Synthese und biologische Evaluierung von Naturstoffderivaten

Dissertation

Zur Erlangung des Doktorgrades der Naturwissenschaften
(Dr. rer. nat.)

der

Naturwissenschaftlichen Fakultät II
Chemie, Physik, Mathematik

der Martin-Luther-Universität
Halle-Wittenberg

vorgelegt von

Frau Marie Christine Renate Kozubek

Gutachter:

1. Prof. Dr. René Csuk
2. Prof. doc. RNDr. Milan Urban

Verteidigt am 14.12.2023, Halle (Saale)

Vorwort

Die vorliegende Arbeit wurde von August 2019 bis Oktober 2022 am Institut für Chemie im Bereich für Organische Chemie der Martin-Luther-Universität Halle-Wittenberg im Arbeitskreis von Prof. Dr. René Csuk angefertigt. Die Dissertation wurde in kumulativer Form verfasst und die Forschungsergebnisse wurden bereits in internationalen „peer-reviewed“ Fachzeitschriften publiziert.

Danksagung

Zuerst möchte ich an dieser Stelle meinem Doktorvater Prof. Dr. René Csuk für die Überlassung dieses interessanten Themas, seinem Vertrauen und die stetige fachliche Beratung und Unterstützung danken. Vielen Dank für die zahlreichen Unterhaltungen, den gewährten Freiraum und die Möglichkeit diese Arbeit durchzuführen.

Außerdem danke ich der gesamten Arbeitsgruppe sowie ehemaligen Mitgliedern für die schöne gemeinsame Zeit und die entgegengebrachte Unterstützung. In diesem Zusammenhang möchte ich mich in besonderer Weise bei M. Sc. O. Kraft, Dr. I. Serbian und DLC T. Schmidt für die hilfreichen Gespräche, die vielen freudigen Momente und die unvergessliche Zeit bedanken. Ein weiterer Dank gilt DLC J. Heisig, sowie M. Sc. T. Denner und M. Sc. N. Heise.

Des Weiteren möchte ich mich bei allen Studenten bedanken, durch deren direkte oder indirekte Hilfe ein Beitrag zum Gelingen dieser Arbeit geleistet wurde.

Ebenso danke ich Dr. D. Ströhl, Y. Schiller und B. Sc. S. Ludwig für die Aufnahme zahlreicher NMR-Spektren. Außerdem danke ich Dr. R. Kluge, DLC T. Schmidt und M. Schneider für die Anfertigung zahlreicher MS-Spektren. Für die Aufnahme der UV/Vis-, IR- und Drehwertmessungen bedanke ich mich bei M. Schneider.

Bei DLC S. Hoenke möchte ich mich für die Durchführung der biologischen Evaluierung bedanken.

Zuletzt möchte ich mich bei meinen Freunden, meiner Familie und besonders meinem Partner bedanken für die konstante Unterstützung, die vielfältige Motivation, jedes aufmunternde Wort und eure Hilfsbereitschaft.

Inhaltsverzeichnis

1.) Einleitung 1

1.1.) Krebs 1

1.2.) Aktuelle Behandlungsstandards und zukünftige Wirkungsziele neuer Zytostatika 3

1.3.) Naturstoffe und deren Konjugate als Quelle neuer Arzneimittel 5

1.4.) Bioaktive Kaffeeinhaltsstoffe 5

1.5.) Triterpene 9

1.6.) Betulin, Betulinsäure und Platansäure 11

2.) Zielstellung 13

3.) Diskussion und Einordnung der Forschungsergebnisse 15

3.1.) Hydroxyzimtsäure-Rhodamin-Konjugate 15

3.2.) Safirinium-Triterpen-Konjugate 16

3.3.) Benzylamide der Betulinsäure 17

..... 19

3.4.) Amide von Betulin und Betulinsäure 19

3.5.) Platansäure-Konjugate 21

3.6.) Vergleich von Betulin-, Betulinsäure- und Glycyrrhetinsäure-Konjugaten 22

3.7.) Der Einfluss des Rhodamin-Substituenten auf die Zytotoxizität von Maslinsäure-Rhodamin-Konjugate 22

4.) Zusammenfassung und Ausblick 26

Literaturverzeichnisse 29

Abbildungsverzeichnis 35

Anhang ..... A

Publikationen ..... A

Erklärung zu den Autorenanteilen der Publikationen ..... F

Lebenslauf ..... H

Selbstständigkeitserklärung I

Angehangene Publikationen ..... J

Abkürzungsverzeichnis

Ac	Acetyl
AChE	Acetylcholinesterase
BA	Betulinsäure
BChE	Butyrylcholinesterase
$CHCl_3$	Chloroform
DC	Dünschichtchromatografie/Dünnschichtchromatogramm
DCM	Dichlormethan
DIPEA	N,N-Diisopropylethylamin
DMAP	4-(Dimethylamino)-pyridin
DMF	N,N-Dimethylformamid
EA	Ethylacetat
EC_{50}	mittlere effektive Konzentration
et al.	lat.: und andere
FACS	Fluorescence-activated Cell Sorting
Hex	Hexan
MeOH	Methanol
NMR	*Nuclear Magnetic Resonance*
PA	Platansäure
S	Selektivitätsfaktor (S = EC_{50}, NIH3T3 / EC_{50} jeweilige Zelllinie)
SRB-Assay	Sulforhodamin B-Assay
TEA	Triethylamin

THF	Tetrahydrofuran
ROS	Reaktive Sauerstoffspezies

1.) Einleitung

1.1.) Krebs

Bösartige Neubildungen als Konsequenz eines unkontrollierten Zellwachstums werden als Krebserkrankung bezeichnet. Im Gegensatz zu gutartigen Neubildungen können Krebszellen in Nachbargewebe einwachsen und/oder über Blut- oder Lymphgefäße in andere Körperregionen streuen. Bei der Entstehung von Metastasen, haben diese vergleichbare Eigenschaften wie der Primärtumor, von dem sie abstammen. Jede Zelle im Köper kann sich zu einem Tumor entwickeln, weshalb eine Unterscheidung in verschiedene Krebserkrankungen hinsichtlich ihres Entstehungsortes vorgenommen werden kann. Die Bildung von Tumoren erfolgt durch eine Schädigung des Genoms. Ursachen für die genetischen Schäden sind Mutationen, die in den Genen selbst oder in den Kontrollsystemen des Genoms auftreten. Die Entwicklung von Mutationen können erblich bedingt sein, zufällig auftreten oder durch die Umwelt ausgelöst werden. Bei genetischen Schädigungen, die zu Krebs führen, kann es zu Störungen lebenswichtiger Funktionen einer Zelle auf allen Ebenen kommen. Hierbei können sowohl die Zellteilung, die Einordnung in den Gewebeverband, die Differenzierung, das Altern (Seneszenz) als auch das Sterben (Apoptose) betroffen sein.[1]

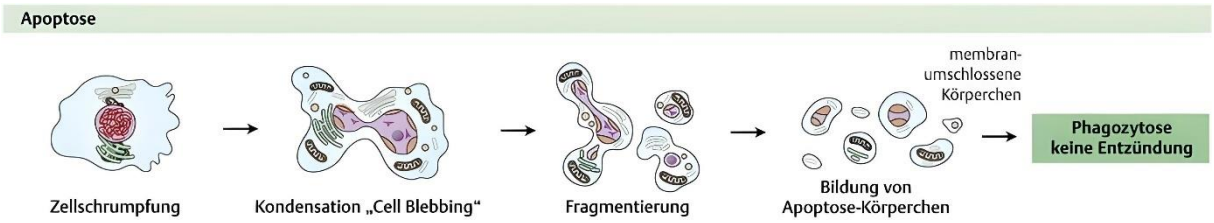

Abbildung 1: Überblick Apoptose[2]

Der Körper verfügt über Kontrollmechanismen, welche Mutationen korrigieren können. Bei schwerwiegender Schädigung, wie beispielsweise unkontrolliertem Wachstum einer Zelle, wird durch Apoptose der Zelle, der Körper vor der Weitergabe genetischer Defekte bei der Zellteilung geschützt. Bei Defekten der genetischen Reparatursysteme und/oder der Apoptose kommt es zur Akkumulation genetischer Schäden mit zunehmendem Alter, wodurch eine Krebserkrankung ausgebildet werden kann. Genetische Veränderungen bedeutender Steuerpositionen der Zelle erklären die Entartung zur Krebszelle. Kennzeichen von Krebszellen

sind unter anderem das Nutzen von Wachstumssignalen, die Resistenz gegen Wachstumsblocker sowie die Inaktivierung des natürlichen Zelltodes. Dies ist möglich, da sie den Stoffwechsel für ihr eigenes Wachstum anpassen und die Bildung neuer Blut- und Lymphgefäße zur Energieversorgung stimulieren. Die bei Entzündungsprozessen nützlichen Abwehrreaktionen werden bei einer Krebserkrankung ebenfalls als Wachstumshilfen missbraucht, da die Angiogenese einer vom Primärtumor abgelösten Krebszelle hilft, rasch Anschluss an das Blutsystem zu finden.[3,4]

Bei Krebs sind Krankheitssymptome am Entstehungsort und in der Umgebung von Metastasen möglich. Natürlich ist eine Früherkennung durch Vorsorgeuntersuchungen bei erworbenen Krebserkrankungen und sogenanntem Alterskrebs mit der größten Chance auf Heilung verbunden. Bei fortgeschrittenen Krebserkrankungen ist eine Beseitigung der Metastasen durch eine Operation oder Bestrahlung meist nicht ausreichend, oder der Tumor kann mit den genannten Methoden nicht behandelt werden, weshalb Chemotherapie als Behandlungsmethode Anwendung findet.[5]

Bei der Chemotherapie greifen chemische Substanzen, die sogenannten Chemotherapeutika oder Zytostatika, in den Vermehrungszyklus der Krebszellen ein, wobei die Wirkstoffe der Chemotherapie in Form von Spritzen, Tabletten oder Infusionen verabreicht werden. Die Wirkung der Zytostatika richtet sich vorrangig gegen die Erbsubstanz jener Zellen, die sich in der Vermehrungsphase befinden, weshalb auch sich üblicherweise rasch teilende, nicht maligne Zellen durch die Wirkstoffe der Chemotherapie beeinflusst werden. Dadurch ergeben sich auch viele Nebenwirkungen dieser Wirkstoffe. Damit beeinflusst die zellschädigende Wirkung der Chemotherapie auch besonders natürlicherweise sich schnell teilende Zellen, wie Zellen der Schleimhaut, der Haarwurzeln oder des Knochenmarks. Weitere Auswirkungen sind Störungen des Verdauungstraktes, Veränderungen der Zusammensetzung des Blutes, Haarausfall, anhaltende Erschöpfungszustände, Konzentrations- und Gedächtnisstörungen, Beeinträchtigung des Menstruationszyklus bei Frauen, Schädigungen der Keimdrüsen sowie Störungen der Fortpflanzungsfähigkeit und ein gesteigertes Risiko für weitere Krebserkrankungen.[6-9]

Bedingt durch die meist sehr hohen Teilungsrate von Krebszellen, sind diese natürlich auch Ziel des Wirkungsmechanismus der Chemotherapeutika. Aufgrund der Vielzahl von

Nebenwirkungen der Chemotherapeutika sollten neue Medikamente zur Krebsbehandlung entwickelt und klinisch erprobt werden, die besonders effektiv, selektiv und besser verträglich sind. Außerdem gibt es bereits Resistenzen gegenüber derzeit eingesetzten Medikamenten, die durch Mutation der Tumore entstehen, wodurch ebenfalls neue Behandlungs-möglichkeiten benötigt werden.[6-9]

Bei Krebszellen sind unter anderem die Zellpermeabilität, die Substanzaufnahme sowie der intrazelluläre pH verändert. Außerdem zeigen sie höhere intrinsische ROS-Spiegel, wobei mit reaktiver Sauerstoffspezies (ROS) hochreaktive Verbindungen wie Peroxide, Hydroxylradikale, Singulett-Sauerstoff und Alpha-Sauerstoff gemeint sind. Die Wirkung neuer Medikamente kann selektiver werden, indem man diese genannten Veränderungen für die chemische Modifikation neuer Substanzen nutzt, um die Beeinträchtigung nicht maligner Zellen durch die Chemotherapie zu verringern.[8,10,11]

Im Gegensatz zur Operation und der Bestrahlung ermöglicht die Chemotherapie eine Verteilung der Wirkstoffe im ganzen Körper, womit auch potenziell verstreute Tumorzellen erreicht und zerstört werden können. Das Gehirn stellt jedoch eine Ausnahme dar, weshalb spezielle Zytostatika nötig sind, welche die Blut-Hirn-Schranke überwinden. Die Chemo-therapie ist neben fortgeschrittenen Krebsstadien auch in Frühstadien unterstützend zu anderen Verfahren einsetzbar, da viele Tumore winzige Tochtergeschwülste bilden, die in bildgebenden Verfahren noch nicht sichtbar sein können.[12,13]

1.2.) Aktuelle Behandlungsstandards und zukünftige Wirkungsziele neuer Zytostatika

In der Chemotherapie gibt es momentan verschiedene Wirkstoffklassen, um Krebszellen in unterschiedlichen Phasen des Zellzyklus angreifen zu können. Vertreter der Zytostatika sind Alkylanzien wie zum Beispiel Cyclophosamid, Antimetabolite wie das Pyrimidin-Analogon 5-Fluorouracil, sowie die zu den Diterpenoiden gehörende Taxane aus der Rinde der pazifischen Eibe.[7,14]

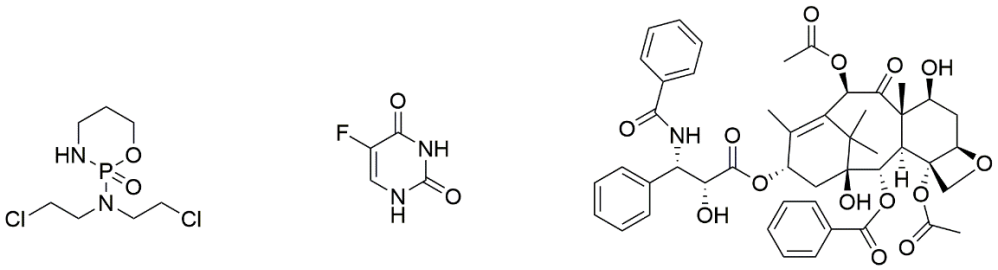

Abbildung 2: verschiedene Zytostatika

Die Wirkung der zuletzt genannten pflanzlichen Zytostatika erfolgt an den sogenannten Mikrotubuli, indem sie den Abbau des Spindelapparates hemmen, wodurch die Teilung des Zellkerns und die Verteilung des Erbgutes verhindert wird.[12,13]

Bei der nächsten Generation von Chemotherapeutika werden unter anderem Verbindungen entwickelt, deren Ziel ihres Wirkmechanismus die Mitochondrien sind. Diese zytoplasmatischen Organellen sind wichtig für die normalen Zellfunktionen, wobei nicht nur die Energiebereitstellung von Bedeutung ist, sondern die Mitochondrien können zudem einen programmierten Zelltod, die Apoptose, induzieren.

Zytostatika mit den Mitochondrien als Ziel des Wirkmechanismus, werden als Mitocane bezeichnet. Diese können je nach Wirkungsmechanismus in unterschiedliche Klassen eingeteilt werden. Eine Übersicht über die Einteilung der Klassen und ihren Wirkungsort ist in der nachfolgenden Tabelle dargestellt.[9]

Tabelle 1: verschiedene Klassen der Mitocane und ihr Wirkort[9]

Klasse	Wirkungsort
1	Hexokinase-Inhibitoren
2	BCl-2-Proteinfamilie
3	Thiol-Redox-Inhibitoren
4	sowie VDAC/ANT
5	Elektronen-Redoxkette
6	Innere Zellmembran (lipophile Kationen)
7	Zitronensäurezyklus
8	mtDNA
9	Unbekannter Wirkort

Zu den Mitocanen gehören strukturell unter anderem lipophile Kationen. Da Studien ein erhöhtes Mitochondrienmembranpotenzial für maligne Zellen im Vergleich zu nicht malignen Zellen nachweisen konnten,[12,13] führt dieser erhöhte Potenzialunterschied zur Begünstigung der Anhäufung von kationischen Verbindungen. Auf Grundlage dieser Befunde wird für neue Wirkstoffstrukturen eine Steigerung der Antitumoraktivität und ein selektiveres zytotoxisches Verhalten gegenüber Krebszellen im Vergleich zu nicht malignen Zellen erwartet.[13,15]

1.3.) Naturstoffe und deren Konjugate als Quelle neuer Arzneimittel

Obwohl nur 1 % aller bekannten organischen Verbindungen Naturstoffe sind und 99 % [16] synthetisch hergestellt wurden, sind 50 % [17] aller zugelassenen Arzneimittel auf Naturstoffe zurückzuführen. Oft wurden Naturstoffe als Leitstruktur für weitere chemische Modifikationen verwendet, da chemische Verbindungen mit natürlichem Ursprung einzigartige komplexe Funktionalisierungsmuster aufweisen, welche schon durch einfache chemische Modifikationen ihre Wirkweise sowie ihren Wirkungsort verändern können.[16] Für die Auswahl geeigneter Strukturen sind daher eine Vielzahl von bioaktiven Molekülen auf pflanzlicher Basis von Interesse, als Alternative für synthetische Wirkstoffe. Mehrere wissenschaftliche Studien zu Tiermodellen und Menschen belegen bereits das krebsvorbeugende Potenzial von Phytochemikalien.[18]

1.4.) Bioaktive Kaffeeinhaltsstoffe

Vor allem Kaffee, als ein sehr häufig konsumiertes Getränk, setzt sich aus einer komplexen Mischung bioaktiver Moleküle zusammen. Beispielsweise die in rohen Kaffeebohnen enthaltenen Diterpene Cafestol und Kahweol, sowie die Hydroxyzimtsäuren stellen interessante Strukturen dar, um chemische Modifikationen vorzunehmen.

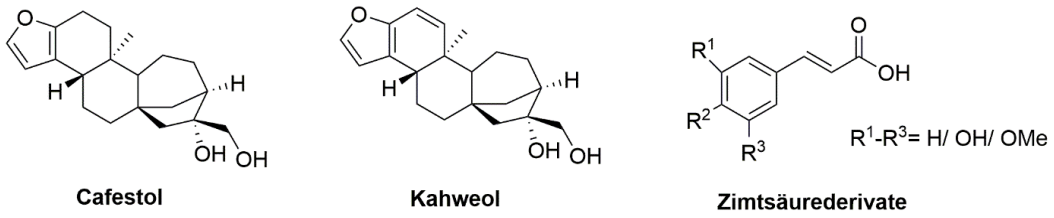

Abbildung 3: Beispiele für bioaktive Inhaltsstoffe in Kaffee

Die chemische Zusammensetzung von ungerösteten Kaffeebohnen besteht aus über 50 % Kohlenhydraten, wobei hier vor allem wasserunlösliche Polysaccharide wie zum Beispiel Cellulose, Mannane oder Galactane, aber auch Saccharose und geringe Anteile an Monosacchariden vorliegen. Die Lipidfraktion setzt sich hauptsächlich aus Triglyceriden zusammen, aber beinhaltet ebenfalls Sterole, Di- und Triterpene sowie deren Fettsäureester. Cafestol und Kahweol unterscheiden sich strukturell nur um eine Doppelbindung zwischen den Kohlenstoffatomen C-1 und C-2. Cafestol und Kahweol sind Derivate des Kaurans, einem Tetracyclophytan mit anelliertem Furanring. Weitere Inhaltstoffe der rohen Kaffeesamen sind Proteine, Chlorogensäuren, Coffein, Trigonellin, organische Säuren und Mineralstoffe. Als Chlorogensäuren bezeichnet man die Summe aller Kaffeoyl-, Feruloyl- und Coumaroyl-chinasäuren, wobei die 5-Caffeoylchinasäure im Kaffee mengenmäßig bedeutend ist.[19,20] Die genaue Zusammensetzung und die Konzentrationen der Inhaltsstoffe im Kaffee hängt jedoch von verschiedenen Faktoren ab und ändert sich mit der Röstung.

Die Diterpene Cafestol und Kahweol sind sehr empfindlich gegenüber Licht, Hitze und Säuren, weshalb bei den Röstprozessen der Kaffeebohnen verschiedene Zersetzungsprodukte wie z.B. das Dehydrocafestol bzw. -kahweol entstehen.[19,21] Hinsichtlich der Einschätzung des anti-karzinogenen Potenzials der Kaffeediterpene gibt es einige Untersuchungen, wie z.B. das die orale Verabreichung von Kahweolacetat und Cafestol zur Hemmung der Proliferation und Migration von Prostatakrebszellen beitragen, indem die Diterpene unter anderem die Apoptose induzieren.[22,23]

Neben den Diterpenen sind phenolische Verbindungen als sekundäre Metaboliten der Pflanze von Relevanz, um positive gesundheitliche Einflüsse für den Menschen zu betrachten. Diverse Phenole zeigten sich bereits als vielversprechende Grundstruktur für zytotoxische Antikrebsmittel, die die Apoptose fördern, die Proliferation reduzieren und auf verschiedene

Aspekte von Krebs abzielen (Angiogenese, Wachstum und Differenzierung sowie Metastasierung).

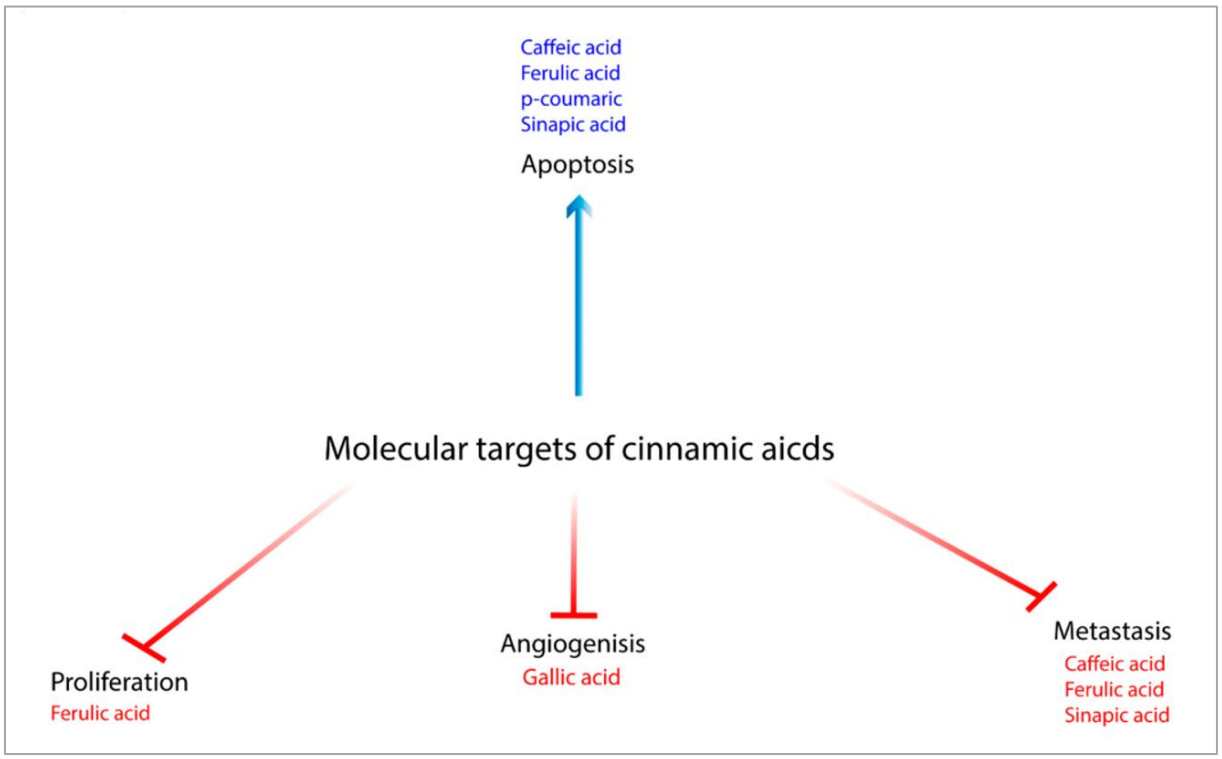

Abbildung 4: Wirkorte der Zimtsäuren[24]

Phenolsäuren gehören zu einer Unterklasse von Pflanzenphenolen, welche wiederum in Benzoe- und Zimtsäuren unterteilt werden können, die in verschiedenen *in-vitro*- und *in-vivo*-Studien mit starken Antikrebsfähigkeiten in Verbindung gebracht werden.[24]

Hydroxyzimtsäuren besitzen sowohl antioxidative sowie entzündungshemmende Eigenschaften, wobei die Wirksamkeit der Zimtsäuren als Antioxidationsmittel abhängig von pH, sowie ihren strukturellen Merkmalen ist und intrinsisch mit dem Vorhandensein von Hydroxylfunktionen in der aromatischen Struktur zusammenhängt. Daher zeigt Kaffeesäure, mit ihrer ortho-Hydrochinonstruktur ein größeres antioxidatives Potential als *p*-Cumarsäure. Hydroxyzimtsäuren finden sich nicht nur in Kaffee, sondern auch in Teeblättern, Getreide, verschiedenen Früchten sowie Gemüsearten. In den Pflanzen sind sie Vorläufermoleküle für Stilbene, Chalcone, Flavonoide, Lignane und Anthocyane.[25,26]

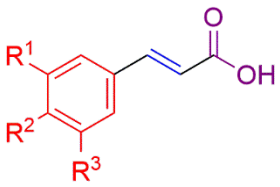

Zimtsäure: R^1 = H, R^2 = H, R^3 = H
p-Cumarsäure: R^1 = H, R^2 = OH, R^3 = H
Kaffeesäure: R^1 = OH, R^2 = OH, R^3 = H
Ferulasäure: R^1 = OMe, R^2 = OH, R^3 = H
Sinapinsäure: R^1 = OMe, R^2 = OH, R^3 = OMe

Abbildung 5: Zimtsäure-Grundgerüst mit verschiedenen Substitutionsmustern

Strukturelles Hauptmerkmal dieser Verbindungen ist ein aromatisches System, an dem eine Propylkette gebunden ist, wobei sowohl die Substitution am aromatischen Ring verändert sein kann, aber auch Reaktionen mit der Doppelbindung sowie der Carbonsäuregruppe möglich sind.

Die Tumorspezifität für phenolische Zimtsäureverbindungen korreliert mit der Form, Größe und dem Ionisationspotential (IP) der Moleküle. Der Ersatz einer Hydroxylgruppe durch eine Methoxygruppe reduziert dabei die zytotoxische Aktivität um ein Vielfaches.[27] Eine Methylierung von Hydroxylgruppen kann zwar die antioxidativen Eigenschaften verbessern, aber das zytotoxische Potenzial signifikant reduzieren.[27] Eine Erhöhung der Phenolsäureaktivität, kann u.a. durch Bildung von Estern erreicht werden, die im Gegensatz zu ihren entsprechenden ungiftigen Phenolsäuren (IC_{50} > 100 µmol/L) eine gewisse zytotoxische Aktivität aufweisen. Andererseits zeigten trihydroxylierte Ester bei Verbindungen gleicher Alkylkettenlänge eine höhere antiproliferative und zytotoxische Wirkung als jene mit zwei OH-Gruppen.[27] In mehreren Experimenten wurde festgestellt, dass Phenolverbindungen die Fluidität von Phospholipidmembranen beeinflussen, ihre Aggregation und Starrheit induzieren, und dieses Merkmal mit der Anzahl hydrophiler Seitenketten zusammenhängt. Polare Hydroxygruppen sind in der Lage, Wasserstoffbindungen mit der Kopfgruppe von Membran-Phospholipiden zu bilden und die Phospholipid-Aggregation zu vermitteln. Dies verursacht eine Verringerung der Membranfläche und die Membran wird unbeweglicher gemacht. Des Weiteren wird angenommen, dass das Vorhandensein von Hydroxygruppen ein Schlüssel zur Wechselwirkung mit Zellmembranen ist. Phenolische Hydroxylgruppen fungieren als Wasserstoffbrückendonoren, während Sauerstoffatome in Phospholipiden als Akzeptoren dienen können.[10,28]

Aktuelle Berichte über die Anti-Krebs-Eigenschaften von Phenolsäuren konzentrieren sich darauf, den Mechanismus ihrer Wirkung aufzuklären, wobei ROS-abhängige Signalwege besonders empfindlich auf das Vorhandensein von Antioxidantien wie Phenolsäuren reagieren.[29] Hydroxylgruppen scheinen besonders wichtig zu sein, bei der Reduktion freier Radikale, sowie bei intermolekularen Wechselwirkungen und der Gestaltung des zytotoxischen Potentials.[10,30]

1.5.) Triterpene

Terpene gehören zu den am weitesten verzweigten sekundären Phytochemikalien. Ihr Grundgerüst lässt sich auf Isopren-Einheiten zurückführen, wodurch durch diverse Bindungsvarianten eine sehr große Anzahl an Kohlenstoffgerüsten und funktionellen Gruppen entsteht, welche sich, wie in Abbildung 6 gezeigt, zu Hemi-, Mono-, Sesqui-, Di-, Tri-, Tetra- und Polyterpenen zusammensetzen.[31]

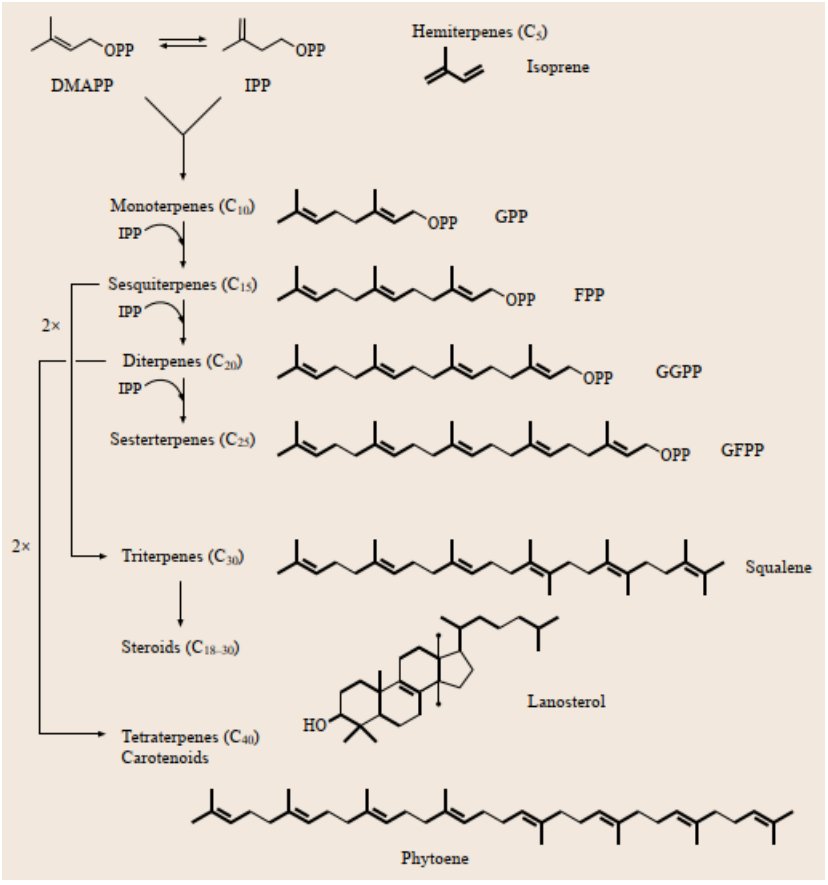

Abbildung 6: Überblick der Terpenoidskelette, welche durch Addition von Isopreneinheiten gebildet werden[32]

In den letzten Jahren wurden verfügbare natürliche pentazyclische Triterpenoide wie Betulin, Betulinsäure-, Ursol-, Oleanol- und Glycyrrhetinsäure als vielversprechende Gerüste für die Entwicklung neuer, auf Mitochondrien abzielende Antikrebsmittel, untersucht. Die Antitumorwirkung nativer Triterpensäuren, die *in vitro* gegen verschiedene Tumorzelllinien (Melanom, Adenokarzinom, Neuroblastom, Medulloblastom und Glioblastom) nachgewiesen wurde, wird durch eine geringe systemische Toxizität ergänzt.[33-39] Diese Sekundärmetaboliten beeinflussen die Funktionalität der Mitochondrien von Tumorzellen, indem sie eine Überproduktion reaktiver Sauerstoffspezies (ROS) initiieren, was zur Bildung von mitochondrialen „Transition Pores“ (Permeabilitätszunahme der inneren Mitochondrienmembran) führt und zur Freisetzung von Cytochrom c in das Zytosol, wodurch es schließlich zur Induktion des Zelltodes kommt.[40,41]

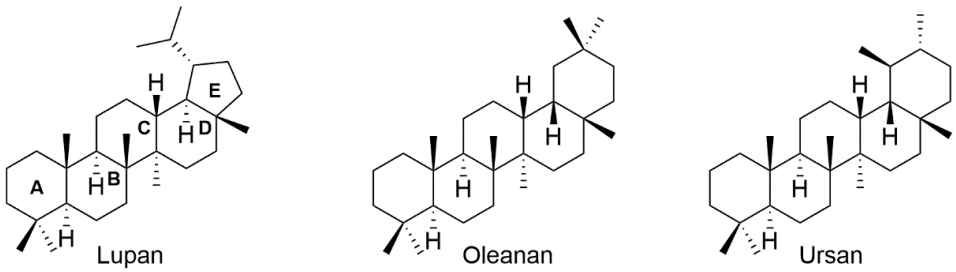

Abbildung 7: Strukturformel pentazyklischer Triterpen-Grundgerüste

Außerdem verleiht das Fehlen einer zytotoxischen Wirkung gegen normale menschliche Zellen (Fibroblasten oder normale Lymphozyten) Triterpensäuren einen signifikanten Vorteil hinsichtlich einer selektiveren Wirkweise. Ihre hohe Hydrophobizität, ihre geringe Bioverfügbarkeit, sowie eine schlechte Löslichkeit im Blutserum erschweren die Entwicklung von Triterpenoiden als Arzneimittelkandidaten gegen Krebs erheblich.[41,42]

Als vielversprechende Verbindungen für die Arzneimittelentwicklung erwiesen sich Konjugate aus pentazyklischen Triterpenoiden und kationischen, lipophilen Molekülen als potenzielle Mitocan-Wirkstoffe. Dabei durchdringen delokalisierte lipophile Kationen, die hydrophoben Barrieren von Plasma und Mitochondrienmembranen, wie z.B. Rhodamin-123, Triphenylphosphonium und Guanidiniumkationen.[41] Der Ansatz Zytostatika zu entwickeln, welche die Mitochondrien als Zielort ihres Wirkmechanismus haben, ist nicht als allgemeine Lösung zu sehen. Man kann aber von einer Wirksamkeit bei Tumoren ausgehen, die nachweislich stark vom oxidativen Stoffwechsel abhängig sind, wie z. B. Hirntumore, akute myeloische

Leukämie,[43,44] Cisplatin-resistente Eierstockkrebszellen[45] oder bestimmte Stadien der Tumorprogression.[41,46]

1.6.) Betulin, Betulinsäure und Platansäure

Betulin und Betulinsäure gehören zu Triterpenoiden vom Lupantyp, die aus der Rinde verschiedener Baumarten, wie der Moor-Birke (*Betula pubescens*), isoliert werden können.[42,47,48] In den natürlichen Quellen kommt Betulinsäure, wie alle anderen Triterpencarbonsäuren, in Form von polareren Konjugaten vor, die hauptsächlich mit Mono- und Oligosacchariden oder Zuckerestern gebildet werden.[49,50]

Im Allgemeinen wurde Betulinsäure in verschiedenen Pflanzen gefunden, sowohl als freies Aglycon als auch in Form von glykosylierten Derivaten, wodurch die Bioverfügbarkeit erhöht wird.[49,51] Die Isolierung aus pflanzlichen Quellen ist durchaus herausfordern, da das Triterpen von einer Reihe anderer Pflanzenprodukte auf Terpenbasis begleitet wird. Betulin hingegen ist ein sehr häufig vorkommender Sekundärmetabolit von verschiedenen Pflanzen, welcher oft in größeren Mengen als Betulinsäure selbst vorhanden ist. Es ist jedoch möglich Betulin mit Hilfe einer Umwandlung in einen Aldehyd zu überführen, welcher gefolgt durch eine weitere Oxidation zur Betulinsäure umgesetzt wird.[47,52] Die Reinigung der Zielverbindungen kann durch eine Kombination verschiedener chromatographischer Methoden, gefolgt von Kristallisation, erreicht werden.[50,52,53]

Betulin wurde erstmals 1788 von Lowitz beschrieben und Betulinsäure 1902 von Retzlaff. Erst im Jahr 1995 entdeckte Pisha et al., dass die Apoptose bestimmter Krebszellen durch Betulinsäure induziert wird, was zu einem signifikanten Anstieg des Interesses an dieser Art von Verbindungen führte.[54,55] Betulin und Betulinsäure zeigen ähnliche Wirkungen auf lebende Organismen und besitzen ein breites Wirkungsspektrum biologische Aktivitäten, wie antitumorale,[56,57] antibakterielle,[58,59] anti-HIV,[60,61] entzündungshemmende,[62,63] antiretrovirale,[64-66] antimalaria-,[59,61,63] antiadipositas,[67] hepatoprotektive,[68,69] und immunmodulatorische Eigenschaften[67].[42] Darüber hinaus sind diese Verbindungen Antioxidantien[70] und reduzieren oxidativen Stress.[61,67] Des Weiteren haben Betulin und Betulinsäure eine positive

Wirkung auf die Behandlung von atopischer Dermatitis[71] und beschleunigen die Wundheilung.[42,72]

Chemische Modifikationen der Triterpenoide erfolgen, wie in Abbildung 8 dargestellt, hauptsächlich an den drei reaktiven funktionellen Gruppen:

an der sekundären Hydroxygruppe (C-3-Position; gelb), an der primären Hydroxygruppe (Betulin; rot) bzw. an der Carbonsäuregruppe (Betulinsäure) an Position C-28, und an der Isopropenyl-Seitenkette (blau). Modifikationen an Position C-2 oder im Triterpenring des Betulin- bzw. Betulinsäuregerüsts sind deutlich seltener.[42]

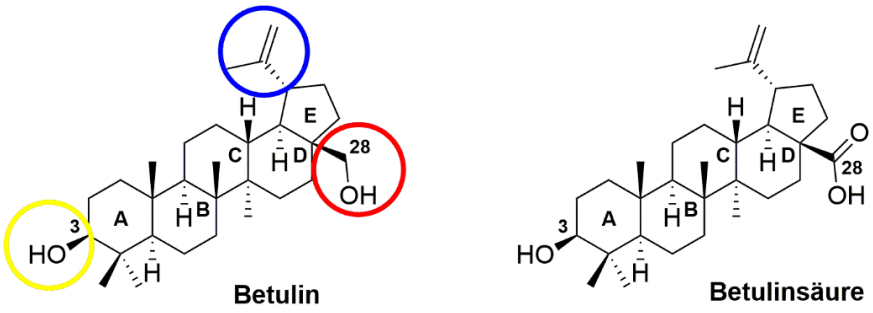

Abbildung 8: wichtigste funktionelle Gruppen für chemische Modifikationen

Platansäure, welche ebenfalls ein Lupan-Grundgerüst aufweist, wurde beispielsweise aus der Rinde von der Ahornblättrigen Platane (*Platanus hybrida*),[73] der Südseemyrte (*Leptospermum scoparium*),[74] der brasilianischen Pflanze *Eugenia moraviana*[75] oder aus dem Kajeputbaum (*Melaleuca leucadendra*)[76] isoliert.[77]

Bei pharmakologischen Untersuchungen der Platansäure bzw. ihrer Konjugate wurden inhibitorische Eigenschaften für die Replikation von HIV,[78] die Inhibierung von Cholinesterase-Inhibitoren (AChE und BChE),[79] was für die Behandlung der Alzheimer Krankheit von Bedeutung ist,[80] und zytotoxische Eigenschaften,[15,81-84] sowie die Inhibierung von Carbo-anhydrase II,[85] nachgewiesen.

2.) Zielstellung

Naturstoffe sind in der Arzneimittelforschung weiterhin ein relevanter Ausgangspunkt, um mithilfe chemischer Modifikationen geeignete Leitstrukturen zu finden, welche die Entdeckung neuer, selektiver und effektiver Wirkstoffe ermöglichen. Hierbei besteht natürlich ein großes Interesse an der Entwicklung von möglichst nebenwirkungsfreien und gleichzeitig hochwirksamen Zytostatika.

In Pflanzen finden sich diverse interessante Stoffklassen mit bioaktiven Eigenschaften, wie z.B. phenolische Verbindungen oder Terpene, welche bereits durch eine Vielzahl von Studien nachgewiesene positive Eigenschaften auf den menschlichen Organismus haben. Jedoch können die in der Natur vorkommenden Verbindungen durch geeignete chemische Modifikationen ihre Wirkweise verändern, sowie steigern.

Im Rahmen dieser Arbeit lag der Schwerpunkt auf Hydroxyzimtsäuren sowie Vertretern der pentazyklischen Triterpene, wie Betulin- und Platansäure als Ausgangspunkt für die Wirkstoffforschung, wobei neuartige Konjugate hergestellt werden sollten.

Um möglichst selektive und zytotoxische Verbindungen zu synthetisieren, wurden Strukturen dahingehend verändert, dass durch die Kupplung von natürlichen Sekundärmetaboliten mit lipophilen, kationischen Verbindungen, wie Rhodamin B, potentielle Mitocane hergestellt werden sollten.

Ein weiteres Ziel beinhaltete zusätzliche chemische Veränderungen an verschiedenen reaktiven Gruppen der pentazyklischen Triterpene, um den Einfluss diverser Substituenten an unterschiedlichen Positionen einschätzen zu können und einen Vergleich mit ähnlichen Strukturen hinsichtlich ihrer Zytotoxizität und Selektivität zu ermöglichen. Bei der strukturellen Modifikation müssen die Änderungen der Verbindungen hinsichtlich der Polarität und Löslichkeit möglichst auf physiologische Verhältnisse angepasst werden. Ansonsten müssten weiter Methoden für den Transport der Zielstruktur zum Wirkort angewendet werden, bzw. kann die entsprechende Bioverfügbarkeit nicht ausreichend für den Einsatz in der Human- oder Tiermedizin gewährleistet werden.

Es sollten in dieser Arbeit u.a. der Einsatz diverser Amino-Substituenten untersucht werden, sowie vergleichbare Modifikationen an Betulin und Betulinsäure vorgenommen werden, um die Struktur-Aktivitäts-Beziehung hinsichtlich geringfügiger Unterschiede besser beurteilen zu können. Des Weiteren sollte neben der Variation der Substitution auch die Relevanz der Position des Substituenten untersucht werden, wobei bereits zuvor gewonnene Erkenntnisse bei der Erforschung der Triterpene berücksichtigt wurden, um eine Verbesserung der biologischen Aktivität ermöglichen zu können.

Nach erfolgreicher Synthese werden die neuen Verbindungen mittels SRB-Assay, Färbeexperimenten mit Annexin V, gefolgt von Durchflusszytometrie und Zellzyklus-untersuchungen hinsichtlich ihrer Zytotoxizität untersucht, wobei für die Abschätzung der Selektivität neben den humanen Tumorzelllinien auch nicht maligne Zelllinien für den SRB-Assay verwendet wurden. Weiterführende biologische Untersuchungen dienten der Aufklärung, ob die eingesetzten Testverbindungen Apoptose oder Nekrose in den Zellen auslösen bzw. in welchem Teil der Zelle eine Anreicherung der Verbindungen erkennbar war.

3.) Diskussion und Einordnung der Forschungsergebnisse

3.1.) Hydroxyzimtsäure-Rhodamin-Konjugate

Es wurden Carbonsäureamide synthetisiert, indem der Fluoreszenzfarbstoff Rhodamin B mit Piperazin umgesetzt wurde, gefolgt von einer Kupplung mit verschiedenen Hydroxyzimtsäuren.

Hierbei wurde zuerst das Säurechlorid von Rhodamin B mit Oxalylchlorid hergestellt, welches mit Piperazin zum Amid überführt wurde. Bei dieser Reaktion findet neben der Monoacylierung des symmetrischen Diamins, eine Nebenreaktion statt, bei der auch das bisacylierte Produkt gebildet wird. Mit entsprechenden Anpassungen der Reaktions-bedingungen, war es möglich eine, für die weiteren Synthesen und der anschließend folgenden Untersuchungen, ausreichende Ausbeute des Produkts herzustellen.

Anschließend wurden Zimtsäure, *p*-Cumarsäure, Ferulasäure und Sinapinsäure in Anwesenheit von TBTU zu Hydroxyzimtsäure-Rhodamin-Konjugaten umgesetzt.

Tabelle 2: verwendete Zelllinien für die biologische Evaluierung

Zelllinie	Krebsart/ursprüngliches Gewebe
A375	Melanom (Hautkrebs)
A2780	Eierstockkarzinom
FaDu	Plattenepithelkarzinom von Kopf und Nacken
HT29	Dickdarmkrebs
MCF-7	Mammakarzinom
NIH3T3	nicht maligne Fibroblasten

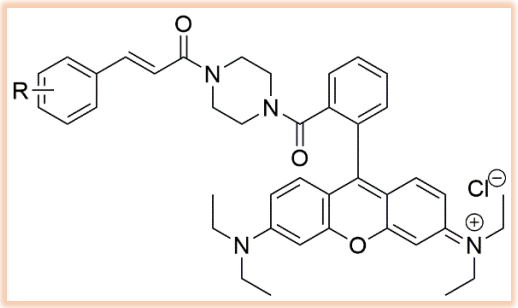

Abbildung 9: Hydroxyzimtsäure-Rhodamin-Konjugate

Die biologische Evaluierung der Zytotoxizität mittels SRB-Assay vom Carbonsäureamid von Rhodamin B und Piperazin ergab für 4 untersuchte Zelllinien EC_{50}-Werte > 30 µM und moderate EC_{50}-Werte von 26 µM für A2780 und 18 µM für MCF-7. Hieraus ersichtlich wird, dass die zytotoxischen Eigenschaften nicht direkt mit dem Rhodamin-B-Gerüst in

Zusammenhang stehen und somit erst durch Kupplung mit einer weiteren Verbindung ein biologisch aktives Produkt entsteht.

Fast alle hergestellten Konjugate zeigten eine gute zytotoxische Aktivität, wobei das Apoptose auslösende Zimtsäure-Konjugat mit Piperazinyl-Spacer für alle getesteten Tumorzelllinien (A375, HT29, MCF-7, A2780, FaDu) niedrige EC_{50}-Werte von 1-3 µM und eine Selektivität von S = 3.5 aufwies. Das Sinapinsäure-Rhodamin-Konjugat hatte mit S = 4.4 den höchsten Selektivitätsfaktor, jedoch waren die zytotoxischen Eigenschaften geringer als die des Zimtsäure-Konjugats. Diese Ergebnisse deuten darauf hin, dass das Vorhandensein einer Hydroxy- oder einer Methoxygruppe in den Hydroxyzimtsäure-Konjugaten die EC_{50}-Werte leicht erhöhen kann, jedoch gleichzeitig die Selektivität nicht deutlich verbessert werden kann.

3.2.) Safirinium-Triterpen-Konjugate

Um die Aktivität der Rhodamin-Triterpen-Konjugate mit anderen kationischen Kupplungskomponenten zu vergleichen, wurden unterschiedlich substituierte Fluorenszenz-marker des Typs Safirinium-P hergestellt, wie in der nachfolgenden Abbildung dargestellt.

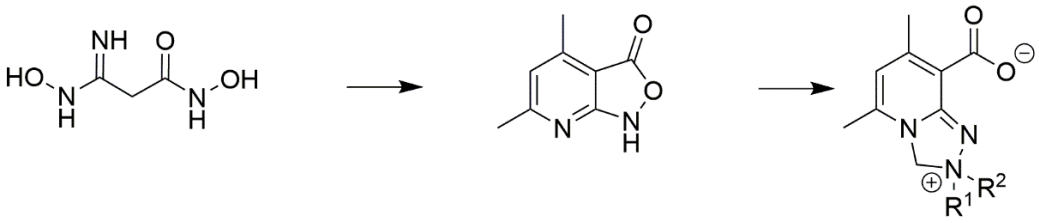

Abbildung 10: Übersicht der Synthese von Safirinium P

4,6-Dimethylisoxazolo[3,4-b]pyridin-3(1H)-on wurde gemäß bereits bekannten Verfahren,[86] aus der Kondensation von *N*-hydroxy-3-(hydroxylamino)-3-iminopropanamid[87] mit Acetyl-aceton in Gegenwart von Piperidin zu dem genannten Zwischenprodukt umgesetzt.

Die nächste Synthesestufe basiert auf einer selektiven Tandem-Mannich-elektrophilen Aminierungsreaktion von fluorogenem 4,6-Dimethyl-isoxazolo[3,4-b]pyridin-3(1H)-on mit Formaldehyd und sekundären Aminen. Aus dieser Mehrkomponentenreaktion wird eine neue

Klasse von photostabilen Fluoreszenzfarbstoffen mit Pyridotriazolium-Kernstrukturen erhalten.[88] Danach erfolgte der Umsatz mit gespacerten Triterpensäuren, welche erneut über ein Carbonsäurechlorid als reaktive Zwischenstufe erhalten wurden. In früheren Veröffentlichungen wurde bekannt, dass Safirinium-Hybride gut in Zellen transportiert werden,[86,88-94] weshalb dieses kationische Grundgerüst für neue Triterpen-Konjugate gewählt wurde. Hierbei zeigten die Safirinium-Stammverbindungen keine zytotoxische Aktivität, während viele Triterpenoid-Safirinium-Konjugate eine mäßige Zytotoxizität aufzeigten. Die aktivste Verbindung war ein Safirinium P Konjugat, welches mit dem Piperazinamid der Betulinsäure verknüpft wurde, mit EC_{50}-Werten von 4.6 µM für Zelllinien des Eierstockkarzinoms (A2780).

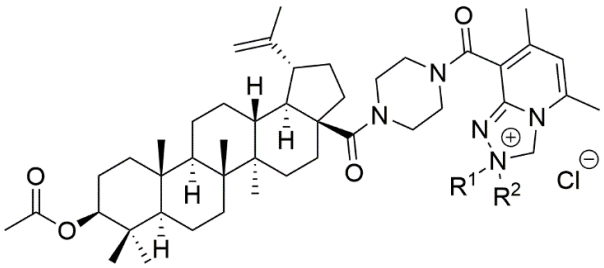

Abbildung 11: Übersichtsstruktur des Safirinium P-Konjugates der acetylierten Betulinsäure mit Piperazin-Spacer (R^1 und R^2 = Ethyl-/Hexyl-/Dodecylest)

Bildgebende Fluoreszenzuntersuchungen ergaben, dass die Safirinium-Grundstrukturen auch bei längeren Inkubationszeiten von 24 Stunden nicht in die Zelle eindringen können, während sich die Konjugate im endoplasmatischen Retikulum, aber nicht in den Mitochondrien anreichern. Diese Ergebnisse könnten ihre verringerte Aktivität im Vergleich zu Rhodamin-B-Analoga erklären, welche in die Mitochondrien gelangen.

3.3.) Benzylamide der Betulinsäure

Es wurden monosubstituierte Benzylamide der acetylierten Betulinsäure hergestellt, um ihre Bioaktivität sowie ihre Selektivität bezüglich Tumorzellen und nicht maligne Zellen in Abhängigkeit des Substitutionsmusters des aromatischen Ringes zu untersuchen.

Fast alle Verbindungen zeigten signifikante zytotoxische Aktivitäten. Beim direkten Vergleich der verschiedenen Substituenten ergab sich, dass die Verbindungen mit einer Methoxygruppe die niedrigsten EC_{50}-Werte erzielten, während die mit Chlor substituierten Strukturen die geringsten Aktivitäten für die verwendeten Tumorzelllinien aufzeigten. Es ist erkennbar, dass die Antitumoraktivität der Benzylamide mit Chlor als Substituent von der ortho- über meta- bis zur para-Position geringer wird. Bei den mit Fluor substituierten Verbindungen ist ein ähnlicher Trend ersichtlich, wobei der Unterschied zwischen den EC_{50}-Werten deutlich geringer ist. Von den Methoxy-Konjugaten hat die meta-Position die niedrigsten EC_{50}-Werte mit 2.1 µM für A375, danach folgt die ortho-Verbindung mit 2.5 µM und die geringste Zytotoxizität besitzen die para-substituierten Benzylamide. Jedoch ist das Methoxy-Konjugat in meta-Position als einzige Verbindung dieser Reihe in geringen Maß für die nicht maligne Zelllinie zytotoxisch, weshalb die Selektivität geringer ist, als die der ortho-substituierten Verbindung. Auch bei den Konjugaten mit Methylgruppe hat die meta-Verbindung die beste Antitumoraktivität, während die para-Position wieder die geringste Aktivität aufweist, wie in Abbildung 12 dargestellt.

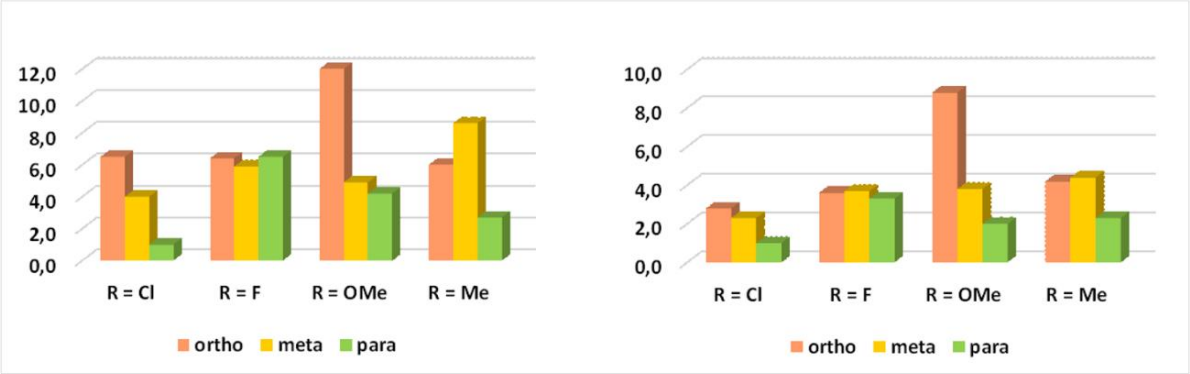

*Abbildung 12: Selektivitätsfaktoren unterschiedlich substituierter Benzylamide der Betulinsäure für die Zelllinie A375 (**links**) und für die Zelllinie A2780 (**rechts**)*

Aus Abbildung 12 ist außerdem erkenntlich, dass bei den ermittelten Selektivitätsfaktoren nicht nur die Art der Substitution, sondern auch die Position des Substituenten einen erkennbaren Einfluss auf die Selektivität der Strukturen haben. Anhand der Ergebnisse wird deutlich, dass mit Ausnahme der fluorhaltigen Konjugate die para-Position die geringsten Selektivitätsfaktoren erreichten, während die selektivste Verbindung für die dargestellten Tumorzelllinien eine Methoxygruppe in ortho-Position ist.

3.4.) Amide von Betulin und Betulinsäure

Wie bereits aus vorherigen Studien[95-98] bekannt, sorgt eine Acetylierung an Position 3 nicht nur für eine höhere Zytotoxizität, sondern erreicht dies wahrscheinlich durch ihre bessere Bioverfügbarkeit. Aus genannten Gründen wurden die Ausgangsverbindungen daher, wie in Abbildung 13 dargestellt, zuerst acetyliert und danach noch mit Benzylamin amidiert. Die erhaltenen Produkte wurden darauf mittels Hydroborierung mit BH_3 in THF, anschließender Oxidation und abschließender Amidierung in die von Betulin und Betulinsäure abgeleiteten 29-Oxo-Amide überführt. Als Amin-Komponente kamen Ethylendiamin, Morpholin, Piperazin und N-Methylpiperazin zum Einsatz. Des Weiteren wurden die Methylpiperazin-Verbindungen mit Methyliodid quarternisiert, wordurch eine kationische Struktur erzielt wurde.

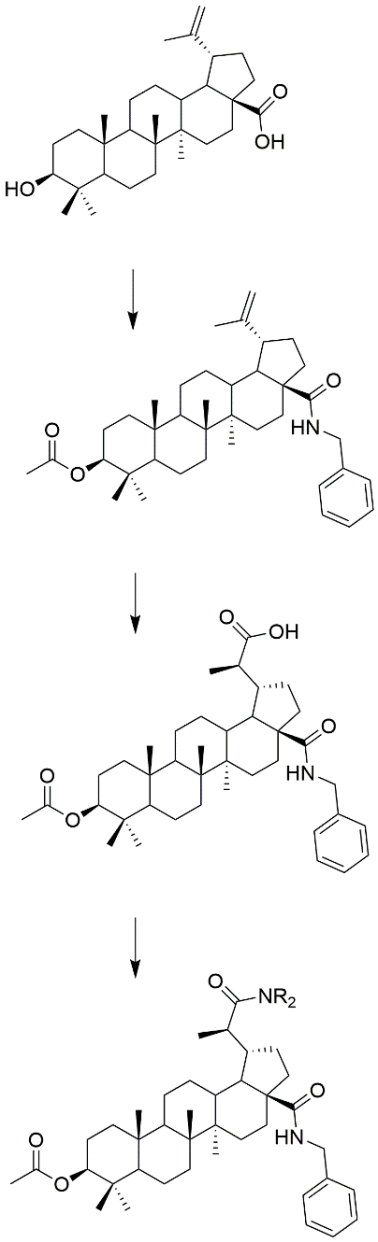

Abbildung 13: Syntheseüberblick der Betulinsäure-Konjugate

Alle hergestellten Verbindungen waren zytotoxisch für eine Reihe menschlicher Tumorzelllinien, wobei die von Ethylendiamin abgeleiteten Strukturen besonders aktiv waren mit EC_{50}-Werten von 1.9 µM für HT29.

Beim direkten Vergleich von der biologischen Aktivität von den Betulin- und Betulinsäurekonjugaten, für die in der folgenden Abbildung dargestellten Tumorzelllinien, fällt auf, dass die von Betulinsäure abgeleiteten Konjugate, welche noch zusätzlich an Position 28 einen Benzylamidrest aufwiesen, minimal höhere EC_{50}-Wert besitzen, im Vergleich zu den Konjugaten des diacetylierten Betulins.

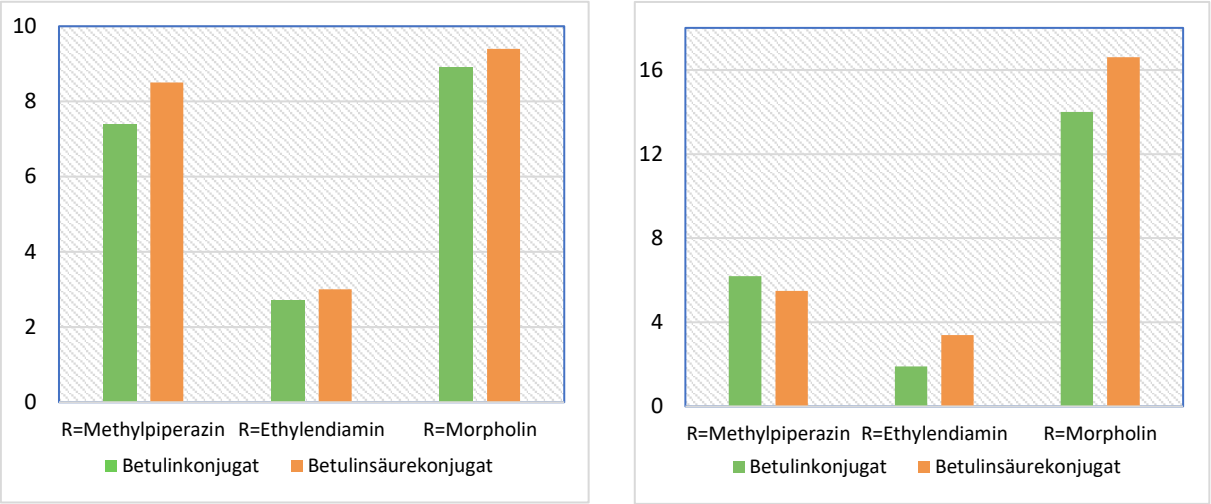

*Abbildung 14: EC_{50}-Werte der Betulin- und Betulinsäurekonjugate für MCF-7 (**links**) und HT29 (**rechts**) in [µM]*

Außerdem war bei dieser Auswahl von Verbindungen auffällig, dass strukturell ähnliche Verbindungen unterschiedliche Wirkmechanismen zeigten, da das Betulinsäurekonjugat mit Methylpiperazin-Einheit hauptsächlich Apoptose verursacht, während diese Verbindung mit Ethylendiamin-Rest bevorzugt Nekrose/Spätapoptose auslöst. Dieses Ergebnis zeigt, dass kleine strukturelle Veränderungen am Molekül einen signifikanten Einfluss auf die Wirkung in den Zellen haben können.

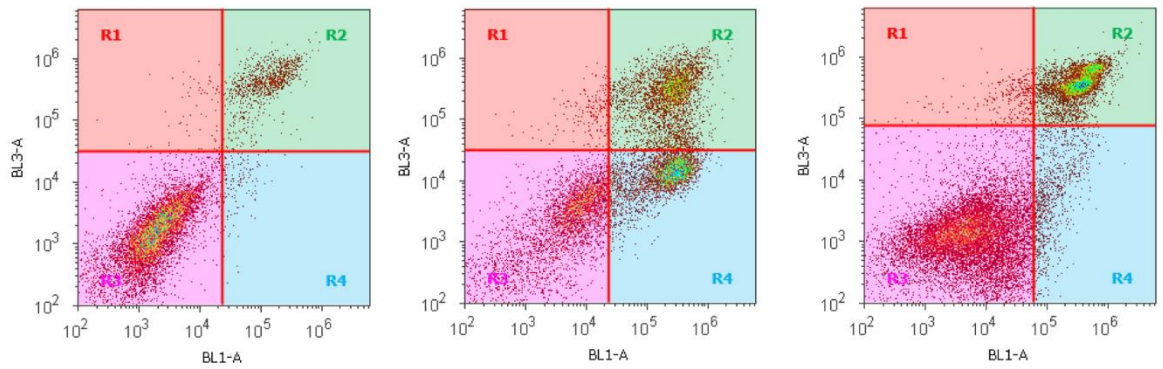

*Abbildung 15: FACS-Untersuchungen von der Kontrolle (**links**; als Vergleich), Betulinsäure-Konjugat mit Methylpiperazin (**Mitte**) und Betulinsäure-Konjugat mit Ethylendiamin (**rechts**) für A375; (R1 = nekrotisch, R2 = sekundär nekrotisch/spätapoptotisch, R3 = vital und R4 = apoptotisch)*

3.5.) Platansäure-Konjugate

Während von Betulinsäure eine große Bandbreite an Konjugaten erforscht wurde, ist der Einsatz von der strukturell ähnlichen Platansäure deutlich weniger erforscht.

Es wurden daher verschiedene Konjugate der 3-*O*-Acetylplatansäure hergestellt. Zuerst erfolgte die Synthese diverser Carbonsäureamide mit *N*-Methylpiperazin, Ethylendiamin, Morpholin, Piperazin und Homopiperazin. Anschließend wurde die Verbindung mit der Methylpiperazin-Einheit mit einem Überschuss an Iodmethan quaternisiert.
Danach erfolgte die Reaktion der Platansäureamide mit Hydroxylammoniumchlorid, wodurch als Endprodukt die (*E*) konfigurierten Oxime gebildet wurden.

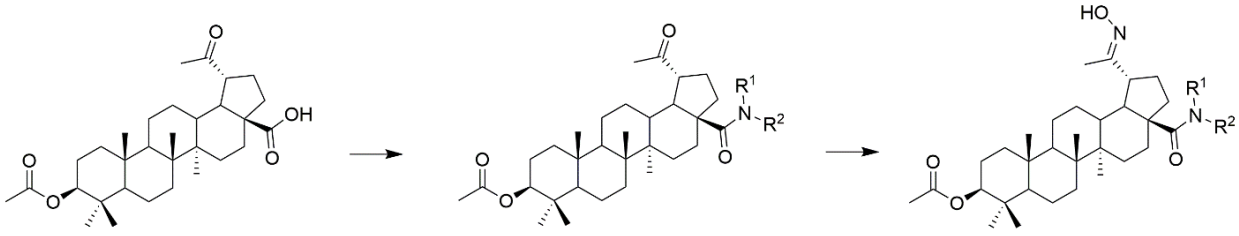

Abbildung 16: Syntheseübersicht Platansäure-Konjugate

Das Ergebnis der biologischen Evaluierung ergab, dass alle Amide zytotoxisch für menschliche Tumorzelllinien waren und vor allem das Konjugat mit der Homopiperazinyl-Einheit die höchste Zytotoxizität mit EC_{50}-Werten von 0.9 µM für die Zelllinie A375 aufwies. Der aktivitätssteigernde Einfluss von Homopiperazin als Spacer im Vergleich zu Piperazin wurde bereits mit verschiedenen Homopiperazinyl-Derivaten von Triterpenoiden in weiteren Studien[13,99] nachgewiesen. Zusätzliche FACS- und Zellzyklusmessungen zeigten, dass diese Verbindung eher durch Apoptose als durch Nekrose auf die A375-Zellen wirkt. Die biologische Aktivität der Oxime war im Vergleich zu der für die entsprechenden Amide bestimmten Zytotoxizität verringert, da sich die Löslichkeit dieser Konjugate deutlich verringerte. Von den hergestellten Oximen hatte das Konjugat mit dem Piperazin-Rest die niedrigsten EC_{50}-Werte mit 2.2 µM für A375.

3.6.) Vergleich von Betulin-, Betulinsäure- und Glycyrrhetinsäure-Konjugaten

Neben den bereits beschriebenen Triterpenen des Lupantyps, wurden zum Vergleich Konjugate der zum β-Amyrintyp gehörende Glycyrrhetinsäure betrachtet, wobei die verschiedenen Positionen der Verknüpfung mit dem gespacerten Rhodamin hinsichtlich der Zytotoxizität verglichen werden sollte. Hierbei wurde anhand der dargestellten Beispiele deutlich, dass die zwei Verbindungen, die über Position 28 verknüpft waren, niedrigere EC_{50}-Werte aufzeigten, als die drei Verbindungen die über C-29 mit dem gespacerten Rhodamin B verbunden sind. Des Weiteren zeigten weiterführende Untersuchungen der Lupantypen der zuletzt genannten Verbindungen, dass diese einen nekrotischen Zelltod verursachen.

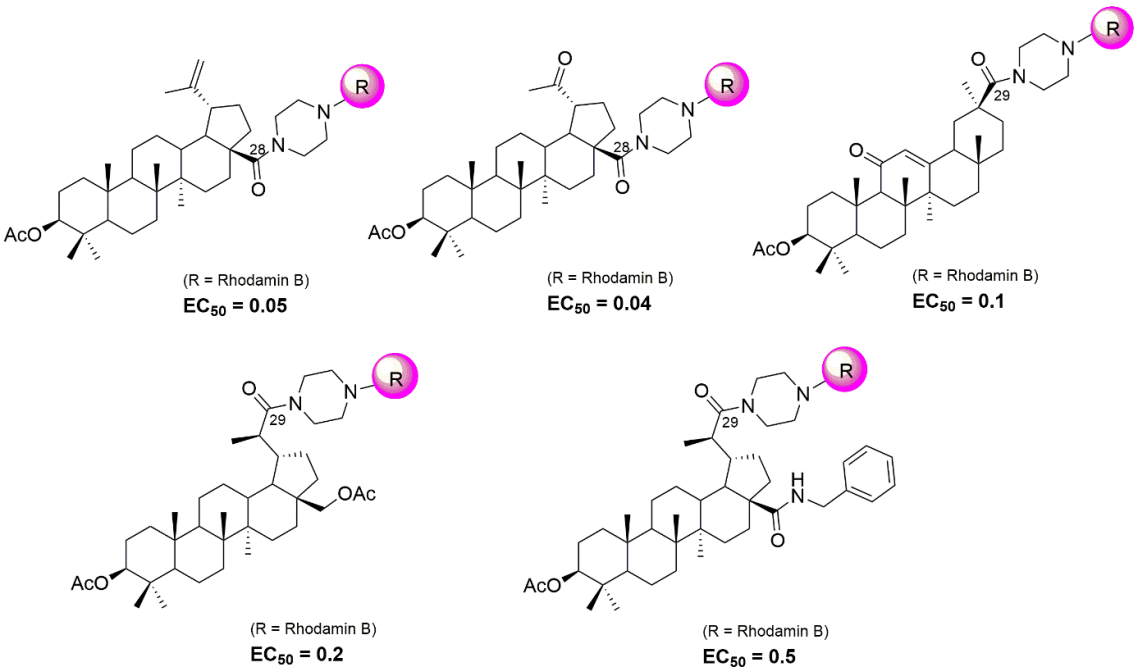

Abbildung 17: Vergleich der Triterpen-Piperazin-Rhodamin-Konjugate mit EC_{50}-Werten in [µM] für A2780

3.7.) Der Einfluss des Rhodamin-Substituenten auf die Zytotoxizität von Maslinsäure-Rhodamin-Konjugate

Nachdem bereits Untersuchungen zur verschiedenen Triterpenen, sowie zum Einsatz von verschiedenen Spacern durchgeführt wurden, erwies sich eine Untersuchung des Einflusses des distalen Rhodaminrests als erforderlich.

Für die Synthese substituierter Rhodamine gibt es verschiedene Synthesemöglichkeiten. Aufgrund der guten kommerziellen Verfügbarkeit des Ausgangsmaterials und der relativ geringen Synthesestufenanzahl, wurde 3-Aminophenol für die Verwendung als Ausgangsstoff gewählt. Dessen Reaktion mit den jeweiligen Alkylhalogeniden ergab Dialkyl-3-aminophenole als entsprechend substituierte Zwischenstufen.

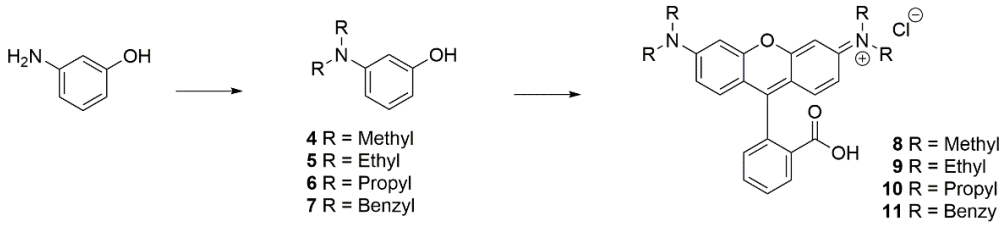

Abbildung 18: Überblick Synthese der Rhodamine

Die Rhodamine wurden durch die Reaktion der zuvor hergestellten Verbindungen mit Phthalsäureanhydrid in Gegenwart katalytischer Mengen Aluminiumtrichlorid erhalten. Maslinsäure wurde nach bereits bekannter Methode aus entkernten Oliven extrahiert. Die Acetylierung der Maslinsäure ergab das Diacetat. Die Reaktion der diacetylierten Maslinsäure mit Oxalylchlorid in Gegenwart katalytischer Mengen Dimethylformamid (DMF) und die anschließende Reaktion mit Piperazin lieferten das Piperazinylamid (**3**). Die zuvor hergestellten Rhodamine wurden mit Oxalylchlorid *in situ* in die entsprechenden Säurechloride umgewandelt. Die Umsetzung der Säurechloride der Rhodamine mit dem Piperazinylamid (**3**) ergab die Piperazinyl-verknüpften Triterpen-Rhodamin-Konjugate.

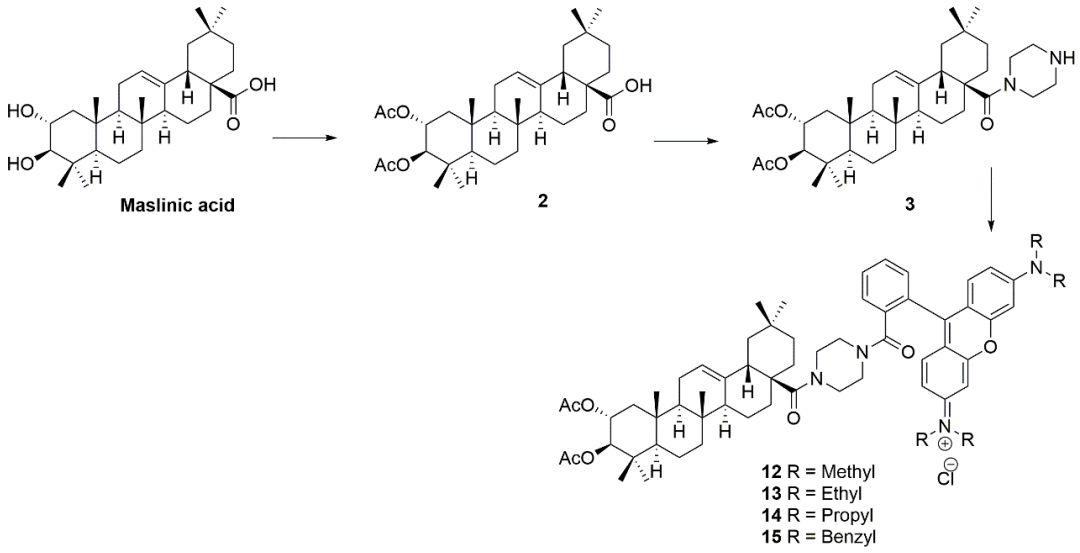

Abbildung 19: Reaktionsschema für die Maslinsäure-Rhodamin-Konjugate

In Tabelle 3 sind die zellbiologischen Ergebnisse zusammengefasst. Für die Rhodamin-Konjugate **12** - **14** wurde im Vergleich zu den Vorstufen ein deutlicher Anstieg der Zytotoxizität bis zu einem etwa 100-fachen Faktor beobachtet. Alle Verbindungen zeigen eine besondere Zytotoxizität für A2780-Zellen (EC50 0,02 bis 0,01 µM). Allerdings ist Verbindung **14** sowohl für A2780-, A375- als auch für MCF-7-Zellen am stärksten zytotoxisch, während für NIH3T3-Zellen eine viel schwächere Zytotoxizität beobachtet wurde. Dies spiegelt sich auch in der berechneten Selektivität S wider (S = EC_{50}, NIH3T3 / EC_{50} jeweilige Zelllinie).

Tabelle 3: SRB-Assay EC50-Werte [µM] nach 72 h Behandlung; gemittelt aus drei unabhängigen Experimenten, die jeweils in dreifacher Ausfertigung durchgeführt wurden; Konfidenzintervall CI = 95 %. Menschliche Krebszelllinien: A375 (Melanom), HT29 (kolorektales Karzinom), MCF-7 (Brustadenokarzinom), A2780 (Ovarialkarzinom), HeLa (Zervixkarzinom), NIH3T3 (nicht-maligne Fibroblasten); Cut-off 30 µM, n.l. nicht löslich; Doxorubicin (DX) wurde als positiver Standard verwendet; Verbindung 15 war unter den Testbedingungen nicht löslich.

[µM]	**A3735**	**HT29**	**MCF-7**	**A2780**	**HeLa**	**NiH3T3**
MA	>30	28.8 ± 0.5	>30	19.5 ± 0.8	>30	21.1 ± 0.2
3	2.0 ± 0.1	1.6 ± 0.1	1.0 ± 0.1	1.9 ± 01	2.1 ± 0.1	3.2 ± 0.02
12	0.07 ± 0.01	0.11 ± 0.04	0.05 ± 0.02	0.02 ± 0.001	0.15 ± 0.02	0.30 ± 0.04
13	0.05 ± 0.01	0.09 ± 0.03	0.03 ± 0.01	0.02 ± 0.005	0.08 ± 0.03	0.25 ± 0.03
14	0.02 ± 0.004	0.07 ± 0.02	0.03 ± 0.005	0.01 ± 0.001	0.05 ± 0.01	0.15 ± 0.04
DX	n.l.	0.9 ± 0.01	1.1 ± 0.3	0.01 ± 0.01	n.l.	0.4 ± 0.0
Selektivität						
12	4.3	2.7	6.0	15.0	2.0	
13	5.0	2.8	8.3	12.5	3.1	
14	7.5	2.1	5.0	15.0	3.0	

Die Zellselektivität ist für A2780-Zellen am höchsten (S = 15,0). Grundsätzlich scheint die Zytotoxizität mit zunehmender Kettenlänge des Alkylsubstituenten am Rhodaminrest zuzunehmen. Dies korreliert auch gut mit den berechneten logarithmischen log $P_{Octanol/Wasser}$ Verteilungskoeffizienten für die Rhodamin-Piperazinyl-Reste. Der Koeffizient steigt von 0,61 (für Methylsubstitution) über 1,72 (für Ethyl) auf 3,05 (für Propyl). Es scheint also ein gewisser, aber nicht abschließend geklärter Zusammenhang zwischen dem Substitutionsmuster am Rhodamin und der beobachteten Zytotoxizität zu bestehen. Zuvor konnte bereits gezeigt

werden, dass Triterpen-Piperazinyl-Rhodamin-Konjugate als Mitocane zu betrachten sind. Ihre zytotoxische Wirkung beruht wahrscheinlich auf einer Wechselwirkung mit der inneren Mitochondrienmembran beruht.

Diese Maslinsäure-Rhodamin-Konjugate waren für eine Reihe menschlicher Tumorzelllinien zytotoxisch, für nichtmaligne Fibroblasten jedoch weniger. Erwähnenswert ist, dass diese Verbindungen eine gewisse Selektivität für A2780-Zellen aufwiesen, und insbesondere Verbindung **14**, ein Rhodamin-Konjugat mit Propyl-Substituenten, zeigte EC_{50}-Werte von nur 0,01 µM und war ca. 15-mal zytotoxischer für die Krebszellen als für die Fibroblasten.

Abschließend ist festzustellen, dass die gemessene Zytotoxizität offensichtlich parallel zum berechneten Oktanol/Wasser-Verteilungskoeffizienten verläuft und lässt, da die Verbindungen als Mitocane wirken, auf eine Wechselwirkung mit der inneren Mitochondrienmembran schließen.

4.) Zusammenfassung und Ausblick

Die große Diversität von natürlich vorkommenden Verbindungen ist Grundlage zahlreicher Studien zur Entwicklung von gezielt wirksamen und nebenwirkungsarmen Medikamenten. Vor allem Triterpene wie Betulinsäure und Maslinsäure als Ausgangsstoffe sind in der Forschung von großem Interesse. Neben ihrer Zugänglichkeit ist auch die chemische Modifikationsmöglichkeit mit dem Ziel selektiver Zytotoxizität von Bedeutung.

Für die Modifikation der Naturstoffe wurden verschiedene Konjugate mit gespacertem Rhodamin B verknüpft. Hierbei wurde zuerst mit einfach zugänglichen Hydroxyzimtsäuren als Modellstruktur gearbeitet, wobei die niedrigsten EC_{50}-Werte von 1-3 µM mit der Zimtsäure-Verbindung erreicht wurde und sich mit Vorhandensein von Hydroxy- bzw. Methoxygruppen nicht weiter erniedrigen ließ. Der höchste Selektivitätsfaktor lag für das Sinapinsäure-Rhodamin-Konjugat bei S = 4.4.

Für weitere Untersuchungen wurden daher pentazyklische Triterpen-Konjugate als aktivere Ausgangsstruktur der Naturstoff-Komponente verwendet. Um den Einfluss des lipophilen Kations hinsichtlich der Zytotoxizität der Gesamtstruktur zu variieren, wurden unterschiedliche Safrinium P Derivate hergestellt, wobei nach Kupplung mit acetylierter Betulinsäure wieder EC_{50}-Werte im einstelligen µM-Bereich erzielt wurden. Mit Hilfe entsprechender Untersuchungen konnte herausgefunden werden, dass die Anreicherung der Konjugate nicht in den Mitochondrien, sondern im endoplasmatischen Retikulum erfolgte.

Eine deutliche Steigerung der Selektivität wurde mittels Synthese verschieden substituierter Benzylamide der acetylierten Betulinsäure erreicht, wobei die EC_{50}-Werte wieder eine Zytotoxizität im zuvor erwähnten Bereich aufwiesen. Die Erhöhung der Selektivität S auf 12.0 bei der ortho-Methoxy-Verbindung beweist, dass neben der Art des Substituenten auch die Position einen erkennbaren Einfluss hat.

Von Betulin und von Betulinsäure abgeleitete 29-Oxo-Amide wurden durch Hydroborierung, gefolgt von Oxidation und anschließender Amidierung der eingeführten Carbonsäure hergestellt, wie in Abbildung 13 dargestellt. Alle Verbindungen zeigten eine signifikante zytotoxische Aktivität für verschiedene menschliche Tumorzelllinien. Kleine Änderungen in der Struktur führten jedoch zu signifikanten Änderungen in der Zytotoxizität der Verbindungen. Bei der Variation der Amin-Einheit zeigten die C-29-Amide, die mit

Ethylendiamin hergestellt wurden, die niedrigsten EC_{50}-Werte und für beide Strukturen konnte in weiteren Untersuchungen hauptsächlich Apoptose nachgewiesen werden. Die vom Betulin abgeleiteten Strukturen waren im Vergleich zu denen der Betulinsäure in geringem Maß zytotoxischer.

Außerdem wurde ausgehend von der acetylierten Platansäure weitere Carbonsäureamide hergestellt und anschließend zu den entsprechenden Oximen umgesetzt, wobei die Amide deutlich zytotoxischer waren und die aktivste Verbindung eine Homopiperazin-Einheit enthielt mit einem EC_{50} von 0.9 µM.

Bei der Gegenüberstellung von Betulin, Betulinsäure, Platansäure und Glycyrrhetinsäure abgeleiteten pentazyklischen Triterpen-Piperazin-Rhodamin B-Konjugate, zeigte sich, dass die Verknüpfungsposition am E-Ring das Ausmaß der Zytotoxizität bestimmt. Die Verbindungen mit veränderte Kupplungsposition des gespacerten Rhodamins waren zytotoxisch, aber signifikant weniger zytotoxisch als diejenigen, die mit dem Piperazin-Fluorophor über C-28 verknüpft sind. Färbeexperimente zeigten, dass die an C-29 verbundenen Rhodamin-B-Konjugate mit Lupan-Grundgerüst nekrotische Verbindungen sind und als Mitocane wirken. Die aktivste Verbindung, die an C-28 amidiert ist, hatte einen EC_{50}-Wert von 0.04 µM für A2780 (Zelllinie des Ovarialkarzinoms). Im Vergleich dazu, wies die aktivste Verbindung von den über C-29 verbundenen Triterpen-Rhodamin-Konjugaten eine Aktivität von 0.2 µM auf.

Bei der Synthese verschieden substituierter Maslinsäure-Rhodamin-Konjugate wurde der Einfluss der Rhodaminstruktur auf die Zytotoxizität untersucht. Die aktivste Verbindung war das Rhodamin-Konjugat mit Propylrest, welches einen EC_{50} Wert von 0,01 µM aufwies und eine Selektivität S von 15. Zudem verläuft die gemessene Zytotoxizität der Maslinsäure-Rhodamin-Konjugate parallel zu den berechneten Oktanol/Wasser-Verteilungskoeffizienten und lässt, da es sich um Mitocane handelt, auf eine Wechselwirkung mit der inneren Mitochondrienmembran schließen.

Zusammenfassend lässt sich feststellen, dass sowohl zytotoxische als auch selektive Verbindungen hergestellt wurden, wobei der Einfluss unterschiedlicher Naturstoffe als Ausgangsstoff, deren chemische Modifikationen sowie eine Variation der eingesetzten Amin-Komponente und der kationischen Struktur vorgenommen wurde.

Abschließend ist zu bemerken, dass neben einer besseren Bioverfügbarkeit, durch das Einführen von Acetylgruppen am Triterpen, auch die Wahl des Spacers von Relevanz ist, um die höchst mögliche Zytotoxizität durch die Verknüpfung von Triterpenen mit einem lipohilen Kation wie Rhodamin B zu ermöglichen. Jedoch muss für die Substitution des Triterpens auch die Selektivität berücksichtigt werden, welche sich nachweislich durch Art und Position der eingebrachten Gruppen verändert. Bei der Wahl des Triterpens für sowohl zytotoxische als auch selektive Mitocane ist neben der Anzahl möglicher Modifikationsposition, wie Hydroxygruppen, die Polarität und damit verbundene Löslichkeitsmerkmale zu berücksichtigen, um die Wirksamkeit der synthetisierten Verbindungen noch weiter optimieren zu können. Hinsichtlich der kationischen Struktureinheit sind weitere chemische Modifikationen an Rhodamin B relevante Optimierungsoptionen, um die Entwicklung optimaler Wirkstoffe voranzutreiben.

Literaturverzeichnisse

(1) Frickhofen, N. In *Onkologie für die Palliativmedizin*; Universitätsverlag Göttingen, 2015, DOI:10.17875/gup2015-850 10.17875/gup2015-850.

(2) Thieme via medici.

(3) Wagener, C.; Müller, O. *Molekulare Onkologie*; 3 ed.; Georg Thieme Verlag KG: Stuttgart, 2010.

(4) Sedlacek, H.-H. *Onkologie - Die Tumorerkrankungen des Menschen*; 2 ed.; De Gruyter: Berlin, Boston, 2021.

(5) Frickhofen, N. In *ELSEVIER ESSENTIALS Onkologie*; 2 ed.; Urban & Fischer in Elsevier, 2017.

(6) Cooper, M. R.; Cooper, M. R. In *American Cancer Society Textbook of Clinical Oncology*; Library of Congress Cataloging, 1991.

(7) Pfreundschuh, M. In *Kompendium Internistische Onkologie Standards in Diagnostik und Therapie - Teil I: Epidemiologie, Tumorbiologie, Zytostatika, Prinzipien der Tumortherapie, Supportive Maßnahmen*; 4 ed.; Springer Berlin, Heidelberg: Berlin, Germany, 2006, DOI:https://doi.org/10.1007/3-540-31303-6 https://doi.org/10.1007/3-540-31303-6.

(8) Panda, V.; Khambat, P.; Patil, S. Mitocans as Novel Agents for Anticancer Therapy: An Overview. *Int. J. Clin. Med.* **2011,** *2*, 515.

(9) Neuzil, J.; Dong, L.-F.; Rohlena, J.; Truksa, J.; Ralph, S. J. Classification of mitocans, anti-cancer drugs acting on mitochondria. *Mitochondrion* **2013,** *13* (3), 199.

(10) Godlewska-Żyłkiewicz, B.; Świsłocka, R.; Kalinowska, M.; Golonko, A.; Świderski, G.; Arciszewska, Ż.; Nalewajko-Sieliwoniuk, E.; Naumowicz, M.; Lewandowski, W. Biologically Active Compounds of Plants: Structure-Related Antioxidant, Microbiological and Cytotoxic Activity of Selected Carboxylic Acids. *Materials* **2020,** *13* (19), 4454.

(11) Zorov, D. B.; Juhaszova, M.; Sollott, S. J. Mitochondrial reactive oxygen species (ROS) and ROS-induced ROS release. *Physiol Rev* **2014,** *94* (3), 909.

(12) Fulda, S.; Kroemer, G. Mitochondria as Therapeutic Targets for the Treatment of Malignant Disease. *Antioxidants & Redox Signaling* **2011,** *15* (12), 2937.

(13) Wolfram, R. K.; Heller, L.; Csuk, R. Targeting mitochondria: Esters of rhodamine B with triterpenoids are mitocanic triggers of apoptosis. *Eur J Med Chem* **2018,** *152*, 21.

(14) The American Cancer Society *The American Cancer Society's Principles of Oncology: Prevention to Survivorship*; Wiley: Hoboken, NJ, USA, 1991.

(15) Sommerwerk, S.; Heller, L.; Kerzig, C.; Kramell, A. E.; Csuk, R. Rhodamine B conjugates of triterpenoic acids are cytotoxic mitocans even at nanomolar concentrations. *Eur J Med Chem* **2017,** *127*, 1.

(16) von Nussbaum, F.; Brands, M.; Hinzen, B.; Weigand, S.; Häbich, D. Antibakterielle Naturstoffe in der medizinischen Chemie - Exodus or Renaissance? *Angew. Chem. Int. Ed.* **2006,** *45* (31), 5072.

(17) Newman, D. J.; Cragg, G. M. Natural Products as Sources of New Drugs from 1981 to 2014. *J Nat Prod* **2016,** *79* (3), 629.

(18) Jabir, N. R.; Islam, M. T.; Tabrez, S.; Shakil, S.; Zaidi, S. K.; Khan, F. R.; Araújo, L. d. S.; de Meneses, A.-A. P. M.; Santos, J. V. d. O.; Melo-Cavalcante, A. A. d. C. An insight towards anticancer potential of major coffee constituents. *BioFactors* **2018,** *44* (4), 315.

(19) Fischer, M.; Glomb, M.; Behr's Verlag, 2015.

(20) Kamm, W.; Dionisi, F.; Fay, L. B.; Hischenhuber, C.; Schmarr, H.-G.; Engel, K.-H. Rapid and simultaneous analysis of 16-O-methylcafestol and sterols as markers for assessment of green coffee bean authenticity by on-line LC-GC. *J. Am. Oil Chem. Soc.* **2002,** *79*, 1109.

(21) Speer, K.; Kölling-Speer, I. The lipid fraction of coffee bean. *Brazilian Journal of Plant Physiology* **2006,** *18*, 201.

(22) Iwamoto, H.; Izumi, K.; Natsagdorj, A.; Naito, R.; Makino, T.; Kadomoto, S.; Hiratsuka, K.; Shigehara, K.; Kadono, Y.; Narimoto, K.et al. Coffee diterpenes kahweol acetate and cafestol synergistically inhibit the proliferation and migration of prostate cancer cells. *Prostate* **2019,** *79* (5), 468.

(23) Lima, C. S.; Spindola, D. G.; Bechara, A.; Garcia, D. M.; Palmeira-Dos-Santos, C.; Peixoto-da-Silva, J.; Erustes, A. G.; Michelin, L. F. G.; Pereira, G. J. S.; Smaili, S. S.et al. Cafestol, a diterpene molecule found in coffee, induces leukemia cell death. *Biomed. Pharmacother.* **2017,** *92*, 1045.

(24) Abotaleb, M.; Liskova, A.; Kubatka, P.; Büsselberg, D. Therapeutic Potential of Plant Phenolic Acids in the Treatment of Cancer. *Biomolecules* **2020,** *10* (2), 221.

(25) Teixeira, J.; Gaspar, A.; Garrido, E. M.; Garrido, J.; Borges, F. Hydroxycinnamic Acid Antioxidants: An Electrochemical Overview. *BioMed Research International* **2013,** *2013*, 251754.

(26) Alam, M. A.; Subhan, N.; Hossain, H.; Hossain, M.; Reza, H. M.; Rahman, M. M.; Ullah, M. O. Hydroxycinnamic acid derivatives: a potential class of natural compounds for the management of lipid metabolism and obesity. *Nutr. Metab. (Lond.)* **2016,** *13* (27), 1.

(27) Fiuza, S. M.; Gomes, C.; Teixeira, L. J.; Girão da Cruz, M. T.; Cordeiro, M. N. D. S.; Milhazes, N.; Borges, F.; Marques, M. P. M. Phenolic acid derivatives with potential anticancer properties—a structure–activity relationship study. Part 1: Methyl, propyl and octyl esters of caffeic and gallic acids. *Biorg. Med. Chem.* **2004,** *12* (13), 3581.

(28) Sirk, T. W.; Brown, E. F.; Sum, A. K.; Friedman, M. Molecular Dynamics Study on the Biophysical Interactions of Seven Green Tea Catechins with Lipid Bilayers of Cell Membranes. *Journal of Agricultural and Food Chemistry* **2008,** *56* (17), 7750.

(29) Deshmukh, P.; Unni, S.; Krishnappa, G.; Padmanabhan, B. The Keap1–Nrf2 pathway: promising therapeutic target to counteract ROS-mediated damage in cancers and neurodegenerative diseases. *Biophys. Rev.* **2017,** *9* (1), 41.

(30) Zhang, L.; Zhang, J.; Jiang, Q.; Zhang, L.; Song, W. Zinc binding groups for histone deacetylase inhibitors. *Journal of Enzyme Inhibition and Medicinal Chemistry* **2018,** *33* (1), 714.

(31) Journal Club. Triterpene - eine vielversprechende und biologisch hochinteressante pflanzliche Stoffklasse. *Complementary Medicine Research* **2015,** *22* (5), 326.

(32) Wüst, M. In *Springer Handbook of Odor*; Springer International Publishing: Cham, Switzerland, 2017.

(33) Csuk, R. Betulinic acid and its derivatives: a patent review (2008 – 2013). *Expert Opin. Ther. Pat.* **2014,** *24* (8), 913.

(34) Pathak, A. K.; Bhutani, M.; Nair, A. S.; Ahn, K. S.; Chakraborty, A.; Kadara, H.; Guha, S.; Sethi, G.; Aggarwal, B. B. Ursolic Acid Inhibits STAT3 Activation Pathway Leading to Suppression of Proliferation and Chemosensitization of Human Multiple Myeloma Cells. *Mol. Cancer Res.* **2007,** *5* (9), 943.

(35) Lin, C.; Wen, X.; Sun, H. Oleanolic acid derivatives for pharmaceutical use: a patent review. *Expert Opin. Ther. Pat.* **2016,** *26* (6), 643.

(36) Hussain, H.; Green, I. R.; Ali, I.; Khan, I. A.; Ali, Z.; Al-Sadi, A. M.; Ahmed, I. Ursolic acid derivatives for pharmaceutical use: a patent review (2012-2016). *Expert Opin. Ther. Pat.* **2017,** *27* (9), 1061.
(37) Zhang, X.; Hu, J.; Chen, Y. Betulinic acid and the pharmacological effects of tumor suppression (Review). *Mol Med Rep* **2016,** *14* (5), 4489.
(38) Damle, A. A.; Pawar, Y. P.; Narkar, A. A. Anticancer activity of betulinic acid on MCF-7 tumors in nude mice. *Indian J. Exp. Biol.* **2013,** *51* (7), 485.
(39) Mullauer, F. B.; van Bloois, L.; Daalhuisen, J. B.; Ten Brink, M. S.; Storm, G.; Medema, J. P.; Schiffelers, R. M.; Kessler, J. H. Betulinic acid delivered in liposomes reduces growth of human lung and colon cancers in mice without causing systemic toxicity. *Anti-Cancer Drugs* **2011,** *22* (3), 223.
(40) Fulda, S.; Galluzzi, L.; Kroemer, G. Targeting mitochondria for cancer therapy. *Nature Reviews Drug Discovery* **2010,** *9* (6), 447.
(41) Spivak, A. Y.; Nedopekina, D. A.; Gubaidullin, R. R.; Dubinin, M. V.; Belosludtsev, K. N. Conjugation of Natural Triterpenic Acids with Delocalized Lipophilic Cations: Selective Targeting Cancer Cell Mitochondria. *Journal of Personalized Medicine* **2021,** *11* (6), 470.
(42) Grymel, M.; Zawojak, M.; Adamek, J. Triphenylphosphonium Analogues of Betulin and Betulinic Acid with Biological Activity: A Comprehensive Review. *Journal of Natural Products* **2019,** *82* (6), 1719.
(43) Molina, J. R.; Sun, Y.; Protopopova, M.; Gera, S.; Bandi, M.; Bristow, C.; McAfoos, T.; Morlacchi, P.; Ackroyd, J.; Agip, A.-N. A.et al. An inhibitor of oxidative phosphorylation exploits cancer vulnerability. *Nat. Med.* **2018,** *24* (7), 1036.
(44) Panina, S. B.; Pei, J.; Kirienko, N. V. Mitochondrial metabolism as a target for acute myeloid leukemia treatment. *Cancer & Metabolism* **2021,** *9* (1), 17.
(45) Zampieri, L. X.; Grasso, D.; Bouzin, C.; Brusa, D.; Rossignol, R.; Sonveaux, P. Mitochondria Participate in Chemoresistance to Cisplatin in Human Ovarian Cancer Cells. *Mol. Cancer Res.* **2020,** *18* (9), 1379.
(46) Faubert, B.; Solmonson, A.; DeBerardinis, R. J. Metabolic reprogramming and cancer progression. *Science* **2020,** *368* (6487), eaaw5473.
(47) Krasutsky, P. A. Birch bark research and development. *Natural Product Reports* **2006,** *23* (6), 919.
(48) Safe, S.; Kasiappan, R. Natural Products as Mechanism-based Anticancer Agents: Sp Transcription Factors as Targets. *Phytother. Res.* **2016,** *30* (11), 1723.
(49) Ríos, J. L.; Máñez, S. New Pharmacological Opportunities for Betulinic Acid. *Planta Med.* **2018,** *84* (01), 8.
(50) Bildziukevich, U.; Özdemir, Z.; Wimmer, Z. Recent Achievements in Medicinal and Supramolecular Chemistry of Betulinic Acid and Its Derivatives (‡). *Molecules* **2019,** *24* (19), 3546.
(51) Moghaddam, M. G.; Ahmad, F. B. H.; Samzadeh-Kermani, A. Biological Activity of Betulinic Acid: A Review. *Pharmacology & Pharmacy* **2012,** *3* (2), 119.
(52) Csuk, R.; Schmuck, K.; Schäfer, R. A practical synthesis of betulinic acid. *Tetrahedron Letters* **2006,** *47* (49), 8769.
(53) Sarek, J.; Kvasnica, M.; Vlk, M.; Urban, M.; Dzubak, P.; Hajduch, M. In *Research on Melanoma - A Glimpse into Current Directions and Future Trends*; IntechOpen: Croatia, 2011, DOI:10.5772/19582 10.5772/19582.
(54) Pisha, E.; Chai, H.; Lee, I.-S.; Chagwedera, T. E.; Farnsworth, N. R.; Cordell, G. A.; Beecher, C. W. W.; Fong, H. H. S.; Kinghorn, A. D.; Brown, D. M.et al. Discovery of

betulinic acid as a selective inhibitor of human melanoma that functions by induction of apoptosis. *Nat. Med.* **1995,** *1* (10), 1046.

(55) Fulda, S. Betulinic Acid for Cancer Treatment and Prevention. *Int. J. Mol. Sci.* **2008,** *9* (6), 1096.

(56) Hordyjewska, A.; Ostapiuk, A.; Horecka, A. Betulin and betulinic acid in cancer research. *Journal of Pre-Clinical and Clinical Research* **2018,** *12* (2), 72.

(57) Fulda, S.; Kroemer, G. Targeting mitochondrial apoptosis by betulinic acid in human cancers. *Drug Discovery Today* **2009,** *14* (17), 885.

(58) Zhao, H.; Liu, Z.; Liu, W.; Han, X.; Zhao, M. Betulin attenuates lung and liver injuries in sepsis. *Int. Immunopharmacol.* **2016,** *30*, 50.

(59) Ghaffari Moghaddam, M.; Ahmad, B. H. F.; Samzadeh-Kermani, A. *Biological activity of betulinic acid: a review. Pharmacol. Pharm* **2012,** *3*, 119.

(60) Zhao, H.; Zheng, Q.; Hu, X.; Shen, H.; Li, F. Betulin attenuates kidney injury in septic rats through inhibiting TLR4/NF-κB signaling pathway. *Life Sciences* **2016,** *144*, 185.

(61) Jonnalagadda, S. C.; Suman, P.; Morgan, D. C.; Seay, J. N. In *Studies in Natural Products Chemistry*; Atta ur, R., Ed.; Elsevier, 2017; Vol. 53.

(62) Kim, E.-C.; Lee, H.-S.; Kim, S. K.; Choi, M.-S.; Lee, S.; Han, J.-B.; An, H.-J.; Um, J.-Y.; Kim, H.-M.; Lee, N.-Y.et al. The bark of Betula platyphylla var. japonica inhibits the development of atopic dermatitis-like skin lesions in NC/Nga mice. *J. Ethnopharmacol.* **2008,** *116* (2), 270.

(63) Alakurtti, S.; Mäkelä, T.; Koskimies, S.; Yli-Kauhaluoma, J. Pharmacological properties of the ubiquitous natural product betulin. *Eur. J. Pharm. Sci.* **2006,** *29* (1), 1.

(64) Baltina, L. A.; Flekhter, O. B.; Nigmatullina, L. R.; Boreko, E. I.; Pavlova, N. I.; Nikolaeva, S. N.; Savinova, O. V.; Tolstikov, G. A. Lupane triterpenes and derivatives with antiviral activity. *Bioorg. Med. Chem. Lett.* **2003,** *13* (20), 3549.

(65) Dang, Z.; Qian, K.; Ho, P.; Zhu, L.; Lee, K.-H.; Huang, L.; Chen, C.-H. Synthesis of betulinic acid derivatives as entry inhibitors against HIV-1 and bevirimat-resistant HIV-1 variants. *Bioorg. Med. Chem. Lett.* **2012,** *22* (16), 5190.

(66) Bori, I. D.; Hung, H.-Y.; Qian, K.; Chen, C.-H.; Morris-Natschke, S. L.; Lee, K.-H. Anti-AIDS agents 88. Anti-HIV conjugates of betulin and betulinic acid with AZT prepared via click chemistry. *Tetrahedron Letters* **2012,** *53* (15), 1987.

(67) Yi, J.; Zhu, R.; Wu, J.; Wu, J.; Xia, W.; Zhu, L.; Jiang, W.; Xiang, S.; Tan, Z. In vivo protective effect of betulinic acid on dexamethasone induced thymocyte apoptosis by reducing oxidative stress. *Pharmacol. Rep.* **2016,** *68* (1), 95.

(68) Dangroo, N. A.; Singh, J.; Rath, S. K.; Gupta, N.; Qayum, A.; Singh, S.; Sangwan, P. L. A convergent synthesis of novel alkyne–azide cycloaddition congeners of betulinic acid as potent cytotoxic agent. *Steroids* **2017,** *123*, 1.

(69) Boryczka, S.; Bębenek, E.; Wietrzyk, J.; Kempińska, K.; Jastrzębska, M.; Kusz, J.; Nowak, M. Synthesis, Structure and Cytotoxic Activity of New Acetylenic Derivatives of Betulin. *Molecules* **2013,** *18* (4), 4526.

(70) Yamashita, K.; Lu, H.; Lu, J.; Chen, G.; Yokoyama, T.; Sagara, Y.; Manabe, M.; Kodama, H. Effect of three triterpenoids, lupeol, betulin, and betulinic acid on the stimulus-induced superoxide generation and tyrosyl phosphorylation of proteins in human neutrophils. *Clin. Chim. Acta* **2002,** *325* (1), 91.

(71) De Benedetto, A.; Agnihothri, R.; McGirt, L. Y.; Bankova, L. G.; Beck, L. A. Atopic Dermatitis: A Disease Caused by Innate Immune Defects? *J. Invest. Dermatol.* **2009,** *129* (1), 14.

(72) Weckesser, S.; Laszczyk, M. N.; Müller, M. L.; Schempp, C. M.; Schumann, H. Topical Treatment of Necrotising Herpes Zoster with Betulin from Birch Bark. *Complementary Medicine Research* **2010,** *17* (5), 271.
(73) Aplin, R. T.; Halsall, T. G.; Norin, T. 607. The chemistry of triterpenes and related compounds. Part XLIII. The constituents of the bark of Platanus x hybrida Brot. and the structure of platanic acid. *Journal of the Chemical Society (Resumed)* **1963**, DOI:10.1039/JR9630003269 10.1039/JR9630003269(0), 3269.
(74) Mayer, R. Three Lupane Derivatives from Leptospermum scoparium. *Arch. Pharm.* **1996,** *329* (10), 447.
(75) Lunardi, I.; Peixoto, J. L. B.; Silva, C. C. d.; Shuquel, I. T. A.; Basso, E. A.; Vidotti, G. J. Triterpenic acids from Eugenia moraviana. *J. Braz. Chem. Soc.* **2001,** *12*, 180.
(76) Lee, C.-K. A New Norlupene from the Leaves of Melaleuca leucadendron. *Journal of Natural Products* **1998,** *61* (3), 375.
(77) Bildziukevich, U.; Malík, M.; Özdemir, Z.; Rárová, L.; Janovská, L.; Šlouf, M.; Šaman, D.; Šarek, J.; Nonappa; Wimmer, Z. Spermine amides of selected triterpenoid acids: dynamic supramolecular system formation influences the cytotoxicity of the drugs. *Journal of Materials Chemistry B* **2020,** *8* (3), 484.
(78) Fujioka, T.; Kashiwada, Y.; Kilkuskie, R. E.; Cosentino, L. M.; Ballas, L. M.; Jiang, J. B.; Janzen, W. P.; Chen, I. S.; Lee, K. H. Anti-AIDS agents, 11. Betulinic acid and platanic acid as anti-HIV principles from Syzigium claviflorum, and the anti-HIV activity of structurally related triterpenoids. *J Nat Prod* **1994,** *57* (2), 243.
(79) Heller, L.; Kahnt, M.; Loesche, A.; Grabandt, P.; Schwarz, S.; Brandt, W.; Csuk, R. Amino derivatives of platanic acid act as selective and potent inhibitors of butyrylcholinesterase. *Eur. J. Med. Chem.* **2017,** *126*, 652.
(80) Davies, P.; Maloney, A. J. Selective loss of central cholinergic neurons in Alzheimer's disease. *Lancet* **1976,** *2* (8000), 1403.
(81) Baratto, L. C.; Porsani, M. V.; Pimentel, I. C.; Pereira Netto, A. B.; Paschke, R.; Oliveira, B. H. Preparation of betulinic acid derivatives by chemical and biotransformation methods and determination of cytotoxicity against selected cancer cell lines. *Eur. J. Med. Chem.* **2013,** *68*, 121.
(82) Abdel Bar, F. M.; Zaghloul, A. M.; Bachawal, S. V.; Sylvester, P. W.; Ahmad, K. F.; El Sayed, K. A. Antiproliferative Triterpenes from Melaleuca ericifolia. *Journal of Natural Products* **2008,** *71* (10), 1787.
(83) Sommerwerk, S.; Heller, L.; Csuk, R. Synthesis and cytotoxic activity of pentacyclic triterpenoid sulfamates. *Arch. Pharm. (Weinheim)* **2015,** *348* (1), 46.
(84) Kim, J. Y.; Koo, H.-M.; Kim, D. S. H. L. Development of C-20 modified betulinic acid derivatives as antitumor agents. *Bioorg. Med. Chem. Lett.* **2001,** *11* (17), 2405.
(85) Schwarz, S.; Sommerwerk, S.; Lucas, S. D.; Heller, L.; Csuk, R. Sulfamates of methyl triterpenoates are effective and competitive inhibitors of carbonic anhydrase II. *Eur J Med Chem* **2014,** *86*, 95.
(86) Sączewski, J.; Kędzia, A.; Jalińska, A. New derivatives of 4,6-dimethylisoxazolo[3,4-b] pyridin-3(1H)-one: synthesis, tautomerism, electronic structure and antibacterial activity. *Heterocycl. Commun.* **2014,** *20* (4), 215.
(87) Bauer, L.; Nambury, C. N. V. Synthesis of Aminoisoxazolones from α-Cyano Esters and Hydroxylamine1. *The Journal of Organic Chemistry* **1961,** *26* (12), 4917.
(88) Sączewski, J.; Hinc, K.; Obuchowski, M.; Gdaniec, M. The Tandem Mannich–Electrophilic Amination Reaction: a Versatile Platform for Fluorescent Probing and Labeling. *Chemistry – A European Journal* **2013,** *19* (35), 11531.

(89) Fedorowicz, J.; Cebrat, M.; Wierzbicka, M.; Wiśniewska, P.; Jalińska, A.; Dziomba, S.; Gdaniec, M.; Jaremko, M.; Jaremko, Ł.; Chandra, K. Synthesis and evaluation of dihydro-[1, 2, 4] triazolo [4, 3-a] pyridin-2-ium carboxylates as fixed charge fluorescent derivatization reagents for MEKC and MS proteomic analyses. *J. Mol. Struct.* **2020,** *1217*, 128426.

(90) Fedorowicz, J.; Sączewski, J.; Drażba, Z.; Wiśniewska, P.; Gdaniec, M.; Wicher, B.; Suwiński, G.; Jalińska, A. Synthesis and fluorescence of dihydro-[1, 2, 4] triazolo [4, 3-a] pyridin-2-ium-carboxylates: An experimental and TD-DFT comparative study. *Dyes and Pigments* **2019,** *161*, 347.

(91) Cebrat, M.; Wierzbicka, M.; Saczewski, J.; Szewczuk, Z. Study on the application of Safirinium P derivatives as signal enhancers in mass spectrometric evaluation of peptides. *J. Pept. Sci.* **2016,** *22*, S98.

(92) Ciura, K.; Fedorowicz, J.; Andrić, F.; Greber, K. E.; Gurgielewicz, A.; Sawicki, W.; Sączewski, J. Lipophilicity determination of quaternary (fluoro) quinolones by chromatographic and theoretical approaches. *Int. J. Mol. Sci.* **2019,** *20* (21), 5288.

(93) Fedorowicz, J.; Sączewski, J. Modifications of quinolones and fluoroquinolones: hybrid compounds and dual-action molecules. *Monatshefte für Chemie-Chemical Monthly* **2018,** *149* (7), 1199.

(94) Fedorowicz, J.; Sączewski, J.; Konopacka, A.; Waleron, K.; Lejnowski, D.; Ciura, K.; Tomašič, T.; Skok, Ž.; Savijoki, K.; Morawska, M. Synthesis and biological evaluation of hybrid quinolone-based quaternary ammonium antibacterial agents. *Eur. J. Med. Chem.* **2019,** *179*, 576.

(95) Friedrich, S.; Serbian, I.; Hoenke, S.; Wolfram, R. K.; Csuk, R. Synthesis and cytotoxic evaluation of malachite green derived oleanolic and ursolic acid piperazineamides. *Med. Chem. Res.* **2020,** *29* (5), 926.

(96) Kahnt, M.; Fischer Née Heller, L.; Al-Harrasi, A.; Csuk, R. Ethylenediamine Derived Carboxamides of Betulinic and Ursolic Acid as Potential Cytotoxic Agents. *Molecules* **2018,** *23* (10), 2558.

(97) Kahnt, M.; Hoenke, S.; Fischer, L.; Al-Harrasi, A.; Csuk, R. Synthesis and Cytotoxicity Evaluation of DOTA-Conjugates of Ursolic Acid. *Molecules* **2019,** *24* (12), 2254.

(98) Wiemann, J.; Heller, L.; Csuk, R. Targeting cancer cells with oleanolic and ursolic acid derived hydroxamates. *Bioorg Med Chem Lett* **2016,** *26* (3), 907.

(99) Wolfram, R. K.; Fischer, L.; Kluge, R.; Ströhl, D.; Al-Harrasi, A.; Csuk, R. Homopiperazine-rhodamine B adducts of triterpenoic acids are strong mitocans. *Eur. J. Med. Chem.* **2018,** *155*, 869.

Abbildungsverzeichnis

Abbildung 1: Überblick Apoptose[2] 1
Abbildung 2: verschiedene Zytostatika 4
Abbildung 3: Beispiele für bioaktive Inhaltsstoffe in Kaffee 6
Abbildung 4: Wirkorte der Zimtsäuren[24] 7
Abbildung 5: Zimtsäure-Grundgerüst mit verschiedenen Substitutionsmustern 8
Abbildung 6: Überblick der Terpenoidskelette, welche durch Addition von Isopreneinheiten gebildet werden[32] 9
Abbildung 7: Strukturformel pentazyklischer Triterpen-Grundgerüste 10
Abbildung 8: wichtigste funktionelle Gruppen für chemische Modifikationen 12
Abbildung 9: Hydroxyzimtsäure-Rhodamin-Konjugate 15
Abbildung 10: Übersicht der Synthese von Safirinium P 16
Abbildung 11: Übersichtsstruktur des Safirinium P-Konjugates der acetylierten Betulinsäure mit Piperazin-Spacer (R^1 und R^2 = Ethyl-/Hexyl-/Dodecylest) 17
Abbildung 12: Selektivitätsfaktoren unterschiedlich substituierter Benzylamide der Betulinsäure für die Zelllinie A375 (**links**) und für die Zelllinie A2780 (**rechts**) 18
Abbildung 13: Syntheseüberblick der Betulinsäure-Konjugate 19
Abbildung 14: EC_{50}-Werte der Betulin- und Betulinsäurekonjugate für MCF-7 (**links**) und HT29 (**rechts**) in [µM] 20
Abbildung 15: FACS-Untersuchungen von der Kontrolle (**links**; als Vergleich), Betulinsäure-Konjugat mit Methylpiperazin (**Mitte**) und Betulinsäure-Konjugat mit Ethylendiamin (**rechts**) für A375; (R1 = nekrotisch, R2 = sekundär nekrotisch/spätapoptotisch, R3 = vital und R4 = apoptotisch) 20
Abbildung 16: Syntheseübersicht Platansäure-Konjugate 21
Abbildung 17: Vergleich der Triterpen-Piperazin-Rhodamin-Konjugate mit EC_{50}-Werten in [µM] für A2780 22
Abbildung 18: Überblick Synthese der Rhodamine 23
Abbildung 19: Reaktionsschema für die Maslinsäure-Rhodamin-Konjugate 23

Anhang

Publikationen

Es folgt eine Auflistung der für diese Arbeit relevanten Publikationen (P-1 bis P-7).

P-1: **Synthesis and cytotoxic evaluation of hydroxycinnamic acid rhodamine B conjugates**

Marie Kozubek, Immo Serbian, Sophie Hoenke, Oliver Kraft, René Csuk *Results in Chemistry* **2020**, 10005, 2211-7156

P-2: **Cytotoxic triterpenoid-safirinium conjugates target the endoplasmic reticulum**

Oliver Kraft, Marie Kozubek, Sophie Hoenke, Immo Serbian, Daniel Major, René Csuk *Eur. J. Med. Chem.* **2021**, 209, 112920

P-3: **Apoptotic activity of substituted 3-*O*-acetyl-betulinic acid benzylamides**

Marie Kozubek, Linda Höhlich, Sophie Hoenke, Hans-Peter Deigner, Ahmed Al-Harrasi, René Csuk *EJMECH Reports* **2021**, 100016, 2772-4174

P-4: **Synthesis and cytotoxicity of betulin and betulinic acid derived 30-oxo-amides**

Marie Kozubek, Sophie Hoenke, Theresa Schmidt, Hans-Peter Deigner, Ahmed Al-Harrasi, René Csuk *Steroids* **2022**, 109014, 0039-128X

P-5: **Platanic acid derived amides are more cytotoxic than their corresponding oximes**

Marie Kozubek, Sophie Hoenke, Theresa Schmidt, Dieter Ströhl, René Csuk

Med Chem Res **2022**, 1554-8120

P-6: **Betulinic acid and glycyrrhetinic acid derived piperazinyl spacered rhodamine B conjugates are highly cytotoxic and necrotic**

Marie Kozubek, Sophie Hoenke, Hans-Peter Deigner, René Csuk *Results in Chemistry* **2022**, 100429, 2211-7156

P-7: **On the influence of the rhodamine substituents onto the cytotoxicity of mitocanic maslinic acid rhodamine conjugates**

Marie Kozubek, Toni C. Denner, Marc Eckert, Sophie Hoenke, René Csuk *Results in Chemistry* **2023**, 100708

Publikation P-1: **Synthesis and cytotoxic evaluation of hydroxycinnamic acid rhodamine B conjugates**

Marie Kozubek, Immo Serbian, Sophie Hoenke, Oliver Kraft, René Csuk *Results in Chemistry* **2020**, 10005, 2211-7156

Abstract

Four different hydroxycinnamic acid rhodamine B conjugates have been prepared and screened for their cytotoxic activity. In the sulforhodamine B (SRB) assay the majority of the conjugates displayed good cytotoxicity in the low µM range for different human tumor cell lines. Low EC50 values were obtained especially for an apoptose-triggering cinnamic acid rhodamine conjugate 3 holding a piperazinyl spacer and a cinnamoyl moiety.

Keywords: **Hydroxycinnamic acid, Amides, Rhodamine B, Cytotoxicity**

DOI: **10.1016/j.rechem.2020.100057**

Link: **https://doi.org/10.1016/j.rechem.2020.100057**

Publikation P-2: **Cytotoxic triterpenoid-safirinium conjugates target the endoplasmic reticulum**

Oliver Kraft, Marie Kozubek, Sophie Hoenke, Immo Serbian, Daniel Major, René Csuk *Eur. J. Med. Chem.* **2021**, 209, 112920

Abstract

Safirinium P and Q fluorescence labels were synthesized and conjugated with spacered triterpenoic acids to access hybrid structures. While the parent safirinium compounds were not cytotoxic at all, many triterpenoid safirinium P and Q conjugates showed moderate cytotoxicity. An exception, however, was safirinium P derived compound 30 holding low EC_{50} = 5.4 mM (for A375 cells) to EC_{50} = 7.5 mM (for FaDu cells) as well as EC_{50} = 6.6 mM for non-malignant fibroblasts NIH 3T3. Fluorescence imaging showed that the safirinium core structures cannot enter the cells (not even after a prolonged incubation time of 24 h), while the conjugates (as exemplified for 30) are accumulating in the endoplasmic reticulum but not in the mitochondria. The development of safirinium-hybrids targeting the endoplasmic reticulum can be regarded as a promising strategy in the development of cytotoxic agents.

Keywords: ***Betulinic acid, Safirinium, Cytotoxicity, Endoplasmic reticulum***

DOI: **10.1016/j.ejmech.2020.112920**

Link: **https://doi.org/10.1016/j.ejmech.2020.112920**

Publikation P-3: **Apoptotic activity of substituted 3-*O*-acetyl-betulinic acid benzylamides**

Marie Kozubek, Linda Höhlich, Sophie Hoenke, Hans-Peter Deigner, Ahmed Al-Harrasi, René Csuk *EJMECH Reports* **2021**, 100016, 2772-4174

Abstract

Acetylated betulinic acid (**BA**) was converted into mono-substituted benzylamides **2–14**. Screening in SRB assays showed them as cytotoxic for a variety of different human tumor cell lines. While parent **BA** was not cytotoxic within the limits of the assay (cut-off 30 µM), the target amides were cytotoxic. Their bioactivity as well as their tumor cell/non-tumor cell selectivity depended on the substitution pattern of the aromatic ring. The most active compound 9 (holding an ortho methoxy substituent) acted mainly by apoptosis.

Keywords: **Betulinic acid, Benzylamides, Cytotoxicity, SRB assay**

DOI: **10.1016/j.ejmcr.2021.100016**

Link: **https://doi.org/10.1016/j.ejmcr.2021.100016**

Publikation P-4: **Synthesis and cytotoxicity of betulin and betulinic acid derived 30-oxo-amides**

Marie Kozubek, Sophie Hoenke, Theresa Schmidt, Hans-Peter Deigner, Ahmed Al-Harrasi, René Csuk *Steroids* **2022** 109014,0039-128X

Abstract

Betulin and betulinic acid derived 30-oxo-amides were prepared by hydroboration, subsequent oxidation and amidation; these novel compounds were screened for their cytotoxic activity by SRB assays. All of the compounds showed significant cytotoxic activity for different human tumor cell lines. Small changes in the structure, however, resulted in significant changes in the cytotoxicity of the compounds. Of special interest were compounds **11** and **12**, each holding an extra ethylenediamine moiety. These C-30 amides which showed low EC_{50} values, and both of them acted mainly by apoptosis.

Keywords: **Betulin, Betulinic acid, Cytotoxicity**

DOI: **10.1016/j.steroids.2022.109014**

Link: **https://doi.org/10.1016/j.steroids.2022.109014**

Publikation P-5: **Platanic acid derived amides are more cytotoxic than their corresponding oximes**

Marie Kozubek, Sophie Hoenke, Theresa Schmidt, Dieter Ströhl, René Csuk *Med Chem Res* **2022**, 1554-8120

Abstract

Albeit platanic acid has been known since 1956, its potential to act as a valuable starting material for the synthesis of cytotoxic agents has been neglected for many years. Hereby we describe the synthesis of a small library of amides and oximes derived from 3-O-acetyl-platanic acid, and the results of their screening as cytotoxic agents for several human tumor cell lines. As a result, while the cytotoxicity of the oximes was diminished as compared to the parent amides, the homopiperazinyl amide **5** held the highest cytoxicity (EC50 =0.9 µM for A375 human melanoma cells). Extra FACS and

cell cycle measurements showed compound **5** to act onto A375 cells rather by apoptosis than by necrosis.

Keywords: **Platanic acid, cytotoxicity, SRB assay**

DOI: **10.1007/s00044-022-02902-1**

Link: **https://doi.org/10.1007/s00044-022-02902-1**

P-6: **Betulinic acid and glycyrrhetinic acid derived piperazinyl spacered rhodamine B conjugates are highly cytotoxic and necrotic**

Marie Kozubek, Sophie Hoenke, Hans-Peter Deigner, René Csuk *Results in Chemistry* **2022**, 100429, 2211-7156

Abstract

Pentacyclic triterpene-piperazine-rhodamine B conjugates with ursane or oleanane backbones have been shown in the past to be highly cytotoxic thereby acting as mitocans. Starting from betulinic acid or glycyrrhetinic acid, new analogues were now made available, and their cytotoxic activity was investigated employing several human tumor cell lines [A375 (melanoma), HT29 (colorectal carcinoma), MCF-7 (breast adenocarcinoma), A2780 (ovarian carcinoma), and for comparison NIH 3T3 (non-malignant fibroblasts)]. For these conjugates it has been established that the linking position at ring E governs the magnitude of cytotoxicity. These conjugates were still highly cytotoxic but significantly less cytotoxic than those holding an oleanane skeleton. Staining experiments showed the rhodamine B conjugates as necrotic compounds and to act as mitocans. The most active compound (8) held an EC50 = 0.04 µM for A2780 ovarian carcinoma cells.

Keywords: **Betulin, Betulinic acid, Glycyrrhetinic acid, Cytotoxicity, Rhodamine B conjugates**

DOI: **10.1016/j.rechem.2022.100429**

Link: **https://doi.org/10.1016/j.rechem.2022.100429**

P-7: **On the influence of the rhodamine substituents onto the cytotoxicity of mitocanic maslinic acid rhodamine conjugates**

Marie Kozubek, Toni C. Denner, Marc Eckert, Sophie Hoenke, René Csuk *Results in Chemistry* **2023**, 100708

Abstract

Maslinic acid was converted via a di-acetylated piperazinyl amide into rhodamine conjugates differing in their alkyl moieties. These conjugates were submitted to cytotoxicity assays employing a panel of human tumor cell lines. These conjugates held high cytotoxicity but also some selectivity especially for A2780 cells. Thereby, a propyl substituted rhodamine conjugate showed EC50 values as low as EC50 = 0.01 µM and was approx. 15 times more cytotoxic for the cancer cells than for non-malignant fibroblasts (NIH 3 T3). Cytotoxicity obviously parallels the lipophilicity of the residue and suggests - since the compounds act as mitocanes - an interaction of the conjugates with the inner mitochondrial membrane.

Keywords: **Maslinic acid, Mitocans, Rhodamine, Cytotoxicity**

DOI: **10.1016/j.rechem.2022.100708**

Link: **https://doi.org/10.1016/j.rechem.2022.100708**

Erklärung zu den Autorenanteilen der Publikationen

Die Dissertation beruht auf sieben Publikationen, wobei in sechs Arbeiten der Schwerpunkt auf der Zytotoxizität der Triterpenkonjugate liegt und in einer Publikation stehen zytotoxische Eigenschaften von Hydroxyzimtsäurederivaten im Vordergrund. Die Manuskripte wurden in Zusammenarbeit mit allen Koautoren verfasst. Prof. Dr. René Csuk betreute zusätzlich die Arbeit und stand für fachliche Diskussionen zur Verfügung. Im Folgenden sollen die Anteile der Autoren an den durchgeführten Synthesen und der biologischen Evaluierung der Derivate näher erläutert werden.

1. "Synthesis and cytotoxic evaluation of hydroxycinnamic acid rhodamine B conjugates"

Marie Kozubek, Immo Serbian, Sophie Hoenke, Oliver Kraft, René Csuk *Results in Chemistry* **2020**, 10005, 2211-7156

Die Synthese wurde von mir durchgeführt und die Auswertung der spektroskopischen Daten wurde von mir vorgenommen. Die Bestimmung der EC_{50}-Werte und weitere zytotoxische Untersuchungen wurde von S. Hoenke durchgeführt. R. Csuk betreute praktische sowie theoretische Aspekte der Arbeit.

2. "Cytotoxic triterpenoid-safirinium conjugates target the endoplasmic reticulum"

Oliver Kraft, Marie Kozubek, Sophie Hoenke, Immo Serbian, Daniel Major, René Csuk *Eur. J. Med. Chem.* **2021**, 209, 112920

Die Synthese aller Konjugate ist in Zusammenarbeit mit O.Kraft, I.Serbian, D.Major und mir entstanden, wobei ich für die Safirinium P Konjugate zuständig war und hierfür auch die spektroskopische Auswertung übernommen habe. O.Kraft war für die Safirinium Q Konjugate verantwortlich, welche nicht Teil dieser Arbeit sind. Die Bestimmung der EC_{50}-Werte und weitere zytotoxische Untersuchungen wurde von S. Hoenke durchgeführt. R. Csuk betreute praktische sowie theoretische Aspekte der Arbeit.

3. "Apoptotic activity of substituted 3-*O*-acetyl-betulinic acid benzylamides"

Marie Kozubek, Linda Höhlich, Sophie Hoenke, Hans-Peter Deigner, Ahmed Al-Harrasi, René Csuk *EJMECH Reports* **2021**, 100016, 2772-4174

Die Synthesen und die Auswertung der spektroskopischen Daten wurden im Rahmen einer von mir betreuten Vertiefungsarbeit von L. Höhlich durchgeführt. Die Bestimmung der EC_{50}-Werte und weitere zytotoxische Untersuchungen wurde von S. Hoenke durchgeführt. R. Csuk betreute praktische sowie theoretische Aspekte der Arbeit.

4. “Synthesis and cytotoxicity of betulin and betulinic acid derived 30-oxo-amides”

Marie Kozubek, Sophie Hoenke, Theresa Schmidt, Hans-Peter Deigner, Ahmed Al-Harrasi, René Csuk *Steroids* **2022** 109014,0039-128X

Die Synthese wurde von mir durchgeführt und die Auswertung der spektroskopischen Daten wurde auch von mir vorgenommen. Die Bestimmung der EC_{50}-Werte und weitere zytotoxische Untersuchungen wurde von S. Hoenke durchgeführt. D. Ströhl führte weitere NMR-Experimente an den Verbindungen durch. R. Csuk betreute praktische sowie theoretische Aspekte der Arbeit.

5. “Platanic acid derived amides are more cytotoxic than their corresponding oximes”

Marie Kozubek, Sophie Hoenke, Theresa Schmidt, Dieter Ströhl, René Csuk *Med Chem Res* **2022**, 1554-8120

Die Synthese wurde von mir durchgeführt und die Auswertung der spektroskopischen Daten wurde auch von mir vorgenommen. Die Bestimmung der EC_{50}-Werte und weitere zytotoxische Untersuchungen wurde von S. Hoenke durchgeführt. R. Csuk betreute praktische sowie theoretische Aspekte der Arbeit.

6. “Betulinic acid and glycyrrhetinic acid derived piperazinyl spacered rhodamine B conjugates are highly cytotoxic and necrotic”

Marie Kozubek, Sophie Hoenke, Hans-Peter Deigner, René Csuk *Results in Chemistry* **2022**, 100429, 2211-7156

Die Synthese wurde von mir durchgeführt und die Auswertung der spektroskopischen Daten wurde auch von mir vorgenommen. Die Bestimmung der EC_{50}-Werte und weitere zytotoxische Untersuchungen wurde von S. Hoenke durchgeführt. R. Csuk betreute praktische sowie theoretische Aspekte der Arbeit.

7. “**On the influence of the rhodamine substituents onto the cytotoxicity of mitocanic maslinic acid rhodamine conjugates”**

Marie Kozubek, Toni C. Denner, Marc Eckert, Sophie Hoenke, René Csuk *Results in Chemistry* **2023**, 100708

Die Synthese der Vorstufen ist in Zusammenarbeit mit T. C. Denner erfolgt, wobei die Synthese der Konjugate und die Auswertung der spektroskopischen Daten im Rahmen einer von mir betreuten Diplomarbeit von M. Eckert durchgeführt wurde. Die Bestimmung der EC50-Werte und weitere zytotoxische Untersuchungen wurde von S. Hoenke durchgeführt. R. Csuk betreute praktische sowie theoretische Aspekte der Arbeit.

Lebenslauf

Persönliche Angaben

Name:	Marie Christine Renate Kozubek
Staatsangehörigkeit:	Deutsch

Bildungsweg

Seit 08/2019	Promotionsstudium am Institut für Chemie im Bereich Organische Chemie, Martin-Luther-Universität Halle-Wittenberg unter der Leitung von Prof. René Csuk
04/2019	Abschluss als **Diplom-Lebensmittelchemikerin** (Dipl.-LMChem)
10/2014 - 04/2019	Lebensmittelchemiestudium an der Martin-Luther-Universität Halle-Wittenberg
09/2005 - 07/2013	Abitur Evangelisches Gymnasium Mühlhausen

Berufserfahrung

Seit 08/2019	Wissenschaftliche Mitarbeiterin Organische Chemie Martin-Luther-Universität Halle-Wittenberg
06/2019 - 07/2019	Wissenschaftliche Hilfskraft Organische Chemie
02/2018	Praktikum am Institut für Lebensmittelhygiene an der Veterinärmedizinischen Fakultät der Universität Leipzig
08/2017	Praktikum im Physiologisch-Chemischen Institut der Veterinärmedizinischen Fakultät der Universität Leipzig

Selbstständigkeitserklärung

Hiermit erkläre ich an Eides statt, dass ich die vorliegende Arbeit selbstständig und nur unter Zuhilfenahme der angegebenen Quellen und Hilfsmittel verfasst habe. Die aus den benutzten Werken wörtlich oder inhaltlich entnommenen Stellen wurden als solche kenntlich gemacht. Die Arbeit wurde bisher an keiner anderen Universität oder Hochschule eingereicht.

Halle (Saale), den 21.05.2023 Marie Christine Renate Kozubek

Angehangene Publikationen

Es folgen die die Volltext-Versionen der Publikationen P1 – P7.

P1

Results in Chemistry 2 (2020) 100057

Contents lists available at ScienceDirect

Results in Chemistry

journal homepage: www.elsevier.com/locate/rechem

Synthesis and cytotoxic evaluation of hydroxycinnamic acid rhodamine B conjugates

Marie Kozubek, Immo Serbian, Sophie Hoenke, Oliver Kraft, René Csuk *

Martin-Luther-University Halle-Wittenberg, Organic Chemistry, Kurt-Mothes-Str. 2, D-06120 Halle (Saale), Germany

ARTICLE INFO

Article history:
Received 8 March 2020
Accepted 18 June 2020
Available online xxxx

Keywords:
Hydroxycinnamic acid
Amides
Rhodamine B
Cytotoxicity

ABSTRACT

Four different hydroxycinnamic acid rhodamine B conjugates have been prepared and screened for their cytotoxic activity. In the sulforhodamine B (SRB) assay the majority of the conjugates displayed good cytotoxicity in the low μM range for different human tumor cell lines. Low EC_{50} values were obtained especially for an apoptose-triggering cinnamic acid rhodamine conjugate **3** holding a piperazinyl spacer and a cinnamoyl moiety.

1. Introduction

Today more than one-third of drug sales are based on products holding a natural product scaffold, although only 1% of all known organic compounds are natural substances. [1] Therefore, natural products have been and will be used, to develop helpful drugs to cure diseases, among them cancer [2–4], neurodegenerative diseases [5,6], diabetes [7–11] or atherosclerosis [12–17]. However, structural modifications are necessary to increase both selectivity and the pharmacological profile of these compounds. Bioactive plant-based molecules are of special interest to be selected as suitable structures because of several reasons: a) they are re-newable and b) several scientific studies on animal models and humans have already demonstrated the cancer-preventing potential of phytochemicals. [18] Polyphenols are secondary metabolites of plants, and – among others - hydroxycinnamic acids (HCAs) seem of importance since they hold antioxidant [19–23] and anti-inflammatory properties [24–27]. HCAs are ubiquitous; they are found not only in coffee but also in tea leaves, cereals, many fruits and vegetables. In these plants, HCAs occur most often as esters, glycosides or conjugated to proteins. Furthermore, HCAs are precursors for the biosynthesis of stilbenes, chalcones, flavonoids, lignans and anthocyanins. [28–30]

Hybrids holding a combination of natural products or drugs and the xanthene dye rhodamine B have previously been prepared. Thus, conjugates of rhodamine B and di- or triterpenes were found to be highly cytotoxic for human tumor cell lines in vitro even on a nanomolar range. In addition, the fluorescent dye rhodamine B targets and enables the conjugate to enter the mitochondria, whereby the conjugates act as mitocan [31–34].

Mitochondria are likely to be the target of the next generation of chemotherapeutic agents because these cytoplasmatic organelles can induce programmed cell death, especially apoptosis. [31,35] A controlled cell death causes the cell to shrink; it also leads to a change of the mitochondrial pH value and, as a consequence, to a breakdown of the mitochondrial membrane potential. [36–38] In addition, condensation of the chromatin and the cytoplasm is observed. [39,40] Furthermore, during phagocytosis, the dying cells transfer phosphatidylserine from the inside of the membrane to the outside of the membrane. [41] This promotes the recognition of apoptotic cells and thus accelerates the process of apoptosis. Accordingly, apoptosis-induced cell death is a desirable goal in the therapy of cancer to minimize unwanted side effects.

Hence, we set out to synthesize hydroxycinnamic acid rhodamine B conjugates and examine their cytotoxicity and selectivity towards human tumor cells.

2. Results and discussion

2.1. Chemistry

The strategy was to synthesize the carboxamide **1** from the condensation of the fluorescent dye rhodamine B and piperazine, followed by the coupling of **1** with the respective hydroxycinnamic acid (Scheme 1). Thereby, the acyl chloride of rhodamine B (prepared in situ from rhodamine B and oxalyl chloride) was used for the amidation of the fluorescent dye and piperazine. In this reaction, a direct monoacylation of a symmetrical diamine has to take place, but the formation of a bisacylated product **2** as a by-product could not be avoided; this

* Corresponding author.
E-mail address: rene.csuk@chemie.uni-halle.de (R. Csuk).

https://doi.org/10.1016/j.rechem.2020.100057

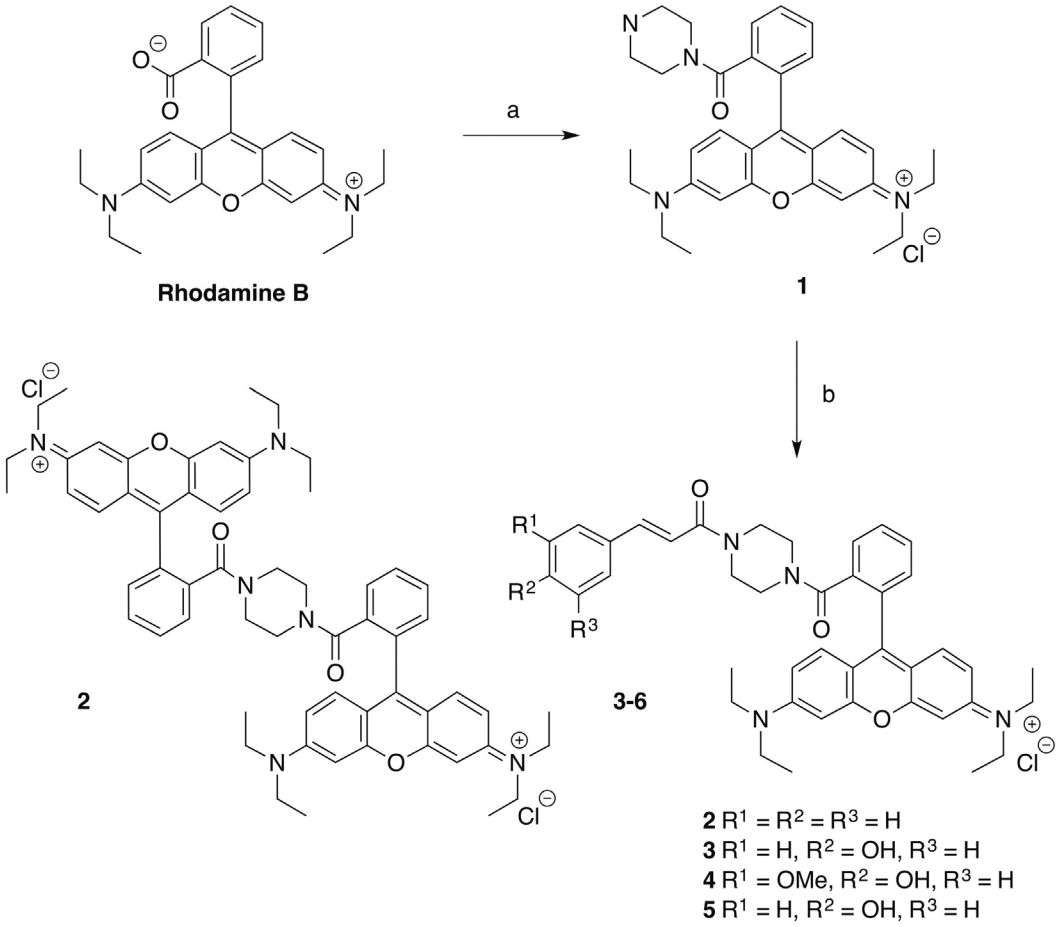

Scheme 1. Structure of rhodamine B and synthesis of the hydroxycinnamic acid conjugates **3–6**; a) 1. DCM, $(COCl)_2$, DMF; 2. DCM, piperazine, 67%; b) cinnamic acid or *p*-coumaric acid or ferulic acid or sinapinic acid, TBTU, DIPEA, DMF, 57% (**3**), 45% (**4**), 48% (**5**), 54% (**6**).

parallels previous findings of Bandgar about the synthesis of monoacylated piperazine derivates. [42]

Compound **1** and cinnamic acid, *p*-coumaric acid, ferulic acid and sinapinic acid were coupled in the presence of TBTU to yield the corresponding conjugates **3–6**.

The structure of the compounds was determined by ^1H and ^{13}C NMR and was further confirmed by MS, IR and UV–vis investigations. Thus, in the ^1H NMR spectra of products **3–6** signals of the methylene groups of the piperazine were detected at $\delta = 3.5$ ppm. These signals showed a significant line-broadening probably due to ring inversion by pyramidal inversion. In the ^{13}C NMR spectra, the signals of the methylene groups of piperazine were detected at $\delta = 47$ ppm; again, these signals show some line broadening. In the UV–vis spectra λ_{max} values between 5.56 and 5.61 nm were recorded; these values are typical for an intact rhodamine B structure.

2.2. Biology

The cytotoxicity of the synthesized carboxamides was evaluated using a colorimetric sulforhodamine B (SRB) assay. The results of the tests are compiled in Table 1.

Compound **1**, the carboxamide of rhodamine B and piperazine shows for four cell lines $EC_{50} > 30$ μM and moderate EC_{50} values of 26.4 μM for A2780 and 17.8 μM for MCF-7 cells; rhodamine B was not cytotoxic at all for these cell lines (cut-off 30 μM; compounds holding EC_{50} values >30 μM are usually regarded as not cytotoxic). This indicates

Table 1
Cytotoxicity of rhodamine B, compounds **1–6**, and staurosporine (**ST**, standard): EC_{50} values in μM from SRB assays after 72 h of treatment; the values are averaged from three independent experiments performed each in triplicate. The human cancer cell lines A375 (epithelial melanoma), HT29 (colorectal adenocarcinoma), MCF-7 (human breast adenocarcinoma), A2780 (ovarian carcinoma), FaDu (pharynx squamous carcinoma) and the non-malignant mouse fibroblasts NIH 3 T3 were used.

	A375	HT29	MCF-7	A2780	FaDu	NIH 3 T3
Rhodamine B	> 30	> 30	> 30	> 30	> 30	> 30
1	> 30	> 30	17.8 ± 3.9	26.4 ± 2.1	> 30	> 30
2	9.0 ± 0.8	10.5 ± 0.8	7.2 ± 0.7	4.3 ± 0.7	7.8 ± 0.3	15.2 ± 1.0
3	3.0 ± 0.1	3.3 ± 0.2	1.0 ± 0.1	1.5 ± 0.1	1.6 ± 0.2	3.3 ± 0.2
4	5.8 ± 0.6	11.3 ± 0.8	3.2 ± 0.2	4.4 ± 0.6	5.3 ± 0.5	10.9 ± 3.6
5	25.6 ± 1.3	> 30	9.3 ± 0.9	14.0 ± 1.1	17.5 ± 1.3	> 30
6	20.5 ± 0.8	> 30	6.8 ± 0.9	11.1 ± 0.6	14.8 ± 0.7	> 30
ST	n.d.	0.2 ± 0.02	0.1 ± 0.01	0.1 ± 0.01	0.1 ± 0.05	0.008 ± 0.001

Table 2
Selectivity factors of compounds **1**–**5** ($F_{SI} = EC_{50,\ NIH\ 3T3}/EC_{50\ tumor\ cell\ line}$).

	F_{SI} (A375)	F_{SI} (HT29)	F_{SI} (MCF-7)	F_{SI} (A2780)	F_{SI} (FaDu)
1	–	–	1.7	1.1	–
2	1.7	1.5	2.1	3.6	2.0
3	1.1	1.0	3.5	2.2	2.1
4	1.9	1.0	3.4	2.5	2.1
5	1.2	–	3.2	2.1	1.7
6	1.5	–	4.4	2.7	2.0

that any relevant cytotoxicity is not directly connected to the rhodamine B scaffold. An improved cytotoxicity was observed for **2**. The highest cytotoxicity was observed for this compound for ovarian carcinoma cells A2780 ($EC_{50} = 4.3$ μM) while this compound was less cytotoxic for non-malignant NIH 3 T3 cells ($EC_{50} = 15.4$ μM). Furthermore, for the fluorescent dye conjugates **3**–**6** cytotoxic effects could be noted with the cinnamic acid conjugate **3** holding the lowest EC_{50}-values for all tested cell lines, ranging from 1 μM to 3 μM. Thereby, all of these compounds were most cytotoxic for MCF-7 human breast adenocarcinoma cells. Besides their cytotoxicity, the selectivity against tumor cell lines (A375, HT29, MCF-7, A2780, FaDu) compared to a non-malignant cell line (NIH 3 T3) is important for the development of novel anticancer agents. For this reason, the maximum selectivity index of the rhodamine B conjugates was calculated ($F_{SI} = EC_{50,\ NIH\ 3T3}/EC_{50\ tumor\ cell\ line}$), and the results are summarized in Table 2.

The highest selectivity index was determined for sinapinic acid conjugate **6** with $F_{SI} = 4.4$. Compound **3** shows an $F_{SI} = 3.5$ for the cell line MCF-7 compared to the non-malignant NIH 3 T3 cells, thus representing the third-highest selectivity factor of this investigation. These results seem to indicate that the presence of a hydroxy or a methoxy groups in the hydroxycinnamic acid conjugates may slightly increase the EC_{50} values but does not significantly improve the selectivity of the compounds. Flow cytometric Annexin V/PI measurements with compound 3 for 48 h at 2 x EC_{50} concentration employing A375 cells showed ca. 27% of apoptotic cells (Fig. 1).

Further studies should aim to access conjugates holding other substituents to improve both the selectivity and to decrease their EC_{50} values for tumor cell lines.

3. Conclusion

In conclusion, substituted hydroxycinnamic acid rhodamine B conjugates **3**–**6** have been synthesized and screened in SRB assays for their cytotoxic acitivity. Thereby a rhodamine B piperazine carboxyamide **1** was prepared in good yields that was then coupled with several hydroxycinnamic acids following a standard amidation protocol. Almost all of the prepared conjugates showed cytotoxic activity with the cinnamic acid conjugate **3** holding low EC_{50} values between 1 and 3 μM for all tested tumor cell lines (A375, HT29, MCF-7, A2780, FaDu). Although the sinapinic acid conjugate **6** was the most selective compound of this study holding a selectivity factor of 4.4, its cytotoxicity was significantly lower than that of compound **3**. The latter compound acted in part by apoptosis on A375 cells. Thus, hydroxycinnamic acid rhodamine B conjugates present an interesting class of rhodamine B conjugates for the development as anticancer drugs, because of their low EC_{50} values. Further studies will show whether their cytotoxic effect as well as their selectivity can be improved by altering the substitution pattern of the cinnamic acid core.

4. Experimental part

4.1. General

NMR spectra were recorded using the Varian spectrometers Unity Inova (500 MHz) or Gemini 2000 (400 MHz). MS spectra were taken on a Finnigan MAT LCQ 7000 instrument. Thin-layer chromatography was performed on pre-coated silica gel plates supplied by Macherey-Nagel. IR spectra were recorded on a Spectrum 1000 FT-IR-spectrometer from Perkin Elmer. The UV/Vis-spectra were recorded on a Lambda 14 spectrometer from Perkin Elmer. The melting points were determined using the Leica hot stage microscope Galen III and are uncorrected. The solvents were dried according to usual procedures. The used chemicals were obtained from different commercial suppliers in bulk quantities.

4.2. Biology

4.2.1. Cell lines and culture conditions

Following human cancer cell lines A375 (epithelial melanoma), HT29 (colorectal adenocarcinoma), MCF-7 (human breast adenocarcinoma), A2780 (ovarian carcinoma), FaDu (pharynx squamous carcinoma) and non-malignant mouse fibroblasts NIH 3 T3 were used. All cell lines were obtained from the Department of Oncology (Martin-Luther-University Halle Wittenberg). Cultures were maintained as monolayers in RPMI 1640 medium with L-glutamine (Capricorn Scientific GmbH, Ebsdorfergrund, Germany) supplemented with 10% heat-inactivated fetal bovine serum (Sigma-Aldrich GmbH, Steinheim, Germany) and penicillin/streptomycin (Capricorn Scientific GmbH,

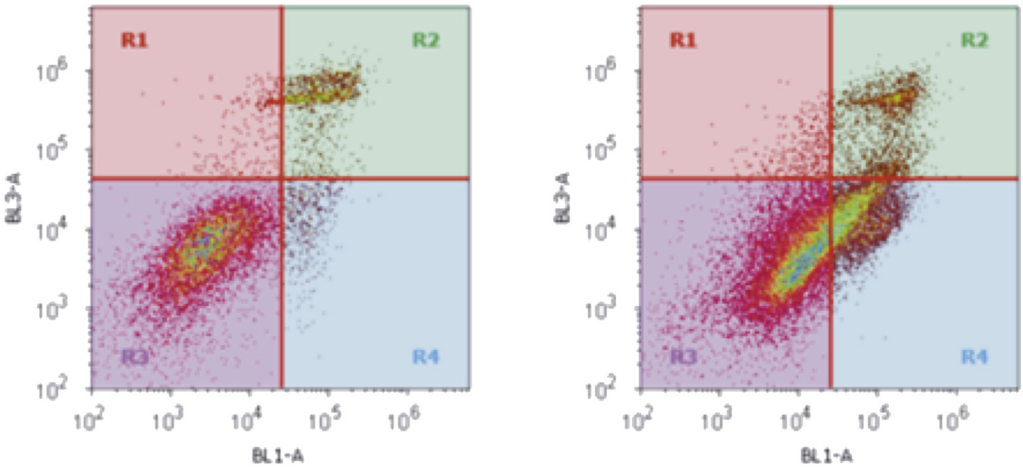

Fig. 1. Annexin V/PI flow cytometry of **3** (incubation for 48 h, 2 x EC_{50}) and A375 cells: left: control, right: treated cells.

Ebsdorfergrund, Germany) at 37 °C in a humidified atmosphere with 5% CO_2.

4.2.2. Cytotoxicity assay (SRB assay)

For the evaluation of the cytotoxicity of the compounds the sulforhodamine-B (Kiton-Red S, ABCR) micro-culture colorimetric assay was used; fluorescence measurements were performed as previously reported [31–35]. The EC_{50} values were averaged from three independent experiments performed each in triplicate calculated from semi-logarithmic dose-response curves applying a non-linear 4P Hills-slope equation.

4.3. Syntheses

*4.3.1. N-(6-(Diethylamino)-9-(2-(piperazin-1-carbonyl)phenyl)-3H-xanthen-3-yliden)-N-ethylethanaminium chloride (**1**)*

The fluorescent dye rhodamine B (10.0 g, 22.3 mmol) was dissolved in dry DCM (250 mL), treated with oxalyl chloride (8.84 mL) at 0 °C. One drop of dry DMF was added, and the solution was allowed to warm up to room temperature. After completion of the reaction, the solvent was removed under reduced pressure. The residue was dissolved in dry DCM (50 mL), and the solution was concentrated again to remove excess oxalyl chloride. The acyl chloride of rhodamine B was diluted with dry DCM (300 mL) and added dropwise to a solution of dry DCM (350 mL) and piperazine (10.0 g). After 24 h, the solvent was removed under reduced pressure followed by chromatographic purification (silica gel, chloroform/methanol, 9:1) of the crude material to yield **1** (7.24 g, 67%) as a dark purple solid; $R_F = 0.14$ (chloroform/methanol, 8:2); m.p. > 350 °C; λ_{max} (log ε) = 260 (0.23), 354 (0.06), 561 (0.82) nm; IR (ATR) ν = 3401*br*, 1589 *m*, 1529*w*, 1411*s*, 1328*s*, 1275*s*, 1246 *m*, 1180*s*, 1132 *m*, 1074 *m*, 1011*w*, 977 *m*, 922 *m*, 820 *m*, 683 *m*; ^{1}H NMR (500 MHz, CD_3OD): δ = 7.79–7.74 (*m*, 3H, 3-H + 4-H + 5-H), 7.52 (*m*, 1H, 6-H), 7.28–7.25 (d, 1H, 10-H), 7.10–7.09 (*m*, 1H, 11-H), 6.98–6.97 (d, 1H, 13-H), 3.72–3.59 (*m*, 6H, 15-H_a + 15-H_b + 17-H_a + 17-H_b + 20-H_a + 20-H_b), 3.08–3.05 (t, 4H, 18-H_a + 18-H_b + 19-H_a + 19-Hb), 1.33–1.30 (t, 3H, 16-H_a + 16-H_b + 16-H_c) ppm; ^{13}C NMR (126 MHz, CD_3OD): δ = 169.53 (C-1), 159.2 (C-8), 157.3 (C-12), 156.7 (C-14), 135.7 (C-7), 133.0 (C-10), 132.3 (C-2), 131.8 (C-6), 131.5 (C-5), 131.4 (C-4), 128.9 (C-3), 115.4 (C-11), 114.8 (C-9), 97.4 (C-13), 46.9 (C-15), 46.8 (C-17 + C-20), 44.5 (C-18 + C-19), 12.8 (C16) ppm; MS (ESI, MeOH): *m/z* = 256.2 (24%, $[M + H]^{2+}$), 511.4 (100%, $[M]^+$); analysis calcd for $C_{32}H_{39}ClN_4O_2$ (547.14): C 70.25, H 7.18, N 10.24; found: C 70.01, H 7.34, N 10.02.

*4.3.2. 9,9′-[Piperazine-1,4-diylbis(carbonyl-2,1-phenylene)]bis[6-(diethylamino)-N,N-diethyl-3H-xanthen-3-iminium] dichloride (**2**)*

To a solution of rhodamine B (500 mg, 1.04 mmol) in dry DCM (15 mL), oxalyl chloride (0.4 mL, 4.18 mmol), DMF (17 mg, 0.23 mmol) and TEA (24 mg, 0.23 mmol) were added, and the mixture was stirred at 25 °C for 3 h. The volatiles were removed under reduced pressure, and the residue was dissolved in dry DCM (15 mL). At 0 °C, piperazine (270 mg, 3.12 mmol), TEA (15 mg, 1.5 mmol) and a catal. Amount of DMAP were added. After stirring for 1 h at 25 °C, the solvents were removed under reduced pressure, and the residue was subjected to column chromatography (SiO_2, chloroform/methanol, 9:1) to yield **2** (284 mg, 54%) as a pink solid; $R_f = 0.27$ (silica gel, $CHCl_3$/MeOH 9:1); m.p. 212–216 °C; IR (ATR): ν = 3414*br*, 2964*w*, 1652 *m*, 1585*s*, 1410*s*, 1329*s*, 1271*s*. 1245*s*, 1178*vs*, 1130*s*, 1072*s*, 1002 *m*, 921 *m*, 821 *m*, 682 s cm^{-1}; UV–Vis (MeOH): λ_{max} (log ε) = 259 (4.55), 307 (4.20), 356 (3.92), 560 (5.07) nm; ^{1}H NMR (500 MHz, $CDCl_3$): δ = 7.59–7.51 (*m*, 4H, 3-H + 5-H), 7.37 (s, 2H, 4-H), 7.23–7.17 (*m*, 2H, 6-H), 7.15–7.02 (*m*, 4H, 10-H + 10'-H), 7.00–6.73 (*m*, 4H, 11-H + 11'-H), 6.66 (s, 4H, 13–H + 13'-H), 3.83 (s, 4H, 17-H + 18-H), 3.60–3.43 (*m*, 16H, 15-H + 15'-H), 1.20 (t, *J* = 7.1 Hz, 24H, 16-H + 16'–H) ppm; ^{13}C NMR (125 MHz, $CDCl_3$): δ = 167.9 (C-1), 157.6 (C-14 + C-14′), 155.6 (C-12 + C-12′ + C-8), 134.3 (C-7), 131.8 (C-11 + C-11′), 130.1 (C-4 + C-2 + C-6 + C-5), 127.6 (C-3), 114.2 (C-10 + C-10′), 113.5 (C-9 + C-9′), 96.1 (C-13 + C-13′), 45.9 (C-15 + C-15′), 12.3 (C-16 + C-16′) ppm; MS (ESI, MeOH): *m/z* (%) = 936.5 ($[M\text{-}2Cl]^{2+}$, 100); analysis calcd for $C_{60}H_{68}Cl_2N_6O_4$ (1008.13): C 71.48, H 6.80, N 8.34; found: C 71.19, H 6.93, N 8.17.

*4.3.3. (E)-N-(9-(2-(4-Cinnamoylpiperazin-1-carbonyl)phenyl)-6-(diethylamino)-3H-xanthen-3-yliden)-N-ethylethanaminium chloride (**3**)*

To an ice cold solution of cinnamic acid (0.5 g, 3.37 mmol) in dry DMF (15 mL) compound **1** (2.69 g, 4.92 mmol), TBTU (1.08 g) and DIPEA (1.2 mL) were added. After completion of the reaction (as indicated by TLC), the mixture was extracted with an aqueous solution of $NaHCO_3$ solution (satd., 100 mL), the organic layer was dried with $MgSO_4$, the solvents were removed under diminished pressure, and the residue was subjected to column chromatography (silica gel, chloroform/methanol, 95:5) to yield **3** (1.23 g, 57%) as a dark purple solid; $R_F = 0.19$ (chloroform/methanol, 95:5); m.p. 172–175 °C; λ_{max} (log ε) = 262 (0.59), 355 (0.09), 561 (1.32) nm; IR (ATR):??ν = 2978*w*, 1633*w*, 1585*s*, 1528*w*, 1411 *m*, 1332*s*, 1271 *m*, 1244 *m*, 1177*s*, 1130 *m*, 1071 *m*, 1005 *m*, 976 *m*, 921 *m*, 823 *m*, 745 *m*, 707 *m*, 682 s, 663 *m*, 546 *m*, 486 *m*; ^{1}H NMR (400 MHz, CD_3OD): δ = 7.80–7.71 (*m*, 3H, 3-H + 6-H + 4-H), 7.61–7.52 (*m*, 3H, 3-H* + 5-H* + 3-H'), 7.39–7.28 (*m*, 4H, 2-H* + 4-H* + 6-H* + 10-H), 7.10–7.04 (*m*, 2H, H2'+ 11-H), 6.96 (d, 1H, 13-H), 3.71–3.64 (q, 2H, H15), 3.58–3.45 (t, 8H, 17-H_a + 17-H_b + 18-H_a + 18-H_b + 19-H_a + 19-H_b + 20-H_a + 20-H_b), 1.32–1.26 (t, 3H, 16-H_a + 16-H_b + 16-H_c) ppm; ^{13}C NMR (101 MHz, CD_3OD): δ = 169.7 (C-1), 168.3 (C-1′), 159.3 (C-8), 157.2 (C-14), 157.0 (C-12), 144.8 (C-3′), 136.5 (C-7), 136.3 (C-1*), 133.2 (C-10), 132.3 (C-2), 131.8 (C-5), 131.3 (C-4), 131.1 (C-4*), 130.0 (C-2* + C-6*), 129.1 (C-3* + C-5*), 129.0 (C-3 + C-6), 117.8 (C-2′), 115.4 (C-11), 114.9 (C-9), 97.4 (C-13), 46.9 (C-15), 43.3 (C-17 + C-18 + C-19 + C-20), 12.9 (C16) ppm; MS (ESI, MeOH): *m/z* = 641.5 (100%, $[M]^+$); analysis calcd for $C_{41}H_{45}ClN_4O_3$ (677.29): C 72.71, H 6.70, N 8.27; found: C 72.45, H 6.91, N 7.97.

*4.3.4. (E)-N-(6-(Diethylamino)-9-(2-(4-(3-(4-hydroxyphenyl)acryloyl)piperazin-1-carbonyl)phenyl)-3H-xanthen-3-yliden)-N-ethylethanaminium chloride (**4**)*

Following the conditions given for the synthesis of **2**, from *p*-coumaric acid (0.31 g, 1.89 mmol), **1** (0.97 g, 1.77 mmol), TBTU (0.61 g) and DIPEA (0.32 mL) followed by column chromatography (silica gel, chloroform/methanol, 95:5) **4** (535 mg, 45%) was obtained as a dark purple solid; $R_F = 0.26$ (chloroform/methanol, 95:5); m.p. 214–218 °C; λ_{max} (log ε) = 259 (0.54), 310 (0.45), 556 (1.16) nm; IR (ATR): ν = 2925*w*, 1585*s*, 1409 *m*, 1333*s*, 1242 *m*, 1178*s*, 1123*s*, 1071*s*, 1004 *m*, 921 *m*, 822 *m*, 682 *m*; ^{1}H NMR (500 MHz, CD_3OD): δ = 7.78–7.58 (*m*, 3H, 5-H + 3-H + H-2′), 7.52–7.36 (*m*, 5H, 3-H* + 5-H* + 3-H'+ H-2* + 6-H*), 7.28–7.19 (*m*, 1H, 10-H), 7.05–7.00 (*m*, 1H, 11-H), 6.91–6.89 (*m*, 1H, 13-H), 3.67–3.61 (*m*, 2H, 15-H_a + 15-H_b), 3.52–3.38 (*m*, 8H, 17-H_a + 17-H_b + 18-H_a + 18-H_b + 19-H_a + 19-H_b + 20-H_a + 20-H_b), 1.35–1.22 (t, 3H, 16-H_a + 16-H_b + 16-H_c) ppm; ^{13}C NMR (126 MHz, CD_3OD): δ = 169.7 (C-1), 168.3 (C-1′), 159.3 (C-8), 157.2 (C-14), 156.9 (C-12 + C-4*), 145.4 (C-3′), 136.5 (C-7), 136.5 (C-1*), 133.1 (C-10), 132.3 (C-2), 131.8 (C-3* + C-5*), 131.3 (C-5), 131.0 (C-2* + C-6*), 130.2 (C-2′), 128.9 (C-3), 127.0 (C-4), 115.4 (C-11), 114.9 (C-9), 97.4 (C-13), 46.9 (C-15), 43.2 (C-17 + C-18 + C-19 + C-20), 12.9 (C-16) ppm; MS (ESI, MeOH): *m/z* = 657.5 (100%, $[M]^+$); analysis calcd for $C_{41}H_{45}ClN_4O_4$ (693.29): C 71.03, H 6.54, N 8.08; found: C 72.84, H 6.75, N 7.73.

*4.3.5. (E)-N-(6-(Diethylamino)-9-(2-(4-(3-(4-hydroxy-3-methoxyphenyl)acryloyl)piperazin-1-carbonyl)phenyl)-3H-xanthen-3-yliden)-N-ethylethanaminium chloride (**5**)*

Following the conditions given for the synthesis of **2**, from ferulic acid (0.22 g, 1.13 mmol), TBTU (0.36 g), **1** (0.58 g, 1.06 mmol) and DIPEA (193 μL) followed by column chromatography (silica gel,

chloroform/methanol, 8:2) **5** (364 mg, 48%) was obtained as a dark purple solid; $R_F = 0.21$ (chloroform/methanol, 9:1); m.p. 188–192 °C; λ_{max} (log ε) = 259 (0.25), 560 (0.47) nm; IR (ATR): *ν* = 2975*w*, 1588*s*, 1411 *m*, 1336*s*, 1273 *m*, 1243 *m*, 1179*s*, 1072 *m*, 1006 *m*, 820 *m*, 744 s, 682 *m*; ^{1}H NMR (500 MHz, CD_3OD): δ = 7.84–7.81 (d, 1H, H-2*), 7.74–7.66 (*m*, 3H, 5-H + H-2′ + 3-H), 7.51–7.42 (*m*, 4H, 5-H* + 6-H + 4-H + 3-H'), 7.24–7.19 (d, 1H, 10-H), 7.05–6.96 (*m*, 2H, 11-H + 6-H*), 6.85–6.63 (*m*, 1H, 13-H), 3.86–3.81 (s, 3H, H-7*$_a$ + H-7*$_b$ + H-7*$_c$), 3.64–3.57 (*m*, 2H, 15-H_a + 15-H_b), 3.51–3.39 (*m*, 8H, 17-H_a + 17-H_b + 18-H_a + 18-H_b + 19-H_a + 19-H_b + 20-H_a + 20-H_b), 1.27–1.21 (t, 3H, 16-H_a + 16-H_b + 16-H_c) ppm; ^{13}C NMR (126 MHz, CD_3OD): δ = 169.5 (C-1), 168.3 (C-1′), 159.1 (C-8), 157.0 (C-12), 156.8 (C-14), 150.1 (C-4*), 149.3 (C-3*), 145.3 (C-3′), 136.4 (C-7), 133.0 (C-10), 132.2 (C-2), 131.2 (C-5), 129.5 (C-1*), 128.8 (C-3), 128.3 (C-5*), 128.2 (C-6), 127.1 (C-4), 124.2 (C-6*) 118.6 (C-2*), 115.4 (C-11), 114.8 (C-9), 111.4 (C-2′), 97.3 (C-13), 56.6 (C-7*), 46.8 (C-15), 43.2 (C-17 + C-18 + C-19 + C-20), 12.8 (C16) ppm; MS (ESI, MeOH): *m*/*z* = 687.4 (100%, $[M]^+$); analysis calcd for $C_{42}H_{47}ClN_4O_5$ (723.31): C 69.74, H 6.55, N 7.75; found: C 69.63, H 6.78, N 7.50.

*4.3.6. (E)-N-(6-(Diethylamino)-9-(2-(4-(3-(4-hydroxy-3,5-dimethoxyphenyl)-acryloyl)piperazin-1-carbonyl)phenyl)-3H-xanthen-3-yliden)-N-ethylethanaminium (**6**)*

Following the conditions given for the synthesis of **2**, from sinapinic acid (0.5 g, 3.05 mmol), **1** (2.0 g, 3.65 mmol), TBTU (0.71 g) and DIPEA (0.7 mL) followed by column chromatography (silica gel, chloroform/methanol, 8:2) **6** (1.14 g, 54%) was obtained as a dark purple solid; $R_F = 0.33$ (chloroform/methanol, 95:5); m.p. 163–175 °C; λ_{max} (log ε) = 239 (0.60), 310 (0.45), 561 (1.65) nm; IR (KBr):? ? = 1584*s*, 1411 *m*, 1332*s*, 1177*s*, 1071 *m*, 1005 *m*, 772 s, 682 *m*; ^{1}H NMR (400 MHz, CD_3OD): δ = 7.80–7.71 (*m*, 4H, 5-H + 4-H + 3-H + 6-H), 7.54–7.44 (*m*, 2H, 5-H* + 3-H'), 7.31–7.26 (d, 1H, 10-H), 7.11–6.89 (*m*, 4H, 11-H + 13-H + H-9 + H-2′), 3.89–3.84 (s, 6H, H-7*$_a$ + H-7*$_b$ + H-7*$_c$ + H-8*$_a$ + H-8*$_b$ + H-8*$_c$), 3.70–3.64 (q, 2H, 15-H_a + 15-H_b), 3.56–3.44 (s, 8H, 17-H_a + 17-H_b + 18-H_a + 18-H_b + 19-H_a + 19-H_b + 20-H_a + 20-H_b), 1.32–1.27 (t, 3H, 16-H_a + 16-H_b + 16-H_c) ppm; ^{13}C NMR (101 MHz, CD_3OD): δ = 169.6 (C-1), 168.3 (C-1′), 159.3 (C-8), 157.2 (C-12), 157.0 (C-14), 149.4 (C-4* + C-2*), 145.7 (C-3′), 139.3 (C-7 + C-3*), 136.5 (C-1*), 133.2 (C-10), 132.3 (C-2), 131.8 (C-5*), 131.3 (C-5), 128.9 (C-6 + C-3 + C-4), 115.4 (C-11),114.9 (C-9), 107.0 (C-2′), 97.4 (C-13), 56.9 (C-7* + C-8*), 46.9 (C-15), 43.2 (C-17 + C-18 + C-19 + C-20), 12.8 (C-16) ppm; MS (ESI, MeOH): *m*/*z* = 717.5 (100%, $[M]^+$); analysis calcd for $C_{41}H_{45}ClN_4O_4$ (693.29): C 71.03, H 6.54, N 8.08; found: C 70.82, H 6.79, N 7.75.

Acknowledgements

We like to thank the late Dr. R. Kluge for measuring the MS spectra and Dr. D. Ströhl and his team for the NMR spectra. Many thanks are also due to Mrs. V. Simon for measuring the IR and UV/Vis spectra. The cell lines were kindly provided by Dr. Th. Müller (Dept. of Haematology/Oncology, Martin-Luther University Halle-Wittenberg).

Appendix A. Supplementary data

Supplementary data to this article can be found online at https://doi.org/10.1016/j.rechem.2020.100057.

References

[1] F. von Nussbaum, M. Brands, B. Hinzen, S. Weigand, D. Häbich, Antibakterielle Naturstoffe in der medizinischen Chemie – Exodus oder Renaissance? Angew. Chem. 118 (2006) 5194–5254.
[2] E.B. Khalid, E.-M. El-Kenawy Ayman, H. Rahman, G. Abdelkarim, A. Najda, Natural products against cancer angiogenesis, Tumor Biol. 37 (2016) 14513–14536.
[3] Y. Wang, J. Zhong, J. Bai, R. Tong, F. An, P. Jiao, L. He, D. Zeng, E. Long, J. Yan, J. Yu, L. Cai, The application of natural products in cancer therapy by targeting apoptosis pathways, Curr. Drug Metab. 19 (2018) 739–749.
[4] Q.-Y. Zhang, F.-X. Wang, K.-K. Jia, L.-D. Kong, Natural product interventions for chemotherapy and radiotherapy-induced side effects, Front. Pharmacol. 9 (2018) 1253.
[5] P.M. Di, L. Papi, F. Gori, E. Turillazzi, Natural products in neurodegenerative diseases: a great promise but an ethical challenge, Int. J. Mol. Sci. 20 (2019), E5170. https://doi.org/10.3390/ijms20205170.
[6] F.F. Ribeiro, F.J.B. Mendonca Jr., J.B. Ghasemi, H.M. Ishiki, M.T. Scotti, L. Scotti, Docking of natural products against neurodegenerative diseases: general concepts, Comb. Chem. High Throughput Screen. 21 (2018) 152–160.
[7] E. Chang, C.Y. Kim, Natural products and obesity: a focus on the regulation of mitotic clonal expansion during adipogenesis, Molecules 24 (2019) 1157/1151-1157/1122.
[8] G.-E. Deligiannidou, E. Philippou, M. Vidakovic, W.V. Berghe, A. Heraclides, N. Grdovic, M. Mihailovic, C. Kontogiorgis, Natural products derived from the Mediterranean diet with antidiabetic activity: from insulin mimetic hypoglycemic to nutriepigenetic modulator compounds, Curr. Pharm. Des. 25 (2019) 1760–1782.
[9] I. Gani, M. Maqbool, M.A. Dar, Anti-diabetic effects of some medicinal plants in experimental animals: a review, Asian J Pharm Res Dev 7 (2019) 66–69.
[10] R. Khursheed, S.K. Singh, S. Wadhwa, B. Kapoor, M. Gulati, R. Kumar, A.K. Ramanunny, A. Awasthi, K. Dua, Treatment strategies against diabetes: success so far and challenges ahead, Eur. J. Pharmacol. 862 (2019) 172625.
[11] J.-L. Rios, I. Andujar, G.R. Schinella, F. Francini, Modulation of diabetes by natural products and medicinal plants via incretins, Planta Med. 85 (2019) 825–839.
[12] W.H. El-Tantawy, A. Temraz, Natural products for controlling hyperlipidemia: review, Arch. Physiol. Biochem. 125 (2019) 128–135.
[13] S. Gholipour, R.D.E. Sewell, Z. Lorigooini, M. Rafieian-Kopaei, Medicinal plants and atherosclerosis: a review on molecular aspects, Curr. Pharm. Des. 24 (2018) 3123–3131.
[14] G.E. Hirsch, P.R. Nazario Viecili, A. Spring de Almeida, S. Nascimento, F.G. Porto, J. Otero, A. Schmidt, B. da Silva, M.M. Parisi, J.Z. Klafke, Natural products with antiplatelet action, Curr. Pharm. Des. 23 (2017) 1228–1246.
[15] Y.E. Koo, J. Song, S. Bae, Use of plant and herb derived medicine for therapeutic usage in cardiology, Medicines 5 (2018) 38/31-38/10.
[16] B.K. Ooi, K.-G. Chan, B.H. Goh, W.H. Yap, The role of natural products in targeting cardiovascular diseases via Nrf2 pathway: novel molecular mechanisms and therapeutic approaches, Front. Pharmacol. 9 (2018) 1308.
[17] M. Sedighi, M. Bahmani, S. Asgary, F. Beyranvand, M. Rafieian-Kopaei, A review of plant-based compounds and medicinal plants effective on atherosclerosis, J Res Med Sci 22 (2017) 30/31-30/16.
[18] N.R. Jabir, M.T. Islam, S. Tabrez, S. Shakil, S.K. Zaidi, F.R. Khan, L.d.S. Araújo, A.-A.P.M. de Meneses, J.V.d.O. Santos, A.A.d.C. Melo-Cavalcante, An insight towards anticancer potential of major coffee constituents, BioFactors 44 (2018) 315–326.
[19] S. Benfeito, C. Oliveira, P. Soares, C. Fernandes, T. Silva, J. Teixeira, F. Borges, Antioxidant therapy: still in search of the 'magic bullet', Mitochondrion 13 (2013) 427–435.
[20] H.R. El-Seedi, A.M.A. El-Said, S.A.M. Khalifa, U. Goeransson, L. Bohlin, A.-K. Borg-Karlson, R. Verpoorte, Biosynthesis, natural sources, dietary intake, pharmacokinetic properties, and biological activities of hydroxycinnamic acids, J Agric Food Chem 60 (2012) 10877–10895.
[21] N. Razzaghi-Asl, J. Garrido, H. Khazraei, F. Borges, O. Firuzi, Antioxidant properties of hydroxycinnamic acids: a review of structure- activity relationships, Curr. Med. Chem. 20 (2013) 4436–4450.
[22] F. Shahidi, A. Chandrasekara, Hydroxycinnamates and their in vitro and in vivo antioxidant activities, Phytochem. Rev. 9 (2010) 147–170.
[23] X. Zhang, X. He, Q. Chen, J. Lu, S. Rapposelli, R. Pi, A review on the hybrids of hydroxycinnamic acid as multi-target-directed ligands against Alzheimer's disease, Bioorg. Med. Chem. 26 (2018) 543–550.
[24] D. Cianciosi, T.Y. Forbes-Hernandez, S. Afrin, M. Gasparrini, P. Reboredo-Rodriguez, P.P. Manna, J. Zhang, L.B. Lamas, S.M. Florez, P.A. Toyos, J.L. Quiles, F. Giampieri, M. Battino, Phenolic compounds in honey and their associated health benefits: a review, Molecules 23 (2018) 2322/2321-2322/2320.
[25] D.L. McKay, J.B. Blumberg, Cranberries (Vaccinium macrocarpon) and cardiovascular disease risk factors, Nutr. Rev. 65 (2007) 490–502.
[26] T. Silva, C. Oliveira, F. Borges, Caffeic acid derivatives, analogs and applications: a patent review (2009–2013), Expert Opin Ther Pat 24 (2014) 1257–1270.
[27] O. Taofiq, I.C.F.R. Ferreira, O. Taofiq, A.M. Gonzalez-Paramas, O. Taofiq, M.F. Barreiro, Hydroxycinnamic acids and their derivatives: cosmeceutical significance, challenges and future perspectives, a review, Molecules 22 (2017) 281, https://doi.org/10.3390/molecules/22020281.
[28] J. Teixeira, A. Gaspar, E.M. Garrido, J. Garrido, F. Borges, Hydroxycinnamic acid antioxidants: an electrochemical overview, BioMed Res Intern 2013 (11) (2013) 25174, https://doi.org/10.1155/2013/251754.
[29] M.A. Alam, N. Subhan, H. Hossain, M. Hossain, H.M. Reza, M.M. Rahman, M.O. Ullah, Hydroxycinnamic acid derivatives: a potential class of natural compounds for the management of lipid metabolism and obesity, Nutrition & Metabolism 13 (2016) 27.
[30] O.L.I. Erukainure, in: R. Watson, V. Preedy, S. Zibadi (Eds.), Polyphenols: Mechanisms of Action in Human Health and Disease, 2nd ed.Academic Press, London, 2018.
[31] S. Sommerwerk, L. Heller, C. Kerzig, A.E. Kramell, R. Csuk, Rhodamine B conjugates of triterpenoic acids are cytotoxic mitocans even at nanomolar concentrations, Eur. J. Med. Chem. 127 (2017) 1–9.
[32] M. Kahnt, J. Wiemann, L. Fischer, S. Sommerwerk, R. Csuk, Transformation of asiatic acid into a mitocanic, bimodal-acting rhodamine B conjugate of nanomolar cytotoxicity, Eur. J. Med. Chem. 159 (2018) 143–148.
[33] J. Wiemann, L. Fischer, J. Kessler, D. Ströhl, R. Csuk, Ugi multicomponent-reaction: syntheses of cytotoxic dehydroabietylamine derivatives, Bioorg. Chem. 81 (2018) 567–576.

[34] R.K. Wolfram, L. Fischer, R. Kluge, D. Ströhl, A. Al-Harrasi, R. Csuk, Homopiperazine-rhodamine B adducts of triterpenoic acids are strong mitocans, Eur. J. Med. Chem. 155 (2018) 869–879.
[35] R.K. Wolfram, L. Heller, R. Csuk, Targeting mitochondria: esters of rhodamine B with triterpenoids are mitocanic triggers of apoptosis, Eur. J. Med. Chem. 152 (2018) 21–30.
[36] S. Matsuyama, J. Llopis, Q.L. Deveraux, R.Y. Tsien, J.C. Reed, Changes in intramitochondrial and cytosolic pH: early events that modulate caspase activation during apoptosis, Nat. Cell Biol. 2 (2000) 318–325.
[37] J.D. Ly, D.R. Grubb, A. Lawen, The mitochondrial membrane potential (deltapsi(m)) in apoptosis; an update, Apoptosis 8 (2003) 115–128.
[38] C. Nilsson, U. Johansson, A.-C. Johansson, K. Kågedal, K. Öllinger, Cytosolic acidification and lysosomal alkalinization during TNF-α induced apoptosis in U937 cells, Apoptosis 11 (2006) 1149, https://doi.org/10.1007/s10495-006-7108-5.
[39] M. Enari, H. Sakahira, H. Yokoyama, K. Okawa, A. Iwamatsu, S. Nagata, Erratum: correction: a caspase-activated DNase that degrades DNA during apoptosis, and its inhibitor ICAD, Nature 393 (1998) 396.
[40] J.F.R. Kerr, A.H. Wyllie, A.R. Currie, Apoptosis: a basic biological phenomenon with wide-ranging implications in tissue kinetics, Br. J. Cancer 26 (1972) 239.
[41] V.A. Fadok, D.R. Voelker, P.A. Campbell, J.J. Cohen, D.L. Bratton, P.M. Henson, Exposure of phosphatidylserine on the surface of apoptotic lymphocytes triggers specific recognition and removal by macrophages, J. Immunol. 148 (1992) 2207–2216.
[42] B.P. Bandgar, S.S. Pandit, Highly rapid and direct synthesis of monoacylated piperazine derivatives from carboxylic acids under mild conditions, Tetrahedron Lett. 44 (2003) 3855–3858.

P2

Cytotoxic triterpenoid-safirinium conjugates target the endoplasmic reticulum

Oliver Kraft, Marie Kozubek, Sophie Hoenke, Immo Serbian, Daniel Major, René Csuk
Eur. J. Med. Chem. 2021, 209, 112920
S. 1-12

Link: https://doi.org/10.1016/j.ejmech.2020.112920

P3

European Journal of Medicinal Chemistry Reports 3 (2021) 100016

HOSTED BY

Contents lists available at ScienceDirect

European Journal of Medicinal Chemistry Reports

journal homepage: www.editorialmanager.com/ejmcr/default.aspx

Apoptotic activity of substituted 3-*O*-acetyl-betulinic acid benzylamides

Marie Kozubek [a], Linda Höhlich [a], Sophie Hoenke [a], Hans-Peter Deigner [b], Ahmed Al-Harrasi [c], René Csuk [a,*]

[a] Martin–Luther–University Halle–Wittenberg, Organic Chemistry, Kurt–Mothes–Str. 2, D, 06120, Halle, Saale, Germany
[b] Furtwangen University, Institute of Precision Medicine, Medical and Life Science Faculty, Jakob–Kienzle–Str. 17, D, 78054, Villigen, Schwenningen, Germany
[c] University of Nizwa, Chair of Oman's Medicinal Plants and Marine Natural Products, P.O. Box 33, PC 616, Birkat Al-Mauz, Nizwa, Oman

ARTICLE INFO

Keywords:
Betulinic acid
Benzylamides
Cytotoxicity
SRB assay

ABSTRACT

Acetylated betulinic acid (**BA**) was converted into mono-substituted benzylamides **2**–**14**. Screening in SRB assays showed them as cytotoxic for a variety of different human tumor cell lines. While parent **BA** was not cytotoxic within the limits of the assay (cut-off 30 μM), the target amides were cytotoxic. Their bioactivity as well as their tumor cell/non-tumor cell selectivity depended on the substitution pattern of the aromatic ring. The most active compound **9** (holding an *ortho* methoxy substituent) acted mainly by apoptosis.

1. Introduction

The therapeutic range of a compound is usually defined as the distance between its therapeutic dose and a dose that leads to a toxic effect [1]. Often, the side effects associated with a particular biological effect can be traced back to a lack of selectivity or insufficient selectivity of complex metabolic pathways. This problem of lack of selectivity is particularly relevant in the use of cytotoxic agents for the therapy of malignant diseases. Cancer remains worldwide the leading cause of death. Thereby alone in 2020, 19.3 million new cases have been reported [2]. It is therefore of particular interest to develop selectively acting substances. Some time ago, we reported on the high cytotoxic activity combined with good selectivity of "EM2" (Fig. 1)[3–10], a diacetylated benzylamide of the naturally occurring triterpene carboxylic acid maslinic acid.

We were therefore interested to find out to what extent these findings can be transferred to betulinic acid **BA** (**1**). **BA** is one of the most frequently studied pentacyclic triterpene carboxylic acids, and an almost unmanageable number of derivatives have been prepared and studied for their biological activities in recent decades. SciFinder held in September 2021 approximately 6000 abstracts containing the keyword "betulinic acid" with 2000 of them dealing with cytotoxic/anti-cancer/anti-tumor activity. This once again showed the unchanged high interest and potential of **BA** and derivatives for possible applications in the therapy of malignant diseases.

2. Results and discussion

Betulinic acid (**BA**) was converted into its acetate **1** (Scheme 1) in 90% yield as previously reported. Compound **1** was activated with oxalyl chloride in the presence of catalytic amounts of dimethylformamide

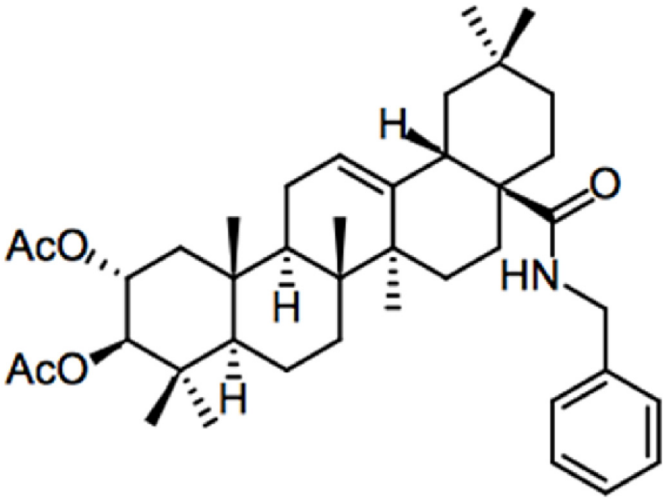

Fig. 1. Structure of cytotoxic lead compound **EM2**.

* Corresponding author.
E-mail address: rene.csuk@chemie.uni-halle.de (R. Csuk).

https://doi.org/10.1016/j.ejmcr.2021.100016
Received 3 October 2021; Received in revised form 4 November 2021; Accepted 5 November 2021
Available online 10 November 2021

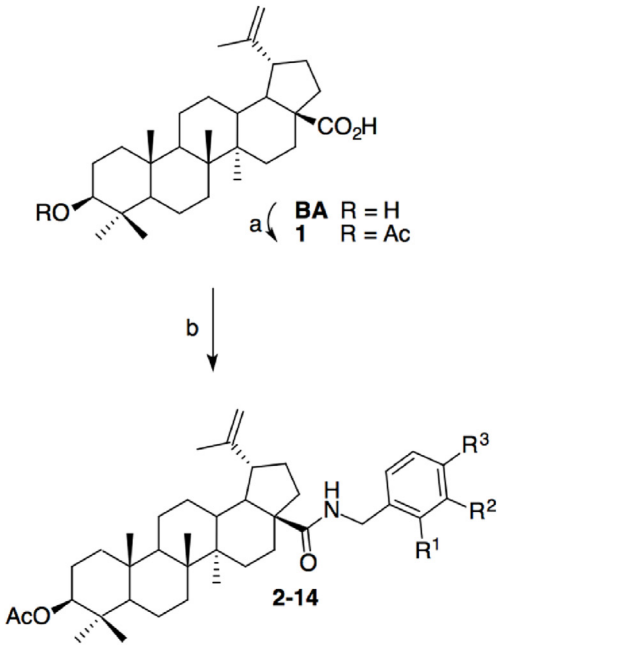

2 $R^1 = R^2 = R^3 = H$; 73%
3 R^1 = Cl, $R^2 = R^3 = H$; 62%
4 $R^1 = R^3 = H$, R^2 = Cl; 78%
5 $R^1 = R^2 = H$, R^3 = Cl; 90%
6 R^1 = F, $R^2 = R^3 = H$; 89%
7 $R^1 = R^3 = H$, R^2 = F; 88%
8 $R^1 = R^2 = H$, R^3 = F; 78%
9 R^1 = OMe, $R^2 = R^3 = H$; 64%
10 $R^1 = R^3 = H$, R^2 = OMe; 62%
11 $R^1 = R^2 = H$, R^3 = OMe; 67%
12 R^1 = Me, $R^2 = R^3 = H$; 86%
13 $R^1 = R^3 = H$, R^2 = Me; 89%
14 $R^1 = R^2 = H$, R^3 = Me; 60%

Scheme 1. Synthesis of the amides **2**–**14**: a) Ac_2O, pyridine, DMAP (cat.), 12 h, 23 °C, 90%; b) $(COCl)_2$, DCM, DMF (cat.), 1 h, 23 °C, then NH_2-Bn-R, NEt_3 (cat.), 1d, 23 °C.

(DMF); addition of the corresponding benzylamines in the presence of catalytic amounts of trimethylamine gave the products **2**–**14** in good yields.

To assess their cytotoxicity, photometric sulforhodamine B (SRB) assays were performed employing a set of human malignant cell lines (A375, HT29, MCF-7, A2780, FaDu) and non–malignant mouse fibroblasts (NIH 3T3). The results from these assays are compiled in Table 1.

All of the compounds (except **5**) showed significant cytotoxic activities, but these compounds also held remarkable selectivity both towards the different human tumor cell lines as well as to non-malignant fibroblasts. While good cytotoxicity was observed for A375 melanoma cells, diminished cytotoxicity was determined for A2780 ovarian carcinoma cells, and an even lower but still noteworthy activity was established for pharynx carcinoma cells FaDu. Rather low or even no cytotoxicity was determined for MCF-7 human breast adenocarcinoma cells (cut-off of the assay 30 μM). Of interest to note that no significant cytotoxicity was found for non-malignant NIH 3T3 fibroblasts. Hence, compound **9** held a selectivity index $S = {}_{EC50,\ NIH\ 3T3}/EC_{50,\ A375} > 12$ for A375 cells and 8.8 for A2780 cells. Fig. 2 shows the selectivity to depend both on the kind of substituent on the aromatic ring as well as the position of the substituent.

In addition, **9** is about two-times more selective than unsubstituted **2**. The finding that **5** was not cytotoxic at all while **9** was among the most cytotoxic compounds underlines once again that even small structural changes might hold a tremendous effect upon the bioactivity of pentacyclic triterpenoids.

Extra FACS measurements (FITC/annexin V/propidium iodide; Fig. 3) showed compound **9** to act mainly by apoptosis. Thus, after an incubation period of 48 h or 72 h only 1% of the A375 cells were necrotic (Fig. 3, R1), 26.6% late apoptotic (R2), 33.4% (48 h) and 30.9% (72 h) viable (R3) and 36.8 (48 h) and 41.3% (after 72 h) apoptotic, respectively.

Furthermore, A375 cells were incubated with **9** to determine its influence onto the cell cycle. As a result (Fig. 4), After 24 h, only 0.8% of all cells were apoptotic, while after another 24 h this number increased by a factor of almost 30. A similarly high rate of apoptotic cells was achieved only after 72 h when incubated with compound **3**.

3. Conclusion

Betulinic acid (**BA**) was acetylated and transformed into monosubstituted benzylamides **2**–**14**. These compounds were screened in SRB assays for cytotoxic activity employing several human tumor cell lines and non-malignant fibroblasts (NIH 3T3). While parent **BA** was not cytotoxic within the limits of the assay (cut-off 30 μM), notable cytotoxicity was established for the final compounds. Cytotoxicity as well tumor cell/non-tumor cell selectivity was strongly dependent on the substitution pattern of the aromatic ring. Extra experiments (FACS, cell

Table 1
SRB assay EC_{50} values [μM] after 72 h of treatment; averaged from three independent experiments performed each in triplicate; confidence interval CI = 95%. Human cancer cell lines: A375 (melanoma), HT29 (colorectal carcinoma), MCF-7 (breast adenocarcinoma), A2780 (ovarian carcinoma), FaDu (pharynx carcinoma), NIH 3T3 (non-malignant fibroblasts); cut-off 30 μM, n.d. not determined. Doxorubicin (**D**) has been used as a positive standard.

Compound	A375	HT29	MCF-7	A2780	FaDu	NIH 3T3
BA	>30	>30	>30	>30	>30	>30
1	19.2 ± 1.7	21.3 ± 2.0	11.0 ± 0.5	18.3 ± 0.5	7.2 ± 1.2	>30
2	4.1 ± 0.2	>30	26.8 ± 6.8	6.29 ± 0.8	9.59 ± 0.9	>30
3	4.6 ± 0.2	>30	>30	10.8 ± 1.8	>30	>30
4	7.5 ± 0.7	>30	>30	13.2 ± 1.4	>30	>30
5	>30	>30	>30	>30	>30	>30
6	4.7 ± 0.6	>30	>30	8.3 ± 2.4	10.2 ± 1.6	>30
7	5.1 ± 1.0	>30	>30	8.2 ± 1.4	11.6 ± 2.6	>30
8	4.6 ± 0.2	>30	>30	9.2 ± 1.6	11.7 ± 1.4	>30
9	2.5 ± 0.1	>30	16.9 ± 1.5	3.4 ± 0.4	5.3 ± 0.2	>30
10	2.1 ± 0.3	>30	11.3 ± 2.6	2.7 ± 0.3	3.6 ± 0.4	10.3 ± 2.1
11	7.2 ± 1.1	>30	>30	14.7 ± 5.4	>30	>30
12	5.0 ± 0.3	>30	18.2 ± 4.7	7.2 ± 0.9	10.0 ± 1.4	>30
13	3.5 ± 0.2	>30	>30	6.8 ± 0.6	13.2 ± 1.6	>30
14	11.2 ± 0.9	>30	>30	>30	>30	>30
DX	n.d.	0.9 ± 0.2	1.1 ± 0.3	0.02 ± 0.01	n.d.	0.06 ± 0.03

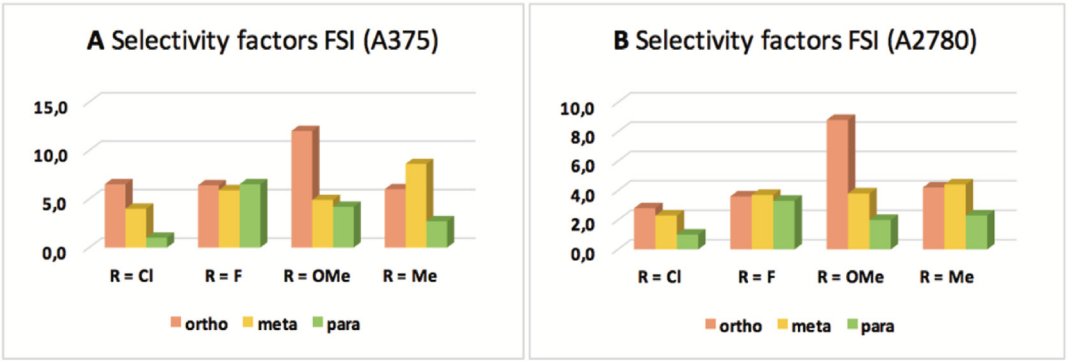

Fig. 2. Selectivity factors depending on the kind of substituent (**A**, A375 cells) as well as on its position (**B**, A2780 cells).

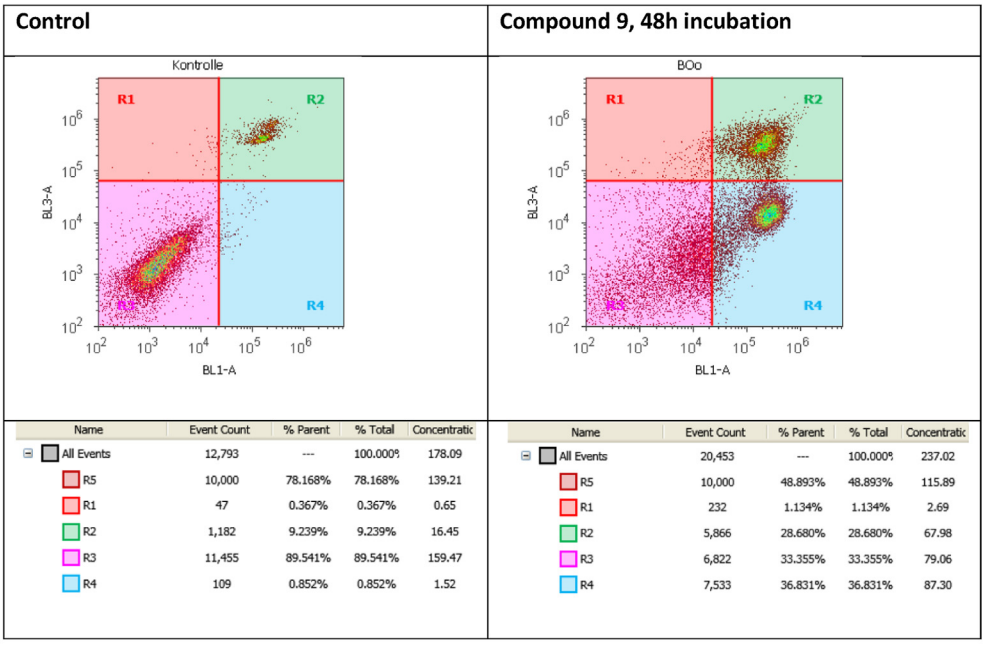

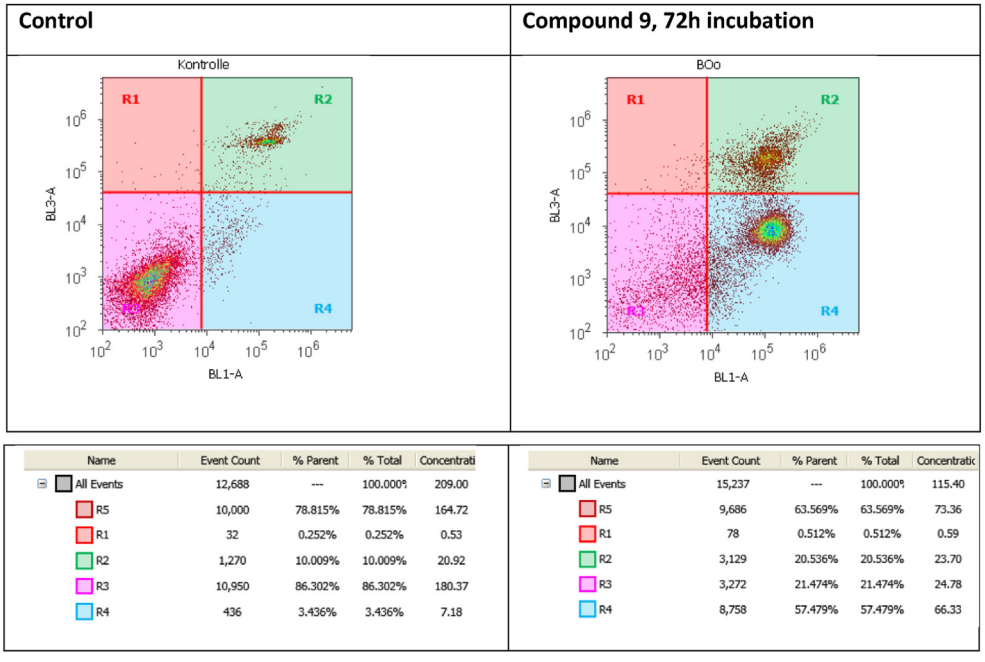

Fig. 3. FACS measurements of compound **9** and A375 cells after an incubation period of 48 h and 72 h, respectively.

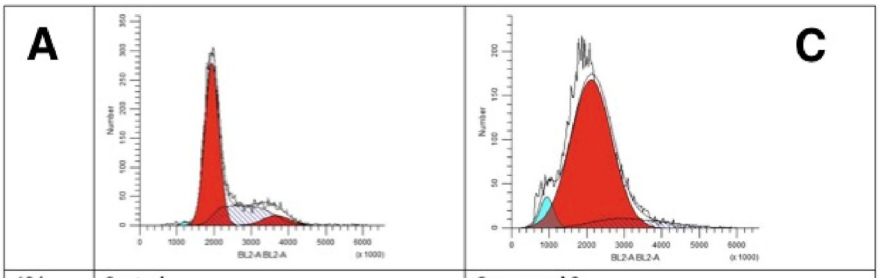

48 h	Control	Compound 3
G1	64.4 %	89.9 %
S	28.2 %	10.1 %
G2/M	7.4 %	0.0 %
Apo	0.7 %	5.8 %

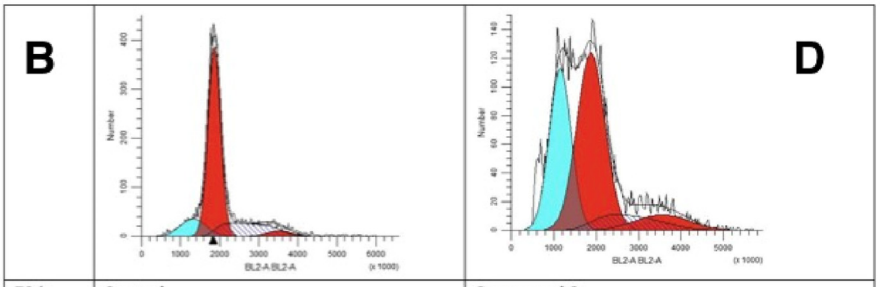

72 h	Control	Compound 3
G1	74.8 %	73.4 %
S	21.0 %	14.3 %
G2/M	4.1 %	12.3 %
Apo	12.0 %	34.1 %

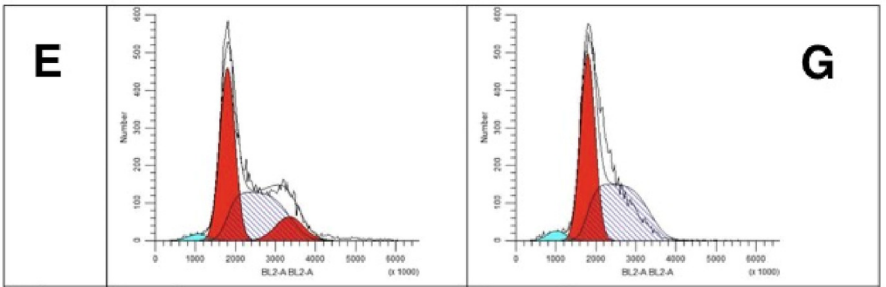

24 h	Control	Compound 9
G1	45.9 %	49.4 %
S	42.2 %	50.6 %
G2/M	11.9 %	0.0 %
Apo	2.4 %	3.3 %

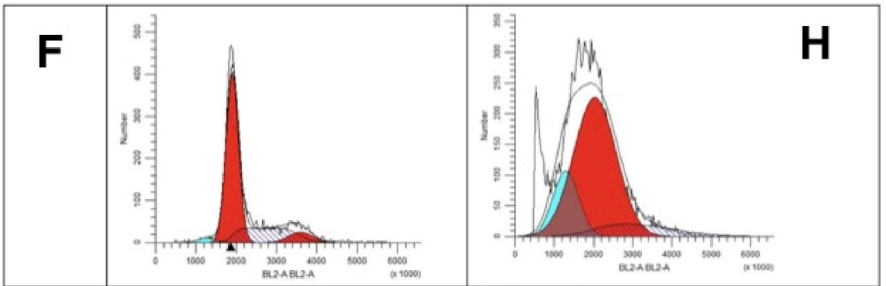

48 h	Control	Compound 9
G1	67.0 %	86.4 %
S	25.0 %	13.6 %
G2/M	7.9 %	0.0 %
Apo	2.5 %	19.8 %

Fig. 4. Investigation of the cell cycle upon incubation with compounds **3** (A and B: control, C: after 48 h, D: after 72 h) and **9** (E and F: control, G: after 24 h, H: after 48 h), respectively.

cycle) showed the most active compound **9** (holding an *ortho* methoxy substituent) to act mainly by apoptosis.

4. Experimental

4.1. General

NMR spectra were recorded using the Varian spectrometers DD2 and VNMRS (400 and 500 MHz, respectively). MS spectra were taken on a Advion expression^{L} CMS mass spectrometer (positive ion polarity mode, solvent: methanol, solvent flow: 0.2 mL/min, spray voltage: 5.17 kV, source voltage: 77 V, APCI corona discharge: 4.2 μA, capillary temperature: 250 °C, capillary voltage: 180 V, sheath gas: N_2). Thin-layer chromatography was performed on pre-coated silica gel plates supplied by Macherey-Nagel. IR spectra were recorded on a Spectrum 1000 FT-IR-spectrometer from Perkin Elmer. The UV/Vis-spectra were recorded on a Lambda 14 spectrometer from Perkin Elmer. The optical rotations were measured either on a JASCO P-2000 or a Perkin-Elmer polarimeter at 20 °C. The melting points were determined using the Leica hot stage microscope Galen III and are uncorrected. The solvents were dried according to usual procedures. Betulinic acid were bought from "Betulinines" (Stříbrná Skalice, Czech Republic) and used as received.

4.2. Biology

4.2.1. Cell lines and culture conditions

Following human cancer cell lines A375 (malignant melanoma), HT29 (colon adenocarcinoma), MCF-7 (breast cancer), A2780 (ovarian carcinoma), FaDu (pharynx carcinoma) and non-malignant mouse fibroblasts NIH 3T3 were used. All cell lines were obtained from the Department of Oncology (Martin-Luther-University Halle Wittenberg). Cultures were maintained as monolayers in RPMI 1640 medium with L-glutamine (Capricorn Scientific GmbH, Ebsdorfergrund, Germany) supplemented with 10% heat-inactivated fetal bovine serum (Sigma-Aldrich GmbH, Steinheim, Germany) and penicillin/streptomycin (Capricorn Scientific GmbH, Ebsdorfergrund, Germany) at 37 °C in a humidified atmosphere with 5% CO_2.

4.2.2. Cytotoxicity assay (SRB assay)

For the evaluation of the cytotoxicity of the compounds the sulforhodamine-B (Kiton-Red S, ABCR GmbH, Karlsruhe, Germany) micro-culture colorimetric assay was used. The EC_{50} values were averaged from three independent experiments performed each in triplicate and calculated from semi-logarithmic dose-response curves applying a non-linear 4P Hills-slope equation.

4.3. Syntheses

4.3.1. General procedure (GP)

Acetylated betulinic acid was dissolved in dry DCM, oxalyl chloride (2 eq) and a catalytic amount of DMF were added at 0 °C. After stirring for 1 h, the excess of oxalyl chloride was removed with THF (3 × 20 mL) under reduced pressure. The residue was dissolved in DCM and the corresponding benzylamine (3 eq) and catalytic amounts of NEt_3 were added. After completion of the reaction (as indicated with TLC), the solution was washed with an aqu. HCl solution (20 mL, 1 M) solution, dried, and the solvent was distilled off under reduced pressure. For purification, the residue was subjected to chromatography.

4.3.2. 3β-Acetyloxylup-20(29)-en-28-oic acid (1)

Betulinic acid (**BA**, 20.0 g, 43.7 mmol) was acetylated in dry pyridine (100 mL) with Ac_2O (12.8 mL, 135.4 mmol) in the presence of catalytic amounts of DMAP as previously described to yield **2** (19.68 g, 90%) as an off-white, crystalline solid; m.p. 285–290 °C (from EtOH) (lit[11].: 277–2780 °C); R_F = 0.41 (silica gel, *n*-hexane/ethyl acetate, 3:1); $[\alpha]_D$ = +20.6° (*c* = 0.14, $CHCl_3$); [lit[11].: $[\alpha]_D$ = +22° (*c* = 0.49, $CHCl_3$)]; MS (ESI, MeOH): *m/z* = 497.5 ($[M - H]^-$, 100%), 995.5 ($[2M - H]^-$, 50%), 1018.1 ($[2M\text{-}2H + Na]^-$, 25%).

4.3.3. 3β-Acetyloxy-N-(phenylmethyl)-lup-20(29)en-28-amide (2)

Following GP; yield: 73%; m.p. 134 °C (from EtOH) (lit [12].: 124–127 °C); R_F = 0.64 (SiO_2, *n*-hexane/ethyl acetate, 7:1); $[\alpha]_D$ = +21.7° (*c* = 0.4, $CHCl_3$) [lit[13].: $[\alpha]_D$ = +23.2° (*c* = 0.35, $CHCl_3$); MS (ESI, MeOH): *m/z* = 588.6 ($[M+H]^+$, 60%), 1197.3 ($[2\ M + Na]^+$, 100%).

4.3.4. 3β-Acetyloxy-N-[(2-chlorophenylmethyl)]-lup-20(29)en-28-amide (3)

Following GP; yield: 62%; m.p. 101–104 °C (from ethyl acetate/*n*-hexane); R_F = 0.32 (SiO_2, *n*-hexane/ethyl acetate, 9:1); $[\alpha]_D$ = +31.6° (*c* = 0.18, $CHCl_3$) IR (KBr): *ν* = 3345w, 2944 m, 2869w, 1735 m, 1667w, 1639 m, 1515 m, 1471 m, 1445 m, 1392w, 1367 m, 1316w, 1244vs, 1197w, 1107w, 1028 m, 979 m, 883 m, 747s, 689w, 680w, 656w, 608w, 544w, 492w, 448w, 431w, 416w cm^{-1}; UV–Vis ($CHCl_3$): λ_{max} (log *ε*) = 264 (3.35) nm; ^{1}H NMR (500 MHz, $CDCl_3$): *δ* = 7.47–7.40 (m, 1H, 36-H), 7.39–7.32 (m, 1H, 37-H), 7.25–7.17 (m, 2H, 38-H + 39-H), 6.15 (*dd*, *J* = 6.1, 6.1 Hz, 1H, N*H*), 4.73 (d, *J* = 2.3 Hz, 1H, 29-H_a), 4.61–4.58 (m, 1H, 29-H_b), 4.54 (*dd*, *J* = 14.6, 6.2 Hz, 1H, 33-H_a), 4.49–4.39 (m, 2H, 3-H + 33-H_b), 3.12 (*td*, *J* = 11.1, 4.4 Hz, 1H, 19-H), 2.37 (*ddd*, *J* = 12.9, 11.4, 3.6 Hz, 1H, 13-H), 2.03 (s, 3H, 32-H), 1.97–1.86 (m, 2H, 16-H_a + 21-H_a), 1.75 (*dd*, *J* = 12.0, 7.8 Hz, 1H, 22-H_a), 1.67 (s, 3H, 30-H), 1.64–0.94 (m, 22H, 1-H + 22-H_b + 12-H + 2-H + 18-H + 16-H_b + 6-H + 11-H + 7-H + 15-H + 9-H), 0.93 (s, 3H, 27-H), 0.84–0.79 (m, 9H, 25-H + 24-H + 23-H), 0.78–0.72 (m, 1H, 5-H), 0.69 (s, 3H, 26-H ppm; ^{13}C NMR (126 MHz, $CDCl_3$): *δ* = 176.1 (C-28), 171.0 (C-31), 150.9 (C-20), 136.3 (C-34), 133.5 (C-35), 130.9 (C-36), 129.4 (C-37), 128.8 (C-39), 127.0 (C-38), 109.4 (C-29), 80.9 (C-3), 55.8 (C-17), 55.4 (C-5), 50.5 (C-9), 50.1 (C-18), 46.8 (C-19), 42.4 (C-14), 41.5 (C-33), 40.7 (C-8), 38.4 (C-1), 38.3 (C-22), 37.8 (C-4), 37.7 (C-13), 37.1 (C-10), 34.3 (C-7), 33.8 (C-16), 30.9 (C-21), 29.3 (C-15), 27.9 (C-23), 25.6 (C-12), 23.7 (C-2), 21.3 (C-32), 20.9 (C-11), 19.5 (C-30), 18.2 (C-6), 16.5 (C-24), 16.2 (C-25), 15.8 (C-26), 14.6 (C-27) ppm; MS [ESI, MeOH/$CHCl_3$ (4:1)]: *m/z* = 620.3 (100%, $[M - H]^-$), 656.2 (92%, $[M+Cl]^-$); analysis calcd for $C_{39}H_{56}ClNO_3$ (622.33): C 75.27, H 9.07, N 2.25; found: C 74.97, H 9.23, N 2.05.

4.3.5. 3β-Acetyloxy-N-[(3-chlorophenylmethyl)]-lup-20(29)en-28-amide (4)

Following GP; yield: 78%; m.p. 134–137 °C (from ethyl acetate/*n*-hexane); R_F = 0.23 (SiO_2, *n*-hexane/ethyl acetate, 9:1); $[\alpha]_D$ = +25.0° (*c* = 0.187, $CHCl_3$); IR (KBr): v = 3365w, 2944 m, 1734 m, 1640 m, 1514 m, 1368 m, 1244vs, 1026 m, 979 m, 882 m, 755 m, 681 m, 444w cm^{-1}; UV–Vis ($CHCl_3$): λ_{max} (log *ε*) = 268 (3.45), 275 (3.33) nm; ^{1}H NMR (400 MHz, $CDCl_3$): *δ* = 7.28–7.26 (m, 1H, 35-H), 7.25–7.21 (m, 2H, 38-H + 37-H) 7.19–7.15 (m, 1H, 39-H), 5.97 (*dd*, *J* = 6.0, 6.0 Hz, 1H, N*H*), 4.74 (d, *J* = 2.3 Hz, 1H, 29-H_a), 4.63–4.57 (m, 1H, 29-H_b), 4.52–4.42 (m, 2H, 3-H + 33-H_a), 4.35–4.25 (m, 1H, 33-H_b), 3.15 (*td*, *J* = 11.1, 4.3 Hz, 1H, 19-H), 2.51–2.42 (m, 1H, 13-H), 2.03 (s, 3H, 32-H), 2.01–1.88 (m, 2H, 21-H_a + 16-H_a), 1.81–1.71 (m, 2H, 22-H_a + 12-H_a), 1.68 (s, 3H, 30-H), 1.66–0-96 (m, 18 H, 1-H_a + 1-H_b + 18-H + 2-H_a + 2-H_b + 16-H_b + 12-H_b + 9-H + 6-H_a + 6-H_b + 15-H_a + 15-H_b + 21-H_b + 11-H_a + 11-H_b + 7-H_a + 7-H_b + 22-H_b), 0.95 (s, 3H, 27-H), 0.88 (s, 3H, 26-H), 0.86–0.80 (m, 9H, 23-H_a + 23-H_b + 23-H_c + 25-H + 24-H_a + 24-H_b + 24-H_c), 0.80–0.74 (m, 1H, 5-H) ppm; ^{13}C NMR (101 MHz, $CDCl_3$): *δ* = 176.2 (C-28), 171.2 (C-31), 151.0 (C-20), 141.5 (C-34), 134.6 (C-36), 130.0 (C-38), 127.9 (C-35), 127.6 (C-37), 126.0 (C-39), 109.6 (C-29), 81.9 (C-3), 55.9 (C-17), 55.6 (C-5), 50.73 (C-9), 50.3 (C-18), 46.8 (C-19), 42.9 (C-14), 42.7 (C-33), 40.9 (C-8), 38.6 (C-1), 38.6 (C-22), 38.0 (C-4), 37.9 (C-13), 37.3 (C-10), 34.5 (C-7), 33.9 (C-16), 31.0 (C-21), 29.6 (C-15), 28.1 (C-23), 25.8 (C-12), 23.9 (C-2), 21.5 (C-32), 21.1 (C-11), 19.6 (C-30), 18.4 (C-6), 16.6 (C-24), 16.4 (C-25), 16.3 (C-26), 14.8 (C-27) ppm; MS [ESI, MeOH/$CHCl_3$ (4:1)]: *m/z* = 620.1 (17%, $[M - H]^-$), 656.1 (100%,

[M+Cl]⁻); analysis calcd for $C_{39}H_{56}ClNO_3$ (622.33): C 75.27, H 9.07, N 2.25; found: C 75.91, H 9.30, N 1.99.

4.3.6. 3β-Acetyloxy-N-[(4-chlorophenylmethyl)]-lup-20(29)en-28-amide (5)

Following GP; yield: 90%; m.p. 126–129 °C (from ethyl acetate/*n*-hexane); $R_F = 0.18$ (SiO_2, *n*-hexane/ethyl acetate, 9:1); $[\alpha]_D = +23.2°$ (*c* = 0.172, $CHCl_3$); IR (KBr): ν = 3359w, 2943 m, 1734 m, 1640 m, 1492 m, 1367 m, 1243vs, 1091 m, 1015 m, 979 m, 882 m, 476w cm^{-1}; UV–Vis (CHCl3): λ_{max} (log ε) = 269 (3.55), 277 (3.42) nm; ^{1}H NMR (400 MHz, $CDCl_3$): δ = 7.31–7.23 (m, 2H, 36-H + 38-H), 7.23–7.16 (m, 2H, 35-H + 39-H), 5.93 (*dd*, *J* = 5.9, 5.9 Hz, 1H, N*H*), 4.73 (d, *J* = 2.3 Hz, 1H, 29-H_a), 4.61–4.55 (m, 1H, 29-H_b), 4.50–4.39 (m, 2H, 3-H + 33-H_a), 4.29 (*dd*, *J* = 14.8, 5.7 Hz, 1H, 33-H_b), 3.14 (*td*, *J* = 11.1, 4.2, 1H, 19-H), 2.50–2.40 (m, 1H, 13-H), 2.02 (s, 3H, 32-H_a + 32-H_b + 32-H_c), 1.97–1.81 (m, 2H, 21-H_a + 16-H_a), 1.78–1.69 (m, 2H, 22-H_a + 12-H_a), 1.67 (s, 3H, 30-H), 1.66–0.95 (m, 18H, 1-H + 2-H + 18-H + 16-H_b + 6-H + 22-H_b + 15-H + 21-H_b + 7-H + 11-H + 9-H + 12-H_b), 0.94 (s, 3H, 27-H), 0.87 (s, 3H, 26-H), 0.83 (s, 9H, 25-H + 24-H + 23-H), 0.80–0.72 (m, 1H, 5-H) ppm; ^{13}C NMR (101 MHz, $CDCl_3$): δ = 176.2 (C-28), 171.1 (C-31), 151.0 (C-20), 138.0 (C-34), 133.2 (C-37), 129.3 (C-35, C-39), 128.9 (C-36, C-38), 109.6 (C-29), 81.1 (C-3), 55.8 (C-17), 55.6 (C-5), 50.7 (C-9), 50.3 (C-18), 46.8 (C-19), 42.7 (C-14), 42.6 (C-33), 40.9 (C-8), 38.6 (C-1), 38.5 (C-22), 38.0 (C-4), 37.9 (C-13), 37.3 (C-10), 34.5 (C-7), 33.9 (C-16), 31.0 (C-21), 29.6 (C-15), 28.1 (C-23), 25.8 (C-12), 23.9 (C-2), 21.5 (C-32), 21.1 (C-11), 19.6 (C-30), 18.3 (C-6), 16.6 (C-24), 16.4 (C-25), 16.3 (C-26), 14.8 (C-27) ppm; MS [ESI, MeOH/$CHCl_3$ (4:1)]: *m/z* = 620.2 (8%, [M − H]⁻), 656.1 (100%, [M+Cl]⁻); analysis calcd for $C_{39}H_{56}ClNO_3$ (622.33): C 75.27, H 9.07, N 2.25; found: C 75.02, H 9.36, N 2.06.

4.3.7. 3β-Acetyloxy-N-[(2-fluorophenylmethyl)]-lup-20(29)en-28-amide (6)

Following GP; yield: 89%; m.p. 125–127 °C (from ethyl acetate/*n*-hexane); $R_F = 0.30$ (SiO_2, *n*-hexane/ethyl acetate, 9:1); $[\alpha]_D = +26.5°$ (*c* = 0.163, $CHCl_3$); IR (KBr): ν = 2936w, 1740 m, 1631 m, 1542 m, 1488 m, 1457w, 1366 m, 1245vs, 1226s, 1033 m, 977 m, 883 m, 832 m, 769s, 695w, 545w, 510w cm^{-1}; UV–Vis ($CHCl_3$): λ_{max} (log ε) = 263 (3.93), 269 (3.86) nm; ^{1}H NMR (400 MHz, $CDCl_3$): δ = 7.41–7.32 (m, 1H, 39-H), 7.29–7.19 (m, 1H, 37-H), 7.07 (*ddd*, *J* = 13.9, 7.0, 1.2 Hz, 1H, 38-H), 7.04–6.98 (m, 1H, 36-H), 6.00 (*dd*, *J* = 6.0, 6.0 Hz, 1H, N*H*), 4.72 (d, *J* = 2.4 Hz, 1H, 29-H_a), 4.61–4.55 (m, 1H, 29-H_b), 4.55–4.35 (m, 3H, 33-H + 3-H), 3.12 (*td*, *J* = 11.1, 4.3 Hz, 1H, 19-H), 2.40 (*ddd*, *J* = 12.9, 11.4, 3.6 Hz, 1H, 13-H), 2.03 (s, 3H, 32-H), 1.99–1.84 (m, 2H, 21-H_a + 16-H_a), 1.73 (*dd*, *J* = 11.8, 7.8 Hz, 1H, 22-H_a), 1.67 (s, 3H, 30-H), 1.66–0.95 (m, 19H, 12-H + 1-H + 2-H + 18-H + 16-H_b + 6-H + 7-H + 11-H + 21-H_b + 15-H + 9-H + 22-H_b), 0.93 (s, 3H, 27-H), 0.82 (d, *J* = 2.4 Hz, 9H, 24-H + 25-H + 23-H), 0.78–0.72 (m, 1H, 5-H), 0.75 (s, 3H, 26-H) ppm; ^{13}C NMR (101 MHz, $CDCl_3$): δ = 176.1 (C-28), 171.0 (C-31), 161.08 (*d*, *J* = 245.7 Hz, C-35), 150.9 (C-20), 129.9 (*d*, *J* = 251.9 Hz, C-39), 129.8 (*d*, *J* = 155.6 Hz, C-37), 125.94 (*d*, *J* = 14.6 Hz, C-34), 124.21 (*d*, *J* = 3.5 Hz, C-38), 115.23 (*d*, *J* = 21.3 Hz, C-36), 109.4 (C-29), 81.0 (C-3), 55.7 (C-17), 55.4 (C-5), 50.5 (C-9), 50.1 (C-18), 46.7 (C-19), 42.4 (C-14), 40.7 (C-8), 38.4 (C-1), 38.3 (C-22), 37.8 (C-4), 37.7 (C-13), 37.5 (C-33), 37.4 (C-33), 37.1 (C-10), 34.3 (C-7), 33.8 (C-16), 30.8 (C-21), 29.3 (C-15), 27.9 (C-23), 25.6 (C-12), 23.7 (C-2), 21.3 (C-32), 20.9 (C-11), 19.5 (C-30), 18.2 (C-6), 16.5 (C-24), 16.2 (C-25), 15.9 (C-26), 14.6 (C-27) ppm; MS [ESI, MeOH/$CHCl_3$ (4:1)]: *m/z* = 604.2 (100%, [M − H]⁻), 640.3 (64%, [M − Cl]⁻); analysis calcd for $C_{39}H_{56}FNO_3$ (605.88): C 77.31, H 9.32, N 2.31; found: C 77.03, H 9.51, N 2.01.

4.3.8. 3β-Acetyloxy-N-[(3-fluorophenylmethyl)]-lup-20(29)en-28-amide (7)

Following GP; yield: 88%; m.p. 228–231 °C (from ethyl acetate/*n*-hexane); $R_F = 0.21$ (SiO_2, *n*-hexane/ethyl acetate, 9:1); $[\alpha]_D = +18.9°$ (*c* = 0.169, $CHCl_3$); IR (KBr): ν = 2943 m, 1734 m, 1666 m, 1450 m, 1375 m, 1244vs, 1193 m, 1027 m, 979 m, 884 m, 742 m, 694 m, 441w cm^{-1}; UV–Vis ($CHCl_3$): λ_{max} (log ε) = 263 (4.02), 270 (3.97) nm; ^{1}H NMR (500 MHz, $CDCl_3$): δ = 7.32–7.24 (m, 1H, 38-H), 7.08–7.03 (m, 1H, 39-H), 7.02–6.91 (m, 2H, 35-H + 37-H), 5.95 (*dd*, *J* = 5.9, 5.9 Hz, 1H, N*H*), 4.74 (d, *J* = 2.3 Hz, 1H, 29-H_a), 4.62–4.57 (m, 1H, 29-H_b), 4.45–4.43 (m, 2H, 3-H + 33-H_a), 4.34 (*dd*, *J* = 14.9, 5.8 Hz, 1H, 33-H_b), 3.15 (*td*, *J* = 11.1, 4.5 Hz, 1H, 19-H), 2.47 (m, 1H, 13-H), 2.03 (s, 3H, 32-H), 1.94 (m, 2H, 22-H_a + 16-H_a), 1.80–1.69 (m, 2H, 22-H_a + 12-H_a), 1.69 (s, 3H, 30-H), 1.66–0.97 (m, 18H, 2-H + 1-H + 16-H_b + 18-H + 6-H + 15-H + 21-H_b + 7-H + 11-H + 9-H + 12-H_b + 22-H_b), 0.96 (s, 3H, 27-H), 0.89 (s, 3H, 25-H), 0.86–0.81 (m, 9H, 23-H + 24-H + 26-H), 0.80–0.74 (m, 1H, 5-H) ppm; ^{13}C NMR (126 MHz, $CDCl_3$): δ = 176.4 (C-28), 171.4 (C-31), 163.4 (*d*, *J* = 246.5 Hz, C-36), 151.2 (C-20), 142.3 (*d*, *J* = 7.1 Hz, C-34), 130.5 (*d*, *J* = 8.2 Hz, C-38), 123.6 (C-39), 114.9 (*d*, *J* = 45.4 Hz, C-35), 130.5 (*d*, *J* = 8.2 Hz, C-37), 109.9 (C-29), 81.4 (C-3), 56.1 (C-17), 55.9 (C-5), 51.0 (C-9), 50.6 (C-18), 47.1 (C-19), 43.2 (C-14), 42.9 (C-33), 41.2 (C-8), 38.8 (C-1), 38.8 (C-22), 38.2 (C-4), 38.1 (C-13), 37.5 (C-10), 34.8 (C-7), 34.2 (C-16), 31.3 (C21), 29.9 (C-15), 28.4 (C-23), 26.0 (C-12), 24.1 (C-2), 21.7 (C-32), 21.4 (C-11), 19.9 (C-30), 18.6 (C-6), 16.9 (C-24), 16.6 (C-25), 16.5 (C-26), 15.0 (C-27) ppm; MS [ESI, MeOH/$CHCl_3$ (4:1)]: *m/z* = 604.5 (100%, [M − H]⁻), 640.5 (20%, [M − Cl]⁻); analysis calcd for $C_{39}H_{56}FNO_3$ (605.88): C 77.31, H 9.32, N 2.31; found: C 77.06, H 9.57, N 1.95.

4.3.9. 3β-Acetyloxy-N-[(4-fluorophenylmethyl)]-lup-20(29)en-28-amide (8)

Following GP; yield: 78%; m.p. 128–131 °C (from ethyl acetate/*n*-hexane); $R_F = 0.17$ (SiO_2, *n*-hexane/ethyl acetate, 9:1); $[\alpha]_D = +23.8°$ (*c* = 0.182, $CHCl_3$); IR (KBr): ν = 3371w, 2943 m, 1733 m, 1640 m, 1509s, 1368 m, 1243vs, 1155 m, 1026 m, 979 m, 882 m, 834 m, 487 m cm^{-1}; UV–Vis ($CHCl_3$): λ_{max} (log ε) = 265 (3.93), 272 (3.87) nm; ^{1}H NMR (400 MHz, $CDCl_3$): δ = 7.29–7.20 (m, 2H, 35-H + 39-H), 7.05–6.94 (m, 2H, 36-H + 38-H), 5.91 (*dd*, *J* = 5.9, 5.9 Hz, 1H, N*H*), 4.74 (d, *J* = 2.4 Hz, 1H, 29-H_a), 4.62–4.57 (m, 1H, 29-H_b), 4.50–4.41 (m, 2H, 3-H + 33H_a), 4.30 (*dd*, *J* = 14.7, 5.7 Hz, 1H, 33-H_b), 3.15 (*td*, *J* = 11.1, 4.2 Hz, 1H, 19-H), 2.52–2.41 (m, 1H, 13-H), 2.03 (s, 3H, 32-H), 2.02–1.85 (m, 2H, 21-H_a + 16-H_a), 1.74 (m, 2H, 22-H_a + 12-H_a), 1.68 (s, 3H, 30-H), 1.66–0.96 (m, 18H, 1-H + 2-H + 18-H + 16-H_b + 6-H + 11-H + 7-H + 15-H, 21-H_b + 9-H + 22-H_b + 12-H_b), 0.95 (s, 3H, 27-H), 0.88 (s, 3H, 26-H), 0.88–0.81 (m, 9H, 25-H + 24-H + 23-H), 0.81–0.73 (m, 1H, 5-H) ppm; ^{13}C NMR (101 MHz, $CDCl_3$): δ = 176.1 (C-28), 171.2 (C-31), 162.2 (*d*, *J* = 245.5 Hz, C-37), 151.0 (C-20), 135.2 (*d*, *J* = 3.1 Hz, C-34), 129.6 (*d*, *J* = 8.1 Hz, C-35, C-39), 115.6 (*d*, *J* = 21.4 Hz, C-36, C-38), 109.6 (C-29), 81.1 (C-3), 55.8 (C-17), 55.6 (C-5), 50.7 (C-9), 50.3 (C-18), 46.9 (C-19), 42.7 (C-14), 42.6 (C-33), 40.9 (C-8), 38.6 (C-1), 38.5 (C-22), 38.0 (C-4), 37.9 (C-13), 37.3 (C-10), 34.5 (C-7), 33.9 (C-16), 31.0 (C-21), 29.6 (C-15), 28.1 (C-23), 25.8 (C-12), 23.9 (C-2), 21.5 (C-32), 21.1 (C-11), 19.6 (C-30), 18.3 (C-6), 16.6 (C-24), 16.4 (C-25), 16.3 (C-26), 14.8 (C-27) ppm; MS [ESI, MeOH/$CHCl_3$ (4:1)]: *m/z* = 604.5 (100%, [M − H]⁻), 640.6 (14%, [M − Cl]⁻); analysis calcd for $C_{39}H_{56}FNO_3$ (605.88): C 77.31, H 9.32, N 2.31; found: C 77.11, H 9.47, N 2.03.

4.3.10. 3β-Acetyloxy-N-[(2-methoxyphenylmethyl)]-lup-20(29)en-28-amide (9)

Following GP; yield: 64%; m.p. 127–131 °C (from ethyl acetate/*n*-hexane); $R_F = 0.22$ (SiO_2, *n*-hexane/ethyl acetate, 9:1); $[\alpha]_D = +33.9°$ (*c* = 0.175, $CHCl_3$); IR (KBr): ν = 2942 m, 1733 m, 1640 m, 1492 m, 1367 m, 1240vs, 1028 m, 979 m, 881 m, 750 s cm^{-1}; UV–Vis ($CHCl_3$): λ_{max} (log ε) = 272 (4.33), 277 (4.30) nm; ^{1}H NMR (400 MHz, $CDCl_3$): δ = 7.30–7.20 (m, 2H, 37-H + 39-H), 6.94–6.83 (m, 2H, 36-H + 38-H), 6.18 (*dd*, *J* = 5.9, 5.9 Hz, 1H, N*H*), 4.72 (d, *J* = 2.4 Hz, 1H, 29-H_a), 4.61–4.55 (m, 1H, 29-H_b), 4.49–4.32 (m, 3H, 3-H + 33-H), 3.85 (s, 3H, 40-H), 3.11 (*td*, *J* = 11.1, 4.0 Hz, 1H, 19-H), 2.34 (*ddd*, *J* = 12.8, 11.4, 3.6 Hz, 1H, 13-H), 2.03 (s, 3H, 32-H), 2.00–1.86 (m, 2H, 16-H_a + 21-H_a), 1.78–1.70 (m, 1H, 22-H_a),1.68 (s, 3H, 30-H) 1.66–0.93 (m, 19H, 1-H + 2-H + 12-H + 18-H + 16-H_b + 6-H + 22-H_b + 7-H + 11-H + 21-H_b + 15-H + 9-H), 0.92 (s, 3H, 27-H), 0.84–0.78 (m, 9H, 25-H + 24-H + 23-H), 0.78–0.71 (m,

1H, 5-H), 0.67 (s, 3H, 26-H) ppm; ^{13}C NMR (101 MHz, $CDCl_3$): δ = 176.0 (C-28), 171.1 (C-31), 157.6 (C-35), 151.2 (C-20), 130.2 (C-37), 128.8 (C-39), 127.1 (C-34), 120.9 (C-38), 110.3 (C-36), 109.4 (C-29), 81.1 (C-3), 55.9 (C-17), 55.6 (C-5), 55.4 (C-40), 50.6 (C-9), 50.2 (C-18), 47.1 (C-19), 42.6 (C-14), 40.8 (C-8), 39.6 (C-33), 38.5 (C-1), 38.4 (C-22), 37.9 (C-4), 37.9 (C-13), 37.2 (C-10), 34.4 (C-7), 34.0 (C-16), 31.0 (C-21), 29.4 (C-15), 28.1 (C-23), 25.7 (C-12), 23.8 (C-2), 21.4 (C-32), 21.1 (C-11), 19.6 (C-30), 18.3 (C-6), 16.6 (C-24), 16.3 (C-25), 15.9 (C-26), 14.7 (C-27) ppm; MS [ESI, MeOH/$CHCl_3$ (4:1)]: *m/z* = 616.7 (100%, $[M - H]^-$); analysis calcd for $C_{40}H_{59}NO_4$ (617.92): C 77.75, H 9.62, N 2.27; found: C 77.48, H 9.82, N 2.11.

4.3.11. 3β-Acetyloxy-N-[(3-methoxyphenylmethyl)]-lup-20(29)en-28-amide (10)

Following GP; yield: 62%; m.p. 124–127 °C (from ethyl acetate/*n*-hexane); R_F = 0.17 (SiO_2, *n*-hexane/ethyl acetate, 9:1); $[\alpha]_D$ = +16.8° (*c* = 0.180, $CHCl_3$); IR (KBr): *ν* = 3359w, 2943 m, 1733 m, 1639 m, 1453 m, 1368 m, 1243vs, 1182 m, 1027 m, 979 m, 881 m, 734 m, 692 m cm^{-1}; UV–Vis ($CHCl_3$): λ_{max} (log *ε*) = 274 (4.32), 281 (4.29) nm; ^{1}H NMR (400 MHz, $CDCl_3$): *δ* = 7.28–7.19 (m, 1H, 38-H), 6.90–6.83 (m, 1H, 39-H), 6.83–6.77 (m, 2H, 35-H + 37-H), 5.87 (*dd*, *J* = 5.8, 5.8 Hz, 1H, N*H*), 4.74 (d, *J* = 2.3 Hz, 1H, 29-H_a), 4.63–4.56 (m, 1H, 29-H_b), 4.51–4.32 (m, 3H, 3-H + 33-H), 3.79 (s, 3H, 40-H), 3.16 (*td*, *J* = 11.1, 4.1 Hz, 1H, 19-H), 2.50 (*ddd*, *J* = 12.8, 11.4, 3.6 Hz, 1H, 13-H), 2.03 (s, 3H, 32-H), 2.02–1.88 (m, 2H, 21-H_a + 16-H_a), 1.80–1.71 (m, 2H, 22-H_a + 12-H_a), 1.69 (d, *J* = 1.4 Hz, 3H, 30-H), 1.67–0.97 (m, 18H, 1-H + 2-H + 18-H + 16-H_b + 15-H + 6-H + 21-H_b + 7-H + 11-H_a + 11-H_b + 9-H + 12-H_b + 22-H_b), 0.95 (s, 3H, 27-H), 0.91 (s, 3H, 26-H), 0.86–0.81 (m, 9H, 25-H + 24-H + 23-H), 0.81–0.73 (m, 1H, 5-H) ppm; ^{13}C NMR (101 MHz, $CDCl_3$): *δ* = 176.0 (C-28), 171.1 (C-31), 160.0 (C-36), 151.1 (C-20), 140.9 (C-34), 129.8 (C-38), 120.1 (C-39), 113.3 (C-37), 113.1 (C-35), 109.6 (C-29), 81.1 (C-3), 55.8 (C-17), 55.6 (C-5), 55.3 (C-40), 50.7 (C-9), 50.3 (C-18), 46.8 (C-19), 43.4 (C-33), 42.6 (C-14), 40.9 (C-8), 38.6 (C-1), 38.6 (C-22), 37.9 (C-4), 37.8 (C-13), 37.3 (C-10), 34.5 (C-7), 33.9 (C-16), 31.0 (C-21), 29.6 (C-15), 28.1 (C-23), 25.8 (C-12), 23.9 (C-2), 21.4 (C-32), 21.1 (C-11), 19.6 (C-30), 18.3 (C-6), 16.6 (C-24), 16.4 (C-25), 16.3 (C-26), 14.7 (C-27) ppm; MS [ESI, MeOH/$CHCl_3$ (4:1)]: *m/z* = 616.6 (100%, $[M - H]^-$); analysis calcd for $C_{40}H_{59}NO_4$ (617.92): C 77.75, H 9.62, N 2.27; found: C 75.47, H 9.81, N 1.96.

4.3.12. 3β-Acetyloxy-N-[(4-methoxyphenylmethyl)]-lup-20(29)en-28-amide (11)

Following GP; yield: 67%; m.p. 125–129 °C (from ethyl acetate/*n*-hexane); R_F = 0.14 (SiO_2, *n*-hexane/ethyl acetate, 9:1); $[\alpha]_D$ = +21.2° (*c* = 0.175, $CHCl_3$); IR (KBr): *ν* = 2943 m, 1732 m, 1640 m, 1512s, 1465 m, 1368 m, 1243vs, 1174 m, 1108w, 1029 m, 979 m, 883w, 829w, 511w cm^{-1}; UV–Vis ($CHCl_3$): λ_{max} (log *ε*) = 277 (4.22) nm; ^{1}H NMR (400 MHz, $CDCl_3$): *δ* = 7.24–7.16 (m, 2H, 35-H + 39-H), 6.89–6.81 (m, 2H, 36-H + 38-H), 5.84–5.77 (m, 1H, N*H*), 4.74 (d, *J* = 2.4 Hz, 1H, 29-H_a), 4.62–4.56 (m, 1H, 29-H_b), 4.51–4.37 (m, 2H, 3-H + 33-H_a), 4.29 (*dd*, *J* = 14.5, 5.4 Hz, 1H, 33-H_b), 3.80 (s, 3H, 40-H), 3.17 (*td*, *J* = 11.0, 4.0 Hz, 1H, 19-H), 2.49 (*ddd*, *J* = 12.9, 11.5, 3.6 Hz, 1H, 13-H), 2.03 (s, 3H, 32-H), 2.02–1.90 (m, 1H, 21-H_a), 1.90–1.84 (m, 1H, 16-H_a), 1.79–1.70 (m, 2H, 22-H_a + H-12$_a$), 1.68 (s, 3H, 30-H), 1.67–0.96 (m, 18H, 1-H + 2-H + 18-H + 16-H_b + 6-H + 15-H + 7-H + 11-H + 21-H_b + 9-H + 12-H_b + 22-H_b), 0.95 (s, 3H, 27-H), 0.91 (s, 3H, 26-H), 0.86–0.81 (m, 9H, 25-H + 24-H + 23-H), 0.80–0.75 (m, 1H, 5-H) ppm; ^{13}C NMR (101 MHz, $CDCl_3$): *δ* = 176.0 (C-28), 171.2 (C-31), 159.1 (C-37), 151.1 (C-20), 131.5 (C-34), 129.2 (C-35, C-39), 114.2 (C-36, C-38), 109.5 (C-29), 81.1 (C-3), 55.8 (C-17), 55.6 (C-5), 55.5 (C-40), 50.7 (C-9), 50.3 (C-18), 46.9 (C-19), 42.9 (C-33), 42.7 (C-14), 40.9 (C-8), 38.6 (C-1), 38.6 (C-22), 38.0 (C-4), 37.9 (C-13), 37.3 (C-10), 34.5 (C-7), 33.9 (C-16), 31.0 (C-21), 29.6 (C-15), 28.1 (C-23), 25.8 (C-12), 23.9 (C-2), 21.5 (C-32), 21.1 (C-11), 19.6 (C-30), 18.3 (C-6), 16.6 (C-24), 16.4 (C-25), 16.3 (C-26), 14.8 (C-27) ppm; MS [ESI, MeOH/$CHCl_3$ (4:1)]: *m/z* = 616.6 (100%, $[M - H]^-$); analysis calcd for $C_{40}H_{59}NO_4$ (617.92): C 77.75, H 9.62, N 2.27; found: C 77.58, H 9.88, N 2.06.

4.3.13. 3β-Acetyloxy-N-[(2-methylphenylmethyl)]-lup-20(29)en-28-amide (12)

Following GP; yield: 86%; m.p. 128–132 °C (from ethyl acetate/*n*-hexane); R_F = 0.28 (SiO_2, *n*-hexane/ethyl acetate, 9:1); $[\alpha]_D$ = +20.4° (*c* = 0.169, $CHCl_3$); IR (KBr): *ν* = 3377w, 2943 m, 1734 m, 1640 m, 1463 m, 1367 m, 1243vs, 1027 m, 979 m, 882 m, 738 s cm^{-1}; UV–Vis ($CHCl_3$): λ_{max} (log *ε*) = 263 (3.55) nm; ^{1}H NMR (400 MHz, $CDCl_3$): *δ* = 7.27–7.19 (m, 2H, 39-H + 37-H), 7.19–7.12 (m, 2H, 36-H + 38-H), 5.66 (*dd*, *J* = 5.3, 5.3 Hz, 1H, N*H*), 4.74 (d, *J* = 2.4 Hz, 1H, 29-H_a), 4.63–4.57 (m, 1H, 29-H_b), 4.51–4.35 (m, 3H, 3-H + 33-H), 3.17 (*td*, *J* = 11.0, 4.1 Hz, 1H, 19-H), 2.51 (*ddd*, *J* = 12.9, 11.3, 3.6 Hz, 1H, 13-H), 2.33 (s, 3H, 40-H), 2.03 (s, 3H, 32-H), 2.03–1.93 (m, 1H, 21-H_a), 1.89 (m, 1H, 16-H_a), 1.80–1.71 (m, 2H, 22-H_a+ 12-H_a), 1.69 (s, 3H, 30-H), 1.67–0.96 (m, 18H, 1-H + 2-H + 16-H_b + 18-H + 15-H + 6-H + 7-H + 11-H + 21-H_b + 9-H + 12-H_b + 22-H_b), 0.95 (s, 3H, 27-H), 0.91 (s, 3H, 26-H), 0.87–0.81 (s, 9H, 25-H + 24-H + 23-H), 0.81–0.74 (m, 1H, 5-H) ppm; ^{13}C NMR (101 MHz, $CDCl_3$): *δ* = 175.9 (C-28), 171.1 (C-31), 151.1 (C-20), 136.6 (C-34), 136.5 (C-35), 130.7 (C-36), 128.8 (C-39), 127.8 (C-37), 126.3 (C-38), 109.6 (C-29), 81.1 (C-3), 55.9 (C-17), 55.6 (C-5), 50.7 (C-9), 50.4 (C-18), 46.8 (C-19), 42.6 (C-14), 41.6 (C-33), 40.9 (C-8), 38.6 (C-1), 38.6 (C-22), 38.0 (C-4), 37.8 (C-13), 37.3 (C-10), 34.5 (C-7), 34.0 (C-16), 31.1 (C-21), 29.6 (C-15), 28.1 (C-23), 25.8 (C-12), 23.9 (C-2), 21.5 (C-32), 21.1 (C-11), 19.6 (C-30), 19.1 (C-40), 18.4 (C-6), 16.6 (C-24), 16.4 (C-25), 16.3 (C-26), 14.7 (C-27) ppm; MS [ESI, MeOH/$CHCl_3$ (4:1)]: *m/z* = 600.7 (100%, $[M - H]^-$), 636.8 (5%, $[M - Cl]^-$); analysis calcd for $C_{40}H_{59}NO_3$ (601.92): C 79.82, H 9.88, N 2.33; found: C 79.65, H 10.04, N 2.00.

4.3.14. 3β-Acetyloxy-N-[(3-methylphenylmethyl)]-lup-20(29)en-28-amide (13)

Following GP; yield: 89%; m.p. 109–113 °C (from ethyl acetate/*n*-hexane); R_F = 0.27 (SiO_2, *n*-hexane/ethyl acetate, 9:1); $[\alpha]_D$ = +26.0° (*c* = 0.132, $CHCl_3$); IR (KBr): *ν* = 2943 m, 1734 m, 1640 m, 1450 m, 1368 m, 1243vs, 1026 m, 979 m, 881 m, 764 m, 442w cm^{-1}; UV–Vis ($CHCl_3$): λ_{max} (log *ε*) = 265 (3.55), 272 (3.42) nm; ^{1}H NMR (400 MHz, $CDCl_3$): *δ* = 7.21 (*dd*, *J* = 7.5, 7.5 Hz, 1H, 38-H), 7.12–7.03 (m, 3H, 35-H + 37-H + 39-H), 5.87 (*dd*, *J* = 5.7, 5.7 Hz, 1H, N*H*), 4.74 (d, *J* = 2.4 Hz, 1H, 29-H_a 4.62–4.57 (m, 1H, 29-H_b), 4.51–4.41 (m, 2H, 3-H + 33-H_a), 4.31 (*dd*, *J* = 14.6, 5.5 Hz, 1H, 33-H_b), 3.17 (*td*, *J* = 11.0, 4.1 Hz, 1H, 19-H), 2.50 (m, 1H, 13-H), 2.33 (s, 3H, 40-H), 2.03 (s, 3H, 32-H), 1.93 (m, 2H, 21-H_a + 16-H_a), 1.81–1.71 (m, 2H, 22-H_a + 12-H_a), 1.69 (s, 3H, 30-H), 1.67–0.97 (m, 18H, 2-H + 1-H + 18-H + 16-H_b + 21-H_b + 6-H + 15-H + 7-H + 11-H + 9-H + 12-H_b + 22-H_b), 0.96 (s, 3H, 27-H), 0.92 (s, 3H, 26-H), 0.90–0.81 (m, 9H, 25-H + 24-H + 23-H), 0.81–0.74 (m, 1H, 5-H ppm; ^{13}C NMR (101 MHz, $CDCl_3$): *δ* = 175.8 (C-28), 171.0 (C-31), 150.9 (C-20), 139.1 (C-34), 138.3 (C-36), 128.5 (C-38, C-35), 128.0 (C-37), 124.8 (C-39), 109.4 (C-29), 80.9 (C-3), 55.7 (C-17), 55.5 (C-5), 50.6 (C-9), 50.2 (C-18), 46.7 (C-19), 43.2 (C-33), 42.5 (C-14), 40.8 (C-8), 38.4 (C-1), 38.4 (C-22), 37.8 (C-4), 37.7 (C-13), 37.1 (C-10), 34.4 (C-7), 33.8 (C-16), 30.9 (C-21), 29.4 (C-16), 27.9 (C-23), 25.6 (C-12), 23.7 (C-2),21.4 (C-40), 21.3 (C-32), 21.0 (C-11), 19.5 (C-30), 18.2 (C-6), 16.5 (C-24), 16.2 (C-25), 16.2 (C-26), 14.6 (C-27) ppm; MS [ESI, MeOH/$CHCl_3$ (4:1)]: *m/z* = 600.5 (100%, $[M - H]^-$), 638.4 (15%, $[M - Cl]^-$); analysis calcd for $C_{40}H_{59}NO_3$ (601.92): C 79.82, H 9.88, N 2.33; found: C 70.66, H 10.2, N 2.19.

4.3.15. 3β-Acetyloxy-N-[(4-methylphenylmethyl)]-lup-20(29)en-28-amide (14)

Following GP; yield: 60%; m.p. 134–137 °C (from ethyl acetate/*n*-hexane); R_F = 0.26 (SiO_2, *n*-hexane/ethyl acetate, 9:1); $[\alpha]_D$ = +21.2° (*c* = 0.175, $CHCl_3$); IR (KBr): *ν* = 2943 m, 1734 m, 1640 m, 1515 m, 1367 m, 1243vs, 1023 m, 979 m, 882 m, 751 m, 474w cm^{-1}; UV–Vis ($CHCl_3$): λ_{max} (log *ε*) = 265 (3.63), 274 (3.52) nm; ^{1}H NMR (500 MHz, $CDCl_3$): *δ* =

7.16 (d, $J = 8.1$ Hz, 2H, 35-H + 39-H), 7.13 (d, $J = 8.0$ Hz, 2H, 36-H + 38-H), 5.83 (*dd*, $J = 5.7$, 5.7 Hz, 1H, N*H*), 4.74 (d, $J = 2.3$ Hz, 1H, 29-H_a), 4.62–4.57 (m, 1H, 29-H_b), 4.50–4.40 (m, 2H, 3-H_a + 33-H_a), 4.32 (*dd*, $J = 14.6$, 5.5 Hz, 1H, 33-H_b), 3.17 (*td*, $J = 11.1$, 4.3 Hz, 1H, 19-H), 2.54–2.45 (m, 1H, 13-H), 2.34 (s, 3H, 40-H), 2.03 (s, 3H, 32-H), 2.02–1.93 (m, 1H, 21-H_a), 1.90 (*dt*, $J = 13.5$, 3.2 Hz, 1H, 16-H_a), 1.79–1.71 (m, 2H, 22-H_a + 12-H_a), 1.68 (s, 3H, 30-H), 1.67–0.97 (m, 18H, 1-H + 2-H + 18-H + 16-H_b + 6-H + 15-H + 11-H+ 21-H_b + 7-H + 9-H + 12-H_b + 22-H_b), 0.95 (s, 3H, 27-H), 0.92 (s, 3H, 26-H), 0.87–0.82 (m, 9H, 25-H + 24-H + 23-H), 0.81–0.75 (m, 1H, 5-H) ppm; ^{13}C NMR (126 MHz, $CDCl_3$): $\delta = 176.0$ (C-28), 171.1 (C-31), 151.1 (C-20), 137.1 (C-34), 136.3 (C-37), 129.5 (C-36, C-38), 127.9 (C-35, C-39), 109.5 (C-29), 81.1 (C-3), 55.8 (C-17), 55.6 (C-5), 50.7 (C-9), 50.3 (C-18), 46.9 (C-19), 43.2 (C-33), 42.6 (C-14), 40.9 (C-8), 38.6 (C-1), 38.6 (C-22), 38.0 (C-4), 37.9 (C-13), 37.3 (C-10), 34.5 (C-7), 33.9 (C-16), 31.0 (C-21), 29.6 (C-15), 28.1 (C-23), 25.8 (C-12), 23.9 (C-2), 21.4 (C-32), 21.2 (C-40), 21.1 (C-11), 19.6 (C-30), 18.4 (C-6), 16.6 (C-24), 16.4 (C-25), 16.3 (C-26), 14.8 (C-27) ppm; MS [ESI, MeOH/$CHCl_3$ (4:1)]: $m/z = 600.7$ (100%, $[M - H]^-$), 636.8 (8%, $[M - Cl]^-$); analysis calcd for $C_{40}H_{59}NO_3$ (601.92): C 79.82, H 9.88, N 2.33; found: C 79.64, H 10.07, N 1.97.

Acknowledgment

We like to thank Dr D. Ströhl and his team for the NMR spectra, Th. Schmidt for the MS spectra, and Mr. M. Schneider for measuring IR and UV/vis spectra as well as optical rotations and micro-analyses. The cell lines were provided by Dr. Th. Müller (Dept. Oncology, Martin-Luther-University Halle-Wittenberg). Experimental help in the lab was provided by Ms V. Karsten.

Appendix A. Supplementary data

Supplementary data to this article can be found online at https://doi.org/10.1016/j.ejmcr.2021.100016.

References

[1] G. Ehninger, U. Schuler, H.D. Waller, Pharmacokinetic aspects in the use of new cytostatic drugs, Onkologie 10 (1987) 218–224.
[2] H. Sung, J. Ferlay, R.L. Siegel, M. Laversanne, I. Soerjomataram, A. Jemal, F. Bray, Global cancer statistics 2020: GLOBOCAN estimates of incidence and mortality worldwide for 36 cancers in 185 countries, CA, A Cancer Journal for Clinicians 71 (2021) 209–249.
[3] S. Schwarz, A. Loesche, S.D. Lucas, S. Sommerwerk, I. Serbian, B. Siewert, E. Pianowski, R. Csuk, Converting maslinic acid into an effective inhibitor of acylcholinesterases, Eur. J. Med. Chem. 103 (2015) 438–445.
[4] B. Siewert, E. Pianowski, A. Obernauer, R. Csuk, Towards cytotoxic and selective derivatives of maslinic acid, Bioorg. Med. Chem. 22 (2014) 594–615.
[5] S. Sommerwerk, L. Heller, J. Kuhfs, R. Csuk, Urea derivates of ursolic, oleanolic and maslinic acid induce apoptosis and are selective cytotoxic for several human tumor cell lines, Eur. J. Med. Chem. 119 (2016) 1–16.
[6] I.Z. Pavel, R. Csuk, C. Danciu, S. Avram, F. Baderca, A. Cioca, E.-A. Moaca, C.-V. Mihali, I. Pinzaru, D.M. Muntean, C.A. Dehelean, Assessment of the antiangiogenic and anti-inflammatory properties of a maslinic acid derivative and its potentiation using zinc chloride, Int. J. Mol. Sci. 20 (2019) 2828.
[7] I.Z. Pavel, C. Danciu, S. Avram, R. Csuk, F. Baderca, A. Cioca, E.-A. Moaca, I. Pinzaru, C.A. Dehelean, C.-V. Mihali, D.M. Muntean, D.M. Muntean, Assessment of the antiangiogenic and anti-inflammatory properties of a maslinic acid derivative and its potentiation using zinc chloride, Int J Mol Sci 20 (2019).
[8] I.Z. Pavel, C. Danciu, C. Oprean, C.A. Dehelean, D. Muntean, R. Csuk, D.M. Muntean, In vitro evaluation of the antimicrobial ability and cytotoxicity on two melanoma cell lines of a benzylamide derivative of maslinic acid, Anal. Cell. Pathol. (2016), 2787623, https://doi.org/10.1155/2016/2787623.
[9] I.Z. Pavel, C.A. Dehelean, L. Farczadi, D.M. Muntean, L. Vlase, C. Danciu, R. Csuk, F. Birsasteanu, D.M. Muntean, Assessment of a maslinic acid derivative and its metabolite in rat blood by liquid chromatography coupled with mass spectrometry, Rev. Chim. (Bucharest, Rom.) 68 (2017) 1089–1094.
[10] I.Z. Pavel, A.E. Parvu, C.A. Dehelean, L. Vlase, R. Csuk, D.M. Muntean, Assessment of the antioxidant effect of a maslinic acid derivative in an experimental model of acute inflammation, Farmacia (Bucharest, Rom.) 65 (2017) 390–395.
[11] M. Urban, J. Sarek, J. Klinot, G. Korinkova, M. Hajduch, Synthesis of A-seco derivatives of betulinic acid with cytotoxic activity, J. Nat. Prod. 67 (2004) 1100–1105.
[12] J. Wiemann, L. Heller, V. Perl, R. Kluge, D. Stroehl, R. Csuk, Betulinic acid derived hydroxamates and betulin derived carbamates are interesting scaffolds for the synthesis of novel cytotoxic compounds, Eur. J. Med. Chem. 106 (2015) 194–210.
[13] S. Hoenke, N.V. Heise, M. Kahnt, H.-P. Deigner, R. Csuk, Betulinic acid derived amides are highly cytotoxic, apoptotic and selective, Eur. J. Med. Chem. 207 (2020) 112815.

P4

Publikation P-4: Synthesis and cytotoxicity of betulin and betulinic acid derived 30-oxo-amides

Marie Kozubek, Sophie Hoenke, Theresa Schmidt, Hans-Peter Deigner, Ahmed Al-Harrasi, René Csuk *Steroids* 2022 109014,0039-128X
S. 1 - 10

Link: https://doi.org/10.1016/j.steroids.2022.109014

P5

Platanic acid derived amides are more cytotoxic than their corresponding oximes

Marie Kozubek, Sophie Hoenke, Theresa Schmidt, Dieter Ströhl, René Csuk*

Martin–Luther–University Halle–Wittenberg, Organic Chemistry, Kurt–Mothes–Str. 2, D–06120 Halle (Saale), Germany.

* Corresponding author; rene.csuk@chemie.uni-halle.de

Abstract

Albeit platanic acid has been known since 1956, its potential to act as a valuable starting material for the synthesis of cytotoxic agents has been neglected for many years. Hereby we describe the synthesis of a small library of amides and oximes derived from 3-O-acetyl-platanic acid, and the results of their screening as cytotoxic agents for several human tumor cell lines. As a result, while the cytotoxicity of the oximes was diminished as compared to the parent amides, the homopiperazinyl amide **5** held the highest cytoxicity (EC_{50} = 0.9 μM for A375 human melanoma cells). Extra FACS and cell cycle measurements showed compound **5** to act onto A375 cells rather by apoptosis than by necrosis.

Keywords: Platanic acid, cytotoxicity, SRB assay

Introduction

Platanic acid (**PA**, Fig. 1) is a 20-oxo-30-norlupane analog to betulinic acid. The compound was first isolated by C. Djerassi [1] in 1956; it occurs in several plants, including *Platanus sp.*, *Melaleucas sp.* or *Melilotus sp*.[2] This pentacyclic triterpenoic acid, however, can also be readily obtained in good yields by oxidative cleavage of the *exo*-cyclic double bond of betulinic acid (**BA**) or derivatives thereof. Typically, OsO_4 [3], RuO_4 [4], or ozone [5] have been utilized for this reaction. Its reconversion can be performed by means of a Wittig reaction [6]; this reaction has been used to access labelled **PA** and derivatives thereof.[7]

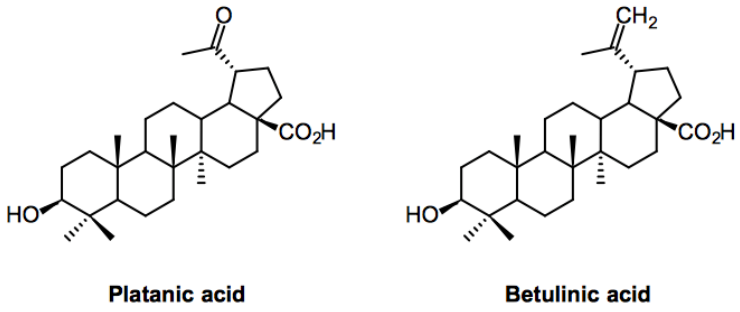

Figure 1. Structures of platanic acid (**PA**) and betulinic acid (**BA**).

Despite the relatively good accessibility of platanic acid, the number of studies and structural modifications has remained relatively small over all these years. This is all the more astonishing since the number of publications on betulinic acid is almost unmanageably large, while less than 100 publications can be found under the keyword "platanic acid" in SciFinder (as of February 2022). This is surprising as several derivatives derived from platanic acid have proven to be strongly cytotoxic or enzyme inhibitors.[8] This included the synthesis of cytotoxic amides [9], access to rhodamine B conjugates that acted as mitocans in several human tumor cell lines even in low nano-molar concentration.[10-13] Several derivatives were potent inhibitors of the enzymes acetyl and butyrylcholinesterase (AChE, BChE)[8] but also of xanthine oxidase.[14, 15] The development of inhibitors for AChE and/or BChE as therapeutics to alleviate the symptoms of neurological disorders such as Alzheimer's disease [16-19], Parkinson [20-26] or Lewy body dementias [27-32] has been in the focus of scientific interest now for many years. Inhibitors of xanthine oxidase are drugs intended for the therapy of hyperuricemia and gout but also for the management of reperfusion injury[33-45]. However, the focus of our own investigations was based on the cytotoxic potential of these compounds

Results and discussion

3-*O*-Acetyl-platanic acid [8] (Scheme 1) was chosen as a starting material for the synthesis of the derivatives. Thus, this very valuable stating material was allowed to react with oxalyl chloride in the presence of catal. amounts of dimethylformamide (DMF) followed by the addition of *N*-methylpiperazine to yield amide **1** in 76% isolated yield. The same procedure was applied for the synthesis of analogs **2** (from ethylenediamine, 87%), **3** (from morpholine, 73%), and **4** (from piperazine, 95%). Activation of **1** with oxalyl chloride followed by the reaction with homopiperazine furnished **5** while from the reaction of **1** with an excess of iodomethane

in dry DCM compound **6** was obtained. Reaction of amides **1**–**4** with hydroxylammonium chloride in dry pyridine at 60 °C for 3h furnished (*E*) configurated oximes **7**–**10**, respectively. A 2D ROESY NMR spectrum (Fig. 2) of compound **9** was recorded to determine the absolute configuration of the oximes **7**-**10**. This spectrum revealed evidence of ROE interactions between the protons from the methyl group (H-29 at δ = 1.66 ppm) with the proton from the hydroxyl group (at δ = 10.04 ppm) indicated by the presence of a ROE cross peak. Based on these results, the oximes hold an (*E*) configuration. This result is in full agreement with previously obtained results. Careful examination of the synthesis of **9** revealed that very small amounts (as indicated via HPTLC-ESI-MS) of (*Z*) configured product were also formed during the reaction, but this material could not be isolated.

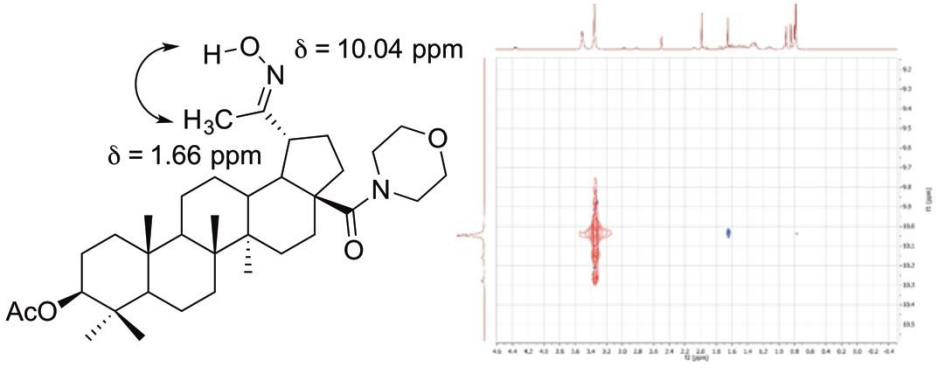

Figure 2. Determination of the absolute configuration of oxime **9** by 2D ROESY NMR.

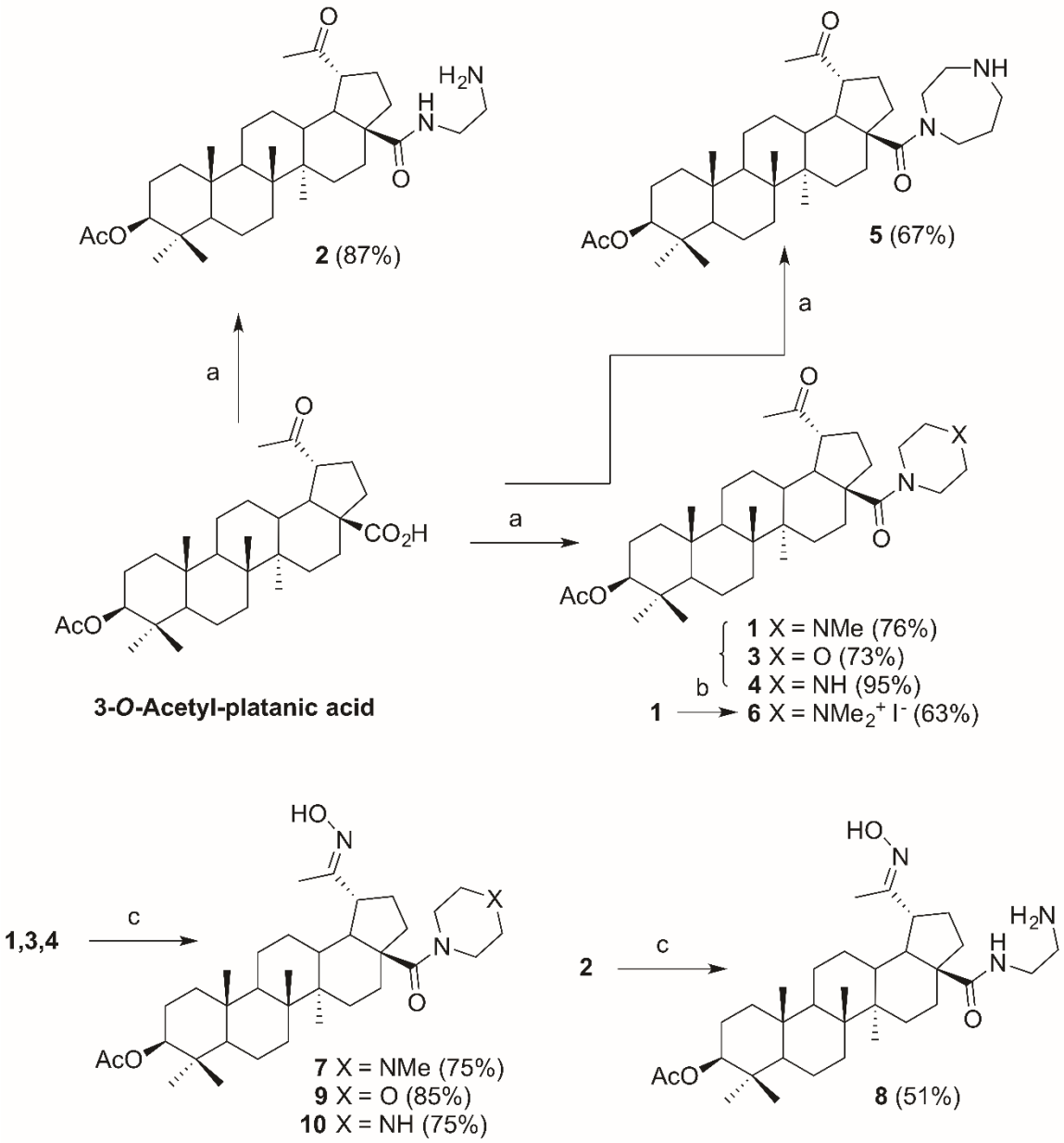

Scheme 1. Reactions and conditions: a) $(COCl)_2$, DCM, DMC (catal.), then *N*-methylpiperazine (→ **1**) or ethylenediamine (→ **2**) or morpholine (→ **3**) or piperazine (→ **4**) or homopiperazine (→ **5**), 3 h, 21 °C; b) MeI, DCM, 24 h, 21 °C; c) hydroxylammonium chloride, pyridine, **1** (→ **7**) or **2** (→ **8**) or **3** (→ **9**) or **4** (→ **10**), 3 h 60 °C,

To assess their cytotoxicity, photometric sulforhodamine B (SRB) assays were performed employing a set of human malignant cell lines (A375, HT29, MCF-7, A2780, HeLa) and non–malignant mouse fibroblasts (NIH 3T3). The results from these assays are compiled in Table 1.

Table 1. SRB assay EC_{50} values [μM] after 72 h of treatment; averaged from three independent experiments performed each in triplicate; confidence interval CI = 95%. Human cancer cell lines: A375 (melanoma), HT29 (colorectal carcinoma), MCF-7 (breast adenocarcinoma), A2780 (ovarian carcinoma), HeLa (cervical cancer), NIH 3T3 (non-malignant fibroblasts), HEK293 (human embryonic kidney cells); cut-off 30 μM, n.s. not soluble, n.d. not determined. Doxorubicin (**DX**) has been used as a positive standard.

Compound	A375	HT29	MCF7	A2780	HeLa	NIH 3T3	HEK293
1	n.s.	n.s.	n.s.	n.s.	n.s.	n.s.	n.s.
2	1.7 ± 0.7	3.8 ± 0.2	3.4 ± 0.2	3.0 ± 0.3	3.7 ± 0.2	1.6 ± 0.6	3.1 ± 0.2
3	n.s.	n.s.	n.s.	n.s.	n.s.	n.s.	n.s.
4	1.9 ± 0.4	3.9 ± 0.2	2.7 ± 0.3	2.6 ± 0.4	2.9 ± 0.4	1.3 ± 0.1	2.7 ± 0.6
5	0.9 ± 0.1	2.3 ± 0.2	1.8 ± 0.2	1.6 ± 0.1	n.d.	0.6 ± 0.1	n.d.
6	n.s.	n.s.	n.s.	n.s.	n.s.	n.s.	n.s.
7	7.9 ± 0.6	11.1 ± 0.3	6.3 ± 0.6	8.1 ± 0.8	9.8 ± 0.6	6.9 ± 0.9	6.1 ± 1.1
8	7.8 ± 1.2	10.1 ± 0.4	8.2 ± 0.4	10.0 ± 0.7	10.0 ± 0.5	5.5 ± 0.6	11.8 ± 1.2
9	9.0 ± 1.4	20.3 ± 1.0	6.8 ± 0.4	10.4 ± 0.8	13.6 ± 0.7	15.4 ± 1.8	7.4 ± 0.4
10	2.2 ± 0.4	4.8 ± 0.4	2.7 ± 0.3	3.5 ± 0.4	4.0 ± 0.2	1.8 ± 0.1	3.8 ± 0.3
DX	n.d.	0.9 ± 0.2	1.1 ± 0.3	0.02 ± 0.01	n.d.	0.06 ± 0.03	n.d.

Amides **2**–**5** were highly cytotoxic for all human tumor cell lines but also for non-malignant NIH 3T3 and HEK293 cells. The highest cytotoxicity was observed for amide **5** holding a homopiperazinyl moiety. This follows previous findings for homopiperazinyl holding derivatives of triterpenoids and their cytotoxicity. This compound showed an EC_{50} value for A375 human melanoma cells as low as 0.9 μM. Compounds **1**, **3** and **6** were not soluble under the conditions of the assay. The cytotoxicity of the oximes was diminished as compared to the cytotoxicity determined for the corresponding amides. Thereby piperazine derived compound **10** showed the lowest EC_{50} value (2.2 ± 0.4 μM) again for A375 tumor cells followed by EC_{50} = 2.7 ± 0.3 μM for human ovarian carcinoma cells A2780.

Extra FACS based investigation (Fig. 3) of compounds **2** and **5** (A375 cells, incubation time 48 h) showed 0.4% of the cells necrotic (R1), 15.5% late-apoptotic (R2) and 3.6% apoptotic (R3), while for **5** the percentage of necrotic cells was also low (0.7%) but the number of apoptotic cells ca. five-times larger (20.8%, R4) than for compound **2**.

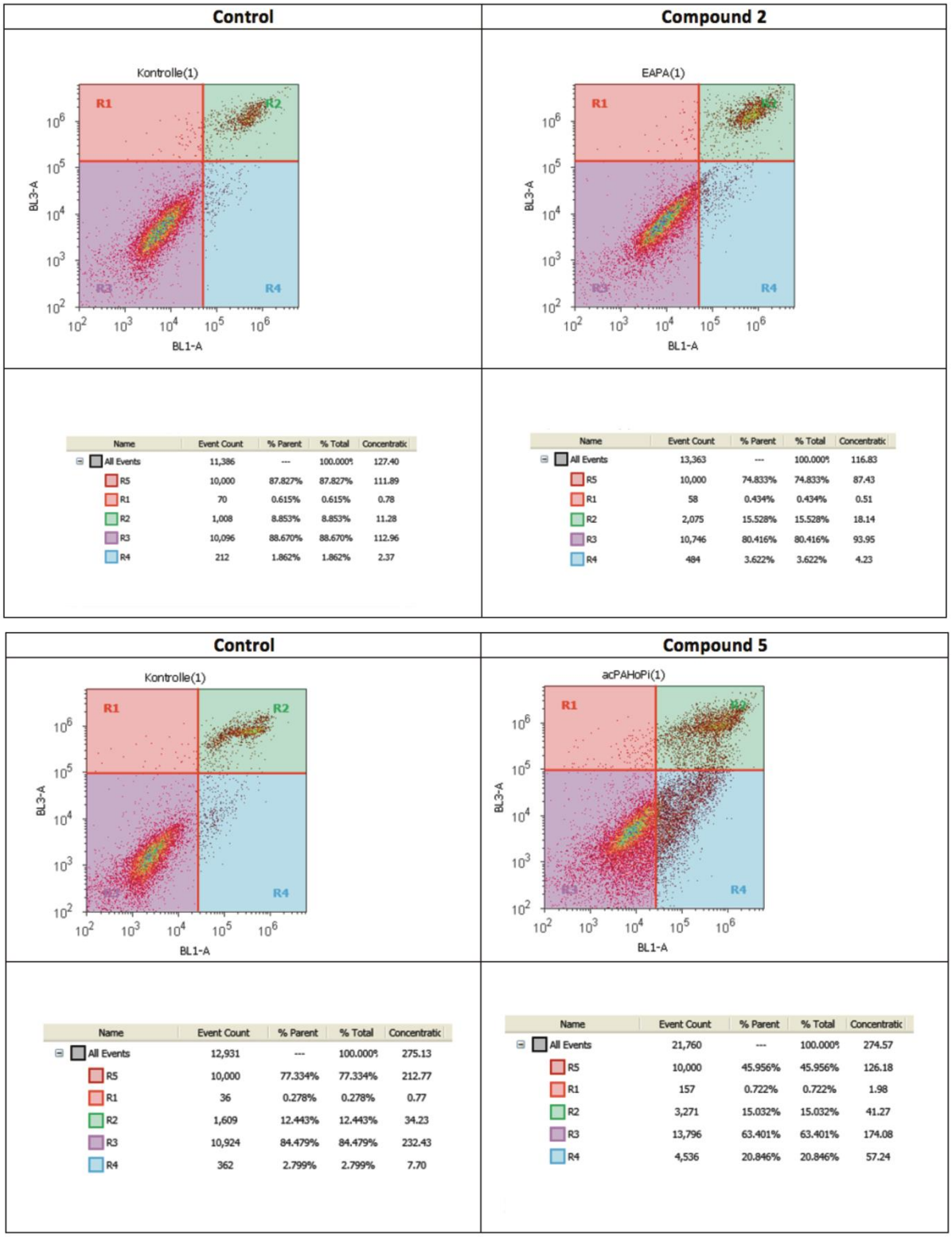

Figure 3. FACS investigation of compounds **2** and **5** (48h incubation, A375 cells).

Investigation of the cell cycle (48 h, A375 cells, Fig. 4) showed for **2** 73.8% of the cells in G1 phase, 15.9% in S, 10.4% in G2/M and 24.5% as apoptotic while for **5** under the same

conditions the percentage of cells in G1 was slightly lowered (65.3%) while those in the S phase were higher (24.4%).

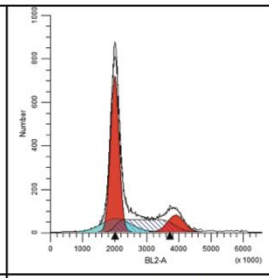
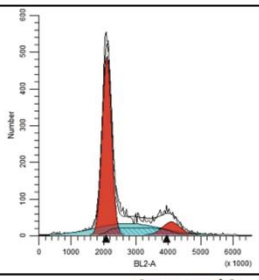
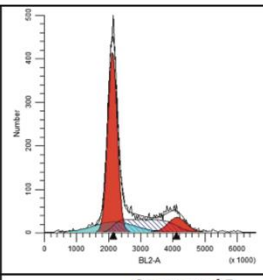

	control	Compound 2	Compound 5
G1	59.9 %	73.8 %	65.3 %
S	27.5 %	15.9 %	24.4 %
G2/M	12.6 %	10.4 %	10.3 %
Apo	15.0 %	24.5 %	13.8 %

Figure 4. Cell cycle investigation for compounds **2** and **5** (incubation 48 h, A375 cells), red G1 G2/M, striped S phase, blue apoptosis.

Conclusion

Long time neglected platanic acid was acetylated and subsequently converted into a variety of amides (**1**–**6**) and their respective oximes (**7**–**10**). Their cytotoxic potential was evaluated in SRB assays employing several human tumor cell lines as well as non-malignant NIH 3T3 and HEK293 cells. As a result, the amides held a higher cytotoxicity than the oximes. The highest cytotoxicity was observed for a homopiperazinyl amide **5** with an EC_{50} = 0.9 µM for human melanoma cells. These results as well as extra FACS and cell cycle measurements reflect that even small changes in the substitution pattern might lead to a significant change in activity and probably in their respective mode of action of these compounds.

Experimental

General

NMR spectra were recorded using the Varian spectrometers DD2 and VNMRS (400 and 500 MHz, respectively). MS spectra were taken on a Advion expression^{L} CMS mass spectrometer (positive ion polarity mode, solvent: methanol, solvent flow: 0.2 mL/min, spray voltage: 5.17 kV, source voltage: 77 V, APCI corona discharge: 4.2 µA, capillary temperature: 250 °C, capillary voltage: 180 V, sheath gas: N_2). Thin-layer chromatography was performed on pre-coated silica gel plates supplied by Macherey-Nagel. IR spectra were recorded on a Spectrum 1000 FT-IR-spectrometer from Perkin Elmer. The UV/Vis-spectra were recorded on a Lambda 14 spectrometer from Perkin Elmer. The optical rotations were measured either on a JASCO P-2000 or a Perkin-Elmer polarimeter at 20 °C. The melting points were determined using the

Leica hot stage microscope Galen III and are uncorrected. The solvents were dried according to usual procedures. Platanic acid was bought from "Betulinines" (Stříbrná Skalice, Czech Republic) and used as received.

Cell lines and culture conditions

Following human cancer cell lines A375 (malignant melanoma), HT29 (colon adenocarcinoma), MCF-7 (breast cancer), A2780 (ovarian carcinoma), HeLa (cervical cancer), NIH 3T3 (non-malignant mouse fibroblasts) and HEK293 (human embryonic kidney cells) were used. All cell lines were obtained from the Department of Oncology (Martin-Luther-University Halle Wittenberg). Cultures were maintained as monolayers in RPMI 1640 medium with L-glutamine (Capricorn Scientific GmbH, Ebsdorfergrund, Germany) supplemented with 10% heat-inactivated fetal bovine serum (Sigma-Aldrich GmbH, Steinheim, Germany) and penicillin/streptomycin (Capricorn Scientific GmbH, Ebsdorfergrund, Germany) at 37 °C in a humidified atmosphere with 5% CO_2.

Cytotoxicity assay (SRB assay)

For the evaluation of the cytotoxicity of the compounds the sulforhodamine-B (Kiton-Red S, ABCR GmbH, Karlsruhe, Germany) micro-culture colorimetric assay was used. The EC_{50} values were averaged from three independent experiments performed each in triplicate and calculated from semi-logarithmic dose-response curves applying a non-linear 4P Hills-slope equation.[10]

General procedure for the synthesis of amides (GPA)

To an ice-cold solution of 3-*O*-acetyl-platanic acid (1.8 g, 3.5 mmol) in dry DCM (20 mL), oxalyl chloride (0.6 mL, 7.0 mmol) and DMF (cat.) were added. After stirring for 3 h at 21 °C, the volatiles were removed under reduced pressure. The residue was dissolved in DCM (25 mL), and at 0 °C 4 equivalents of the corresponding amine were added; stirring at 21 °C was continued for 12 h. Usual aqueous workup followed by chromatographic purification of the crude product yielded the amides.

General procedure for the synthesis of oximes (GPB)

To a solution of the carboxamide in dry pyridine (19 mL), hydroxylammonium chloride was added, and the mixture was stirred at 60 °C for 3h. The solvent was removed under reduced

pressure by co-evaporating with toluene (3 × 20 mL). The residue was fractionated by column chromatography.

*3β-Acetyloxy-N-(1-methylpiperazinyl) 20-oxo-30-norlupan-28-amide (**1**)*

According to GPA with methylpiperazine (1.7 mL, 15.6 mmol) followed by column chromatography (silica gel, *n*-hexane/chloroform/methanol, 5:4.75:0.25) gave **1** (1.8 g, 76 %) as a white solid; m. p. > 300 °C; R_F = 0.22 (*n*-hexane/chloroform/methanol, 5:4.75:0.25); $[\alpha]_D$ = -21.8° (*c* 0.12, $CHCl_3$); IR (ATR): ν = 2988w, 2970m, 2940m, 2867m, 2793m, 1733s, 1716m, 1622s, 1458m, 1413m, 1369m, 1346m, 1300m, 1289m, 1248s, 1222m, 1195m, 1167m, 1143m, 1133m, 1111m, 1077m, 1036m, 1027m, 1009m, 977m, 900m, 782m, 751w, 695m, 656w, 598m, 549w, 509m cm^{-1}; ^1H NMR (500 MHz, $CDCl_3$) δ = 4.45 (dd, *J* = 10.8, 5.4 Hz, 1H), 3.62 (s, 4H, 32-H + 32'-H), 3.22 (dt, *J* = 11.4, 6.0 Hz, 1H), 2.67 (td, *J* = 12.5, 3.8 Hz, 1H), 2.39 (s, 4H, 33-H + 33'-H), 2.32 (s, 3H, 34-H), 2.14 (s, 3H, 29-H), 2.10-2.03 (m, 2H, 16-H_a + 18-H), 2.01 (s, 3H, 31-H), 1.99-1.85 (m, 2H, 22-H_a + 21-H_a), 1.66-1.55 (m, 4H, 1-H_a + 16-H_b + 2-H), 1.50-1.43 (m, 3H, 22-H_b + 21-H_b + 6-H_a), 1.43-1.32 (m, 5H, 11-H_a + 6-H_b + 7-H + 15-H_a), 1.31-1.25 (m, 2H, 11-H_b + 9-H), 1.18-1.13 (m, 1H, 15-H_b), 1.06-1.00 (m, 1H, 12-H_a), 0.98-0.92 (m, 5H, 1-H_b + 27-H + 12-H_b), 0.90 (s, 3H, 26-H), 0.83 (s, 3H, 25-H), 0.82 (s, 3H, 23-H), 0.81 (s, 3H, 24-H), 0.79-0.75 (m, 1H, 5-H) ppm; ^{13}C NMR (126 MHz, $CDCl_3$) δ = 212.9 (C-20), 173.2 (C-28), 170.8 (C-30), 80.8 (C-3), 55.4 (C-5), 55.0 (C-33 + C-33'), 54.3 (C-17), 52.4 (C-18), 50.5 (C-9), 49.9 (C-19), 45.7 (C-34), 41.6 (C-32 + C-32'), 40.5 (C-14), 38.2 (C-1), 37.7 (C-8), 37.0 (C-4 + C-10), 35.8 (C-13), 35.5 (C-22), 34.1 (C-7), 31.9 (C-16), 30.2 (C-29), CH3, 29.7 (C-15), 28.6 (C-21), 27.8 (C-23), 27.4 (C-12), 23.6 (C-2), 21.2 (C-31), 21.0 (C-11), 18.0 (C-6), 16.4 (C-24), 16.1 (C-25), 15.9 (C-26), 14.5 (C-27) ppm; MS (ESI, MeOH:$CHCl_3$, 4:1): m/z 605.4 ($[M+H+Na]^+$, 100%); analysis calcd for $C_{36}H_{58}N_2O_4$ (582.87): C 74.18, H 10.03, N 4.81; found: 73.86, H 10.29, N 4.57.

*3β-Acetyloxy-N-(2-aminoethyl) 20-oxo-30-norlupan-28-amide (**2**)*

According to GPA with ethylenediamine (0.7 mL, 11.0 mmol) followed by chromatography (silica gel, chloroform/methanol/ammonium hydroxide, 9:1:0.1) gave **2** (2.4 g, 87 %) as a white solid; m.p. 230-233 °C (lit.:[46] 231-234 °C); R_F = 0.17 (chloroform/methanol/ammonium hydroxide, 9:1:0.1); $[\alpha]_D$ = -13.9° (*c* 0.13, $CHCl_3$) [lit.:[47] $[\alpha]_D$ = -8.5° (c=0.16, $CHCl_3$); IR (ATR): ν = 2941m, 2866m, 1732m, 1703m, 1633m, 1524m, 1467m, 1449m, 1391m, 1367m, 1317m, 1247s, 1196m, 1163m, 1108w, 1073w, 1028m, 979m, 945m, 901m, 866m, 820w, 753m, 657m, 610m, 556m, 506m cm^{-1}; ^1H NMR (500 MHz, $CDCl_3$) δ = 4.44 (dd, *J* = 10.9, 5.3

Hz, 1H, 3-H), 3.42-3.24 (m, 3H, 19-H + 32-H), 2.86 (t, *J* = 5.9 Hz, 2H, 33-H), 2.21 (td, *J* = 12.0, 4.2 Hz, 1H, 13-H), 2.14 (s, 3H, 29-H), 2.12-2.02 (m, 2H, 18-H + 21-H_a), 2.01 (s, 3H, 31-H), 1.99-1.95 (m, 1H, 16-H_a), 1.81-1.76 (m, 1H, 22-H_a), 1.66-1.56 (m, 4H, 1-H_a + 16-H_b + 2-H), 1.52-1.43 (m, 3H, 22-H_b + 21-H_b + 6-H_a), 1.43-1.34 (m, 4H, 15-H_a + 11-H_a + 6-H_b + 7-H_a), 1.33-1.29 (m, 1H, 7-H_b), 1.28-1.20 (m, 2H, 11-H_b + 9-H), 1.18-1.13 (m, 1H, 15-H_b), 1.10-0.99 (m, 2H, 12-H), 0.97 (s, 3H, 27-H), 0.95-0.91 (m, 1H, 1-H_b), 0.89 (s, 3H, 26-H), 0.83-0.81 (m, 6H, 25-H + 23-H), 0.80 (s, 3H, 24-H), 0.78-0.74 (m, 1H, 5-H); ^{13}C NMR (126 MHz, $CDCl_3$) δ = 213.0 (C-20), 176.8 (C-28), 171.1 (C-30), 81.0 (C-3), 55.7 (C-17), 55.5 (C-5), 51.3 (C-19), 50.5 (C-9), 50.2 (C-18), 42.4 (C-14), 41.5 (C-33), 41.1 (C-32), 40.8 (C-8), 38.5 (C-1), 38.1 (C-22), 37.9 (C-4), 37.2 (C-10), 36.9 (C-13), 34.4 (C-7), 33.0 (C-16), 30.2 (C-29), 29.6 (C-15), 28.7 (C-21), 28.0 (C-23), 27.3 (C-12), 23.8 (C-2), 21.4 (C-31), 21.0 (C-11), 18.3 (C-6), 16.6 (C-24), 16.3 (C-25), 16.2 (C-26), 14.8 (C-27) ppm; MS (ESI, MeOH:$CHCl_3$, 4:1): m/z 541.3 ($[M]^-$, 100%); analysis calcd for $C_{33}H_{54}N_2O_4$ (542.79): C 73.02, H 10.03, N 5.16; found: 72.86, H 10.29, N 46.

*3β-Acetyloxy-N-(4-morpholinyl) 20-oxo-30-norlupan-28-amide (**3**)*

According to GPA with morpholine (1.4 mL, 16.4 mmol) followed by chromatography (silica gel, *n*-hexane/chloroform/acetone, 5:4.75:0.25) gave **3** (1.7 g, 73 %) as a white solid; m.p. 255-258 °C; R_F = 0.17 (*n*-hexane/chloroform/acetone, 5:4.75:0.25); $[\alpha]_D$ = -20.5° (*c* 0.14, $CHCl_3$); IR (ATR): ν = 2943m, 2864m, 1732m, 1709m, 1634s, 1452m, 1409m, 1367m, 1314w, 1263m, 1244s, 1188s, 1173w, 1116s, 1066w, 1031s, 979m, 901w, 844w, 751w, 609w, 598w, 577w, 556w, 507w cm^{-1}; ^{1}H NMR (400 MHz, $CDCl_3$) δ = 4.45 (dd, *J* = 10.5, 5.5 Hz, 1H, 3-H), 3.67-3.53 (m, 8H, 33-H + 33'-H + 32-H + 32'-H), 3.26 – 3.18 (m, 1H, 19-H), 2.68 (td, *J* = 12.2, 4.0 Hz, 1H, 13-H), 2.16 (s, 3H, 29-H), 2.11-2.03 (m, 2H, 16-H_a + 18-H), 2.02 (s, 3H, 31-H), 1.97-1.86 (m, 2H, 22-H_a + 21-H_a), 1.65-1.58 (m, 3H, 1-H_a + 16-H_b + 2-H_a), 1.58-1.45 (m, 4H, 2-H_b + 22-H_b + 21-H_b + 6-H_a), 1.44-1.42 (m, 1H, 11-H_a), 1.41-1.34 (m, 4H, 6-H_b + 7-H + 15-H_a), 1.31-1.23 (m, 2H, 9-H + 11-H_b), 1.21-1.14 (m, 1H, 15-H_b), 1.07-1.01 (m, 1H, 12-H_a), 0.97 (s, 3H, 27-H), 0.96-0.92 (m, 2H, 1-H_b + 12-H_b), 0.91 (s, 3H, 26-H), 0.83 (s, 3H, 25-H), 0.82 (s, 3H, 23-H), 0.82 (s, 3H, 24-H), 0.80-0.76 (m, 1H, 5-H) ppm;^{13}C NMR (101 MHz, $CDCl_3$) δ = 213.0 (C-20), 173.7 (C-28), 171.1 (C-30), 81.0 (C-3), 67.1 (C-33 + C-33' + C-32 + C-32'), 55.6 (C-5), 54.6 (C-17), 52.6 (C-18), 50.8 (C-9), 50.1 (C-19), 41.9 (C-14), 40.7 (C-8), 38.5 (C-1), 37.9 (C-4), 37.3 (C-10), 36.1 (C-13), 35.7 (C-22), 34.4 (C-7), 32.1 (C-16), 30.5 (C-29), 30.0 (C-15), 28.9 (C-21), 28.1 (C-23), 27.6 (C-12), 23.8 (C-2), 21.4 (C-31), 21.3 (C-11), 18.3 (C-6), 16.6 (C-24), 16.4 (C-25), 16.2 (C-26), 14.8 (C-27) ppm; MS (ESI, MeOH:$CHCl_3$, 4:1): m/z

592.5 ($[M+H+Na]^+$, 100%); analysis calcd for $C_{35}H_{55}NO_5$ (569.81): C 73.77, H 9.73, N 2.46; found: C 73.55, H 9.97, N 2.11.

*3β-Acetyloxy-N-(1-piperazinyl) 20-oxo-30-norlupan-28-amide (**4**)*

According to GPA with piperazine (0.7 g, 8.0 mmol) followed chromatography (silica gel, $CHCl_3$/MeOH, 9:1) gave compound **4** (1.1 g, 95 %) as a white solid; m.p. 220-223 °C (lit.:[10]115-125 °C); R_F = 0.15 ($CHCl_3$/MeOH, 9:1); $[\alpha]_D$ = -20.3° (*c* 0.13, $CHCl_3$); IR (ATR): ν = 2941m, 2866m, 1731m, 1709m, 1628s, 1450m, 1413m, 1393m, 1367m, 1318w, 1244s, 1193s, 1163m, 1133m, 1110w, 1102w, 1027s, 979m, 900w, 858w, 803w, 752m, 679w, 659w, 608w, 572w, 552w 507w, 453w cm^{-1}; ^1H NMR (500 MHz, $CDCl_3$) δ = 4.45 (dd, *J* = 10.7, 5.4 Hz, 1H, 3-H), 3.78-3.63 (m, 4H, 32-H + 32'-H), 3.20 (t, *J* = 11.4 Hz, 1H, 19-H), 3.00-2.89 (m, 4H, 32-H + 32'-H), 2.64 (t, *J* = 10.3 Hz, 1H, 13-H), 2.15 (s, 3H, 29-H), 2.10-2.03 (m, 2H, 18-H + 16-H_a), 2.02 (s, 3H, 31-H), 1.94-1.84 (m, 2H, 22-H_a + 21-H_a), 1.67-1.55 (m, 4H, 1-H_a + 16-H_b + 2-H), 1.53-1.45 (m, 3 H, 22-H_b + 6-H_a + 21-H_b), 1.42-1.30 (m, 5H, 11-H_a + 6-H_b + 7-H + 15-H_a), 1-29-1.28 (m, 1H, 9-H), 1.25-1.21 (m, 1H, 11-H_b), 1.20-1.15 (m, 1H, 15-H_b), 1.07-1.00 (m, 1H, 12-H_a), 0.99-0.94 (m, 5H, 1-H_b + 27-H + 12-H_b), 0.90 (s, 3H, 26-H), 0.83 (s, 3H, 25-H), 0.82 (s, 3H, 23-H), 0.81 (s, 3H, 24-H), 0.80-0.75 (m, 1H, 5-H) ppm; ^{13}C NMR (126 MHz, $CDCl_3$): δ = 212.9 (C-20), 173.7 (C-28), 171.1 (C-30), 81.0 (C-3), 58.5 (C-33 + C-33'), 55.6 (C-5), 54.6 (C-17), 52.6 (C-18), 50.7 (C-9), 50.1 (C-19), 45.4 (C-32 + C-32') 41.9 (C-14), 40.7 (C-8), 38.5 (C-1), 37.9 (C-4), 37.3 (C-10), 36.1 (C-13), 35.7 (C-22), 34.3 (C-7), 32.1 (C-16), 30.5 (C-29), 30.0 (C-15), 28.9 (C-21), 28.0 (C-23), 27.6 (C-12), 23.8 (C-2), 21.4 (C-31), 21.3 (C-11), 18.3 (C-6), 16.6 (C-24), 16.4 (C-25), 16.2 (C-26), 14.8 (C-27) ppm; MS (ESI, MeOH:$CHCl_3$, 4:1): m/z 569.6 ($[M]^+$, 100%); analysis calcd for $C_{35}H_{56}N_2O_4$ (568.83): C 73.90, H 9.92, N 4.92; found: C 73.65, H 10.13, N 4.75.

*3β-Acetyloxy-N-(1-homopiperazinyl) 20-oxo-30-norlupan-28-amide (**5**)*

According to GPA with homopiperazine (0.4 g, 4.0 mmol) followed by column chromatography (silica gel, $CHCl_3$/ MeOH, 95:5) gave **5** (387 mg, 67%) as a white solid; m. p. 160-165 °C; R_F = 0.14 ($CHCl_3$/MeOH, 9:1); $[\alpha]_D$ = -29.2° (*c* 0.16, $CHCl_3$); IR (ATR): ν = 2940*m*, 1732*s*, 1622*s*, 1367*m*, 1244*vs*, 979*m*, 750*s* cm^{-1}; ^1H NMR (500 MHz, $CDCl_3$): δ = 4.45 (*dd*, *J* = 10.7, 5.4 Hz, 1H, 3-H), 3.24 (*td*, *J* = 11.4, 3.6 Hz, 1H, 19-H), 3.89 – 2.55 (*m*, 8H, 32-H, 33-H, 34-H, 36-H), 2.73 (*t*, *J* = 12.4 Hz, 1H, 13-H), 2.15 (*s*, 3H, 29-H), 2.14 – 2.02 (*m*, 3H, 16-H_a, 18-H, 22-H_a), 2.02 (*s*, 3H, 31-H), 1.98 – 1.87 (*m*, 1H, 21-H_a), 1.68 – 1.12 (*m*, 17H, 35-H, 1-H_a, 2-H, 16-H_b, 22-H_b, 21-H_b, 6-H, 11-H_a, 7-H, 15-H_a, 9-H, 11-H_b, 15-H_b), 1.06 – 0.99 (*m*,

2H, 12-H), 0.97 (*s*, 3H, 27-H), 0.96 – 0.94 (*m*, 1H, 1-H_b), 0.91 (*s*, 3H, 26-H), 0.82 (*s*, 3H, 25-H), 0.82 (*s*, 3H, 23-H), 0.81 (*s*, 3H, 24-H), 0.79 – 0.74 (*m*, 1H, 5-H); ^{13}C NMR (126 MHz, $CDCl_3$): δ = 213.4 (C-20), 174.7 (C-28), 171.3 (C-30), 81.3 (C-3), 55.9 (C-5), 55.3 (C-17), 53.2 (C-18), 51.0 (C-9), 50.5 (C-19), 42.2 (C-14), 41.0 (C-8), 38.8 (C-1), 38.2 (C-4), 37.5 (C-10), 36.3 (C-13), 36.3 (C-22), 34.6 (C-7), 32.2 (C-16), 30.7 (C-29), 30.3 (C-15), 29.2 (C-21), 28.3 (C-23), 27.8 (C-12), 24.1 (C-2), 21.7 (C-31), 21.6 (C-11), 18.5 (C-6), 16.9 (C-24), 16.6 (C-25), 16.4 (C-26), 15.1 (C-27) ppm; MS (ESI, MeOH): m/z 583.3 ($[M]^+$, 100%); analysis calcd. for $C_{36}H_{58}N_2O_4$ (582.86): C 74.18, H 10.03, N 4.81; found: C 73.82, H 10.31, N 4.56.

*3β-Acetyloxy-N-(1,1-dimethylpiperazin-1-ium-4-yl) 20-oxo-30-norlupan-28-amide iodide (**6**)*

A solution of **1** (1.8 g, 3.0 mmol) and iodomethane (3.2 mL, 51 mmol) in dry DCM (60 mL) was stirred for 1 day at 21 °C. The volatiles were removed under reduced pressure followed by chromatography (silica gel, chloroform/methanol/formic acid, 4.5:0.4:0.1) to afford **6** (1.2 g, 63 %) as a yellowish solid; m.p. 130-231 °C; R_F = 0.27 (chloroform/methanol/formic acid, 4.5:0.4:0.1); $[\alpha]_D$ = -1.3° (*c* 0.13, $CHCl_3$); IR (ATR): ν = 2825m, 2776w, 2740w, 2696w, 1646m, 1578s, 1382m, 1351s, 1227m, 1066m, 790m, 764m, 726m cm^{-1}; ^{1}H NMR (500 MHz, CD_3OD): δ = 4.44-4.39 (m, 1H, 3-H), 4.05-3.89 (m, 4H, 32-H + 32'-H), 3.45 (s, 4H, 33-H + 33'-H), 3.25 (s, 6H, 34-H + 35-H), 3.19-3.11 (m, 1H, 19-H), 2.70-2.61 (m, 1H, 13-H), 2.15 (s, 3H, 29-H), 2.14-2.01 (m, 3H, 21-H_a + 18-H + 22-H_a), 1.99 (s, 3H, 31-H), 1.97-1.88 (m, 1H, 16-H_a), 1.71-1.55 (m, 4H, 1-H_a + 21-H_b + 2-H), 1.55-1.33 (m, 9H, 16-H_b + 22-H_b + 6-H_a + 11-H_a + 6-H_b + 7-H + 15-H_a + 9-H), 1.32-1.23 (m, 2H, 11-H_b + 15-H_b), 1.11-1.05 (m, 1H, 12-H_a), 0.99 (s, 3H, 27-H), 0.98-0.94 (m, 2H, 1-H_b + 12-H_b), 0.92 (s, 3H, 26-H), 0.87 (s, 3H, 25-H), 0.83 (s, 3H, 23-H), 0.83 (s, 3H, 24-H), 0.81-0.78 (m, 1H, 5-H) ppm; ^{13}C NMR (126 MHz, CD_3OD) δ = 215.6 (C-20), 175.6 (C-28), 172.9 (C-30), 82.5 (C-3), 62.4 (C-33 + C-33'), 56.9 (C-5), 55.8 (C-17), 53.9 (C-18), 52.0 (C-34 + C-35), 52.0 (C-9), 51.6 (C-19), 42.9 (C-14), 41.9 (C-8), 39.6 (C-1), 39.5 (C-32 + C-32'), 38.8 (C-4), 38.3 (C-10), 37.4 (C-13), 36.5 (C-22), 35.4 (C-7), 32.8 (C-21), 31.1 (C-15), 29.8 (C-29), 29.7 (C-16), 28.5 (C-12), 28.4 (C-23), 24.6 (C-2), 22.4 (C-11), 21.1 (C-31), 19.2 (C-6), 16.9 (C-24), 16.8 (C-25), 16.6 (C-26), 15.0 (C-27) ppm; MS (ESI, MeOH:$CHCl_3$, 4:1): m/z 597.0 ($[M-I]^+$, 100%); analysis calcd for $C_{37}H_{61}IN_2O_4$ (724.79): C 61.31, H 8.48, N 3.87; found: C 61.03, H 8.67, N 3.58.

*(3β, 20E) 3-Acetyloxy-20-hydroxyimino-N-(1-methylpiperazinyl)-30-norlupan-28-amide (**7**)*

According to GPB from **1** (1.9 g, 3.3 mmol) and hydroxylammonium chloride (1.5 g, 22 mmol) followed by chromatography (silica gel, *n*-hexane/chloroform/methanol, 5:4.5:0.5) **7** (1.5 g, 75

%) was obtained as a white solid; m.p. 295-300 °C; R_F = 0.27 (*n*-hexane/chloroform/methanol, 5:4.5:0.5); $[\alpha]_D$ = + 0.21° (*c* 0.12, MeOH); IR (ATR): ν = 2944m, 2872m, 2686w, 2583w, 2513w, 2452w, 1712m, 1627s, 1456m, 1449m, 1488m, 1373s, 1315w, 1300w, 1249s, 1206m, 1153m, 1130w, 1086w, 1049m, 1025m, 975s, 947m, 911w, 850w, 763m, 746m, 690m, 667m, 606m, 545m, 511m, 476m cm^{-1}; ^1H NMR (500 MHz, DMSO-d_6) δ 4.36 (dd, *J* = 11.6, 4.6 Hz, 1H, 3-H), 3.70-3.30 (m, 6H, 33-H + 33'-H + 32-H), 3.00 – 2.93 (m, 1H, 19-H), 2.93-2.82 (m, 2H, 32'-H), 2.80-2.75 (m, 1H, 13-H), 2.74 (s, 3H, 34-H), 2.10-2.01 (m, 1H, 16-H_a), 1.98 (s, 3H, 31-H), 1.95-1.90 (m, 1H, 22-H_a), 1.77-1.70 (m, 1H, 21-H_a), 1.66 (s, 3H, 29-H), 1.64-1.37 (m, 9H, 18-H + 1-H_a + 2-H_a + 12-H_a + 16-H_b + 2-H_b + 22-H_b + 6-H_a + 21-H_b), 1.37-1.24 (m, 6H, 11-H_a + 6-H_b + 7-H + 9-H + 15-H_b), 1.16-1.08 (m, 2H, 11-H_b + 15-H_b), 0.97-0.92 (m, 1H, 1-H_b), 0.91 (s, 3H, 27-H), 0.85 (s, 3H, 26-H), 0.83-0.81 (m, 1H, 12-H_b), 0.80 (s, 3H, 25-H), 0.79-0.74 (m, 7H, 23-H + 24-H + 5-H) ppm; ^{13}C NMR (126 MHz, DMSO-d_6) δ = 172.8 (C-28), 170.1 (C-30), 159.9 (C-20), 79.9 (C-3), 54.7 (C-5), 53.6 (C-17), 52.1 (C-33 + C-33' + C-32 + C-32'), 51.5 (C-18), 49.8 (C-9), 43.3 (C-19), 41.8 (C-34), 41.4 (C-14), 40.2 (C-8), 37.8 (C-1), 37.4 (C-4), 36.6 (C-10), 35.0 (C-22), 35.8 (C-13), 33.7 (C-7), 31.5 (C-16), 29.3 (C-15), 28.5 (C-21), 27.6 (C-23), 25.1 (C-12), 23.4 (C-2), 21.0 (C-31), 20.6 (C-11), 17.7 (C-6), 16.4 (C-24), 15.9 (C-25), 15.7 (C-26), 14.3 (C-27), 10.7 (C-29) ppm; MS (ESI, MeOH:$CHCl_3$, 4:1): m/z 598.6 ($[M+CH_3OH+H]^+$, 100%) 1197.3 ($[2M+2CH_3OH+H]^+$, 10%); analysis calcd for $C_{36}H_{59}N_3O_4$ (597.87): C 72.32, H 9.95, N 7.03; found: 72.08, H 10.15, N 6.80.

*(3β, 20E) 3-Acetyloxy-20-hydroxyimino-N-(2-aminoethyl)-30-norlupan-28-amide (**8**)*

According to GPB from **2** (1.3 g, 2.5 mmol) and hydroxylammonium chloride (1.2 g, 17 mmol) followed by chromatography (silica gel, *n*-hexane/chloroform/methanol, 4:3.5:1.5) **8** (0.7g, 51%) was obtained as a white solid; m.p. > 300 °C; R_F = 0.22 (*n*-hexane/chloroform/methanol, 4:3.5:1.5); $[\alpha]_D$ = + 3.12° (*c* 0.10, MeOH); IR (ATR): ν = 2940s, 2872m, 1733m, 1709m, 1657m, 1639m, 1516m, 1467m, 1451m, 1367s, 1317w, 1245s, 1195m, 1172w, 1156w, 1131w, 1108w, 1024s, 978s, 946m, 902m, 878w, 850m, 803w, 774w, 691m, 611m, 560m, 548m, 500m, 471m cm^{-1}; ^1H NMR (500 MHz, DMSO-d_6) δ = 4.36 (dd, *J* = 11.5, 4.6 Hz, 1H, 3-H), 3.32-3.28 (m, 2H, 32-H), 3.10 (dt, *J* = 11.0, 5.6 Hz, 1H, 19-H), 2.82-2.73 (m, 2H, 33-H), 2.54-2.46 (m, 1H, 13-H), 2.24-2.17 (m, 1H, 16-H_a), 1.99 (s, 3H, 31-H), 1.90-1.84 (m, 1H, 22-H_a), 1.74-1.66 (m, 1H, 21-H_a), 1.64 (s, 3H, 29-H), 1.60-1.46 (m, 5H, 1-H_a + 2-H_a + 18-H + 12-H_a + 2-H_b), 1.46-1.37 (m, 3H, 6-H_a + 16-H_b + 22-H_b), 1.37-1.22 (m, 7H, 11-H_a + 21-H_b + 6-H_b + 7-H + 9-H + 15-H_a), 1.19-1.08 (m, 1H, 11-H_b), 1.06-1.01 (m, 1H, 15-H_b), 0.97-0.91 (m, 1H, 1-H_b), 0.90 (s, 3H, 27-H), 0.84 (s, 3H, 26-H), 0.83-0.81 (m, 1H, 12-H_b), 0.80 (s, 3H, 25-H), 0.79-

0.74 (m, 7H, 23-H + 24-H + 5-H) ppm; ^{13}C NMR (126 MHz, DMSO-d_6) δ = 176.1 (C-28), 170.1 (C-30), 159.7 (C-20), 79.9 (C-3), 54.7 (C-5), 54.6 (C-17), 49.7 (C-9), 49.4 (C-18), 44.0 (C-19), 41.8 (C-14), 40.2 (C-8), 38.6 (C-33), 37.7 (C-1), 37.4 (C-4), 37.3 (C-22), 36.6 (C-10), 36.5 (C-32), 36.3 (C-13), 33.7 (C-7), 32.0 (C-16), 28.9 (C-15), 28.2 (C-21), 27.6 (C-23), 25.1 (C-12), 23.4 (C-2), 21.0 (C-31), 20.4 (C-11), 17.7 (C-6), 16.4 (C-24), 15.9 (C-25), 15.8 (C-26), 14.3 (C-27), 10.6 (C-29) ppm; ; MS (ESI, MeOH:$CHCl_3$, 4:1): m/z 558.1 ($[M+H]^+$, 100%) 1170.5 ($[2M+H]^+$, 50%); analysis calcd for $C_{33}H_{55}N_3O_4$ (557.81): C 71.06, H 9.94, N 7.53; found: C 70.78, H 10.12, N 7.35.

*(3β, 20E) 3-Acetyloxy-20-hydroxyimino-N-(4-morpholinyl)-30-norlupan-28-amide (**9**)*

According to GPB from **3** (1.5 g, 2.6 mmol) and hydroxylammonium chloride (1.2 g, 17 mmol) followed by chromatography (silica gel, *n*-hexane/chloroform/methanol, 5:4.75:0.25) compound **9** (1.3 g, 85%) was obtained as a white solid; m.p. 283-286 °C; R_F = 0.24 (*n*-hexane/chloroform/methanol, 5:4.75:0.25); $[\alpha]_D$ = + 0.76 ° (*c* 0.10, MeOH); IR (ATR): ν = 3400m, 2967m, 2940m, 2927m, 2860m, 1735w, 1706s, 1636s, 1467w, 1445m, 1393m, 1385m, 1363m, 1313w, 1299w, 1268s, 1224w, 1185m, 1119s, 1065w, 1046m, 1031m, 978m, 948w, 915w, 904w, 881w, 854m, 751w, 662m, 646m, 596m, 550w, 510w cm^{-1}; ^{1}H NMR (500 MHz, DMSO-d_6) δ = 4.37 (dd, *J* = 11.6, 4.7 Hz, 1H, 3-H), 3.56-3.46 (m, 8H, 33-H + 33'-H + 32-H + 32'-H), 2.98 (q, *J* = 6.5 Hz, 1H, 19-H), 2.86-2.79 (m, 1H, 13-H), 2.11-2.05 (m, 1H, 16-H_a), 1.99 (s, 3H, 31-H), 1.97-1.92 (m, 1H, 22-H_a), 1.74-1.68 (m, 1H, 21-H_a), 1.65 (s, 3H; 29-H), 1.64-1.43 (m, 8H, 18-H + 1-H_a + 12-H_a + 2-H_a + 2-H_b + 16-H_b + 22-H_b + 6-H_a), 1.42-1.29 (m, 7H, 21-H_b + 6-H_b + 11-H_a + 7-H + 9-H + 15-H_a), 1.19-1.08 (m, 2H, 11-H_b + 15-H_b), 0.98-0.92 (m, 1H, 1-H_b), 0.91 (s, 3H, 27-H), 0.85 (s, 3H, 26-H), 0.84-0.82 (m, 1H, 12-H_b), 0.81 (s, 3H, 25-H), 0.79 (m, 7H, 23-H + 24-H + 5-H) ppm; ^{13}C NMR (126 MHz, DMSO-d_6) δ = 172.5 (C-28), 170.1 (C-30), 159.8 (C-20), 79.9 (C-3), 66.3 (C-33 + C-33' + C-32 + C-32'), 54.7 (C-5), 53.5 (C-17), 51.6 (C-18), 49.8 (C-9), 43.4 (C-19), 41.4 (C-14), 40.2 (C-8), 37.8 (C-1), 37.4 (C-4), 36.6 (C-10), 35.8 (C-13), 35.0 (C-22), 33.7 (C-7), 31.4 (C-16), 29.2 (C-15), 28.5 (C-21), 27.6 (C-23), 25.1 (C-12), 23.4 (C-2), 20.9 (C-31), 20.6 (C-11), 17.7 (C-6), 16.4 (C-24), 15.9 (C-25), 15.7 (C-26), 14.3 (C-27), 10.6 (C-29) ppm; MS (ESI, MeOH:$CHCl_3$, 4:1): m/z 585.7 ($[M+H]^+$, 86%) 1115.2 ($[2M+H]^+$, 20%); analysis calcd for $C_{35}H_{56}N_2O_5$ (584.83): C 71.88, H 9.65, N 4.79; found: 71.64, H 9.87, N 4.51.

*(3β, 20E) 3-Acetyloxy-20-hydroxyimino-N-(1-piperazinyl)-30-norlupan-28-amide (**10**)*

According to GPB from **4** (1.5 g, 2.6 mmol) and hydroxylammonium chloride (1.2 g, 17 mmol) followed by chromatography (silica gel, *n*-hexane/chloroform/methanol, 4:3.5:1.5) compound **10** (1.1 g, 75%) was obtained as white solid; m.p. 211-215 °C; R_F = 0.17 (*n*-hexane/chloroform/methanol, 4:3.5:1.5); $[\alpha]_D$ = - 14.4° (*c* 0.11, $CHCl_3$); IR (ATR): ν = 2943s, 2713s, 2667s, 2163w, 1983w, 1894w, 1732m, 1623m, 1577m, 1506m, 1468m, 1393m, 1372m, 1315m, 1246m, 1193m, 1160m, 1146m, 1027m, 999s, 981m, 947m, 901m, 850m, 575s, 540s, 510s, 471s, 419s cm^{-1}; ^1H NMR (500 MHz, $CDCl_3$) δ = 4.48 – 4.43 (m, 1H, 3-H), 3.78-3.67 (m, 4H, 33-H + 33'-H), 3.07 (m, 1H, 19-H), 3.04-2.90 (m, 4H, 32-H + 32'-H), 2.81 (m,1H, 13-H), 2.11-2.04 (m, 1H, 16-H_a), 2.03 (s, 3H, 31-H), 2.00-1.82 (m, 2H, 22-H_a + 21-H_a), 1.80 (s, 3H, 29-H), 1.75-1.46 (m, 9H, 18-H + 1-H_a + 2-H + 16-H_b + 12-H_a + 21-H_b + 6-H_a + 22-H_b), 1.43-1.39 (m, 1H, 11-H_a), 1.39-1.31 (m, 4H, 6-H_b + 7-H + 15-H_a), 1.30-1.24 (m, 2H, 9-H + 11-H_b), 1.19-1.13 (m, 1H, 15-H_b), 0.98-0.93 (m, 2H, 1-H_b + 12-H_b), 0.92 (s, 3H, 27-H), 0.90 (s, 3H, 26-H), 0.83 (s, 3H, 25-H), 0.82 (s, 3H, 23-H), 0.82 (s, 3H, 24-H), 0.79-0.75 (m, 1H, 5-H) ppm; ^{13}C NMR (126 MHz, $CDCl_3$) δ = 173.4 (C-28), 171.2 (C-30), 162.7 (C-20), 81.1 (C-3), 58.5 (C-33 + C-33'), 55.7 (C-5), 54.4 (C-17), 52.7 (C-18), 50.8 (C-9), 45.0 (C-32 + C-32'), 44.0 (C-19), 41.9 (C-14), 40.8 (C-8), 38.6 (C-1), 37.9 (C-4), 37.3 (C-10), 36.5 (C-13), 35.8 (C-22), 34.4 (C-7), 32.5 (C-16), 29.9 (C-15), 29.3 (C-21), 28.1 (C-23), 26.0 (C-12), 23.8 (C-2), 21.4 (C-31), 21.3 (C-11), 18.3 (C-6), 16.6 (C-24), 16.4 (C-25), 16.2 (C-26), 14.7 (C-27), 11.8 (C-29) ppm; MS (ESI, MeOH:$CHCl_3$, 4:1): m/z 584.0 ($[M+H]^+$, 50%) 1167.0 ($[2M+H]^+$, 100%); analysis calcd for $C_{35}H_{57}N_3O_4$ (583.86): C 72.00, H 9.84, N 7.20; found: 71.86, H 10.03, N 6.97.

Acknowledgment

We like to thank Y. Schiller and S. Ludwig for the NMR spectra, and Mr. M. Schneider for measuring IR and UV/vis spectra as well as optical rotations and micro-analyses. The cell lines were provided by Dr. Th. Müller (Dept. Oncology, Martin-Luther-University Halle-Wittenberg). We like to thank V. Karsten for her help with thy cytotoxicity assays.

Declarations:

Conflict of Interest:

The authors declare that they have no conflict of interest.

Funding:
No external funding has been received.

Autor contribution:
RC conceived the work, M.K., S.H., T. S. and D. S. generated the data; all authors analyzed the data and wrote the manuscript.

Data Availability:
The datasets generated during and/or analysed during the current study are available from the corresponding author on reasonable request.

Ethics:
No animal or human studies are involed

Consent to publish
All authors have agreed on the final version of this manuscript

Plant reproducibility
No plants are involved in this study

Clinical trial registration
No clinical trials are associated with this study

Gels and plots
No gels and plots have been used; images have not been manipulated.

References
1. Djerassi C, Ehrlich R. Optical Rotatory Dispersion Studies .4. Steroidal Sapogenins. J Am Chem Soc. 1956;78(2):440-6. doi:DOI 10.1021/ja01583a052.
2. Aplin RT, Halsall TG, Norin T. Chemistry of Triterpenes and Related Compounds .43. Constituents of Bark of Platanus X Hybrida Brot and Structure of Platanic Acid. J Chem Soc. 1963:3269-73. doi:DOI 10.1039/jr9630003269.
3. Baratto LC, Porsani MV, Pimentel IC, Netto ABP, Paschke R, Oliveira BH. Preparation of betulinic acid derivatives by chemical and biotransformation methods and determination of

cytotoxicity against selected cancer cell lines. Eur J Med Chem. 2013;68:121-31. doi:10.1016/j.ejmech.2013.07.012.
4. Denisenko MV, Odinokova LE, Denisenko VA, Uvarova NI. Oxidation of Betulin, Dihydrobetulin and 3-Beta-28-Dihydroxy-18-Lupene by Ruthenium Tetraoxide. Khim Prir Soedin+. 1991(3):430-1.
5. Zhang C, Wang X, Cui J, Li X, Zhang Y, Wang X et al. Synthetic Analogues of Betulinic Acid as Potent Inhibitors of PS1/BACE1 Interaction to Reduce Aβ Generation. Chin J Chem. 2017;35(1):103-12. doi:10.1002/cjoc.201600611.
6. Tietze LF, Heinzen H, Moyna P, Rischer M, Neunaber H. Synthesis of [C-13]Betulin and [H-2]Betulin for Biological Transformations. Liebigs Ann Chem. 1991(12):1245-9.
7. Vlk M, Urban M, Elbert T, Sarek J. Synthesis of selectively deuterated and tritiated lupane derivatives with cytotoxic activity. J Radioanal Nucl Ch. 2013;298(2):1149-57. doi:10.1007/s10967-013-2533-8.
8. Heller L, Kahnt M, Loesche A, Grabandt P, Schwarz S, Brandt W et al. Amino derivatives of platanic acid act as selective and potent inhibitors of butyrylcholinesterase. Eur J Med Chem. 2017;126:652-68. doi:10.1016/j.ejmech.2016.11.056.
9. Hoenke S, Christoph MA, Friedrich S, Heise N, Brandes B, Deigner HP et al. The Presence of a Cyclohexyldiamine Moiety Confers Cytotoxicity to Pentacyclic Triterpenoids. Molecules. 2021;26(7). doi:10.3390/molecules26072102.
10. Sommerwerk S, Heller L, Kerzig C, Kramell AE, Csuk R. Rhodamine B conjugates of triterpenoic acids are cytotoxic mitocans even at nanomolar concentrations. Eur J Med Chem. 2017;127:1-9. doi:10.1016/j.ejmech.2016.12.040.
11. Wiemann J, Fischer L, Kessler J, Stroehl D, Csuk R. Ugi multicomponent-reaction: Syntheses of cytotoxic dehydroabietylamine derivatives. Bioorg Chem. 2018;81:567-76. doi:10.1016/j.bioorg.2018.09.014.
12. Wolfram RK, Fischer L, Kluge R, Stroehl D, Al-Harrasi A, Csuk R. Homopiperazine-rhodamine B adducts of triterpenoic acids are strong mitocans. Eur J Med Chem. 2018;155:869-79. doi:10.1016/j.ejmech.2018.06.051.
13. Wolfram RK, Heller L, Csuk R. Targeting mitochondria: Esters of rhodamine B with triterpenoids are mitocanic triggers of apoptosis. Eur J Med Chem. 2018;152:21-30. doi:10.1016/j.ejmech.2018.04.031.

14. Ali MS, Ashfaq A, Lateef M, Sultan A, Zikr-ur-Rehman S, Shaikh Q-u-a et al. Phytochemical screening and biological evaluation of young stems of alstonia scholaris. J Chem Soc Pak. 2021;43(5):606-10.
15. Nguyen MTT, Nguyen NT. A new lupane triterpene from Tetracera scandens L., xanthine oxidase inhibitor. Nat Prod Res. 2013;27(1):61-7. doi:10.1080/14786419.2011.652960.
16. Cummings JL. Alzheimer's disease. N Engl J Med. 2004;351(1):56-67. doi:10.1056/nejmra040223.
17. Goedert M, Spillantini MG. A Century of Alzheimer's Disease. Science (Washington, DC, U S). 2006;314(5800):777-81. doi:10.1126/science.1132814.
18. Huang Y, Mucke L. Alzheimer Mechanisms and Therapeutic Strategies. Cell (Cambridge, MA, U S). 2012;148(6):1204-22. doi:10.1016/j.cell.2012.02.040.
19. Masters CL, Bateman R, Blennow K, Rowe CC, Sperling RA, Cummings JL. Alzheimer's disease. Nat Rev Dis Primers. 2015;1:15056. doi:10.1038/nrdp.2015.56.
20. Bohnen NI, Kaufer DI, Hendrickson R, Ivanco LS, Lopresti BJ, Constantine GM et al. Cognitive correlates of cortical cholinergic denervation in Parkinson's disease and parkinsonian dementia. J Neurol. 2006;253(2):242-7. doi:10.1007/s00415-005-0971-0.
21. Connolly BS, Lang AE. Pharmacological treatment of Parkinson disease: a review. JAMA, J Am Med Assoc. 2014;311(16):1670. doi:10.1001/jama.2014.3654.
22. Hilker R, Thomas AV, Klein JC, Weisenbach S, Kalbe E, Burghaus L et al. Dementia in Parkinson disease: functional imaging of cholinergic and dopaminergic pathways. Neurology. 2005;65(11):1716-22. doi:10.1212/01.wnl.0000191154.78131.f6.
23. Jellinger KA, Korczyn AD. Are dementia with Lewy bodies and Parkinson's disease dementia the same disease? BMC Med. 2018;16:34/1. doi:10.1186/s12916-018-1016-8.
24. Klein JC, Eggers C, Kalbe E, Weisenbach S, Hohmann C, Vollmar S et al. Neurotransmitter changes in dementia with Lewy bodies and Parkinson disease dementia in vivo. Neurology. 2010;74(11):885-92. doi:10.1212/wnl.0b013e3181d55f61.
25. Mueller MLTM, Bohnen NI. Cholinergic Dysfunction in Parkinson's Disease. Curr Neurol Neurosci Rep. 2013;13(9):1-9. doi:10.1007/s11910-013-0377-9.
26. Perry EK, Curtis M, Dick DJ, Candy JM, Atack JR, Bloxham CA et al. Cholinergic correlates of cognitive impairment in Parkinson's disease: comparisons with Alzheimer's disease. J Neurol Neurosurg Psychiatry. 1985;48(5):413-21. doi:10.1136/jnnp.48.5.413.
27. Balestrino R, Schapira AHV. Parkinson disease. Eur J Neurol. 2020;27(1):27-42. doi:10.1111/ene.14108.

28. Bose A, Beal MF. Mitochondrial dysfunction in Parkinson's disease. J Neurochem. 2016;139(S1):216-31. doi:10.1111/jnc.13731.

29. Jenner P, Olanow CW. Understanding cell death in Parkinson's disease. Ann Neurol. 1998;44(3):S72.

30. Kalia LV, Lang AE. Parkinson's disease. Lancet. 2015;386(9996):896-912. doi:10.1016/s0140-6736(14)61393-3.

31. Lucking CB, Brice A. Alpha-synuclein and Parkinson's disease. Cell Mol Life Sci. 2000;57(13/14):1894-908. doi:10.1007/pl00000671.

32. Nussbaum RL, Ellis CE. Alzheimer's disease and Parkinson's disease. N Engl J Med. 2003;348(14):1356-64. doi:10.1056/nejm2003ra020003.

33. Berry CE, Hare JM. Xanthine oxidoreductase and cardiovascular disease: molecular mechanisms and pathophysiological implications. J Physiol (Oxford, U K). 2004;555(3):589-606. doi:10.1113/jphysiol.2003.055913.

34. Borges F, Fernandes E, Roleira F. Progress towards the discovery of xanthine oxidase inhibitors. Curr Med Chem. 2002;9(2):195-217. doi:10.2174/0929867023371229.

35. Granger DN. Role of xanthine oxidase and granulocytes in ischemia-reperfusion injury. Am J Physiol. 1988;255(6):H1269.

36. Harrison R. Structure and function of xanthine oxidoreductase: where are we now? Free Radical Biol Med. 2002;33(6):774-97. doi:10.1016/s0891-5849(02)00956-5.

37. Kumar R, Darpan, Sharma S, Singh R. Xanthine oxidase inhibitors: a patent survey. Expert Opin Ther Pat. 2011;21(7):1071-108. doi:10.1517/13543776.2011.577417.

38. Battelli MG, Polito L, Bortolotti M, Bolognesi A. Xanthine oxidoreductase in cancer: more than a differentiation marker. Cancer Med. 2016;5(3):546-57. doi:10.1002/cam4.601.

39. Dawson J, Walters M. Uric acid and xanthine oxidase: future therapeutic targets in the prevention of cardiovascular disease? Br J Clin Pharmacol. 2006;62(6):633-44. doi:10.1111/j.1365-2125.2006.02785.x.

40. Diaz-Torne C, Perez-Herrero N, Perez-Ruiz F. New medications in development for the treatment of hyperuricemia of gout. Curr Opin Rheumatol. 2015;27(2):164-9. doi:10.1097/bor.0000000000000146.

41. Isaka Y, Takabatake Y, Takahashi A, Saitoh T, Yoshimori T. Hyperuricemia-induced inflammasome and kidney diseases. Nephrol, Dial, Transplant. 2016;31(6):890-6. doi:10.1093/ndt/gfv024.

42. Kostic DA, Dimitrijevic DS, Gordana S S, Palic IR, Dordevic AS, Ickovski JD. Xanthine oxidase: isolation, assays of activity, and inhibition. J Chem. 2015:294858. doi:10.1155/2015/294858.
43. Ling X, Bochu W. A review of phytotherapy of gout: perspective of new pharmacological treatments. Pharmazie. 2014;69(4):243-56. doi:10.1691/ph.2014.3642.
44. Luna G, Dolzhenko AV, Mancera RL. Inhibitors of Xanthine Oxidase: Scaffold Diversity and Structure-Based Drug Design. ChemMedChem. 2019;14(7):714-43. doi:10.1002/cmdc.201900034.
45. Wortmann RL. Recent advances in the management of gout and hyperuricemia. Curr Opin Rheumatol. 2005;17(3):319-24. doi:10.1097/01.bor.0000162060.25895.a5.
46. Hoenke S, Christoph MA, Friedrich S, Heise N, Brandes B, Deigner H-P et al. The presence of a cyclohexyldiamine moiety confers cytotoxicity to pentacyclic triterpenoids. Molecules. 2021;26(7):2102. doi:10.3390/molecules26072102.
47. Kahnt M, Heller L, Al-Harrasi A, Schaefer R, Kluge R, Wagner C et al. Platanic acid-derived methyl 20-amino-30-norlupan-28-oates are potent cytotoxic agents acting by apoptosis. Med Chem Res. 2018;27(7):1757-69. doi:10.1007/s00044-018-2189-6.

P6

Results in Chemistry 4 (2022) 100429

Contents lists available at ScienceDirect

Results in Chemistry

journal homepage: www.sciencedirect.com/journal/results-in-chemistry

Betulinic acid and glycyrrhetinic acid derived piperazinyl spacered rhodamine B conjugates are highly cytotoxic and necrotic

Marie Kozubek [a], Sophie Hoenke [a], Hans-Peter Deigner [b], René Csuk [a,*]

[a] Martin–Luther–University Halle–Wittenberg, Organic Chemistry, Kurt–Mothes–Str. 2, D–06120 Halle (Saale), Germany
[b] Furtwangen University, Institute of Precision Medicine, Medical and Life Science Faculty, Jakob–Kienzle–Str. 17, D-78054 Villingen–Schwenningen, Germany

ARTICLE INFO

Keywords:
Betulin
Betulinic acid
Glycyrrhetinic acid
Cytotoxicity
Rhodamine B conjugates

ABSTRACT

Pentacyclic triterpene-piperazine-rhodamine B conjugates with ursane or oleanane backbones have been shown in the past to be highly cytotoxic thereby acting as mitocans. Starting from betulinic acid or glycyrrhetinic acid, new analogues were now made available, and their cytotoxic activity was investigated employing several human tumor cell lines [A375 (melanoma), HT29 (colorectal carcinoma), MCF-7 (breast adenocarcinoma), A2780 (ovarian carcinoma), and for comparison NIH 3T3 (non-malignant fibroblasts)]. For these conjugates it has been established that the linking position at ring E governs the magnitude of cytotoxicity. These conjugates were still highly cytotoxic but significantly less cytotoxic than those holding a oleanane skeleton. Staining experiments showed the rhodamine B conjugates as necrotic compounds and to act as mitocans. The most active compound (**8**) held an EC_{50} = 0.04 μM for A2780 ovarian carcinoma cells.

Introduction

For a long time, the potential of pentacyclic triterpene carboxylic acids was underestimated. Although betulin (**BN**, Fig. 1) was first isolated and described by J. T. Lowitz [1] as early as 1788, it was not until 1995 that the cytotoxic effect of the BN-derived betulinic acid (**BA**) against melanoma was recognized by E. Pisha et al. [2] For decades since then, a large number of pentacyclic triterpene carboxylic acids have been isolated from a wide variety of different plant sources and also studied for their cytotoxic potential. [3–11] However, many of these compounds were only weakly cytotoxic or not cytotoxic at all. Even **BA**-derived platanic acid (**PA**) did not live up to the expectations placed in it, since **PA** itself is also practically not cytotoxic and, in addition, it is even more poorly soluble than betulinic acid in biological fluids. [12–21].

More recently, a renaissance of this class of compounds has been achieved, as acylated amides have been shown to have good cytotoxicity, in particular a diacetylated benzylamide ("**EM2**") [22–27] derived from maslinic acid or (iso)-quinolinyl amides ("**IQAA**") [28] derived from augustic acid.

Triterpenoid piperazine amides also stand out as cytotoxic, but are far surpassed [29] by derivatives that have a general structure as an acetylated triterpene carboxylic acid-piperazine-rhodamine B conjugate. [30–36] Thereby, a triterpene carboxylic acid – acetylated one or more times in ring A – is linked to rhodamine B via a piperazine residue (attached to the triterpene carboxylic acid as an amide) at its distal nitrogen to form a cationic, lipophilic conjugate. These compounds are supposed to interact with mitochondrial membranes and therefore act as mitocans (mitochondria targeted drugs) even in the low nanomolar concentration range. [29].

Thereby, compounds of the ursane or oleanane type were mainly investigated. Little is known about derivatives of this type with a lupane or with a β-amyrin backbone, such as in compounds derived from betulin (**BN**), betulinic acid (**BA**), platanic acid (**PA**) or glycyrrhetinic acid (**GA**). This will be the subject of this study.

Results and discussion

BN, **BA**, **PA** and **GA** were selected as starting materials. They are available in large quantities and very good purity from local suppliers. Their acetylation (Scheme 1) gave the known acetates **1**–**3**. Reaction of **1**–**3** with oxalyl chloride followed by reaction with piperazine gave the amides **4**–**6**, and their reaction with rhodamine B (which was previously converted into the corresponding acid chloride with oxalyl chloride) led to the formation of the acetylated piperazinyl-spacered triterpene-rhodamine B conjugates **7**–**9**. These compounds are pink colored thus indicating the presence of an intact cationic rhodamine B moiety. This is

* Corresponding author.
E-mail address: rene.csuk@chemie.uni-halle.de (R. Csuk).

https://doi.org/10.1016/j.rechem.2022.100429
Received 23 May 2022; Accepted 30 June 2022
Available online 2 July 2022

usually regarded as a pre-requisite for obtaining compounds of mitocanic activity. [29].

Especially for a comparison with the corresponding glycyrrhetinic acid derivatives, two additional compounds were prepared (Scheme 2). **BN** was acetylated to form known diacetate **10** whose reduction with BH_3 in THF at 0 °C [37] gave **11**. Jones oxidation of the latter afforded **12** whose reaction with oxalyl chloride followed by the addition of piperazine yielded **13**. Reaction of **13** with rhodamine B (activated with oxalyl chloride) gave **14**. **BA** acetate **1** was converted into its corresponding benzylamide **15** whose reduction with BH_3 yielded **16**. The latter compound was oxidized, and acid **17** was obtained in 52% yield. Coupling of this compound with **18** (having been accessed from the reaction of rhodamine B with oxalyl chloride followed by the addition of piperazine) finally gave **19**.

To assess their cytotoxicity these compounds were subjected to sulforhodamine B (SRB) assays employing several human tumor cell lines. The results of these assays have been compiled in Table 1.

The results from extra staining experiments employing A375 cells (having been incubated with either **14** or **19** at 2 × EC_{50} concentration for 24 h and 48 h, respectively) are depicted in Fig. 2 and Fig. 3. These FITC/annexin V/propidium iodide staining experiments allowed a quantification of the apoptosis/necrosis inducing activity of compounds **14** and **19**, respectively. Thereby, cells found in R1 (upper left) are regarded necrotic, those in R2 (upper right) late apoptotic, in R3 (bottom left) viable cells can be found and in R4 (bottom right) apoptotic cells are registered. Treatment of A375 cells with **14** for 24 h showed 42% of the cells being necrotic; after 2 days 50% of the cells were necrotic, and only 1.6% of the cells had died by apoptosis.

As shown in Figs. 2 and 3, the number of necrotic cells after treatment with **19** for 2 days amounted to 32.8% and 5.7% of the cells having died by apoptosis. This clearly indicates that A375 cells die rather by necrosis than by apoptosis.

Although generalizations are always difficult, betulin derived **14** is more cytotoxic than betulinic acid derived **19**. Compounds **7**–**9** are approximately equally cytotoxic but significantly better than **14**. This might be caused by a higher bioavailability of the former compounds due to an increased solubility. Tumor/non-tumor cell selectivity is approximately the same in all cases but significantly worse than that previously measured for **EM2**. However, the results also show that betulin, betulinic acid and glycyrrhetinic acid derived conjugates are slightly less cytotoxic than the previously reported corresponding oleanolic and ursolic-piperazinyl-rhodamine-B hybrids. All compounds together, however, are significantly worse than those derivatives previously accessed from maslinic acid [38], tormentic acid [29] or madecassic acid [31]. This proves the original assumption that both the type of spacer (piperazine being better than ethylenediamine) is crucial, but also that the presence of a second acetoxy group in ring A improves cytotoxicity, and that the mode of attachment of the rhodamine residue (spacered better than directly bound) and the corresponding triterpene skeleton are also of crucial importance. Worthwhile to mention that **15** (albeit being not a rhodamine derivative) seems perhaps to be a more valuable compound over both, **14** and **19**, because **15** is much less cytotoxic to the non-malignant cells than **14** and **19**. Moreover, it shows certain selectivity in its effect.

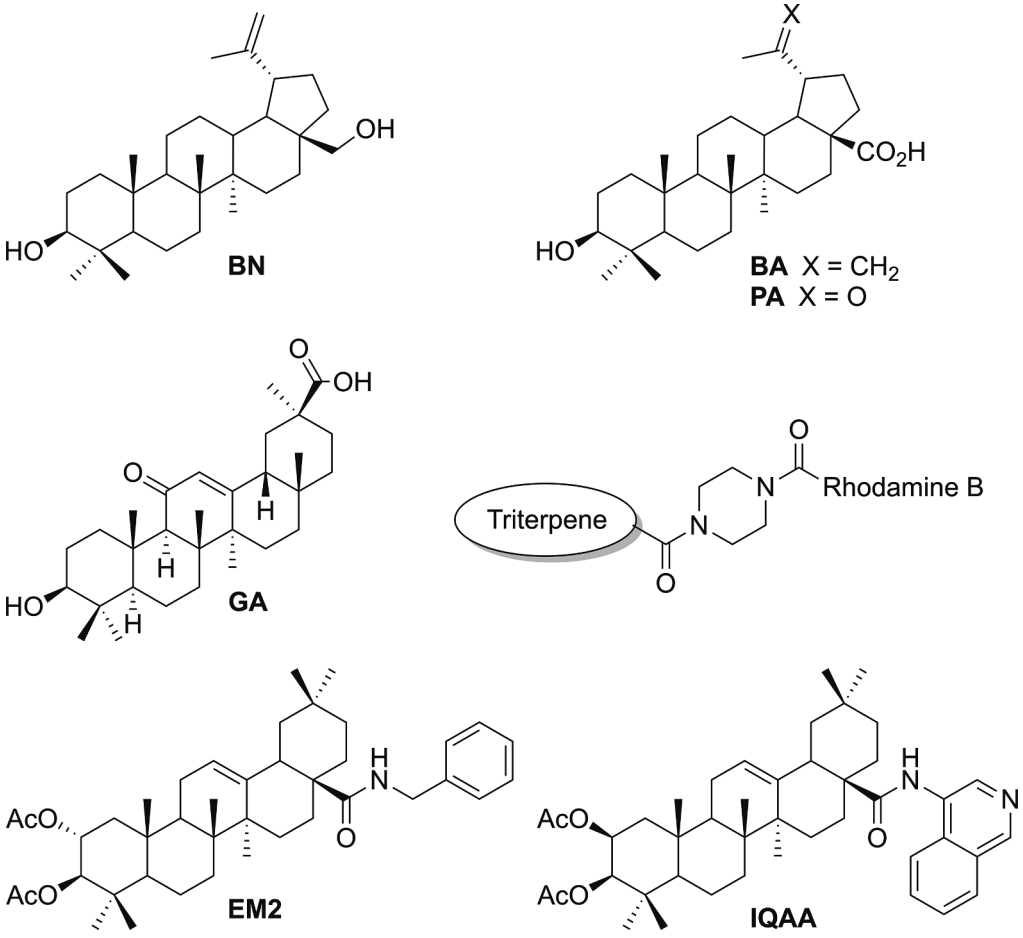

Fig. 1. Structure of betulin (**BN**), betulinic acid (**BA**), platanic acid (**PA**) and the generalized depiction of a piperazinyl spacered triterpene-rhodamine B conjugate as well as of most cytotoxic derivatives **EM2** and **IQAA**.

Conclusion

Pentacyclic triterpene-piperazine-rhodamine B conjugates derived from betulin, betulinic acid or glycyrrhetinic acid were synthesized and screened for their cytotoxic activity. This study is based on previous investigations showing similar compounds holding an ursane or oleanane backbone of high cytotoxicity thereby acting as mitocans. For these new conjugates it was shown, however, that the linking position at ring E governs the magnitude of cytotoxicity. As a result, these conjugates were still highly cytotoxic but significantly less cytotoxic than those holding a oleanane skeleton. Staining experiments showed the rhodamine B conjugates as necrotic compounds and to act as mitocans. The most active compound (**8**) held an EC_{50} = 0.04 μM for A2780 ovarian carcinoma cells.

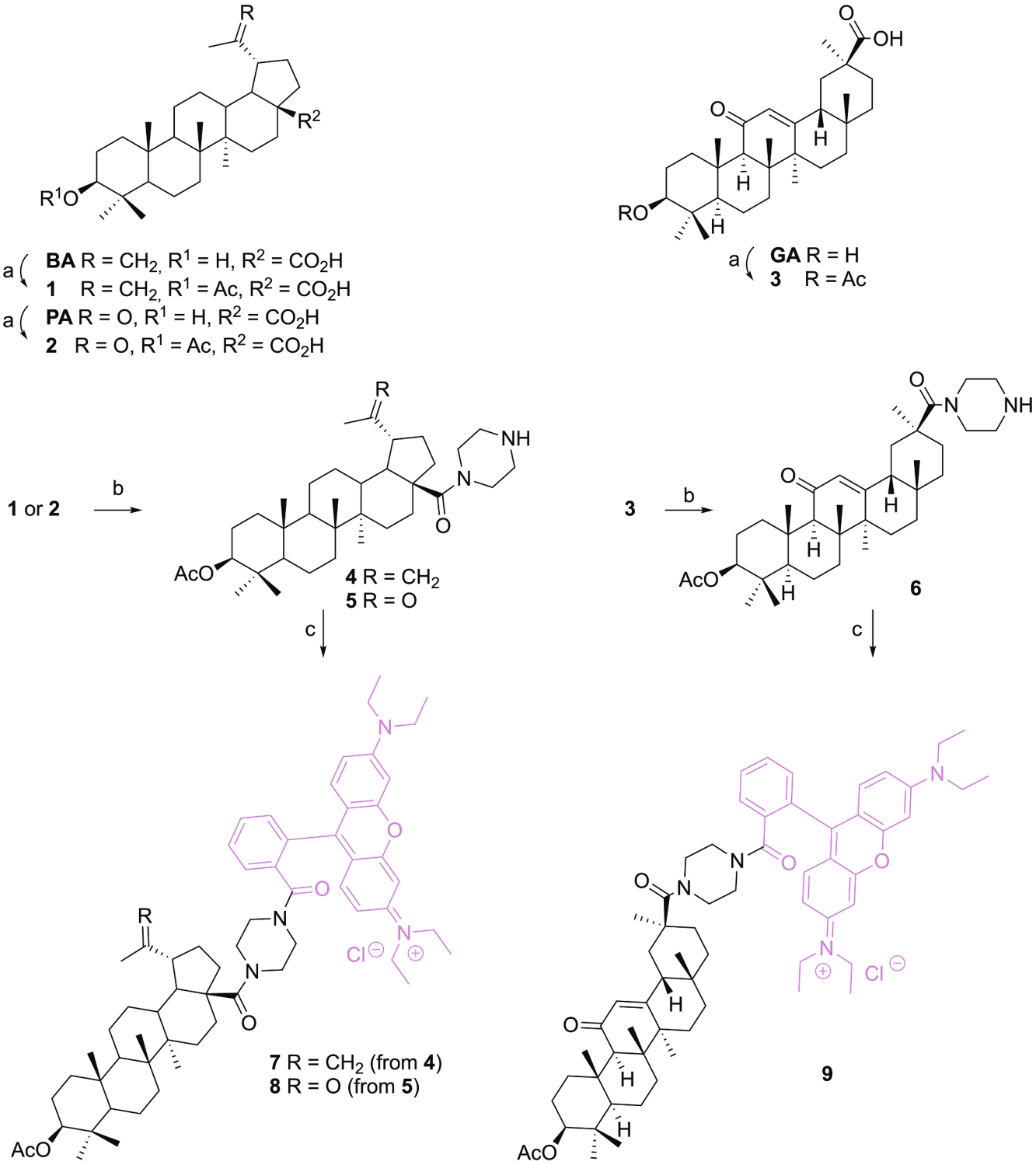

Scheme 1. Synthesis of compounds **1**–**9**: a) Ac_2O, py, DMAP (cat.), 21 °C, 12 h, →**1** (75%), →**2** (79%), →**3** (91%); b) DCM, $(COCl)_2$, DMF (cat.) then piperazine, DCM, 21 °C, 12 h, →**4** (73%), →**5** (68%), →**6** (67%); c) rhodamine B, DCM, $(COCl)_2$, DMF (cat.), then **4**, **5** or **6**, DCM, 21 °C, 24 h, **4** → **7** (67%), **5** → **8** (70%), **6** → **9** (64%); the rhodamine B part has been colored in pink.

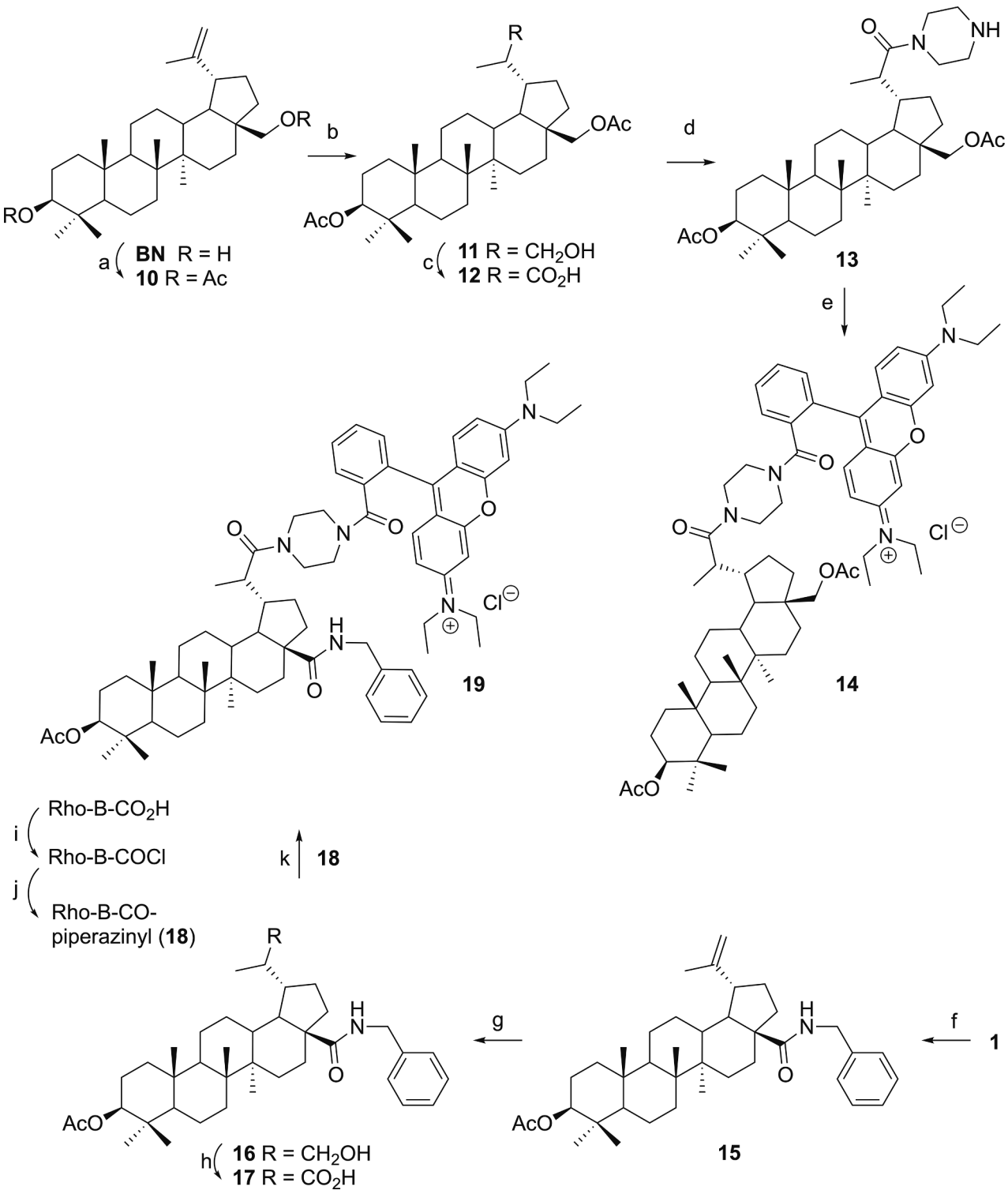

Scheme 2. Synthesis of conjugates **14** and **19**: a) Ac_2O, py, DMAP (cat.), 21 °C, 12 h, 83%; b) THF, BH_3·THF, 1 h, 0 °C then NaOAc, H_2O_2, 1 h, 0 °C, 67%; c) Jones oxidation (CrO_3/H_2SO_4), 0 °C, 1 h, 81%; d) $(COCl)_2$, DCM, DMF (cat.), then piperazine, 12 h, 21 °C, 91%; e) rhodamine B, $(COCl)_2$, DCM, DMF (cat.), then **13**, 24 h, 21 °C, 24%; f) DCM, $(COCl)_2$, DMF (cat.) then Bn-NH_2, 12 h, 21 °C, 67%; g) THF, BH_3·THF, 1 h, 0 °C then NaOAc, H_2O_2, 1 h, 0 °C, 70%; h) Jones oxidation (CrO_3/H_2SO_4), 0 °C, 1 h, 52%; i) $(COCl)_2$, DCM, DMF (cat.); j) piperazine, 12 h, 21 °C, 67%; k) DCM, $(COCl)_2$, DMF (cat), then **18**, DCM, 21 °C, 24 h, 9%.

Experimental

Equipment and general methods are described in the supplementary materials file.

3β-Acetyloxy-lup-20(29)-en-28-oic acid (1)

Following GPA, from betulinic acid (**BA**, 5.0 g, 0.011 mol) **1** (4.1 g, 75%) was obtained as a colorless solid; $R_f = 0.71$ (toluene/ethyl acetate/*n*-heptane/formic acid, 80:26:10:5); m.p. 274–277 °C (lit.: [39] 277–278 °C); $[\alpha]_D = +21.5°$ ($c = 0.40$, $CHCl_3$), lit.: [40] $[\alpha]_D = +26.4°$

Table 1
SRB assay EC_{50} values [μM] after 72 h of treatment; averaged from three independent experiments performed each in triplicate; confidence interval CI = 95%. Human cancer cell lines: A375 (melanoma), HT29 (colorectal carcinoma), MCF-7 (breast adenocarcinoma), A2780 (ovarian carcinoma), NIH 3T3 (non-malignant fibroblasts); cut-off 30 μM, n.d. not determined; n.s. not soluble under the conditions of the assay; doxorubicin (**DX**) has been used as a positive standard.

Compound	A375	HT29	MCF-7	A2780	NIH 3T3
1	19.2 ± 1.7	21.3 ± 2.0	11.0 ± 0.5	18.3 ± 0.5	>30
2	>30	>30	>30	>30	>30
3	>30	>30	>30	>30	>30
4	1.5 ± 0.3	1.0 ± 0.1	1.4 ± 0.1	1.9 ± 0.1	0.9 ± 0.06
5	1.9 ± 0.4	3.9 ± 0.2	2.7 ± 0.3	2.6 ± 0.4	1.3 ± 0.1
6	3.7 ± 0.4	4.5 ± 0.6	8.4 ± 0.8	8.2 ± 0.5	8.7 ± 0.7
7	0.1 ± 0.04	0.2 ± 0.04	0.1 ± 0.05	0.05 ± 0.002	0.2 ± 0.05
8	0.1 ± 0.03	0.1 ± 0.04	0.1 ± 0.03	0.04 ± 0.006	0.2 ± 0.06
9	0.1 ± 0.05	0.1 ± 0.05	0.1 ± 0.05	0.1 ± 0.05	0.1 ± 0.03
10	18.7 ± 0.9	15.9 ± 1.3	20.4 ± 2.6	11.1 ± 1.4	>30
11	10.0 ± 0.3	18.2 ± 1.5	11.5 ± 1.7	9.9 ± 0.8	15.9 ± 0.8
12	21.5 ± 1.1	27.7 ± 0.8	16.1 ± 1.3	12.5 ± 1.8	25.3 ± 0.6
13	n.s.	n.s.	n.s.	n.s.	n.s.
14	0.5 ± 0.05	0.3 ± 0.04	0.3 ± 0.05	0.2 ± 0.06	0.5 ± 0.07
15	4.1 ± 0.2	>30	26.8 ± 6.8	6.3 ± 0.8	>30
16	>30	>30	25.1 ± 5.7	16.8 ± 2.6	>30
17	16.2 ± 1.4	26.1 ± 1.2	13.6 ± 0.9	14.1 ± 1.1	21.2 ± 1.5
18	>30	>30	17.8 ± 3.9	26.4 ± 2.1	>30
19	1.3 ± 0.1	0.7 ± 0.1	0.6 ± 0.2	0.5 ± 0.1	1.6 ± 0.1
DX	n.d.	0.9 ± 0.01	1.1 ± 0.3	0.01 ± 0.006	0.4 ± 0.07

(c = 0.54, $CHCl_3$); MS (ESI): m/z (%) = 497.1 ($[M-H]^-$, 25), 995.3 ([2 M−H]$^-$, 100).

3β-Acetyloxy-20-oxo-30-norlupan-28-oic acid (2)

Following GPA, from platanic acid (**PA**, 5.0 g, 0.011 mol) **2** (4.3 g, 79%) was obtained as a colorless solid; R_f = 0.52 (toluene/ethyl acetate/*n*-heptane/formic acid, 80:26:10:5); m.p. 259–261 °C (lit.: [41] 252–255 °C); $[\alpha]_D$ = –9.0° (c = 0.35, $CHCl_3$), [lit.: [41] $[\alpha]_D$ = –9.5° (c = 0.80, $CHCl_3$)]; MS (ESI): m/z (%) = 499.0 ([M−H]$^-$, 14), 999.2 ([2 M−H]$^-$, 100).

3β-Acetyloxy-11-oxo-olean-12-en-29-oic acid (3)

Following GPA, from glycyrrhetinic acid (**GA**, 5.0 g, 0.011 mol) **3** (5.0 g, 91%) was obtained as a colorless solid; R_f = 0.50 (*n*-hexane/ethyl acetate, 7:3); m.p. 316–318 °C (decomp.) (lit.: [42] 310–313 °C); $[\alpha]_D$ = +165.7° (c = 0.5, $CHCl_3$) [lit.: [42] $[\alpha]_D$ = +163.2° (c = 1.0, $CHCl_3$)]; MS (ESI): m/z (%) = 513.5 ($[M + H]^+$, 100), 535.5 ($[M + Na]^+$, 60), 567.0 ($[M + MeOH + Na]^+$,69).

3β-Acetyloxy-28-(1-piperazinyl)-lup-20(29)-en-28-one (4)

Following GPD, from **1** (2.5 g, 5 mmol) and piperazine (1.6 g, 20.0 mmol), compound **4** (2.1 g, 73%) was obtained as a colorless solid; R_f = 0.38 (chloroform/methanol, 9:1); m.p. = 166–173 °C (lit.: [38] 162–167 °C); $[\alpha]_D$ = − 1.4° (c = 0.21, MeOH), [lit.: [38] $[\alpha]_D$ = − 1.8° (c = 0.32, MeOH); MS (ESI): m/z (%) = 567.3 ($[M + H]^+$, 100).

3β-Acetyloxy-28-(1-piperazinyl)- 30-norlupane −20,28- dione (5)

Following GPD, from **2** (2.5 g, 5.0 mmol) and piperazine (1.6 g, 20.0 mmol), **5** (1.93 g, 68%) was obtained as a colorless solid; R_f = 0.40 (chloroform/methanol, 9:1); m.p. = 126–129 °C (lit: [38] 115–125 °C); $[\alpha]_D$ = − 20.3° (c = 0.13, $CHCl_3$); MS (ESI): m/z (%) = 569.3 ($[M + H]^+$, 100).

3β-Acetyloxy-30-(1-piperazinyl)-olean-12-ene-11,30-dione (6)

Following GPD, from **3** (0.5 g, 1.0 mmol) and piperazine (0.3 g, 4.0 mmol), **6** (0.4 g, 67%) was obtained as a colorless solid; R_f = 0.30 (chloroform/methanol, 9:1); m.p. 162–164 °C [lit.: [38] 160 °C (decomp.]; MS (ESI): m/z (%) = 581.4 ($[M + H]^+$, 42).

9- [2- [[4-(3β-Acetyloxy-28-oxo-lup-20(29)en-28-yl)-1-piperazinyl] carbonyl] phenyl] -3,6-bis(diethylamino] -xanthylium chloride (7)

Following GPE, from **4** (360 mg, 0.64 mmol) and rhodamine B, **7** (440 mg, 67%) was obtained as a dark purple solid; R_f = 0.37 (chloroform/methanol, 9:1); m.p. 246–251 °C (lit.: [38] m.p. 246–250 ∘C); MS (ESI, MeOH): m/z (%) = 991.6 ($[M-Cl]^+$, 100).

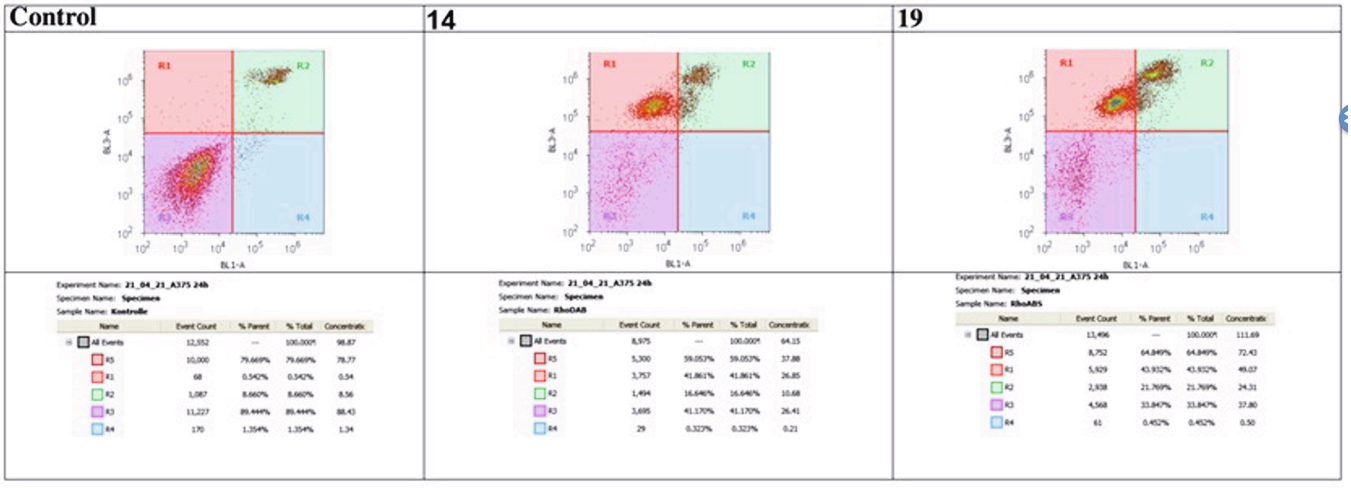

Fig. 2. FITC/Annexin V/Propidium iodide assay utilizing compounds **14** and **19** (A375 cells, 24 h, 2 × EC_{50} concentration).

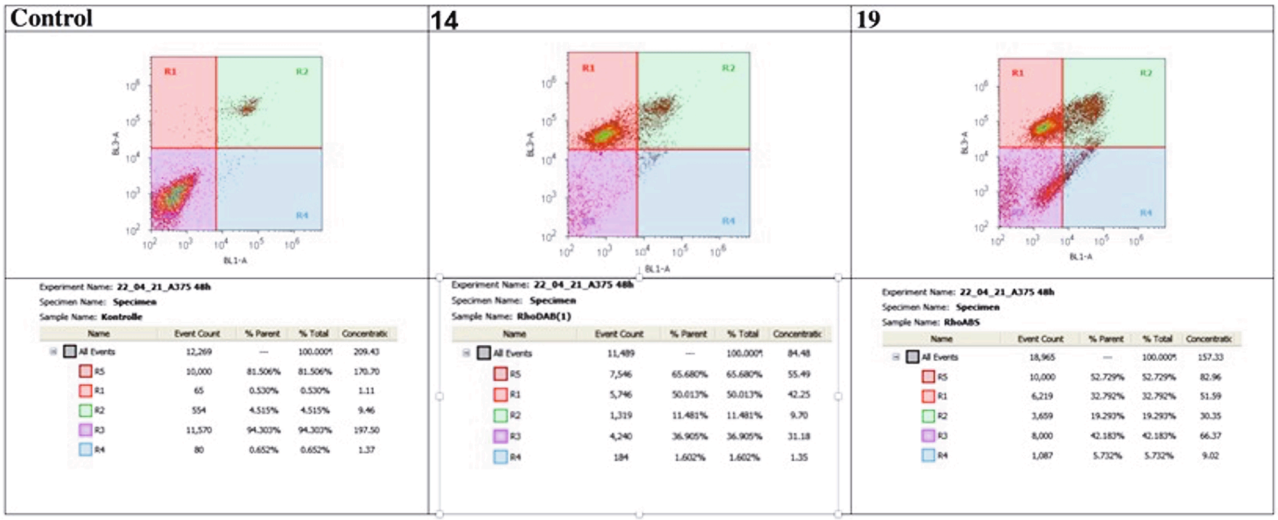

Fig. 3. FITC/Annexin V/propidium iodide assay utilizing compounds **14** and **19** (A375 cells, 48 h, 2 × EC_{50} concentration).

9-[2-[[4-(3β, 20*R*) 3-Acetyloxy-20,28-dioxo-30-norlupan-28-yl)-1-piperazinyl] carbonyl] phenyl] -3,6-bis(diethylamino)-xanthylium chloride (8)

Following GPE from **5** (360 mg, 0.64 mmol) and rhodamine B, **8** (460 mg, 70%) was obtained as a dark purple solid; $R_f = 0.35$ (chloroform/methanol, 9:1); m.p. 246–252 °C (lit.: [38] 235–243 ∘C); MS (ESI, MeOH): *m/z* (%) = 993.7 ($[M-Cl]^+$, 100).

9-[2-[[4-(3β, 20β)-3-Acetyloxy-11,29-dioxo-olean-12-en-29-yl) piperazinyl] carbonyl] phenyl] -3,6-bis(diethylamino] -xanthylium chloride (9)

As previously described, **9** (214 mg, 64%) was obtained as a violet solid; $R_f = 0.32$ (chloroform/methanol, 9:1); m.p. 237–240 °C (lit.: [38] 235–238 °C); MS (ESI): *m/z* (%) = 1005.8 ($[M-Cl]^+$, 100).

3β, 28-Diacetyloxylup-20(29)-ene (10)

Following GPA, betulin (20.0 g, 39.0 mmol) was acetylated, and **10** (16.6 g, 83%) was obtained as a colorless, crystalline solid; $R_f = 0.66$ (*n*-hexane/ethyl acetate, 7:1); m.p. 216–219 °C (lit.: [43] 223–224 °C); $[\alpha]_D$ = +21.0° (*c* = 0.20, $CHCl_3$) [lit.: [44] $[\alpha]_D$ = +23° (*c* = 0.46, $CHCl_3$)]; MS (ESI, MeCN): *m/z* (%) = 549.7 ($[M-Na]^+$, 34), 1075.7 ($[2M + Na]^+$, 100).

(3β, 20*R*) 3,28,29-lupanetriol-3,28-diacetate (11)

Following GPB from **10** (5.7 g, 10.8 mmol) and chromatographic purification (silica gel, chloroform/*n*-hexane/ethyl acetate, 8:7:1) **11** (2.6 g, 67%) was obtained as white solid; $R_f = 0.30$ (silica gel, chloroform/*n*-hexane/ethyl acetate, 8:7:1); m.p. 231–233 °C (lit.: [45,46] 235–236 °C); $[\alpha]_D$ = -13.4° (*c* = 0.15, $CHCl_3$) (lit.: [45,46] $[\alpha]_D$ = -14.0° (c = 0.65, $CHCl_3$)); MS (ESI, MeOH): *m/z* (%) = 567.6 ($[M + Na]^+$, 85), 1111.3 ($[2M + Na]^+$, 100).

(3β, 20*R*) 3, 28-Bis(acetyloxy)-lupan-39-oic acid (12)

Following GPC from **11** (3.5 g, 6.4 mmol) **12** (3.2 g, 81%) was obtained as a white solid; $R_f = 0.25$ (chloroform/*n*-hexane/ethyl acetate, 8:7:1); m.p. 231–234 °C (lit.: [45,46] 239–241 °C; 238–240 °C); $[\alpha]_D$ = -43.2° (*c* = 0.2, $CHCl_3$) (lit.: [45,46] $[\alpha]_D$ = -44.0° (c = 0.68, $CHCl_3$), $[\alpha]_D$ = -56° (c = 1, $CHCl_3$)[29,38]); MS (ESI, MeOH): *m/z* (%) = 557.4 ($[M-H]^-$, 75), 1115.3 ($[2M-H]^-$, 100).

(3β, 20*R*) 3, 28-Bis(acetyloxy)-(1-piperazinyl)-lupan-29-amide (13)

Following GPD from **12** (1.4 g, 2.5 mmol) and piperazine (0.86 g, 10 mmol), compound **13** (1.4 g, 91%) was obtained as white solid; R_f = 0.24 (*n*-heptane/chloroform/isopropanol, 6:2:2); m.p. 125–128 °C (lit.: [37] m.p. 127–130 °C); $[\alpha]_D$ = -19.4° (c = 0.20, $CHCl_3$) (lit.: [37] $[\alpha]_D$ = -18.3° (*c* = 0.16, $CHCl_3$); MS (ESI, MeOH/DCM (4:1)): *m/z* (%) = 627.5 ($[M-H]^+$, 100%).

9-[2-[[4-(3β-Diacetyloxy-(29-piperazinyl)-lupan-30-amid-37-oyl)-1-piperazinyl] carbonyl] phenyl] -3,6-bis(diethylamino] -xanthylium chloride (14)

Following GPE from **13** (0.5 g, 0.8 mmol) and rhodamine B (0.5 g, 1.0 mmol), **14** (0.2 g, 24 %) was obtained as a dark purple solid; R_f = 0.34 (chloroform/methanol, 9:1); IR (ATR): ν = 2970w, 2935w, 2870w, 1720 m, 1645 m, 1584 s, 1556 m, 1529 m, 1480 m, 1466 m, 1433 m, 1410 s, 1394 m, 1334 s, 1272 s, 1245 s, 1196 m, 1177 s, 1160 m, 1130 s, 1072 s, 1006 m, 976 m, 921 m, 868w, 822 m,758 m,709 m, 681 m, 666w, 619w, 608w, 580w, 547w, 520w, 496w, 486w, 465w, 456w cm^{-1}; UV–Vis (MeOH): λ_{max} (log ε) = 223 (4.6), 257 (4.6), 556 (5.1) nm; ^1H NMR (500 MHz, $CDCl_3$) δ = 8.28 (d, *J* = 7.8 Hz, 1H, 47-H), 7.83–7.66 (m, 3H, 46-H + 39-H + 42-H), 7.40–7.29 (m, 2H, 40-H + 41-H), 7.08–7.04 (m, 1H, 47-H), 6.89–6.86 (m, 1H, 47-H'), 6.81(m, 1H, 49′-H), 4.46 (m, 1H, 3-H), 4.20 (m, 1H, 28-H_a), 3.76–3.26 (m, 21H, 28-H_b + 35-H + 35′-H + 36-H + 36′-H + 51-H + 51′-H + 51′′-H + 51′′′-H), 2.24–2.17 (m, 1H, 2-H_a), 2.11 (m, 1H, 19-H), 2.05–2.01(m, 6H, 32-H + 34-H), 1.84–1.71 (m, 3H, 20-H + 16-H_a + 21-H_a), 1.67–1.62 (m, 4H, 1-H_a + 13-H + 15-H_a + 2-H_b), 1.55–1.40 (m, 5H, 12-H_a + 6-H_a + 12-H_b + 9-H + 11-H_b), 1.37–1.20 (m, 20H, 6-H_b + 7-H + 52-H + 52-H'+52′'-H + 52′′'-H + 11-H_b + 22-H_b + 18-H + 16-H_b + 21-H_b), 1.01 (s, 3H, 26-H), 0.99–0.92 (m, 2H, 1-H_b + 15-H_b), 0.90–0.77 (m, 15H, 27-H + 25-H + 24-H), 0.77–0.73 (m, 1H, 5-H) ppm; ^{13}C NMR (126 MHz, $CDCl_3$) δ = 175.3 (C-29), 171.7 (C-33), 171.2 (C-31), 167.9 (C-37), 165.6 (C-48), 159.1 (C-50), 159.1 (C-50′), 157.9 (C-48‘), 155.7 (C-45), 133.8 (C-50‘) 133.3 (C-46), 133.1 (C-39), 131.4 (C-42), 131.4 (C-47), 130.9 (C-46′), 130.6 (C-42), 130.4 (C-49), 130.3 (C-41), 129.9 (C-38), 114.3 (C-47′), 113.7 (C-43), 113.7 (C-45′), 96.6 (C-49‘), 81.1 (C-3), 62.9 (C-28), 55.6 (C-5), 50.2 (C-18), 48.8 (C-9), 46.9 (C-17), 46.4 (C-35 + C-35′+C-36 + C-36′), 46.3 (C-51 + C-51′+C-51′'+C-51′''), 43.9 (C-20), 43.0 (C-14), 41.0 (C-8), 38.7 (C-1), 37.9 (C-4), 37.2 (C-10), 36.8 (C-13), 34.3 (C-7), 33.8 (C-22), 29.8 (C-16), 29.8 (C-21), 28.1 (C-23), 27.7 (C-12), 27.0 (C-15), 23.8 (C-2), 21.7 (C-19), 21.4 (C-34), 21.1 (C-32), 20.9 (C-11), 18.3

(C-6), 16.6 (C-24 + C-25 + C-27), 16.2 (C-26), 16.1 (C-30), 12.8 (C-52 + C-52′+C-52′'+C-52′''') ppm; MS (ESI, MeOH): *m/z* (%) = 1051.6 ([M−Cl]$^+$, 100).

3β-Acetyloxylup-*N*-benzyl-lup-20(29)-en-28-amide (15)

Following GPD from **1** (3. g, 6.6 mmol) and benzylamine (1.9 mL, 17.6 mmol) followed by usual work-up and chromatographic purification (silica gel, *n*-hexane/ethyl acetate, 9:1) **15** (2.6 g, 67%) was obtained as a white solid; R_f = 0.26 (silica gel, *n*-hexane/ethyl acetate, 7:1); m.p. 124–126 °C (lit.: [37] 124–127 °C); $[\alpha]_D$ = +22.3° (*c* = 0.51, $CHCl_3$) [lit.: [37] $[\alpha]_D$ = +23.2° (*c* = 0.35, $CHCl_3$); MS (ESI, MeOH): *m/z* (%) = 588.4 ([M−H]$^+$, 100).

(20*R*) 3β-Acetyloxy-30-hydroxy-*N*-benzyl-lupan-17-carboxamide (16)

Following GPB, from **15** (7.0 g, 11.9 mmol) and chromatographic purification (silica gel, chloroform/*n*-hexane/ethyl acetate, 8:5:3) **16** (5.0 g, 70%) was obtained as a white solid; R_f = 0.35 (chloroform/*n*-hexane/ethyl acetate, 8:5:3); m.p. 142–144 °C (lit.: [37] m.p. 143–145 °C; $[\alpha]_D$ = -0.25° (c = 0.11, $CHCl_3$) (lit.: [37] $[\alpha]_D$ = -0.2° (*c* = 0.18, $CHCl_3$); MS (ESI, MeOH): *m/z* (%) = 604.0 ([M−H] $^-$, 100%).

(20*R*) 3β-Acetoxy-17-benzyl-carbamoyl-lupan-30-oic acid (17)

Following GPC from **16** (2.5 g, 4.1 mmol) **17** (1.3 g, 52%) was obtained as a white solid; R_F = 0.35 (chloroform/*n*-hexane/ethyl acetate, 8:7:1); m.p. 163–167 °C (lit.: [37] m.p. 162–165 °C; $[\alpha]_D$ = -26.5° (c = 0.15, $CHCl_3$) lit.: [37] $[\alpha]_D$ = -27.0° (*c* = 0.12, $CHCl_3$); MS (ESI, MeOH/$CHCl_3$ (4:1)): *m/z* (%) = 618.1 ([M−H]$^-$, 100%).

3,6-Bis(diethylamino)-9 [2-(1-piperazinyl)carbonyl] -xanthylium chloride (18)

Reaction of rhodamine B (10.0 g, 22.3 mmol) in dry DCM (250 mL) with oxalyl chloride (8.84 mL) at 0 °C followed by the addition of piperazine (10.0 g) as described above gave after 24 h and chromatographic purification (silica gel, chloroform/methanol, 9:1) **18** (7.2 g, 67%) as a dark purple amorphous solid; R_f = 0.12 (chloroform/methanol, 8:2); m.p. > 250 °C; MS (ESI, MeOH): *m/z* = 256.2 (26%, [M + H-Cl]$^{2+}$), 511.6 (100%, [M−Cl]$^+$); analysis calcd for $C_{32}H_{39}ClN_4O_2$ (547.14): C 70.25, H 7.18, N 10.24; found: C 69,98, H 7.29, N 9.97.

9- [2- [[4-(3β-Acetyloxy-17β-benzyl-carbamoyl-lupan-29-amid-40-oyl)-piperazinyl] carbonyl] phenyl] -3,6-bis(diethylamino] -xanthylium chloride (19)

Compound **17** (0.4 g, 0.6 mmol) was dissolved in dry DCM (20 mL), oxalyl chloride (0.3 mL) and DMF were added at 0 °C. After 2 h, the volatiles were removed under reduced pressure. The residue was dissolved in dry DCM (10 mL), and the solution was concentrated again to remove excess oxalyl chloride. The acyl chloride of **17** was diluted with dry DCM (15 mL) and added dropwise to a solution of **18** in dry DCM (20 mL). After completion of the reaction (as indicated by TLC), the solvent was removed under diminished pressure, and the residue was subjected to column chromatography (silica gel, chloroform/methanol, 9:1) to yield **19** (51 mg, 9 %) as a dark purple amorphous solid; R_f = 0.30 (chloroform/methanol, 9:1); ^{1}H NMR (500 MHz, $CDCl_3$): δ = 8.16–8.10 (m, 1H), 8.09–8.02 (m, 1H), 7.95–7.53 (m, 4H), 7.48–7.14 (m, 8H), 7.08–6.64 (m, 3H), 4.52–4.43 (m, 1H), 3.96–3.95 (m, 1H), 3.76–3.69 (m, 5H), 3.69–3.53 (m, 6H), 3.50–3.48 (m, 2H), 3.44–3.42 (m, 1H), 3.41–3.23 (m, 4H), 3.19–3.08 (m, 1H), 3.04–2.86 (m, 2H), 2.08–2.01 (m, 6H), 1.99–1.89 (m, 8H), 1.88–1.79 (m, 3H), 1.75–1.57 (m, 6H), 1.55–1.38 (m, 9H), 1.37–1.30 (m, 9H), 1.28–1.22 (m, 8H), 1.19–1.11 (m, 3H), 1.10–1.06 (m, 3H), 1.05–0.96 (m, 2H), 0.93–0.79 (m, 12H), 0.79–0.71 (m, 1H) ppm; ^{13}C NMR (126 MHz, $CDCl_3$): δ = 175.6, 175.3, 170.1, 168.4, 157.2, 155.8, 155.3, 139.7, 137.2, 136.0, 132.2, 130.6, 129.4, 129.4, 128.3, 127.6, 114.7, 114.1, 113.4, 113.2, 98.5, 96.5, 80.2, 55.8, 53.5, 51.3, 50.7, 46.1, 45.7, 45.6, 45.0, 42.6, 42.4, 41.5, 40.0, 39.6, 38.7, 37.8, 37.0, 33.7, 32.6, 31.5, 29.4, 28.2, 27.4, 25.7, 24.2, 21.6, 19.0, 17.8, 16.6, 16.2, 15.7, 14.6, 12.4, 12.0 ppm; MS (ESI, MeOH): *m/z* (%) = 1113.9 ([M−Cl]$^+$, 12%) ppm; analysis calcd for $C_{71}H_{94}N_5O_6Cl$ (1148.99): C 74.22, H 8.25, N 6.10; found: C 73.87, H 8.51, N 5.86.

CRediT authorship contribution statement

Marie Kozubek: Investigation, Writing – review & editing. **Sophie Hoenke:** Investigation, Writing – original draft. **Hans-Peter Deigner:** Conceptualization, Writing – original draft, Writing – review & editing. **René Csuk:** Conceptualization, Writing – original draft, Writing – review & editing.

Declaration of Competing Interest

The authors declare that they have no known competing financial interests or personal relationships that could have appeared to influence the work reported in this paper.

Acknowledgment

We like to thank Dr. D. Ströhl, Y. Schiller and S. Ludwig for the NMR spectra, and M. Schneider for measuring IR and UV/vis spectra as well as optical rotations and micro-analyses. The cell lines were provided by Dr. Th. Müller (Dept. Oncology, Martin-Luther-University Halle-Wittenberg). Experimental help in the lab was provided by V. Karsten (assays) and Dr. R. K. Wolfram (synthesis). We like to thank T. Schmidt for numerous MS spectra.

References

[1] J.T. Lowitz, Über eine neue fast benzoesäureartige Substanz der Birken, Crell's Ann. Chem. 2 (1788,) 312–317.
[2] E. Pisha, H. Chai, I.S. Lee, T.E. Chagwedera, N.R. Farnsworth, G.A. Cordell, C.W. W. Beecher, H.H.S. Fong, A.D. Kinghorn, D.M. Brown, M.C. Wani, M.E. Wall, T. J. Hieken, T.K. Dasgupta, J.M. Pezzuto, Discovery of betulinic acid as a selective inhibitor of human-melanoma that functions by induction of apoptosis, Nat. Med. 1 (10) (1995) 1046–1051.
[3] U. Bildziukevich, Z. Ozdemir, Z. Wimmer, Recent achievements in medicinal and supramolecular chemistry of betulinic acid and its derivatives, Molecules 24, (19) (2019) 3546.
[4] L. Borkova, J. Hodon, M. Urban, Synthesis of betulinic acid derivatives with modified a-rings and their application as potential drug candidates, Asian J. Org. Chem. 7 (8) (2018) 1542–1560.
[5] N. Gupta, A Review on recent developments in the anticancer potential of oleanolic acid and its analogs (2017–2020), Mini Rev. Med. Chem. 22 (4) (2022) 600–616.
[6] J. Hodon, L. Borkova, J. Pokorny, A. Kazakova, M. Urban, Design and synthesis of pentacyclic triterpene conjugates and their use in medicinal research, Eur. J. Med. Chem. 182 (2019), 111653.
[7] H. Hussain, I. Ali, D. Wang, F.L. Hakkim, B. Westermann, I. Ahmed, A.M. Ashour, A. Khan, A. Hussain, I.R. Green, S.T.A. Shah, Glycyrrhetinic acid: a promising scaffold for the discovery of anticancer agents, Expert Opin. Drug Discovery 16 (12) (2021) 1497–1516.
[8] Islam, M. T.; Ali, E. S.; Uddin, S. J.; Khan, I. N.; Shill, M. C.; de Castro e Sousa, J. M.; Barros de Alencar, M. V. O.; Melo-Cavalcante, A. A. C.; Mubarak, M. S., Anti-Cancer Effects of Asiatic Acid, a Triterpene from Centilla asiatica L: A Review. *Anti-Cancer Agents Med. Chem.* **2020,** 20, (5), 536-547.
[9] M. Olech, W. Ziemichod, N. Nowacka-Jechalke, The occurrence and biological activity of tormentic acid-a review, Molecules 26, (13) (2021) 3797.
[10] A. Sureda, M. Martorell, X. Capo, M. Monserrat-Mesquida, M.M. Quetglas-Llabres, M. Rasekhian, S.M. Nabavi, S. Tejada, Antitumor effects of triterpenes in hepatocellular carcinoma, Curr. Med. Chem. 28 (13) (2021) 2465–2484.
[11] A.K. Surowiak, L. Balcerzak, S. Lochynski, D.J. Strub, Biological activity of selected natural and synthetic terpenoid lactones, Int. J. Mol. Sci. 22, (9) (2021) 5036.
[12] L.C. Baratto, M.V. Porsani, I.C. Pimentel, A.B. Pereira Netto, R. Paschke, B. H. Oliveira, Preparation of betulinic acid derivatives by chemical and biotransformation methods and determination of cytotoxicity against selected cancer cell lines, Eur. J. Med. Chem. 68 (2013) 121–131.
[13] U. Bildziukevich, M. Malík, Z. Özdemir, L. Rárová, L. Janovská, M. Šlouf, D. Šaman, J. Šarek, N. Nonappa, Z. Wimmer, Spermine amides of selected

triterpenoid acids: dynamic supramolecular system formation influences the cytotoxicity of the drugs, J. Mater. Chem. B 8 (3) (2020) 484–491.
[14] B.A. Ganaie, M. Shahid, A. Rashid, T. Ara, J. Ahmad Banday, F. Malik, B.A. Bhat, Platanic acid-aryl enones as potential anticancer compounds: synthesis and biological profiling against breast, prostate and lung cancer cell lines, Chem. Biodiversity 18, (10) (2021) e2100292.
[15] S. Hoenke, M.A. Christoph, S. Friedrich, N. Heise, B. Brandes, H.-P. Deigner, A. Al-Harrasi, R. Csuk, The presence of a cyclohexyldiamine moiety confers cytotoxicity to pentacyclic triterpenoids, Molecules 26, (7) (2021) 2102.
[16] S. Hoenke, N.V. Heise, M. Kahnt, H.-P. Deigner, R. Csuk, Betulinic acid derived amides are highly cytotoxic, apoptotic and selective, Eur. J. Med. Chem. 207 (2020), 112815.
[17] M. Kahnt, L. Fischer, A. Al-Harrasi, R. Csuk, Ethylenediamine derived carboxamides of betulinic and ursolic acid as potential cytotoxic agents, Molecules 23 (10) (2018) 1–19.
[18] M. Kahnt, L. Heller, P. Grabandt, A. Al-Harrasi, R. Csuk, Platanic acid: A new scaffold for the synthesis of cytotoxic agents, Eur. J. Med. Chem. 143 (2018) 259–265.
[19] J.Y. Kim, H.M. Koo, D.S.H.L. Kim, Development of C-20 modified betulinic acid derivatives as antitumor agents, Bioorg. Med. Chem. Lett. 11 (17) (2001) 2405–2408.
[20] O. Kraft, M. Kozubek, S. Hoenke, I. Serbian, D. Major, R. Csuk, Cytotoxic triterpenoid-safirinium conjugates target the endoplasmic reticulum, Eur. J. Med. Chem. 209 (2021), 112920.
[21] S. Sommerwerk, L. Heller, R. Csuk, Synthesis and cytotoxic activity of pentacyclic triterpenoid sulfamates, Arch. Pharm. (Weinheim, Ger.) 348 (1) (2015) 46–54.
[22] S. Schwarz, A. Loesche, S.D. Lucas, S. Sommerwerk, I. Serbian, B. Siewert, E. Pianowski, R. Csuk, Converting maslinic acid into an effective inhibitor of acylcholinesterases, Eur. J. Med. Chem. 103 (2015) 438–445.
[23] B. Siewert, E. Pianowski, A. Obernauer, R. Csuk, Towards cytotoxic and selective derivatives of maslinic acid, Bioorg. Med. Chem. 22 (1) (2014) 594–615.
[24] S. Sommerwerk, L. Heller, J. Kuhfs, R. Csuk, Urea derivates of ursolic, oleanolic and maslinic acid induce apoptosis and are selective cytotoxic for several human tumor cell lines, Eur. J. Med. Chem. 119 (2016) 1–16.
[25] I.Z. Pavel, R. Csuk, C. Danciu, S. Avram, F. Baderca, A. Cioca, E.-A. Moaca, C.-V. Mihali, I. Pinzaru, D.M. Muntean, C.A. Dehelean, Assessment of the antiangiogenic and anti-inflammatory properties of a maslinic acid derivative and its potentiation using zinc chloride, Int. J. Mol. Sci. 20, (11) (2019) 2828.
[26] I.Z. Pavel, C. Danciu, C. Oprean, C.A. Dehelean, D. Muntean, R. Csuk, D. M. Muntean, In vitro evaluation of the antimicrobial ability and cytotoxicity on two melanoma cell lines of a benzylamide derivative of maslinic acid, Anal. Cell. Pathol. 2016 (2016) 1–6.
[27] I.Z. Pavel, C.A. Dehelean, L. Farczadi, D.M. Muntean, L. Vlase, C. Danciu, R. Csuk, F. Birsasteanu, D.M. Muntean, Assessment of a maslinic acid derivative and its metabolite in rat blood by liquid chromatography coupled with mass spectrometry, Rev. Chim. (Bucharest, Rom.) 68 (5) (2017) 1089–1094.
[28] S. Sommerwerk, L. Heller, J. Kuhfs, R. Csuk, Selective killing of cancer cells with triterpenoic acid amides - The substantial role of an aromatic moiety alignment, Eur. J. Med. Chem. 122 (2016) 452–464.
[29] S. Hoenke, I. Serbian, H.-P. Deigner, R. Csuk, Mitocanic Di- and triterpenoid rhodamine B conjugates, Molecules 25, (22) (2020) 5443.
[30] M. Kahnt, J. Wiemann, L. Fischer, S. Sommerwerk, R. Csuk, Transformation of asiatic acid into a mitocanic, bimodal-acting rhodamine B conjugate of nanomolar cytotoxicity, Eur. J. Med. Chem. 159 (2018) 143–148.
[31] O. Kraft, A.-K. Hartmann, S. Hoenke, I. Serbian, R. Csuk, Madecassic acid-a new scaffold for highly cytotoxic agents, Int J Mol Sci 23 (2022) (8).
[32] I. Macasoi, I.Z. Pavel, A.E. Moaca, S. Avram, V.L. David, D. Coricovac, A. Mioc, D. A. Spandidos, A. Tsatsakis, C. Soica, V. Dumitrascu, C. Dehelean, Mechanistic investigations of antitumor activity of a rhodamine B-oleanolic acid derivative bioconjugate, Oncol. Rep. 44 (3) (2020) 1169–1183.
[33] I. Serbian, S. Hoenke, R. Csuk, Synthesis of some steroidal mitocans of nanomolar cytotoxicity acting by apoptosis, Eur. J. Med. Chem. 199 (2020), 112425.
[34] J. Wiemann, L. Fischer, J. Kessler, D. Stroehl, R. Csuk, Ugi multicomponent-reaction: Syntheses of cytotoxic dehydroabietylamine derivatives, Bioorg. Chem. 81 (2018) 567–576.
[35] R.K. Wolfram, L. Fischer, R. Kluge, D. Ströhl, A. Al-Harrasi, R. Csuk, Homopiperazine-rhodamine B adducts of triterpenoic acids are strong mitocans, Eur. J. Med. Chem. 155 (2018) 869–879.
[36] R.K. Wolfram, L. Heller, R. Csuk, Targeting mitochondria: Esters of rhodamine B with triterpenoids are mitocanic triggers of apoptosis, Eur. J. Med. Chem. 152 (2018) 21–30.
[37] M. Kozubek, S. Hoenke, T. Schmidt, H.-P. Deigner, A. Al-Harrasi, R. Csuk, Synthesis and cytotoxicity of betulin and betulinic acid derived 30-oxo-amides, Steroids 182 (2022) 109014.
[38] S. Sommerwerk, L. Heller, C. Kerzig, A.E. Kramell, R. Csuk, Rhodamine B conjugates of triterpenoic acids are cytotoxic mitocans even at nanomolar concentrations, Eur. J. Med. Chem. 127 (2017) 1–9.
[39] M. Urban, J. Sarek, J. Klinot, G. Korinkova, M. Hajduch, Synthesis of a-seco derivatives of betulinic acid with cytotoxic activity, J. Nat. Prod. 67 (7) (2004) 1100–1105.
[40] D. Thibeault, C. Gauthier, J. Legault, J. Bouchard, P. Dufour, A. Pichette, Synthesis and structure-activity relationship study of cytotoxic germanicane- and lupane-type 3 beta-O-monodesmosidic saponins starting from betulin, Bioorg. Med. Chem. 15 (18) (2007) 6144–6157.
[41] A. Vystrcil, Budesins.M, Triterpenes., 16. Unusual epimerisation of C(19)-acetyl group of 20-Oxo-30-norlupane derivatives, Collect. Czech. Chem. Comm. 35 (1) (1970) 295–311.
[42] I. Beseda, L. Czollner, P.S. Shah, R. Khunt, R. Gaware, P. Kosma, C. Stanetty, M. C. del Ruiz-Ruiz, H. Amer, K. Mereiter, T. Da Cunha, A. Odermatt, D. Classen-Houben, U. Jordis, Synthesis of glycyrrhetinic acid derivatives for the treatment of metabolic diseases, Bioorg. Med. Chem. 18 (1) (2010) 433–454.
[43] L. Ruzicka, O. Isler, Polyterpene und polyterpenoide, CVI, Oxydation des dihydro-betulins and der dihydro-betulonsäure mit salpetersäure, Helv. Chim. Acta 19 (1936) 506–519.
[44] I.C. Sun, H.K. Wang, Y. Kashiwada, J.K. Shen, L.M. Cosentino, C.H. Chen, L. M. Yang, K.H. Lee, Anti-AIDS agents. 34. Synthesis and structure-activity relationships of betulin derivatives as anti-HIV agents, J. Med. Chem. 41 (23) (1998) 4648–4657.
[45] A. Vystrcil, V. Krecek, M. Budesinsky, Triterpenes., 42. Photooxidation of (20R)- and (20S)-29-Lupanol Derivatives, Collect. Czech. Chem. Commun. 40 (5) (1975) 1593–1603.
[46] A. Vystrcil, V. Pouzar, V. Krecek, Triterpenes., 32. absolute-configuration at C(20) in 29-substituted lupane derivatives, Collect. Czech. Chem. Commun. 38 (12) (1973) 3902–3911.

P7

Results in Chemistry 5 (2023) 100708

Contents lists available at ScienceDirect

Results in Chemistry

journal homepage: www.sciencedirect.com/journal/results-in-chemistry

On the influence of the rhodamine substituents onto the cytotoxicity of mitocanic maslinic acid rhodamine conjugates

Marie Kozubek, Toni C. Denner, Marc Eckert, Sophie Hoenke, René Csuk *

Organic Chemistry, Martin-Luther University Halle-Wittenberg, Kurt-Mothes-Str. 2, D-06120 Halle (Saale), Germany

ARTICLE INFO

Keywords:
Maslinic acid
Mitocans
Rhodamine
Cytotoxicity

ABSTRACT

Maslinic acid was converted via a di-acetylated piperazinyl amide into rhodamine conjugates differing in their alkyl moieties. These conjugates were submitted to cytotoxicity assays employing a panel of human tumor cell lines. These conjugates held high cytotoxicity but also some selectivity especially for A2780 cells. Thereby, a propyl substituted rhodamine conjugate showed EC_{50} values as low as $EC_{50} = 0.01$ μM and was approx. 15 times more cytotoxic for the cancer cells than for non-malignant fibroblasts (NIH 3 T3). Cytotoxicity obviously parallels the lipophilicity of the residue and suggests - since the compounds act as mitocanes - an interaction of the conjugates with the inner mitochondrial membrane.

Introduction

Compounds that selectively address mitochondria of cancer cells are currently considered an innovative and promising option for cancer chemotherapy. [1–12] This is partly due to the discovery that mitochondria are more than just the "power plants" of cells. [13–18].

Some time ago, we showed that pentacyclic triterpenes are ideal starting materials for the development of cytotoxic compounds. [19–22] Thereby, we revealed that the following prerequisites must be present: an amide-bound spacer between the carboxyl group of the triterpene and a distal cationic group. While "simple" quaternary ammonium salts showed improved cytotoxicity as compared to the parent compounds, a breakthrough could be achieved by accessing lipophilic rhodamine B derivatives. The use of a piperazinyl spacer proved to be particularly advantageous. [23–32].

While a hybrid of acetylated oleanolic acid (Fig. 1) with piperazinyl spacer and rhodamine B already showed good cytotoxicity towards human tumor cells, the corresponding analogue from maslinic acid, [33] which - in comparison to oleanolic acid - also carries an additional hydroxyl group at C-2, was clearly more cytotoxic; at the same time the latter compound showed a higher selectivity towards tumor cells in comparison to non-malignant cells (NIH 3 T3). [21] This trend of better cytotoxicity was also observed for the corresponding benzylamides. The benzylamide of 3-*O*-acetyloleanolic acid showed an EC_{50} of 4.3 μM for A2780 human ovarian adenocarcinoma cells, while the benzylamide of di-acetylated maslinic acid (**EM2**) held a significantly higher cytotoxicity ($EC_{50} = 0.5$ μM) for the same cell line. [34] The same applies to the acetylated piperazinyl amides. After already having carried out investigations on the spacer (ethylenediamine or piperazine), the piperazinyl spacer proved to be beneficial for obtained low EC_{50} values. Thus, an investigation of the influence of the distal rhodamine residue [25] was called for.

Results and discussion

Several routes have been suggested for the synthesis of substituted rhodamines. [35,36] Due to good commercial availability of the starting material and the shortness of the route (Scheme 1), we decided to use 3-aminophenol as a starting material, whose reaction with alkyl-halides gave the dialkyl-3-aminophenols **4**–**7**. The rhodamines **8**–**11** were accessed from the reaction of **4**–**7** with phthalic anhydride in the presence of catalytic amounts of aluminum trichloride.

Maslinic acid (**1**) was extracted from pitted olives as previously described; [34,37] its acetylation (Scheme 2) gave known di-acetate **2**. [33] The reaction of **2** with oxalyl chloride in the presence of catalytic amounts of dimethylformamide (DMF) followed by a reaction with piperazine furnished piperazinyl-amide **3**. [30].

The reaction of **8**–**11** with oxalyl chloride converted the rhodamines *in situ* into the corresponding acid chlorides; these were allowed to react with **3** to afford the piperazinyl-spacered triterpene-rhodamine conjugates **12**–**15**.

To assess the cytotoxicity of these compounds sulforhodamine B

* Corresponding author.
E-mail address: rene.csuk@chemie.uni-halle.de (R. Csuk).

https://doi.org/10.1016/j.rechem.2022.100708
Received 5 November 2022; Accepted 2 December 2022
Available online 6 December 2022

(SRB) assays were performed employing several human tumor cell lines. The results from these assays as well the tumor/non-tumor cell selectivity S [$EC_{50\ (NIH\ 3T3)}$ / $EC_{50\ (respective\ cell\ line)}$] are summarized in Table 1.

As a result, compound **1** was cytotoxic to only a minor extent; much stronger cytotoxicity was observed for piperazinyl amide **3**. This compound is cytotoxic to all tumor cell lines but also to non-malignant fibroblasts (NIH 3 T3) to about the same extent. In contrast, a marked increase in cytotoxicity up to an approximately 100-fold factor was observed for the rhodamine conjugates **12**–**14**. All compounds show a particular cytotoxicity for A2780 cells (EC_{50} 0.02 to 0.01 μM). However, **14** is the most cytotoxic for both A2780, A375 and MCF-7 cells, while a much weaker cytotoxicity was observed for NIH 3 T3 cells. This is also reflected in the calculated selectivity S (S = $EC_{50,\ NIH\ 3T3}$ / $EC_{50\ respective\ cell\ line}$). The cell selectivity is highest (S = 15.0) for A2780 cells. In principle, the cytotoxicity seems to increase with a longer chain length of the alkyl substituent on the rhodamine moiety. This also correlates well with the calculated log $p_{octanol/water}$ partition coefficients for the rhodamine-piperazinyl residues: this coefficient increases from 0.61 (for methyl-substitution) to 1.72 (for ethyl) to 3.05 (for propyl). Thus, there seems to be a certain - but not conclusively clarified - correlation between the substitution pattern on the rhodamine and the observed cytotoxicity. Earlier we could show that triterpene-piperazinyl-rhodamine conjugates are to be considered and act as mitocanes and their cytotoxic effect is probably due to an interaction with the inner mitochondrial membrane.

Conclusion

Maslinic acid (from the extraction of pitted olives) was acetylated and converted into the corresponding piperazinyl amide **3** whose coupling with rhodamines differing in their alkyl moieties led to the formation of triterpene-rhodamine conjugates **12**–**15**. These conjugates were cytotoxic to a panel of human tumor cell lines but less to non-malignant fibroblasts. Worthwhile to mention that these compounds held some selectivity for A2780 cells, and especially compound **14**, a propyl substituted rhodamine conjugate showed EC_{50} values as low as EC_{50} = 0.01 μM and was approx. 15 times more cytotoxic for the cancer cells than for the fibroblasts. The measured cytotoxicity obviously parallels the calculated octanol/water partition coefficient and suggests - since the compounds act as mitocanes - an interaction with the inner mitochondrial membrane.

Experimental

General

NMR spectra were recorded using the Varian spectrometers DD2 and VNMRS (400 and 500 MHz, respectively). MS spectra were taken on a Advion expression^{L} CMS mass spectrometer (positive or negative ion polarity mode, solvent: methanol, solvent flow: 0.2 mL/min, spray voltage: 5.17 kV, source voltage: 77 V, APCI corona discharge: 4.2 μA, capillary temperature: 250 °C, capillary voltage: 180 V, sheath gas: N2). Thin-layer chromatography was performed on pre-coated silica gel plates supplied by Macherey-Nagel. IR spectra were recorded on a Spectrum 1000 FT-IR-spectrometer from Perkin-Elmer. The UV/Vis-spectra were recorded on a Lambda 14 spectrometer from Perkin-Elmer. The optical rotations were measured either on a JASCO P-2000 or a Perkin-Elmer polarimeter 341 at 20 °C. The melting points were determined using the Leica hot stage microscope Galen III and are uncorrected. Elemental analyses were performed on a Foss-Heraeus Vario EL (CHNS) unit. The solvents were dried according to usual procedures.

Biological testing

Cell lines and culture conditions

Following human cancer cell lines A375 (malignant melanoma), HT29 (colon adenocarcinoma), MCF-7 (breast cancer), A2780 (ovarian carcinoma), HeLa (cervical cancer) and NIH 3 T3 (non-malignant mouse fibroblasts) were used. All cell lines were obtained from the Department of Oncology (Martin-Luther-University Halle Wittenberg). Cultures were maintained as monolayers in RPMI 1640 medium with L-glutamine (Capricorn Scientific GmbH, Ebsdorfergrund, Germany) supplemented with 10 % heat-inactivated fetal bovine serum (Sigma-Aldrich GmbH, Steinheim, Germany) and penicillin/streptomycin (Capricorn Scientific GmbH, Ebsdorfergrund, Germany) at 37 °C in a humidified atmosphere with 5 % CO_2.

Cytotoxicity assay (SRB assay)

For the evaluation of the cytotoxicity of the compounds the sulforhodamine-B (Kiton-Red S, ABCR GmbH, Karlsruhe, Germany) micro-culture colorimetric assay was used. The EC_{50} values were averaged from three independent experiments performed each in triplicate and calculated from semi-logarithmic dose–response curves applying a non-linear 4P Hills-slope equation.

Syntheses

General procedure a (GPA)

3-Aminophenol (7.6 g, 69.6 mmol) was dissolved in DMF (50 mL) and the respective alkyl halide (205 mmol) and potassium carbonate (18.0 g, 130 mmol) were added; stirring was continued at 100 °C for 3–8 h. Usual aqueous workup followed by chromatographic purification furnished compounds **4**–**7**.

General procedure B (GPB)

The rhodamines **8**–**11** were synthesized by heating a mixture of the respective dialkyl-3-aminophenol **4**–**7** (28.4–41.4 mmol), phthalic

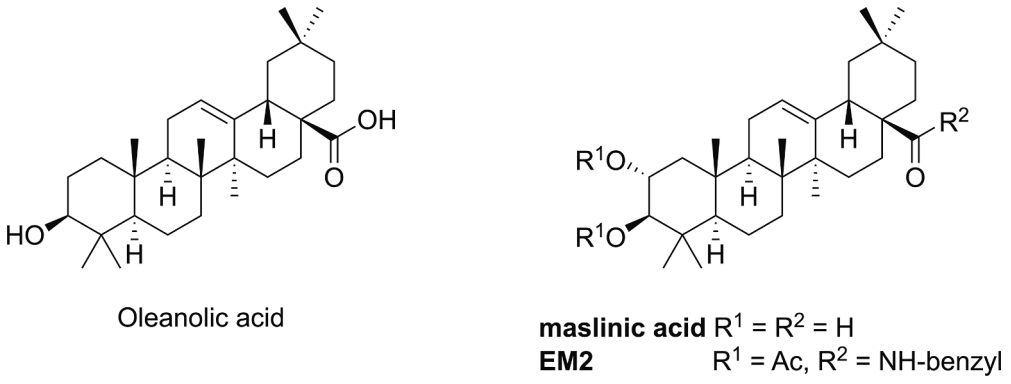

Fig. 1. Structure of oleanolic acid (OA), maslinic acid (MA, 1) and cytotoxic derivative EM2.

anhydride (14.2 – 20.7 mmol) and a catalytic amount of aluminum trichloride to 200 °C for 5–60 min (completion of the reaction checked by TLC). After the completion of the reaction the crude product was purified by column chromatography.

General procedure C (GPC)

Compounds **8**–**11** (0.4 mmol) were dissolved each in dry DCM (10 mL) and at 0 °C oxalyl chloride (0.1 mL, 1.4 mmol) and a catalytic amount of DMF were added, stirring continued at room temperature for 2 h. The volatiles were removed under reduced pressure, and the residue was re-dissolved with THF (3 × 10 mL), and the solvent was removed again. The residue was dissolved in dry DCM (5 mL) and added to a solution of compound **3** (330 mg, 0.5 mmol), triethylamine (0.9 mL, 0.7 mmol) and a catalytic amount of DMAP in dry DCM (5 mL); the mixture was stirred at room temperature for 24 h. The solvent was removed, and the residue subjected to chromatography to yield **12**–**15**.

*Maslinic acid (**1**)*

Pitted green olives (bought from a local discounter, 10 kg) were crushed into small pieces and dried for 2 days at 130–135 °C. The dry material (2.6 kg) was suspended in methanol (3 L) and allowed to stand (with occasional swaying) for 2 days. The mixture was filtered, and the filter cake was extracted with methanol (each 3 L, 2 days, procedure repeated 3 times). The solvent was removed, and the residue subjected to chromatography (silica gel, *n*-hexane/ethyl acetate/methanol, 5:5:1). re-crystallization (*n*-hexane/ethyl acetate) yielded **1** (13.8 g) as a colorless solid; m.p. 264–267 °C (decomp.), (lit.: [38] 265–268 °C (decomp.); R_F = 0.36 (*n*-hexane/ethyl acetate, 1:2).

*2α, 3β-Bis(acetyloxy)-olean-12-en-28-oic acid (**2**)*

Maslinic acid (1) was acetylated as previously described followed by a chromatographic purification of the crude product (silica gel, *n*-hexane/ethyl acetate, 9:1) to yield **2** (78 %); m.p. 280–283 °C (lit.: [33] 287–289 °C); R_F = 0.31 (silica gel, *n*-hexane/ethyl acetate, 6:4).

*2α, 3β-Bis(acetyloxy)-olean-12-en-28-oyl piperazine (**3**)*

Compound **2** was converted into its piperazinyl amide **3** as previously reported in 86 % yield. m.p. 156–159 °C (lit.: [30] 157–160 °C); R_F = 0.35 (silica gel, chloroform/methanol, 9:1).

*3-(Dimethylamino)phenol (**4**)*

According to GPA from methyl iodide followed by chromatography (silica gel, *n*-hexane/ethyl acetate, 4:1) **4** (52 %) was obtained as a white solid; m.p. 82–85 °C (lit: [39] 84–85 °C); R_F = 0.55 (chloroform/methanol, 95:5).

*3-(Diethylamino)phenol (**5**)*

According to GPA from ethyl bromide followed by chromatography (silica gel, *n*-hexane/ethyl acetate, 9:1), **5** (67 %) was obtained as an off-white solid; m.p. 52–55 °C (lit.: [40] 55 °C); R_F = 0.42 (chloroform/methanol, 95:5).

*3-(Dipropylamino)phenol (**6**)*

According to GPA from *n*-propyl bromide followed by chromatography (silica gel, *n*-hexane/ethyl acetate, 9:1) **6** (61 %) was obtained as an off-white solid; m.p. 98–99 °C (lit: [41] 99.7–100.1 °C); R_F = 0.37 (chloroform/methanol, 95:5).

*3-(Dibenzylamino)phenol (**7**)*

According to GPA with benzyl bromide (25 mL) followed by chromatography (silica gel, *n*-hexane/ethyl acetate, 9:1) **7** (8.3 g, 41 %) was obtained as a white solid; m.p. 61–63 °C (lit.: [42] 62–64 °C); R_F = 0.68 (chloroform/methanol, 95:5); IR (ATR): ν = 3514br, 3387br, 3084w, 3061 m, 3027 m, 2905 m, 2865 m, 1703 m, 1615 s, 1603 s, 1578 s, 1502 s, 1494 s, 1451 s, 1395 s, 1359 s, 1328 s, 1297 s, 1277 s, 1262 s, 1166 s, 1074 s, 1044 m, 1027 s, 1001w cm^{-1}; ^1H NMR (400 MHz, $CDCl_3$): δ = 7.42 – 7.18 (m, 10*H*, 9-H + 10-H + 11-H), 7.01 (t, *J* = 8.1 Hz, 1H, 5-H), 6.37 (d, *J* = 5.4 Hz, 1H, 6-H), 6.26 (br s, 1H, 2H), 4.63 (s, 4H, 7-H) ppm; ^{13}C NMR (101 MHz, $CDCl_3$): δ = 156.8 (C-1), 151.0 (C-3), 138.5 (C-8), 130.3 (C-5), 128.8 (C-10), 127.1 (C-11), 126.8 (C-9), 105.5 (C-4), 104.0 (C-6), 99.7 (C-2), 54.3 (C-7) ppm; MS (ESI, MeOH/chloroform, 4:1): *m/z* = 288.1 (56 %, $[M-H]^-$), 290.1 (40 %, $[M + H]^+$).

*9-(2-Carboxyphenyl)-3,6-bis(dimethylamino)xanthylium chloride (**8**)*

According to GPB from **4** followed by chromatography (silica gel, chloroform/MeOH, 9:1) **8** (35 %) was obtained as a violet solid; [43] m. p. 250 °C; R_F = 0.12 (chloroform/methanol, 9:1); UV–vis (MeOH): λ^{max} (log ε) = 254 (3.81), 354 (3.30), 541 (4.28) nm; IR (ATR): ν = 3362br, 2925br, 1718 m, 1645 s, 1590 s, 1537 s, 1514 s, 1490 s, 1407 s, 1364 s, 1346 s, 1262 m, 1220 s, 1187 s, 1138 s, 1090 m, 1071 s cm^{-1}; ^1H NMR (500 MHz, DMSO-d_6): δ = 7.96 (d, *J* = 7.6 Hz, 1H, 3-H), 7.77 (td, *J* = 7.5, 1.0 Hz, 1H, 5-H), 7.70 (td, *J* = 7.6 Hz, 1H, 4-H), 7.20 (d, *J* = 7.6 Hz, 1H, 6-H), 6.64 – 6.33 (m, 6H, 10-H + 10′-H + 11-H + 11′-H + 13-H + 13′-H), 2.93 (s, 12H, 15-H + 15‘-H) ppm; ^{13}C NMR (101 MHz, DMSO-d_6): δ = 168.9 (C-1), 152.5 (C-7), 152.2 (C-14), 152.2 (C-14′), 151.9 (C-12), 151.9 (C-12′), 135.3 (C-5), 129.9 (C-4), 128.3 (C-10), 128.3 (C-10′), 126.6 (C-2), 124.4 (C-3), 124.0 (C-6), 109.0 (C-11), 109.0 (C-11′), 106.1 (C-9), 106.1 (C-9′), 98.0 (C-13), 98.0 (C-13‘), 84.7 (C-8), 39.8 (C-15), 39.8 (C-15‘) ppm; MS (ESI, methanol/chloroform 4:1): *m/z* = 387.2 (64 %, $[M-Cl]^+$), 409.2 (24 %, $[M-Cl + Na]^+$).

*9-(2-Carboxyphenyl)-3,6-bis(diethylamino)xanthylium chloride (**9**)*

According to GPBA from **5** followed by chromatography (silica gel, chloroform/MeOH, 12:1) **8** (45 %) was obtained as a violet solid; m.p. 163–166 °C; R_F = 0.25 (chloroform/methanol, 9:1); identical with commercial material (m.p., m.m.p., ^1H and ^{13}C NMR).

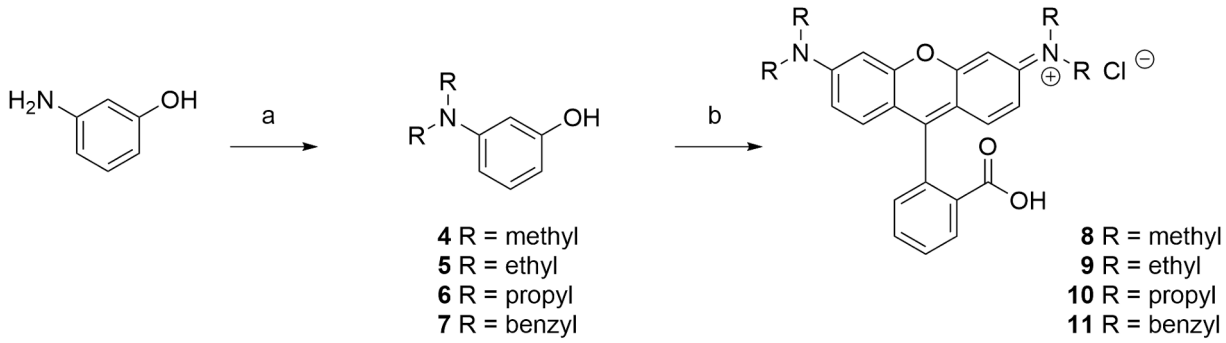

Scheme 1. Reactions and conditions of the rhodamine synthesis: (a) DMF, potassium carbonate and methyl iodide (→4 (52 %)), ethyl bromide (→5 (67 %)), *n*-propyl bromide (→6 (61 %)), or benzyl bromide (→7 (41 %)), 3–8 h, 21 °C; (b) phthalic anhydride, aluminum trichloride (cat.), 5–60 min, 200 °C, yield: 8 (35 %), 9 (45 %), 10 (42 %), 11 (35 %).

*9-(2-Carboxyphenyl)-3,6-bis(dipropylamino)xanthylium chloride (**10**)*

According to GPB from **6** followed by chromatography (silica gel, chloroform/MeOH, 12:1) **10** (42 %) was obtained as a violet solid; m.p. 185–188 °C; R_F = 0.34 (chloroform/methanol, 9:1); UV–vis (MeOH): λ^{max} (log ε) = 224 (4.47), 259 (4.48), 284 (4.18), 305 (4.17), 550 (4.95) nm; IR (ATR): ν = 2957 m, 2931 m, 2872 m, 1741 s, 1637 s, 1614 s, 1589 s, 1544 s, 1519 s, 1464 s, 1430 s, 1410 s, 1370 s, 1337 s, 1286 s, 1265 s, 1232 s, 1216 s, 1196 s, 1180 s, 1157 m, 1126 s, 1113 s, 1102 s, 1038w, 1010 m cm^{-1}; ^1H NMR (500 MHz, $CDCl_3$): δ = 8.21 (d, *J* = 8.4 Hz, 1H, 3-H), 7.65 – 7.55 (m, 2H, 5-H + 4-H), 7.19 – 7.13 (m, 1H, 6-H), 6.91 (d, *J* = 9.0 Hz, 2H, 10-H + 10'-H), 6.61 – 6.52 (m, 4H, 13-H + 13'-H + 11-H + 11'-H), 3.39 – 3.33 (m, 8H, 15-H + 15'-H), 1.67 (dt, *J* = 15.3, 7.6 Hz, 8H, 16-H + 16'-H), 0.95 (t, *J* = 7.4 Hz, 12H, 17-H + 17'-H) ppm; ^{13}C NMR (101 MHz, $CDCl_3$): δ = 168.3 (C-1), 156.1 (C-7), 155.6 (C-14), 155.6 (C-14'), 152.8 (C-12), 152.8 (C-12'), 132.9 (C-5), 130.8 (C-7), 130.4 (C-4), 130.4 (C-10), 130.4 (C-10′), 129.6 (C-3), 128.9 (C-2), 126.6 (C-6), 113.7 (C-9), 113.7 (C-9′), 111.0 (C-11), 111.0 (C-11′), 97.0 (C-13), 97.0 (C-13′), 86.6 (C-8), 53.3 (C-15), 53.3 (C-15'), 20.6 (C-16), 20.6 (C-16'), 11.4 (C-17), 11.4 (C-17') ppm; MS (ESI, methanol/ chloroform 4:1): *m/z* = 517.3 (100 %, $[M-Cl]^+$).

*9-(2-Carboxyphenyl)-3,6-bis(dibenzylamino)xanthylium chloride (**11**)*

According to GPB from **7** followed by chromatography (silica gel, chloroform/MeOH, 9.8:0.2) **11** (35 %) was obtained as a violet solid; m.p. 111–114 °C; R_F = 0.60 (chloroform/methanol, 9:1); UV–vis (MeOH): λ^{max} (log ε) = 256 (4.49), 352 (4.21), 540 (4.80) nm; IR (ATR): ν = 3061w, 3028w, 2908w, 2862w, 1753 s, 1721 s, 1631 s, 1613 s, 1592 s, 1582 s, 1549 s, 1516 s, 1494 s, 1465 s, 1451 s, 1426 s, 1404 s, 1392 s, 1342 s, 1330 s, 1284 s, 1241 s, 1229 s, 1201 s, 1156 s, 1129 s, 1108 s, 1077 s, 1028 m, 1002w cm^{-1}; ^1H NMR (500 MHz, $CDCl_3$): δ = 8.09 (d, *J* = 9.6 Hz, 1H, 3-H), 7.62 (td, *J* = 7.5, 1.2 Hz, 1H, 5-H), 7.51 – 7.47 (td, *J* = 7.8, 1.1 Hz, 1H, 4-H), 7.35 – 7.16 (m, 20H, 18-H + 18′-H + 19-H + 19′-H + 17-H + 17′-H), 6.87 (d, *J* = 9.1 Hz, 1H, H-6), 6.75 (d, *J* = 9.9 Hz, 2H, 10-H + 10′-H), 6.64 – 6.56 (m, 4H, 13-H + 13′-H + 11-H + 11′-H), 4.71 (s, 8H, 15-H + 15′-H) ppm; ^{13}C NMR (126 MHz, $CDCl_3$): δ = 165.5 (C-1), 155.8 (C-14), 155.8 (C-14'), 155.1 (C-12), 155.1 (C-12') 153.6 (C-7), 136.6 (C-16), 136.6 (C-16'), 134.9 (C-6), 133.5 (C-5), 130.3 (C-10), 130.3 (C10'), 129.8 (C-4), 129.1 (C-18), 129.1 (C-18'), 128.1 (C-2), 127.6 (C-19), 127.6 (C-19'), 127.5 (C-3), 126.5 (C-17), 126.5 (C-17'), 111.3 (C-9), 111.3 (C-9'), 111.1 (C-11), 111.1 (C-11'), 98.4 (C-13), 98.4 (C-13'), 84.9 (C-8), 54.5 (C-15), 54.5 (C-15') ppm; MS (ESI, MeOH/ chloroform 4:1) *m/z* = 713.2 (3 %, $[M-Cl + Na-2H]^-$), 691.3 (50 %, $[M-Cl]^+$); analysis calcd for $C_{48}H_{39}ClN_2O_3$ (727.30): C 79.27, H 5.41, N 3.85; found: C 78.90, H 5.63, N 3.69.

Table 1
SRB assay EC_{50} values [μM] after 72 h of treatment; averaged from three independent experiments performed each in triplicate; confidence interval CI = 95 %. Human cancer cell lines: A375 (melanoma), HT29 (colorectal carcinoma), MCF-7 (breast adenocarcinoma), A2780 (ovarian carcinoma), HeLa (cervical carcinoma), NIH 3 T3 (non-malignant fibroblasts); cut-off 30 μM, n.d. not determined; doxorubicin (DX) has been used as a positive standard; compound 15 was not soluble under the conditions of the assay.

[μM]	A375	HT29	MCF-7	A2780	HeLa	NIH 3 T3
MA	>30	28.8 ± 0.5	>30	19.5 ± 0.8	>30	21.1 ± 0.2
3	2.0 ± 0.1	1.6 ± 0.1	1.0 ± 0.1	1.9 ± 0.1	2.1 ± 0.1	3.2 ± 0.02
12	0.07 ± 0.01	0.11 ± 0.04	0.05 ± 0.02	0.02 ± 0.001	0.15 ± 0.02	0.30 ± 0.04
13	0.05 ± 0.01	0.09 ± 0.03	0.03 ± 0.01	0.02 ± 0.005	0.08 ± 0.03	0.25 ± 0.03
14	0.02 ± 0.004	0.07 ± 0.02	0.03 ± 0.005	0.01 ± 0.001	0.05 ± 0.01	0.15 ± 0.04
DX	n.d.	0.9 ± 0.01	1.1 ± 0.3	0.01 ± 0.01	n.d.	0.4 ± 0.0
Selectivity						
12	4.3	2.7	6.0	15.0	2.0	
13	5.0	2.8	8.3	12.5	3.1	
14	7.5	2.1	5.0	15.0	3	

*9-[2-[[4-(2α,3β-Bis(acetyloxy)-olean-12-en-28-oyl)-1-piperazinyl] carbonyl]phenyl]-3,6-bis(dimethylamino]-xanthylium chloride (**12**)*

According to GPC with **8** (0.2 g) followed by chromatography (silica gel, chloroform/MeOH, 9:1) **12** (168 mg, 46 %) was obtained as a violet solid; m.p. 211–214 °C; R_F = 0.32 (chloroform/methanol, 9:1); UV–vis (MeOH): λ^{max} (log ε) = 257 (4.38), 304 (4.05), 555 (4.84) nm; IR (ATR):

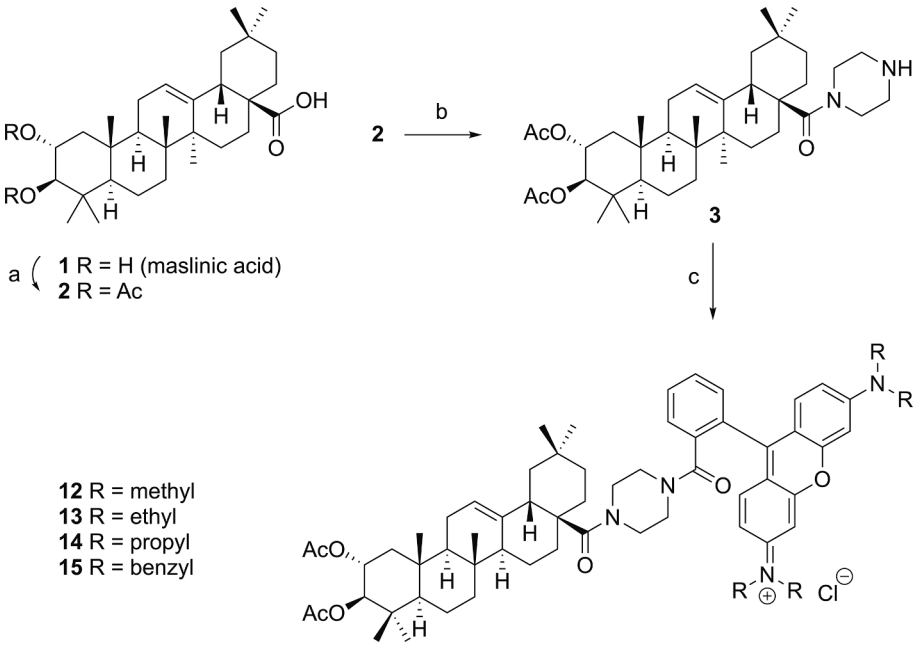

Scheme 2. Reactions and conditions: (a) Ac_2O, NEt_3, DMF (cat.), DCM, 21 °C, 1 day, →2 (78 %); (b) oxalyl chloride, NEt_3, DMF (cat.), DCM, 21 °C, 5 h, then piperazine, DCM, NEt_3, DMAP, 0 °C → 21 °C, 30 min, →3 (86 %); (c) rhodamines 8–11, oxalyl chloride, DMF (cat.), DCM, 0 °C → 21 °C, 2 h, then 3, NEt_3, DMAP (cat.), DCM, 21 °C, 24 h, yield: 12 (46 %), 13 (61 %), 14 (58 %), 15 (52 %).

ν = 2924 s, 2856 m, 1738 s, 1632 s, 1592 s, 1534 m, 1494 s, 1456 s, 1408 s, 1364 s, 1343 s, 1281 s, 1252 s, 1232 s, 1184 s, 1124 s, 1064 m, 1042 s, 1032 s, 1002 s cm^{-1}; ^1H NMR (500 MHz, $CDCl_3$): δ = 7.71 – 7.62 (m, 1H, 41-H), 7.55 – 7.50 (m, 1H, 39-H), 7.39 – 7.36 (m, 1H, 40-H), 7.31 – 7.27 (m, 2H, 46-H + 46′-H), 6.99 (d, J = 9.3 Hz, 2H, 47-H + 47′-H), 6.85 (d, J = 4.7 Hz, 2H, 49-H + 49′-H), 5.19 (m, 1H, 12-H), 5.06 (td, J = 11.1, 4.5 Hz, 1H, 2-H), 4.72 (d, J = 10.3 Hz, 1H, 3-H), 3.33 (s, 12H, 51-H + 51′-H), 3.27 (br s, 8H, 36-H + 35-H), 2.97 (d, J = 9.6 Hz, 1H, 18-H), 2.11 – 2.05 (m, 1H, 16-Ha), 2.03 (s, 3H, 33-H), 2.01 – 1.96 (m, 1H, 1-Ha), 1.95 (s, 3H, 32-H), 1.93 – 1.77 (m, 2H, 11-Ha + 11-Hb), 1.67 – 1.47 (m, 5H, 19-Ha + 16-Hb + 7-Ha + 6-Ha + 15-Ha), 1.46 – 1.39 (m, 1H, 22-Ha), 1.37 – 1.27 (m, 3H, 6-Hb + 21-Ha + 16-Hb), 1.27 – 1.21 (m, 2H, 7-Hb + 22-Hb), 1.18 – 1.09 (m, 2H, 21-Hb + 19-Hb), 1.08 (s, 3H, 27-H), 1.06 – 1.02 (m, 2H, 15-Hb + 1-Hb), 1.00 (s, 3H, 26-H), 0.94 (d, J = 10.3 Hz, 1H, 5-H), 0.88 (s, 6H, 23-H + 24-H), 0.86 (s, 3H, 29-H), 0.86 (s, 3H, 30-H), 0.63 (s, 3H, 25-H) ppm; ^{13}C NMR (126 MHz, $CDCl_3$): δ = 175.7 (C-28), 170.9 (C-31), 170.6 (C-24), 167.8 (C-37), 157.6 (C-50), 157.6 (C-50‘), 157.6 (C-44), 157.5 (C-48),157.5 (C-48‘), 144.8 (C-13), 135.2 (C-43), 132.2 (C-46), 132.2 (C-46‘), 130.5 (C-42), 130.5 (C-38), 130.4 (C-40), 130.3 (C-41), 127.8 (C-39), 121.2 (C-12), 114.5 (C-47), 114.5 (C-47′), 114.1 (C-45), 114.0 (C-45′), 97.0 (C-49‘), 97.0 (C-49), 80.7 (C-3), 70.1 (C-2), 55.0 (C-5), 47.7 (C-9), 47.6 (C-36), 46.4 (C-17), 46.3 (C-19), 43.9 (C-1), 43.6 (C-18), 42.0 (C-35), 41.4 (C-51′), 41.3 (C-51), 39.4 (C-4), 39.4 (C-14), 39.2 (C-8), 38.3 (C-10), 34.0 (C-21), 33.1 (C-30), 32.7 (C-22), 30.4 (C-20), 29.8 (C-7), 28.5 (C-24), 27.9 (C-15), 25.9 (C-27), 24.1 (C-29), 23.5 (C-11), 22.8 (C-16), 21.2 (C-32), 21.0 (C-33), 18.3 (C-6), 17.7 (C-23), 17.0 (C-25), 16.5 (C-26) ppm; MS (ESI, methanol/chloroform, 4:1): m/z = 993.8 (100 %, $[M-Cl]^+$), 1027.8 (10 %, $[M-Cl + MeOH + H]^+$); analysis calcd for $C_{61}H_{79}ClN_4O_7$ (1015.77): C 72.13, H 7.84, N 5.52; found: C 71.87, H 8.03, N 5.31.

*9-[2-[[4-(2α,3β-Bis(acetyloxy)-olean-12-en-28-oyl)-1-piperazinyl] carbonyl]phenyl]-3,6-bis(dimethylamino]-xanthylium chloride **(13)***

As previously reported from **9** in 70 % yield as a violet solid: m.p. 245–248 °C (lit.: [30] 247–249 °C); R_F = 0.30 (silica gel, chloroform/methanol, 9:1).

*9-[2-[[4-(2α,3β-Bis(acetyloxy)-olean-12-en-28-oyl)-1-piperazinyl] carbonyl]phenyl]-3,6-bis(dipropylamino]-xanthylium chloride **(14)***

According to GPC with **10** (0.2 g) followed by chromatography (silica gel, chloroform/MeOH, 11:1) **14** (291 mg, 58 %) was obtained as a violet solid; m.p. 236–239 °C; R_F = 0.38 (chloroform/methanol, 9:1); UV–vis (methanol): λ^{max} (log ε) = 260 (4.48), 307 (4.14), 566 (5.02) nm; IR (ATR): ν = 2938 m, 2874 m, 1737 s, 1632 s, 1586 s, 1528 m, 1508 s, 1468 s, 1429 s, 1411 s, 1393 s, 1363 s, 1336 s, 1300 s, 1252 s, 1230 s, 1177 s, 1132 s, 1100 s, 1033 s, 1001 s cm^{-1}; ^1H NMR (500 MHz, $CDCl_3$): δ = 7.70 – 7.61 (m, 1H, 41-H), 7.53 – 7.50 (m, 1H, 39-H), 7.34 – 7.17 (m, 4H, 40-H + 46-H + 46‘-H + 42-H), 6.97 (d, J = 8.4 Hz, 2H, 47-H + 47‘-H), 6.74 – 6.72 (m, 2H, 49-H + 49‘-H), 5.18 (t, J = 3.3 Hz, 1H, 12-H), 5.05 (td, J = 11.0, 4.6 Hz, 1H, 2-H), 4.71 (d, J = 10.3 Hz, 1H, 3-H), 3.50 (m, 8H, 51-H + 51′-H), 3.30 (m, 8H, 36-H + 35-H), 2.97 (d, J = 13.2 Hz, 1H, 18-H), 2.11 – 2.04 (m, 1H, 16-Ha), 2.02 (s, 3H, 33-H), 1.99 – 1.94 (m, 1H, 1-Ha), 1.94 (s, 3H, 32-H), 1.91 – 1.47 (m, 16H, 11-Ha + 11-Hb + 52-H + 52′-H + 16-Hb + 19-Hb + 7-Ha + 7-Hb + 6-Ha + 15-Ha), 1.46 – 1.37 (m, 1H, 22-Ha), 1.37 – 1.26 (m, 2H, 21-Ha + 6-Hb), 1.21 (d, J = 12.7 Hz, 1H, 22-Hb), 1.15 – 1.01 (m, 4H, 21-Hb + 19-Hb + 1-Hb + 15-Hb), 1.07 (s, 3H, 27-H), 0.99 (t, J = 7.3 Hz, 15H, 53-H + 53′-H + 26-H, 0.94 (d, J = 10.6 Hz, 1H, 5-H), 0.87 (s, 6H, 23-H + 24-H), 0.85 (s, 3H, 29-H), 0.85 (s, 3H, 30-H), 0.63 (s, 3H, 25-H) ppm; ^{13}C NMR (126 MHz, $CDCl_3$): δ = 175.8 (C-28), 170.9 (C-31), 170.6 (C-34), 167.8 (C-37), 157.8 (C-50), 157.8 (C-50‘), 156.3 (C-44), 156.1 (C-48), 156.1 (C-48‘), 144.8 (C-13), 135.2 (C-43), 132.3 (C-46), 132.3 (C-46′), 130.7 (C-38), 130.4 (C-42), 130.4 (C-40), 130.3 (C-41), 127.7 (C-39), 121.2 (C-12), 114.5 (C-47), 114.5 (C-47′), 114.0 (C-45), 114.0 (C-45′), 96.6 (C-49‘), 96.5 (C-49), 80.7 (C-3), 70.1 (C-2), 55.0 (C-5), 53.9 (C-51′), 53.8 (C-51), 47.7 (C-9), 47.6 (C-36), 47.6 (C-17), 46.3 (C-19), 43.91 (C-1), 43.6 (C-18), 42.0 (C-35), 39.4 (C-4), 39.4 (C-14), 39.2 (C-8), 38.3 (C-10), 34.0 (C-21), 33.0 (C-30), 32.7 (C-22), 30.4 (C-20), 29.9 (C-7), 28.5 (C-24), 27.8 (C-15), 25.9 (C-27), 24.1 (C-29), 23.5 (C-11), 22.5 (C-16), 21.2 (C-32), 21.0 (C-33), 20.9 (C-52), 20.9 (C-52‘), 18.3 (C-6), 17.7 (C-23), 17.0 (C-25), 16.5 (C-26), 11.4 (C-53), 11.4 (C-53‘) ppm; MS (ESI, MeOH/chloroform 4:1): m/z = 1106.0 (100 %, $[M-Cl]^+$); analysis calcd for $C_{69}H_{95}ClN_4O_7$ (1127.99): C 73.47, H 8.49, N 4.97; found: C 73.14, H 8.68, N 4.75.

*9-[2-[[4-(2α,3β-Bis(acetyloxy)-olean-12-en-28-oyl)-1-piperazinyl] carbonyl]phenyl]-3,6-bis(dibenzylamino]-xanthylium chloride **(15)***

According to GPC with **11** (followed by chromatography (silica gel, chloroform/MeOH, 9.5:0.5) **15** (52 %) was obtained as a violet solid; m.p. 216–219 °C; R_F = 0.45 (chloroform/methanol, 9:1); UV–vis (MeOH): λ^{max} (log ε) = 259 (4.61), 302 (4.25), 556 (5.06) nm; IR (ATR): ν = 2941 m, 2863 m, 1737 s, 1633 s, 1590 s, 1580 s, 1550 m, 1525 m, 1480 s, 1451 s, 1426 s, 1409 s, 1388 s, 1341 s, 1298 s, 1281 s, 1252 s, 1252 s, 1221 s, 1181 s, 1152 s, 1079 m, 1041 s, 1029 s, 1002 s cm^{-1}; ^1H NMR (500 MHz, $CDCl_3$): δ = 7.67 – 7.63 (m, 1H, 41-H), 7.53 – 7.51 (m, 1H, 39-H), 7.40 – 7.38 (m, 2H, H-46 + H-46′), 7.36 – 7.17 (m, 21H, 40-H + 42-H + 54-H + 54‘-H + 52-H + 52′-H + 53-H + 53′-H), 7.12 – 7.10 (m, 2H, 47-H + 47‘-H), 6.88 – 6.83 (m, 2H, 49-H + 49‘-H), 5.23 (t, J = 3.5 Hz, 1H, 12-H), 5.07 (td, J = 11.1, 4.7 Hz, 1H, 2-H), 4.95 – 4.68 (m, 9H, 51-H + 51‘-H + 3-H), 3.51 – 3.34 (m, 3H, 35-Ha + 36-Ha + 36-Hb), 3.25 (br s, 1H, 35-Hb), 3.04 – 2.99 (m, 1H, 18-H), 2.14 – 2.04 (m, 1H, 16-Ha), 2.03 (s, 3H, 33-H), 2.02 – 1.97 (m, 1H, 1-Ha), 1.95 (s, 3H, 32-H), 1.94 – 1.77 (m, 2H, 11-Ha + 11-Hb), 1.70 – 1.46 (m, 5H, 16-Hb + 19-Ha + 7-Ha + 7-Hb + 15-Ha + 6-Ha), 1.43 (dd, J = 12.3, 2.6 Hz, 1H, 22-Ha), 1.39 – 1.27 (m, 2H, 6-Hb + 21-Ha), 1.25 (d, J = 12.7 Hz, 1H, 22-Hb), 1.18 – 1.12 (m, 2H, 19-Hb + 21-Hb), 1.10 (s, 3H, 27-H), 1.10 – 1.01 (m, 2H, 15-Hb + 1-Hb), 1.01 (s, 3H, 26-H), 0.95 (d, J = 8.0 Hz, 1H, 5-H), 0.89 (s, 3H, 29-H), 0.87 (s, 9H, 23-H + 24-H + 30-H), 0.68 (s, 3H, 25-H) ppm; ^{13}C NMR (126 MHz, $CDCl_3$): δ = 175.6 (C-28), 170.9 (C-31), 170.6 (C-34), 167.5 (C-37), 158.0 (C-50), 158.0 (C-50‘), 157.9 (C-44), 157.7 (C-48), 157.7 (C-48‘), 144.9 (C-13), 134.9 (C-43), 134.7 (C-52), 134.6 (C-52‘), 132.7 (C-46), 132.7 (C-46‘), 131.0 (C-38), 130.7 (C-42), 130.5 (C-40), 130.4 (C-41), 129.4 (C-54), 129.4 (C-54), 128.3 (C-55′), 128.3 (C-55), 127.9 (C-39), 126.5 (C-53′), 126.5 (C-53), 121.2 (C-12), 115.3 (C-47), 115.3 (C-47′), 115.0 (C-45), 115.0 (C-45′), 97.8 (C-49′), 97.7 (C-49), 80.7 (C-3), 70.1 (C-2), 55.2 (C-51), 55.2 (C-51′), 55.0 (C-5), 47.7 (C-9), 47.6 (C-36), 47.6 (C-17), 46.4 (C-19), 43.9 (C-1), 43.7 (C-18), 42.0 (C-35), 39.4 (C-4), 39.4 (C-14), 39.2 (C-8), 38.3 (C-10), 34.0 (C-21), 33.0 (C-30), 32.7 (C-22), 30.4 (C-20), 29.8 (C-7), 28.5 (C-24), 27.9 (C-15), 25.9 (C-27), 24.1 (C-29), 23.5 (C-11), 22.6 (C-16), 21.2 (C-32), 21.0 (C-33), 18.3 (C-6), 17.7 (C-23), 17.0 (C-25), 16.6 (C-26) ppm; MS (ESI, MeOH/chloroform, 4:1): m/z = 1298.7 (32 %, $[M-Cl + H]^+$), 1297.7 (29 %, $[M-Cl]^+$); analysis calcd for $C_{85}H_{95}ClN_4O_7$ (1320.17): C 77.33, H 7.25, N 4.24; found: C 76.97, H 7.65, N 3.97.

CRediT authorship contribution statement

Marie Kozubek: Investigation. **Toni C. Denner:** Investigation. **Marc Eckert:** Investigation. **Sophie Hoenke:** Investigation. **René Csuk:** Conceptualization, Writing – original draft, Writing – review & editing.

Declaration of Competing Interest

The authors declare that they have no known competing financial interests or personal relationships that could have appeared to influence the work reported in this paper.

Data availability

No data was used for the research described in the article.

Acknowledgments

We would like to thank Th. Schmidt for measuring the MS spectra, and Dr. D. Ströhl, Y. Schiller and S. Ludwig for the NMR spectra. Many thanks are also due to M. Schneider for measuring the IR as well as the UV/vis spectra and for the microanalyses. The cell lines have been provided by Dr. Th. Müller (Dept. Oncology).

References

[1] W. Chen, Z. Sun, L. Lu, Targeted Engineering of Medicinal Chemistry for Cancer Therapy: Recent Advances and Perspectives, Angew. Chem., Int. 60 (2021) 5626–5643.
[2] K.-M. Debatin, D. Poncet, G. Kroemer, Chemotherapy: targeting the mitochondrial cell death pathway, Oncogene 21 (2002) 8786–8803.
[3] L. Galluzzi, N. Larochette, N. Zamzami, G. Kroemer, Mitochondria as therapeutic targets for cancer chemotherapy, Oncogene 25 (2006) 4812–4830.
[4] P. Ghosh, C. Vidal, S. Dey, L. Zhang, Mitochondria targeting as an effective strategy for cancer therapy, Int. J. Mol. Sci. 21 (2020) 3363.
[5] V. Gogvadze, S. Orrenius, B. Zhivotovsky, Mitochondria as targets for cancer chemotherapy, Semin. Cancer Biol. 19 (2009) 57–66.
[6] X. Guo, N. Yang, W. Ji, H. Zhang, X. Dong, Z. Zhou, L. Li, H.-M. Shen, S.Q. Yao, W. Huang, Mito-Bomb: Targeting Mitochondria for Cancer Therapy, Adv. Mater. (Weinheim, Ger.), 33 (2021) 2007778.
[7] T. Rodrigues, L.S. Ferraz, Therapeutic potential of targeting mitochondrial dynamics in cancer, Biochem. Pharmacol. (Amsterdam, Neth.), 182 (2020) 114282.
[8] A. Rovini, A. Savry, D. Braguer, M. Carre, Microtubule-targeted agents: When mitochondria become essential to chemotherapy, Biochim. Biophys. Acta, Bioenerg. 1807 (2011) 679–688.
[9] K.A. Sarosiek, T. Ni Chonghaile, A. Letai, Mitochondria: gatekeepers of response to chemotherapy, Trends Cell Biol. 23 (2013) 612–619.
[10] F.A. Urra, S. Fuentes-Retamal, C. Palominos, R. Araya-Maturana, Recent advances in molecular mechanisms of anticancer natural products that target mitochondrial bioenergetics, Stud. Nat. Prod. Chem. 71 (2021) 1–43.
[11] E. Zhang, C. Zhang, Y. Su, T. Cheng, C. Shi, Newly developed strategies for multifunctional mitochondria-targeted agents in cancer therapy, Drug Discovery Today 16 (2011) 140–146.
[12] X. Zhang, Q. Su, J. Zhou, Z. Yang, Z. Liu, L. Ji, H. Gao, G. Jiang, To betray or to fight? The dual identity of the mitochondria in cancer, Future Oncol. 17 (2021) 723–743.
[13] S. Fulda, L. Galluzzi, G. Kroemer, Targeting mitochondria for cancer therapy, Nat. Rev. Drug Discovery 9 (2010) 447–464.
[14] N. Lane, Mitochondrial disease: Powerhouse of disease, Nature (London, U. K.), 440 (2006) 600-602.
[15] C. Ma, F. Xia, S.O. Kelley, Mitochondrial Targeting of Probes and Therapeutics to the Powerhouse of the Cell, Bioconjugate Chem. 31 (2020) 2650–2667.
[16] H.M. McBride, M. Neuspiel, S. Wasiak, Mitochondria: More Than Just a Powerhouse, Curr. Biol. 16 (2006) R551.
[17] M. Scheibye-Knudsen, E.F. Fang, D.L. Croteau, D.M. Wilson III, V.A. Bohr, Protecting the mitochondrial powerhouse, Trends Cell Biol. 25 (2015) 158–170.
[18] P.T. Schumacker, M.N. Gillespie, K. Nakahira, A.M.K. Choi, E.D. Crouser, C. A. Piantadosi, J. Bhattacharya, Mitochondria in lung biology and pathology: more than just a powerhouse, Am. J. Physiol. 306 (2014) L962.
[19] R. Csuk, Betulinic acid and its derivatives: a patent review (2008–2013), Expert Opin. Ther. Pat. 24 (2014) 913–923.
[20] R. Csuk, H.-P. Deigner, The potential of click reactions for the synthesis of bioactive triterpenes, Bioorg. Med. Chem. Lett. 29 (2019) 949–958.
[21] S. Hoenke, I. Serbian, H.-P. Deigner, R. Csuk, Mitocanic Di- and triterpenoid rhodamine B conjugates, Molecules 25 (2020) 5443.
[22] H. Hussain, A. Al-Harrasi, R. Csuk, U. Shamraiz, I.R. Green, I. Ahmed, I.A. Khan, Z. Ali, Therapeutic potential of boswellic acids: a patent review (1990–2015), Expert Opin. Ther. Pat. 27 (2017) 81–90.
[23] N. Heise, S. Hoenke, V. Simon, H.-P. Deigner, A. Al-Harrasi, R. Csuk, Type and position of linkage govern the cytotoxicity of oleanolic acid rhodamine B hybrids, Steroids 172 (2021), 108876.
[24] N.V. Heise, S. Hoenke, I. Serbian, R. Csuk, An improved partial synthesis of corosolic acid and its conversion to highly cytotoxic mitocans, Eur. J. Med. Chem. Rep. 6 (2022), 100073.
[25] N.V. Heise, D. Major, S. Hoenke, M. Kozubek, I. Serbian, R. Csuk, Rhodamine 101 Conjugates of Triterpenoic Amides Are of Comparable Cytotoxicity as Their Rhodamine B Analogs, Molecules 27 (2022) 2220.
[26] M. Kahnt, J. Wiemann, L. Fischer, S. Sommerwerk, R. Csuk, Transformation of asiatic acid into a mitocanic, bimodal-acting rhodamine B conjugate of nanomolar cytotoxicity, Eur. J. Med. Chem. 159 (2018) 143–148.
[27] M. Kozubek, S. Hoenke, H.-P. Deigner, R. Csuk, Betulinic acid and glycyrrhetinic acid derived piperazinyl spacered rhodamine B conjugates are highly cytotoxic and necrotic, Results Chem. 4 (2022), 100429.
[28] O. Kraft, A.-K. Hartmann, S. Hoenke, I. Serbian, R. Csuk, Madecassic Acid-A New Scaffold for Highly Cytotoxic Agents, Int. J. Mol. Sci. 23 (2022) 4362.
[29] O. Kraft, S. Hoenke, R. Csuk, A tormentic acid-homopiperazine-rhodamine B conjugate of single-digit nanomolar cytotoxicity and high selectivity for several human tumor cell lines, Eur. J. Med. Chem. Rep. 5 (2022), 100043.
[30] S. Sommerwerk, L. Heller, C. Kerzig, A.E. Kramell, R. Csuk, Rhodamine B conjugates of triterpenoic acids are cytotoxic mitocans even at nanomolar concentrations, Eur. J. Med. Chem. 127 (2017) 1–9.
[31] R.K. Wolfram, L. Fischer, R. Kluge, D. Stroehl, A. Al-Harrasi, R. Csuk, Homopiperazine-rhodamine B adducts of triterpenoic acids are strong mitocans, Eur. J. Med. Chem. 155 (2018) 869–879.
[32] R.K. Wolfram, L. Heller, R. Csuk, Targeting mitochondria: Esters of rhodamine B with triterpenoids are mitocanic triggers of apoptosis, Eur. J. Med. Chem. 152 (2018) 21–30.
[33] B. Siewert, E. Pianowski, R. Csuk, Esters and amides of maslinic acid trigger apoptosis in human tumor cells and alter their mode of action with respect to the substitution pattern at C-28, Eur. J. Med. Chem. 70 (2013) 259–272.
[34] B. Siewert, E. Pianowski, A. Obernauer, R. Csuk, Towards cytotoxic and selective derivatives of maslinic acid, Bioorg. Med. Chem. 22 (2014) 594–615.
[35] M. Beija, C.A.M. Afonso, J.M.G. Martinho, Synthesis and applications of Rhodamine derivatives as fluorescent probes, Chem. Soc. Rev. 38 (2009) 2410–2433.
[36] M. Fu, X. Zhang, J. Wang, H. Chen, Y. Gao, Progress of Synthesis and Separation of Regioisomerically Pure 5(6)-Substituted Rhodamine, Curr. Org. Chem. 20 (2016) 1584–1590.
[37] S. Hoenke, I. Serbian, R. Csuk, A Malaprade cleavage, a McMurry ring closure and an intramolecular aldol contraction of maslinic acid's ring A, Results Chem. 4 (2022), 100547.
[38] S. Sommerwerk, L. Heller, I. Serbian, R. Csuk, Straightforward partial synthesis of four diastereomeric 2,3-dihydroxy-olean-12-en-28-oic acids from oleanolic acid, Tetrahedron 71 (2015) 8528–8534.
[39] F.G. Bordwell, P.J. Boutan, Conjugate effects of dimethylsulfonio and trimethylammonio groups, J. Am. Chem. Soc. 78 (1956) 87–91.
[40] J.C. Jacquesy, M.P. Jouannetaud, G. Morellet, Y. Vidal, Direct hydroxylation of anilines and aminophenols, Bull. Soc. Chim. Fr. 625 (1986).
[41] M.I.P.S. Leitao, B. Rama Raju, N.M.F.S.A. Cerqueira, M.J. Sousa, M.S.T. Goncalves, Benzo[a]phenoxazinium chlorides: Synthesis, antifungal activity, in-silico studies and evaluation as fluorescent probes, Bioorg. Chem. 98 (2020), 103730.
[42] M. Chouhan, K. Kumar, R. Sharma, V. Grover, V.A. Nair, NiCl2·6H2O/NaBH4 in methanol: a mild and efficient strategy for chemoselective deallylation/ debenzylation of aryl ethers, Tetrahedron Lett. 54 (2013) 4540–4543.
[43] C. Arambula, J. Rodrigues, J.J. Koh, Z. Woydziak, Synthesis of Rhodamines and Rosamines Using 3,6-Difluoroxanthone as a Common Intermediate, J. Org. Chem. 86 (2021) 17856–17865.